Transactions

of the

ASME

FEBRUARY, 1952

VOL. 74, NO. 2

Transactions

of The American Society of Mechanical Engineers

Published on the tenth of every month, **except March, June, September, and December**

Published monthly by The American Society of Mechanical Engineers. Publication office at 20th and Northampton Streets, Easton, Pa. The editorial department is located at the headquarters of the Society, 29 West Thirty-Ninth Street, New York 18, N. Y. Cable address, "Dynamic," New York. Price $1.50 a copy, $12.00 a year for Transactions and the *Journal of Applied Mechanics;* to members and affiliates, $1.00 a copy, $6.00 a year. Changes of address must be received at Society headquarters four weeks before they are to be effective on the mailing list. Please send old as well as new address. . . . By-Law: The Society shall not be responsible for statements or opinions advanced in papers or . . . printed in its publications (B13, Par. 4). . . . Entered as second-class matter March 2, 1928, at the Post Office at Easton, Pa., under the Act of August 24, 1912. . . . Copyrighted, 1952, by The American Society of Mechanical Engineers. Reprints from this publication may be made on condition that full credit be given the Transactions of the ASME and the author, and that date of publication be stated.

The Creep and Stress-Rupture Testing of Steam-Boiler Materials

By J. B. Romer[1] and H. D. Newell[2]

This paper points out the necessity of having adequate data on the high-temperature properties of metals used in steam-boiler construction. The significance of the time factor in testing in relationship to long-life high-performance steam-generating equipment is discussed as are the general effects of metal oxidation from steam and combustion atmospheres. Metallurgical stability of steels is important in maintaining creep strength and is necessary to prevent severe modification of mechanical properties through effects such as spheroidization of carbide phase, graphitization or formation of sigma phase in highly alloyed steels. The relative merits of long-time creep tests and stress-rupture tests are considered, and typical test data are cited for each form of test. These data are necessary for design of superheater tubes and headers, alloy baffles, hangers and fittings, and are an aid to the Code Committee in assigning suitable stress allowances for materials. The paper gives suggestions for temperature limits for superheater-tube materials and a résumé of field experience on carbon and alloy steels. Conclusions are drawn that high-temperature creep and rupture testing have been very useful in evaluating the relative strength of steels for high-temperature use, in aiding in the development of superior materials, and in permitting the increases in steam temperature and pressure which have led to much greater economy in power production. Further advances are forecast for the future through a well-co-ordinated program of metal testing now in progress.

Introduction

The modern steam generator or high-capacity power boiler has been evolved through a period of about 80 years to its present state of efficiency and reliability of operation (1).[3] Present-day large boiler units may range in capacity up to 1,380,000 lb of steam per hr. Superheat temperatures are approaching 1100 F at the turbine throttle with design as high as 2600 psi. Process steam is produced at even higher temperatures (1300 to 1500 F), but at lower pressures than in boilers for power generation. The reheat cycle recently described by Rowand (2), and others (3, 4) is again gaining favor and adds an increment to over-all thermal efficiency of the steam cycle.

There is a decided trend toward providing only one boiler unit per turbine which is practical because of the high availability of present boiler equipment. Advances in temperature and pressure conditions through the years are shown in Fig. 1.

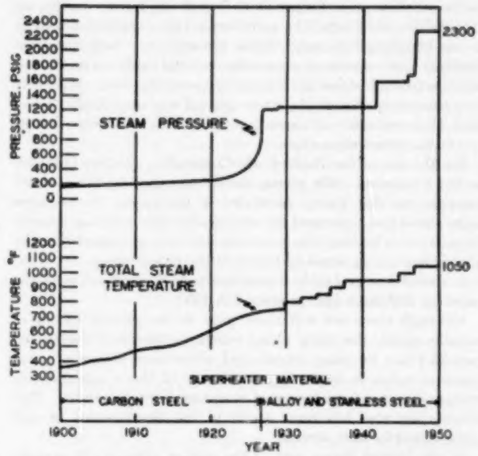

Fig. 1 Trend in Central-Station Boilers, 1900–1950

This improvement in boiler performance has come about gradually through the years and is in no small measure due to studies which have been made during the past 25 years relating to the properties and behavior of metals under long-time exposure to stress at elevated temperatures. These investigations have led to the development of superior materials of construction for the superheater and its headers and to improvements in those other parts which operate at lower temperatures such as drums, steam and waterwall tubes, economizer tubes, and piping. Such studies are continuing on an even more extended scale so as to bring about further improvement and extend present design limits.

Drums, generating tubes, economizer tubes, and so forth, operating at a temperature below 700 F may be designed on the basis of a percentage of the ordinary mechanical properties in accordance with stresses designated by the ASME Boiler Code. Superheaters and other parts operate at higher temperatures where creep becomes operative. The amount of extension is a function of temperature and of the stress imposed and is time-dependent.

Other factors enter the problem of metal selection and usually are of greater significance as the temperature increases—for example, thermal expansivity, heat conductance, elastic moduli, resistance to scaling and corrosive attack of the metal, and structural changes which might in some way affect its useful properties. Strength properties continue, however, to be of primary significance so as to limit working stresses to a level where expected life of equipment is obtained. Because of the long life

---

[1] Consultant, Research and Development Department, The Babcock & Wilcox Company, Alliance, Ohio.

[2] Chief Metallurgist, The Babcock & Wilcox Tube Company, Beaver Falls, Pa.

[3] Numbers in parentheses refer to the Bibliography at the end of the paper.

Contributed by the Joint ASTM-ASME Committee on Effect of Temperature on the Properties of Metals and presented at the Annual Meeting, New York, N. Y., November 26–December 1, 1950, of The American Society of Mechanical Engineers.

expected of boiler equipment, it is of extreme importance to make a careful choice of material and to allow adequate but not excessive factors of safety. Methods of fabrication and physical size of parts also must be considered.

High-Temperature Testing

It has long been known that certain nonmetallic materials, such as glass, when subjected to stress, undergo slow and continuous deformation with time.

The concept of creep in metallic materials, however, is comparatively new. Chevenard (5) in 1919, and Dickenson (6) in 1922, were among the first to draw attention to the phenomena. In the next few years, French (7, 8), Lynch (9), Kanter and Spring (10), White and Clark (11), and Norton (12) contributed heavily to our knowledge of creep. These investigations indicating conclusively that rupture of a metallic material could occur when it is subjected to a stress at elevated temperatures for a sufficiently long time, even though the stress applied was considerably lower than that necessary to cause fracture in the short-time tensile test at the same temperature.

For the use of the Boiler Code Committee, Jacobus (13) presented a paper in 1929, giving the stresses used by the authors' company at that time. As stated in the paper, the so-called creep stress had been used for setting allowable working stresses. In so far as is known, this paper was the first to suggest that the allowable working stress be based on the rate of creep.

A recent and valuable contribution to the subject was the paper by Robinson (14) presented in 1950.

Although there are still many gaps in the present theory of metallic creep, the creep characteristics established during the past 25 years for many metals and alloys have proved of great practical value in indicating the fitness of these materials for continuous service under stress at elevated temperatures. This information also has been useful in the development of still better alloys for such service.

In the United States, one of the earliest attempts to investigate creep in a comprehensive manner was made by the companies with which the authors are associated. Early in 1926 a joint fellowship was established at the Massachusetts Institute of Technology under the direction of Prof. F. H. Norton for these studies. Many steels now used successfully in power-generating units and in the petroleum-refining and chemical industries were tested and proved in the course of this investigation. Extensive studies of the creep characteristics of metals are now continuously under way in the Research and Development Laboratory of the authors' company at Alliance, Ohio.

The need for the most precise data for design purposes and the desirability of developing alloys suitable for use at even higher temperatures and pressures led the company to expand its creep and stress-rupture facilities.

Presently installed in the laboratory are five twelve-station stress-rupture units for operation up to 1500 F, sixteen Baldwin-Southwark units suitable for both stress-rupture and creep tests up to 1800 F, and twenty creep units of M.I.T. design, and thirty-two creep units of company design for testing up to 2000 F. A complete description of these testing facilities already has been published (15). The testing procedures and equipment used fully comply with the ASTM Recommended Practices (16).

Changing fuel supplies, special forms of corrosion, and requirements for better metals which will lend themselves to fabrication into boiler parts, drums, tubing, and headers, present a challenge to the materials engineer and metallurgist. Many of these problems are being overcome, and metals are being applied more intelligently through a better understanding of the effects of temperature in relation to time of exposure while under stress.

Significance of Time Factor in Short-Time Tensile, Creep, and Stress-Rupture Tests

In the engineering of high-temperature equipment, the time factor is of the greatest significance. It may vary, in the case of rockets, from a few seconds, through several hundred hours or more in turbojet aircraft engines to several decades in the service life of large turbines and boilers. The engineer must take into consideration growth or clearance of parts and allow for dimensional changes due to stress and temperature. His design must be based on such data as will give him assurance that performance will be as expected. In the engineering of steam boilers, we are concerned with selection of suitable materials, with provision of sufficient long-time strength, and with surface and internal stability of the metal, so as to avoid failure or rupture with consequent outage of equipment and economic loss. It is the long-time end of the time scale which concerns steam-boiler engineering.

(*a*) *Short-Time Tensile Tests.* Obviously, short-time tensile data are of value for design only in that part of the lower-temperature range where creep of the metal is not significant. Ordinarily, this temperature is considered to be in the vicinity of 650 F for carbon steels and perhaps 750 F for alloy steels. Consequently, steam and water drums, steam-generating tubes, water-wall tubes and headers, and economizer tubes are normally considered to be in this category. Such tubes may suffer a rise in temperature and sometimes inadvertently enter the creep range of temperature and even suffer rupture when scaling or other causes result in unexpected temperature increases. That such events happen can be confirmed by many boiler operators who have experienced such tube failures, not only in superheater tubes, but in furnace-wall and steam-generating tubes. Special forms of corrosion are sometimes a factor in these cases.

Working stresses for these lower temperatures usually are selected on the basis of the familiar room-temperature tensile test, using, for static conditions, a load less than the yield strength. Normally, this is provided by taking one fourth of the minimum ultimate strength for the particular material. The short-time test may be used to confirm the suitability of the stress used at a specific temperature. In fact, one may find that some steels actually increase in strength with moderate increases in temperature. This feature may be noted by reference to Fig. 2 from the recent ASTM publication compiled by Miller and Heger (17) for the principal low-alloy steels which have been used in boiler work. The higher-alloy and stainless steels generally exhibit a fairly gradual decline in short-time strength properties up to 800–900 F with tensile strength falling more abruptly thereafter.

The short-time tensile test has provided some useful information relating to temperatures suitable for fabricating operations of metals and may be used in a preliminary way for evaluating roughly the quick strength of steels having a common heat-treatment or condition of structure. The high strain rate and the short elapsed time of the test preclude using such data for design for long life of steel operated in the creep range. Furthermore, there is not necessarily any relationship between creep resistance and short-time strength; some steels with good short-time properties may exhibit poor creep properties and vice versa.

(*b*) *Creep Tests.* Metallic creep has been studied in large part by most investigators by performing creep tests on many metals and alloys rather than by purely theoretical studies of this phenomenon. Such empirical investigation has been ahead of the purely theoretical studies of the phenomenon of creep behavior in metals. Some investigators have contributed to this phase of the matter, and several of the more recent publications devoted

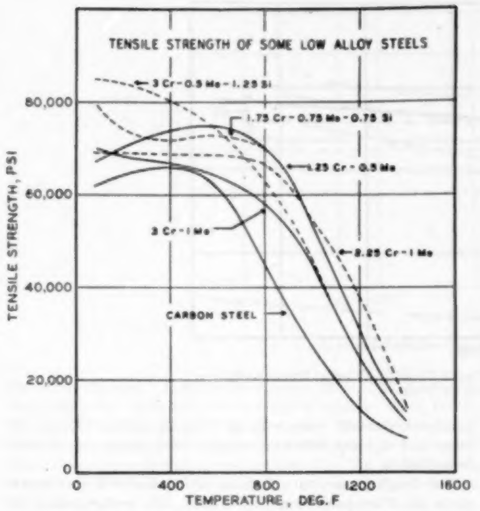

Fig. 2 Tensile Strength of Some Low-Alloy Steels

considerable space to the theoretical aspects of the subject of creep. Theories are described in some detail by Sully (18), Stanford (19), Clark (20), and Smith (21).

Since it is convenient to apply tensile loading, most commercial creep tests are conducted under uniaxial tensile stress although such a simple stress system does not necessarily correspond to that encountered in beams, shells, heavy steam pipes, or other structures. Most of the creep tests conducted by the authors' company have been pointed toward determination of steady-state creep under constant load and temperature using solid tensile-type specimens. Those where high precision was desired were of 10 in. gage length, while others for the higher temperatures, where uniformity of temperature and control is more difficult, were of 2 in. or 3 in. gage length. Since loading was constant, the strain rate may have accelerated gradually with diminution of cross section due to combined action of deformation and scaling of the specimen during the test. These effects are usually not too significant unless the testing is done in a range where scaling of the metal is severe or high stresses are imposed so as to cause appreciable deformation. Other effects such as phase changes in the metal, recrystallization, or precipitation may cause a greater change in the creep rate even though load and temperature are held quite constant.

It always has been our practice to make metallurgical examinations of the creep specimens after creep testing. This procedure includes hardness and microscopic examination for surface condition and structural or phase changes in the metal as compared with the original untested material. Where sufficient gage length permits the necessary subsize specimens to be obtained, the mechanical properties and impact strength are determined and compared with the metal in its initial condition. Thus the relative stability of various materials under stress and temperature have been ascertained for many prominent ferrous materials used in steam-boiler work. Stress has an accelerating action in inducing structural changes, and this is quite pronounced in carbon steels with lesser effects in the more stable alloy steels. Oxidation, which may lead to scaling or intergranular penetration, may be increased sharply under stress concentration such as may exist in welds of dissimilar metals as described by Carpenter (22), and Blaser and Eberle (23).

Creep Testing of Superheater-Tube Alloys

Full-scale creep tests are time-consuming and expensive and are not considered suitable for acceptance tests. Some short methods such as Hatfield's time-yield and the quick creep DIN (DVM) method used in Germany have not received acceptance in this country. Tests of long duration are favored as they permit phase changes in the metal to become complete and allow the effects of surface oxidation to manifest themselves. The Joint High Temperature Committee of the ASME-ASTM has reported on the inadequacy of these short methods (24).

In the early years of testing there was a dearth of information and basic data had to be developed quickly. Even then, the importance of the time element was recognized, and while a number of early tests were carried only to 1600 to 2000 hr, many were run for from 3000 to about 6000 hr. Present practice, in creep laboratory of the authors' company, has been to extend these times on important materials and run both creep and stress-rupture tests on a material to 10,000 hr or longer at temperatures throughout its use range. Generally, testing periods less than 1 per cent of expected life of equipment are not at all significant, and a test period of at least 10 per cent of the service life is preferred. Since boiler superheaters generally are expected to have a life of more than 100,000 hr, this 10,000-hr practice seems well justified.

The principal object of the creep test is to ascertain the steady-state creep rate $V_0 = (de)/(dt)$ for a given condition of temperature and stress so as to determine plastic deformation as a function of time. In the idealized form this may be shown as in Fig. 3.

In many cases tests of short duration will fail to indicate the beginning of third-stage creep which ultimately leads to rupture. Long-time tests, on the other hand, generally will indicate the trend in a given alloy, and working stresses can then be selected to circumvent failure.

Creep and/or rupture in superheater tubes, operating under heat input in the plastic range and under pressure stress, appears to be due mainly to simple tensile stress. This is evident from the general longitudinal nature of both the surface fissures which eventually may develop or when a complete rupture of the tube wall occurs. Invariably, these parallel the longitudinal axis of the tube and only tend to show shear effects at the ends of the rupture where tearing from the bursting reaction occurs at high strain rates. Undoubtedly, some temperature swings occur in the superheater which are dependent on the operating rate of the boiler and other conditions. These may be expected to accelerate the creep rate. Superheaters in many boilers operate under what may be considered steady-state creep. They may undergo cooling to room temperature once or twice a year or perhaps oftener in emergency. In these instances, the metal cools through the plastic range and enters the elastic range where certain residual stresses may develop. These stresses probably tend to wash out when the unit goes back on the line, except at the extreme low end of the creep-temperature range. Bending and vibratory stresses may be superimposed during service but in the main, the stress system is tension from internal pressure.

In many installations the boiler may undergo cyclic operation, being operated at high rating for a portion of the day and then being banked awaiting recurrence of the peak-load condition. This mode of operation likely will accelerate creep action and may induce other stresses in the low-temperature end of the

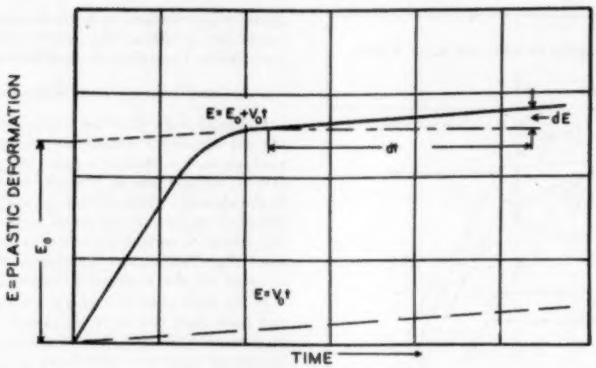

Fig. 3 Idealized Form of Tension-Creep Curve; Plastic Deformation as a Function of Time

cycle which will impose more severe conditions on the metal parts and shorten life.

Deformation—enlargement or expansion—of tubing in a boiler does not necessarily hamper or influence operation of the unit. An expansion of 1 per cent or even 5 per cent might be tolerated in contrast to the limits for total creep permitted for running clearances in turbines or rotating equipment. Small deformations on tubing in high-temperature service are difficult to measure because of oxidation, slag and ash deposits, and because of the difficulty of maintaining reference points. When appreciable overheating occurs the strain rates increase so greatly that rupture is the usual result.

Construction of the superheater, in the newer high temperature, high-pressure units, is by welding to insure tight joints. Small stubs may be welded integrally to the superheater header in the shop and the superheater-tube element is later attached to the stub by welding in the field. This method serves a double purpose of securing a good heat path between tube and header, thus offsetting thermal-expansion difficulties, and it eliminates leakage such as might develop in a mechanically expanded joint should small temperature differences bring about differential creep between the parts.

In the other form, i.e., the expanded or rolled joint used at lower temperatures, the initial elastic and plastic strain must be considered as well as the steady creep rate. One then becomes concerned with the "total" creep rather than the secondary rate of creep. The total deformation at any time up to the beginning of the third-stage creep may be determined from the time-elongation curve by following the method outlined by Smith (21). Summation of the quantity C_0, which is the intercept of the minimum rate of slope on the ordinate axis and the product of the minimum creep rate and the time, gives

$$C_t = C_0 + C_m t$$

where C_t is the total creep at time t, C_0 is the intercept, C_m is the minimum creep rate, and t any time less than the beginning of the third-stage creep. Thus, to calculate total deformation for various stresses, the relations between stress and the quantities: Intercept C_0, minimum creep rate, and time for beginning of third-stage creep are required. These are obtained by testing a number of specimens at each temperature under different stresses.

The form of the creep-time curve for constant load and temperature, if carried on sufficiently far, or if under stress high enough to enter third-stage creep is well known. At high temperatures, primary creep may be virtually absent while at low loads and at more moderate temperatures, creep may cease or be negligible.

The designer must use a working stress which will provide adequate life of the part, structure, or tube. The working stress will have to be limited so that fracture does not occur during expected service life. In tubes, since considerable strain (diametral expansion) can be tolerated, one must chiefly guard against fracture. In theory, high-temperature equipment must be designed with a contemplated or definite service life. How to give long life with economy and avoid failure is the crux of the problem.

Evaluation of alloy steels for superheater service normally has been done on the basis of securing stresses for rates of steady-state creep at several temperatures. Usually these are compared on the basis of the stress producing rates of 0.0001 and 0.00001 per cent per hr, or the more familiar terms of 1 per cent in 10,000 and 100,000 hr, respectively. This makes necessary an unavoidable extrapolation for the long-time rate. Total deformation can be secured for design use, when required, from the actual time-elongation curves.

This paper is not intended to cover the design of tubes for high-temperature service where the metal is operating well into the "plastic range." However, log-log plots of creep rate versus stress are not entirely suitable in their usual form, and the design engineer may create his own curves from the basic data so as to provide a variety of strain rates versus temperature.

Stress-Rupture Tests

Stress-rupture tests, perhaps more properly termed creep-rupture tests, are conducted to determine the stress required for fracturing the metal under prolonged loading. They are made by stressing the specimens so as to cause rupture in time periods ranging from 100 to 10,000 hr, or more. Data are plotted to log-log co-ordinates and if no structural change or intergranular oxidation occurs during testing, a straight-line relationship holds.

Rough strain measurements are made frequently in this form of test since it is important to gain some idea of the flow rate. Final elongation values are obtained by measuring the specimen after fracture. The test has become a popular means of evaluating load-carrying ability and has had increasing use in the high-temperature metals-testing field since its proposal by White, Clark, and Wilson (25). Extrapolation may be dangerous since structural changes or surface-oxidation effects may become manifest only after considerable time under load and as influenced by

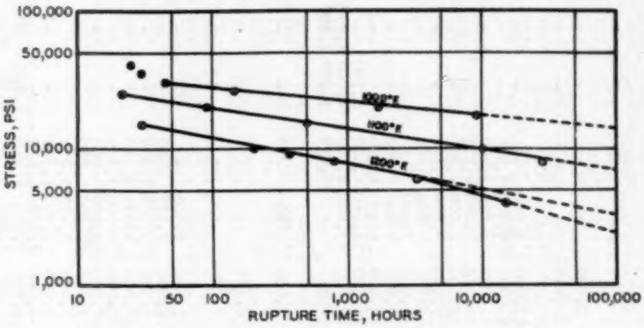

Fig. 4 Stress-Rupture Relationship for B&W Croloy $2^1/_4$

the stress imposed. Rupture tests longer than 1000 hr are preferred on boiler steels and over a range of stresses which bridge the gap between creep and rupture tests. Therefore many of our present rupture tests are run to 10,000 hr or more. The extreme importance of this may be illustrated in Fig. 4 which gives rupture time versus stress on Croloy $2^1/_4$ grade T-22 SA-213 material at several temperatures. In this series of tests it may be noted that no change in slope took place at 1000 F nor at 1100 F even though the final point on the 1100-deg curve was a test extended to 29,286 hr. At 1200 F, however, a change in slope due to surface oxidation took place sometime between a 3320-hr test and one which ruptured after 15,189 hr. This, in effect, suggests a limiting service temperature for this material of 1100 F or a rather drastic reduction in stress allowance if used at higher temperature. A rupture test limited to 3000 hr would not have disclosed these facts. Steels of poorer oxidation resistance show breaks in the stress-rupture time curves at shorter times and lower temperatures. At these more extended times, the relative importance of creep and rupture testing for boiler work is somewhat controversial. Both are useful and desired.

Composition, manufacturing history, particularly deoxidation, grain size, and structural condition all affect the high-temperature strength and ductility of metals. The effect of these variables has received considerable study as is indicated by the literature on the subject (26, 27, 28, 29). In addition, the ability to stand creep strain and suffer deformation varies greatly with the strain rate. At a fast rate, a metal may extend appreciably, whereas with slow rates and longer fracture times, it may suffer intergranular fracture with little or no apparent deformation. The stiffer and more creep-resistant the metal, the more is this characteristic in evidence. Grain-coarsening heat-treatments may be practiced and usually result in improvement in resistance to creep or rupture but at some sacrifice toward withstanding elongation before fracture. It is sometimes preferable, therefore, to apply such heat-treatments to the metal as will give a suitable balance in high-temperature strength and ductility with adjustment of the working stress to a more moderate level, rather than heat-treat the steel for maximum creep strength and have it suffer abrupt fracture. This has been proved in oil-refinery heater work where fine-grained austenitic 18-8 still tubes have given much better over-all service than tubes subjected to a creep-strengthening grain-coarsening heat-treatment.

Tubular Stress Rupture

Before proceeding to the discussion of the tabulated test data, we would like to refer to a development that has been under way for the past year and a half at our research laboratory. We refer to "tubular stress-rupture tests." Considerable work has been done on this important phase of testing. The tests more closely simulate service conditions as the specimens consist of sections of heavy-wall commercial tubing which are subjected to internal steam pressure at superheater temperatures. In order to develop the required hoop stresses, very high steam pressures are required.

This method of testing shows considerable promise in that the ruptures obtained on specimens closely simulate the mode of failure observed on actual tube failures in service. A few tests have been run in excess of 10,000 hr but, in general, the work has not progressed to the point where actual data can be published. Indications are that the information obtained from these tests may be of sufficient interest and value to be made the subject of another paper in the near future.

Test Data

A wide variety of steels of different types and compositions have been subjected to high-temperature tests during the 25 years the authors' company has been doing creep and rupture testing. Many of these were intended for use as tubing or pipe in boilers or other high-temperature equipment. Others were for drum plate, castings, forgings, studs, or bolting. Some tests have been made also on deposited weld metals in connection with welded construction of pressure equipment.

From these tests a number of the most popular and widely used alloy steels have been developed for high-temperature tubing applications. These, and others, are recognized in the ASME Boiler Code as suitable materials for use in steam boilers under the rules which apply. There is presented in this section a compilation of creep and rupture test data from our records. Some rupture-strength curves for recently completed tests on two stainless grades are also given.

Table 1 gives stress values, psi, for creep rates of 0.0001 and 0.00001 per cent per hr for many of the most popular currently used steels employed as superheater tubes, superheater headers, or as piping in boilers and in other high-temperature equipment.

Table 2 gives a supplementary list of similar creep data for a number of steels of grades or kinds which have enjoyed limited utility.

Table 3 lists various plate steels, castings, and others on which creep information has been developed.

Tables 4 and 5 present compositions and tentative stress-rupture data for 1000, 10,000, and 100,000 hr, for several of the commercial austenitic stainless steels now in common use. It is expected that these values will be readjusted when the rupture times have extended to 10,000 hr or more since the tests on these

TABLE 1 CREEP-STRESS DATA* ON BABCOCK & WILCOX CROLOYS AND OTHER TUBULAR MATERIALS FOR HIGH-TEMPERATURE SERVICE

Creep Stress in Lb. Per Sq. In. for a Rate of 1 Per Cent Elongation in 10,000 and 100,000 Hours

ASME SPEC. NO. SA.-	GRADE	MATERIAL B&W DESIGNATION	ANALYSIS		800F	900F	1000F	1100F	1200F	1350F	1500F
			1% - 10,000 Hr. (0.0001%/Hr.)								
SA-83 SA-178	A A	Carbon Steel, Rimmed.......	0.08- 0.18% C;	Si-Trace	12,000	6,300	3,300	1,000	300	-	-
SA-192	-	Carbon Steel, Killed.......	0.10- 0.20% C;	0.25% Max. Si	19,500	11,000	7,200	-	-	-	-
SA-206 SA-209	P1 T1	Carbon-Moly, 0.50% Mo......	0.10- 0.20% C;	0.45- 0.65% Mo	33,500	24,500	12,400	-	-	-	-
SA-280	-	Croloy ½....................	0.50- 0.70%Cr;	0.45- 0.65% Mo	-	35,000	12,000	3,600	-	-	-
SA-213	T11	Croloy 1¼....................	1.00- 1.50%Cr;	0.45- 0.65% Mo	-	35,000	14,700	5,500	3,375	-	-
SA-213	T14	Croloy 2....................	1.75- 2.25%Cr;	0.45- 0.65% Mo	-	28,000	11,000	5,875	3,400	-	-
SA-213	T22	Croloy 2¼....................	2.00- 2.50%Cr;	0.90- 1.10% Mo	-	40,500	16,350	9,200	4,175	-	-
SA-213	T21	Croloy 3M....................	2.75- 3.25%Cr;	0.80- 1.00% Mo	-	19,500	12,500	8,000	4,000	-	-
SA-213	T5	Croloy 5....................	4.00- 6.00%Cr;	0.45- 0.65% Mo	-	17,900	9,200	4,800	1,800	-	-
SA-213	T13	Croloy 5 Si..................	4.00- 6.00%Cr;	0.45- 0.65% Mo **	-	-	8,200	4,400	1,600	-	-
SA-213	T16	Croloy 5 Ti..................	4.00- 6.00%Cr;	0.45- 0.65% Mo ***			13,000	7,300			
SA-213	T7	Croloy 7....................	6.00- 8.00%Cr;	0.45- 0.65% Mo	-	14,500	8,000	4,400	2,000	-	-
SA-213	T9	Croloy 9M....................	8.00-10.00%Cr;	0.90- 1.10% Mo	-	33,250	12,000	6,950	2,300	-	-
SA-213	TP304	Croloy 18-8S (Type 304)....	18.00-20.00%Cr;	8.00-11.00% Ni	-	24,000	18,300	11,550	6,600	2,500	-
SA-213	TP316	Croloy 16-13-3 (Type 316)..	16.00-18.00%Cr;	11.00-14.00% Ni ****	-	-	22,800	13,800	8,200	4,200	1,840
-	-	Croloy 25-20 (Type 310)....	24.00-26.00%Cr;	19.00-22.00% Ni	-	-	-	-	7,400	3,300	1,100
			1% - 100,000 Hr. (0.00001%/Hr.)								
SA-83 SA-178	A A	Carbon Steel, Rimmed.......	0.08- 0.18% C;	Si-Trace	7,000	4,900	2,000	630	70	-	-
SA-192	-	Carbon Steel, Killed.......	0.10- 0.20% C;	0.25% Max. Si	13,500	8,400	2,150	-	-	-	-
SA-206 SA-209	P1 T1	Carbon-Moly, 0.50% Mo......	0.10- 0.20% C;	0.45- 0.65% Mo	23,500	17,200	5,200	-	-	-	-
SA-280	-	Croloy ½....................	0.50- 0.70%Cr;	0.45- 0.65% Mo	32,000	21,000	5,600	1,300	-	-	-
SA-213	T11	Croloy 1¼....................	1.00- 1.50%Cr;	0.45- 0.65% Mo	-	20,000	8,200	2,125	910	-	-
SA-213	T14	Croloy 2....................	1.75- 2.25%Cr;	0.45- 0.65% Mo	-	18,000	6,300	3,325	1,075	-	-
SA-213	T22	Croloy 2¼....................	2.00- 2.50%Cr;	0.90- 1.10% Mo	-	22,000	7,600	4,910	2,510	-	-
SA-213	T21	Croloy 3M....................	2.75- 3.25%Cr;	0.80- 1.00% Mo	-	12,000	7,000	4,000	1,550	-	-
SA-213	T5	Croloy 5....................	4.00- 6.00%Cr;	0.45- 0.65% Mo	-	15,000	7,200	2,400	900	-	-
SA-213	T13	Croloy 5 Si..................	4.00- 6.00%Cr;	0.45- 0.65% Mo **	-	-	5,700	2,700	850	-	-
SA-213	T16	Croloy 5 Ti..................	4.00- 6.00%Cr;	0.45- 0.65% Mo ***			7,000	3,400	1,250		
SA-213	T7	Croloy 7....................	6.00- 8.00%Cr;	0.45- 0.65% Mo	-	9,200	5,000	2,500	1,300	-	-
SA-213	T9	Croloy 9M....................	8.00-10.00%Cr;	0.90- 1.10% Mo	-	24,750	8,500	3,775	1,600	-	-
SA-213	TP304	Croloy 18-8S (Type 304)....	18.00-20.00%Cr;	8.00-11.00% Ni	25,300	18,000	11,500	7,100	4,250	1,600	-
SA-213	TP316	Croloy 16-13-3 (Type 316)..	16.00-18.00%Cr;	11.00-14.00% Ni ****	-	-	14,800	8,700	5,000	2,500	930
-	-	Croloy 25-20 (Type 310)....	24.00-26.00%Cr;	19.00-22.00% Ni	-	-	-	-	5,400	2,800	800

* Data by Prof. F. H. Norton, Babcock & Wilcox Fellow, Massachusetts Institute of Technology.
** 1.00–2.00 per cent Si.
*** 4 × per cent C min, 0.70 per cent max.
**** 2.00–3.00 per cent Mo.
NOTE: Values for Croloys 1¼ to 9M, inclusive, are for 0.15 per cent carbon maximum alloys. (Except Croloy 5 Ti which is a 0.12 per cent carbon maximum alloy.)

TABLE 2 SUPPLEMENTARY CREEP DATA
(Stress values in psi)

GRADE	ANALYSIS C	Mn	Si	Cr	Ni	W	Mo	V	Al	CONDITION	RATE OF CREEP PER CENT PER 1000 HOURS	800	900	1000	1100	1200	1350
			CARBON STEELS														
Open Steel	.08	.41	.01	..	..	..	..	..	..	As Rolled	.01%	6,750	4,900	2,800	630	70	...
											.10%	11,000	6,300	3,300	1,000	300	...
Open Steel	.16	.55	.01	..	..	..	..	..	..	Normalized	.01%	8,400	5,500	1,400	...	...	...
											.10%	13,500	8,200	3,100	...	...	...
SAE 1030	.31	.68	.14	..	..	..	..	..	..	Annealed	.01%	9,900	3,700	2,200	1,150	495	...
											.10%	16,000	8,000	...	1,800	800	...
SAE X1040	.45	.42	.20	..	..	..	..	..	..	Annealed	.01%	...	...	3,200	1,500	550	...
											.10%	...	...	4,500	2,100	900	...
			MANGANESE STEELS														
Mn	.40	2.22	.25	..	..	..	..	..	..	Annealed	.01%	...	9,600	...	1,700	450	...
											.10%	...	12,500		2,600	750	...
Mn-Mo	.13	1.87	.18	..	..	..	.23	..	..	Annealed	.01%	...	...	3,200	935	325	...
											.10%	...	...	5,000	1,500	500	...
Mn-Mo	.12	2.92	.11	..	..	..	.27	..	..	Annealed	.01%	10,200	7,400	1,500	790	300	...
											.10%	16,000	12,000	2,300	1,200	450	...
			TUNGSTEN STEELS														
W-.75	.34	.46	.17	..	..	.74	..	..	..	Annealed	.01%	...	9,600	5,000	1,700	700	...
											.10%	...	12,500	6,500	2,600	1,200	...
W-2	.25	.57	.25	.38	.22	1.95	..	..	..	Annealed	.01%	...	...	...	...	900	...
											.10%	...	...	...	...	2,100	...
			MOLYBDENUM STEELS														
1% Mo	.22	.50	.13	..	..	..	1.06	..	..	Annealed	.01%	25,000	11,000	5,400	...	...	...
											.10%	35,000	27,000	11,500	...	...	...
1% Mo Calorized	.14	.44	.24	..	..	..	.98	..	..	Annealed	.01%	...	...	...	3,500	720	640*
											.10%	...	...	...	5,300	3,000	1,330*
			S.A.E. STEELS														
SAE 4140	.41	.65	.27	1.04	..	..	.21	..	..	Annealed	.01%	...	8,900	3,500	...	...	...
											.10%	...	21,500	8,500	...	...	...
SAE 3140	.40	.59	.20	.66	1.30	..	..	..	..	Annealed	.01%	...	10,500	4,500	1,600	550	...
											.10%	...	...	6,000	2,200	750	...
SAE 2335	.34	.57	.19	..	3.46	..	..	..	..	Annealed	.01%	...	...	3,500	1,200	...	...
											.10%	...	...	5,000	1,700	...	...
Cr-V	.40	.62	.25	.79	..	..	..	.57	..	Annealed	.01%	...	...	5,000	1,700	700	...
											.10%	...	...	6,000	2,300	1,100	...
Nitralloy G	.36	.46	.20	1.38	..	..	.18	..	1.19	Annealed	.01%	15,000	5,170	...	1,910	220	...
											.10%	26,000	17,000	...	3,000	1,900	...
Nitralloy G	.36	.46	.20	1.38	..	..	.18	..	1.19	Nitrided	.01%	...	...	...	3,700	490	...
											.10%	...	...	...	...	...	...

(Continued on page 164)

TABLE 2 (continued)

GRADE	ANALYSIS C	Mn	Si	Cr	Ni	W	Mo	V	Al	CONDITION	RATE OF CREEP PER CENT PER 1000 HOURS	TEMPERATURE DEGREES F. 800	900	1000	1100	1200	1350
				5% CHROMIUM STEELS													
5% Cr	.21	.44	.08	5.60	..	..	..	..	..	Annealed	.01%	10,200	5,100	3,300	1,320	450	...
											.10%	23,000	12,000	7,500	2,000	800	...
5% Cr-W	.11	.33	.20	5.81	..	.92	..	..	..	Annealed	.01%	...	6,800	5,000	1,600	740	...
											.10%	...	10,000	7,000	4,000	...	...
5% Cr Al	.13	.42	1.01	4.84	..	..	.52	..	.58	Annealed	.01%	...	...	5,130	2,440	890	...
											.10%	...	...	8,350	4,430	1,640	...
5 Cr 1% Mo	.11	.32	.73	5.17	..	..	.98	..	..	Annealed	.01%	...	...	6,000	3,200	1,800	...
											.10%	...	...	10,000	5,400	3,500	...
5 Cr 1½% Mo	.08	.25	.87	5.24	..	..	1.60	..	..	Annealed	.01%	...	...	6,100	3,300	1,500	...
											.10%	...	...	11,000	6,800	2,800	...
				STAINLESS STEELS													
Croloy 12	.11	.45	.30	13.22	..	..	..	..	..	Normalized and Tempered	.01%	...	...	10,000	4,000	1,600	900
											.10%	...	...	13,000	5,200	2,100	1,400
Croloy 12 W	.07	.42	.25	11.75	..	1.83	..	..	..	Annealed	.01%	23,000	...	7,200	4,200	...	...
											.10%	33,000	...	10,000	6,000	...	...
Croloy 12-3W	.09	.32	.34	13.05	..	2.76	..	..	..	Annealed	.01%	...	...	...	...	3,000	...
											.10%	...	...	...	...	5,200	...
Croloy 18	.10	.31	.86	17.30	..	..	..	..	..	Annealed	.01%	...	12,000	7,000	4,500	1,600	900
											.10%	...	16,000	8,500	5,200	2,100	1,200
Croloy 27	.20	.80	.36	26.94	..	..	..	..	..	Annealed	.01%	...	...	...	...	1,000	180
											.10%	...	...	...	...	1,600	400
18-14	.12	.46	1.06	17.99	14.80	..	..	..	..	Annealed	.01%	22,800	18,300	13,500	...	2,800	...
											.10%	36,000	30,000	22,000	...	4,000	...
18-8 W	.12	.42	.43	18.33	8.38	1.14	..	..	..	Annealed	.01%	...	12,300	9,800	5,000	3,150	...
											.10%	...	23,000	18,000	8,000	5,000	...
Cyclops No. 17	.14	.53	1.09	6.37	19.01	..	..	..	..	As Rolled	.01%	...	...	20,000	9,500	5,500	2,800
											.10%	...	...	25,000	11,000	6,100	3,200

* Tested at 1300 F

TABLE 3 SUPPLEMENTARY CREEP DATA ON PLATE, CASTINGS, AND WELDED METAL

(Stress values in psi)

Serial Number	Material	Condition	Chemical Composition, Percent C	Mn	Si	Cr	Ni	Mo	Others	Rate of Creep % Per 1000 Hrs.	Temperature F 800	900	1000	1100	1200	1350	BHN Rm. Temp.
Plate																	
118	Open Steel	Boiler Plate, As Rolled	0.20	0.36	-	-	-	-	-	0.01	8,600	7,800	3,200	925	440	-	116
										0.10	13,000	10,500	3,900	1,500	700	-	
119	Open Steel	Navy Plate, As Rolled	0.42	0.53	-	-	-	-	-	0.01	9,600	8,800	3,500	740	130	-	151
										0.10	15,000	11,500	4,200	1,200	400	-	
147	.20C Boiler Plate	Calorized	0.20	0.36	-	-	-	-	-	0.01	-	-	-	620	100	-	116
										0.10	-	-	-	1,000	450	-	
160	Izette Plate	Annealed	0.18	0.50	0.03	-	-	-	(Al deoxide)	0.01	5,600	2,700	800	-	-	-	104
										0.10	9,000	4,500	1,600	-	-	-	
161	Izette Plate	As Received	0.18	0.50	0.03	-	-	-	" "	0.01	11,000	-	-	-	-	-	127
										0.10	14,000	-	-	-	-	-	
176	High Tensile Boiler Plate	Stress Relieved	0.32	0.77	0.17	-	-	-	-	0.01	5,000	3,400	1,700*	-	-	-	121
										0.10	16,000	6,000	3,800*	-	-	-	
239	C-Mo Plate Longitudinal	Stress Relieved at 1200 F	0.17	0.60	0.22	-	-	0.45		0.01	-	22,500	21,000*	-	-	-	-
										0.10	-	42,500	-	-	-	-	
240	C-Mo Plate Transverse	Stress Relieved at 1200 F	0.17	0.60	0.22	-	-	0.45		0.01	-	-	17,000*	-	-	-	-
										0.10	-	-	38,000*	-	-	-	
Castings																	
125	25Cr-20Ni,Si	As Cast	0.59	0.32	2.22	27.52	22.50	-	-	0.01	35,500**	-	16,250	-	-	2,300	174
										0.10	55,000**	-	25,500	-	-	3,700	
135	.23C Casting	As Cast	0.23	0.72	0.35	-	0.02	-	-	0.01	-	5,400	-	-	-	-	127
										0.10	-	8,000	-	-	-	-	
136	.23C Casting	Annealed	0.23	0.72	0.35	-	0.02	-	-	0.01	-	6,300	-	-	-	-	148
										0.10	-	10,000	-	-	-	-	
137	Ni-Cr-Mo Casting	As Cast	0.31	0.77	0.38	0.60	1.37	0.17	-	0.01	-	5,800	-	-	-	-	240
										0.10	-	9,000	-	-	-	-	
138	Ni-Cr-Mo Casting	Annealed	0.31	0.77	0.38	0.60	1.37	0.17	-	0.01	-	6,400	-	-	-	-	193
										0.10	-	10,000	-	-	-	-	
140	18Cr-8Ni	As Cast (sand)	0.10	0.31	0.70	17.84	8.83	-	-	0.01	-	-	-	4,300	1,900	-	150
										0.10	-	-	-	7,000	3,000	-	
141	18Cr-8Ni	Cent'r Cast	0.10	0.31	0.70	17.84	8.83	-	-	0.01	-	-	-	4,600	1,850	-	136
										0.10	-	-	-	7,000	3,000	-	
167	K6	Annealed —	0.28	0.66	0.35	-	-	-	-	0.01	18,000***	-	2,450	-	-	-	-
										0.10	25,000***	-	3,500	-	-	-	
168	K6	Normalized	0.28	0.66	0.35	-	-	-	-	0.01	18,000***	-	2,300	-	-	-	-
										0.10	25,000***	-	3,500	-	-	-	
179	25Cr-12Ni	2100F-W.Q.	0.184	0.50	0.99	24.01	11.72	-	-	0.01	-	-	-	13,000	6,500	3,000	142
										0.10	-	-	-	-	13,500	6,400	
180	SAE 4140 + O.S.M.	Annealed	0.35	1.01	0.76	1.13	0.16	0.58	-	0.01	-	24,500	2,300	-	-	-	209
										0.10	-	32,000	5,500	-	-	-	
181	25Cr-20Ni	2100F-W.Q.	0.115	0.61	0.94	25.17	19.67	-	-	0.01	-	-	-	-	2,350	1,500-2,000	140
										0.10	-	-	-	-	5,000	-	-

(Continued on page 166)

TABLE 3 (*continued*)

Serial Number	Material	Condition	C	Mn	Si	Cr	Ni	Mo	Others	Rate of Creep % Per 1000 Hrs.	800	900	1000	1100	1200	1350	BHN Rm. Temp.
			Chemical Composition, Percent								Temperature F						
Castings (Cont'd.)																	
183	18-8Mo	Quenched	0.07	0.47	0.49	16.83	8.69	3.25	-	0.01	-	-	10,000	-	6,400	2,700	269
										0.10	-	-	-		11,500	3,600	
184	4-6%Cr + 1% Mo	Annealed	0.18	0.47	0.36	5.00	-	1.05	-	0.01	36,000	14,000	3,800	1,900	-	-	163
										0.10	45,500	22,500	7,500	4,300	-	-	
188	4-6%Cr + .50% Mo	Annealed	0.15	0.46	0.17	4.85	-	0.51	-	0.01	16,300	10,500	6,700	3,400	-	-	146
										0.10	24,800	15,000	10,500	5,700	-	-	
192	C-Mo Steel	Annealed	0.22	0.50	0.13	-	-	1.06		0.01	21,000	13,000	-	-	-	-	146
										0.10	27,500	19,500	9,000-11,000	-	-	-	
195	SAE 3135	Annealed	0.35	0.50	0.24	0.70	1.67	-	-	0.01	6,600	3,400	1,150	-	-	-	179
										0.10	13,000	7,200	2,850	-	-	-	
198	SAE 3135 + .50% Mo	Annealed	0.27	0.58	0.24	0.84	1.94	0.55	-	0.01	13,500	4,600	2,300	-	-	-	187
										0.10	22,000	12,500	6,000	-	-	-	
Weld Metal																	
162	L.C. Weld Metal + N_2	Stress Relieved	0.087	0.40	0.14	-	-	-	0.029 N_2	0.01	-	6,300	-	-	-	-	150
										0.10	-	11,000	-	-	-	-	
175	L.C. Weld Metal + N_2	Fully Protected and Stress Relieved	0.089	0.55	0.24	-	-	-	0.019 N_2	0.01	9,800	3,600	1,300	-	-	-	118
										0.10	16,200	6,500	3,000	-	-	-	
196	L.C. Weld Metal + N_2	Fully Protected and Stress Relieved at 1200 F	0.08	0.40	0.15	-	-	-	0.017 N_2	0.01	-	4,800*	-	-	-	-	131
										0.10	-	10,300*	-	-	-	-	
197	L.C. Weld Metal + N_2	Fully Protected, 1700 F Stress Relieved at 1200 F	0.08	0.40	0.15	-	-	-	0.017 N_2	0.01	-	7,300*	-	-	-	-	112
										0.10	-	11,800*	-	-	-	-	
228	High Tensile Weld Metal	Stress Relieved at 1150 F	0.13	0.64	0.17	-	-	0.17	0.016 N_2	0.01	-	8,000*	-	-	-	-	-
										0.10	-	-	-	-	-	-	-
242	C-Mo Weld Metal	Stress Relieved at 1200 F	0.08	0.44	0.16	-	-	0.60	0.021 N_2	0.01		18,000	11,000*	-	-	-	-
										0.10		-	22,000*	-	-	-	-
244	C-Mo Weld Metal	Stress Relieved at 1200F	0.07	0.38	0.11	-	-	0.64		0.01		16,500	10,400*	-	-	-	-
										0.10		-	-	-	-	-	-
245	C-Mo Weld Metal	Stress Relieved at 1200 F	0.09	0.40	0.15	-	-	0.45		0.01		-	10,200*	-	-	-	-
										0.10		-	19,000*	-	-	-	-

* 950 F.
** 650 F.
*** 750 F.

TABLE 4 CHEMICAL COMPOSITION, GRAIN SIZE, AND ROOM-TEMPERATURE HARDNESS OF SEVERAL AUSTENITIC STAINLESS STEELS NOW BEING SUBJECTED TO CREEP AND STRESS RUPTURE

Alloy	AISI Type	B&W Creep Material No.	Heat** Treatment	Chemical Composition C	Mn	Si	Cr	Ni	Mo	Cb	Ti	ASTM Grain Size	V.H.N. 5Kg Load
Croloy 18-8Cb	347	283	A-1	.07	1.75	.46	17.30	12.42	.10	.71	-	2-6 (D***)	137
Croloy 25-20*	310	284	A-2	.084	2.00	.31	24.80	20.95	-	-	-	4-6	161
Croloy 18-8Cb	347	300	B	.058	1.68	.24	17.29	12.44	.13	.75	-	6-7 (5)	144
			S									6-7 (5)	149
Croloy 18-8 Ti	321	301	A	.06	1.77	.50	17.88	12.28	.08	-	.42	3-7 (D)	130
			B									3-7 (D)	140
			S									3-6 (D)	137
Croloy 16-13-3	316	302	B	.063	1.73	.43	16.88	13.44	2.38	-	-	4-5	145
			S									3-5	156
Croloy 16-13-3Cb	None	303	A	.07	1.62	.51	17.17	14.96	2.07	.72	-	7-8 (6)	168
			B									7-8 (6)	165
			S									7-8 (5)	167
Croloy 18-8 S	304	304	A	.076	1.81	.39	18.54	10.04	.18	-	-	3-4	151
			B									3-4 (5)	161
			S									3-4	170
Croloy 18-8Si	302-B	305	B	.070	1.68	2.11	18.12	12.78	.09	-	-	1-7 (D)	159
			S									1-7 (D)	185

* This alloy was melted by the Allegheny Ludlum Steel Corporation, while all the others are of B&W Tube Company manufacture.
** Heat-treatment is described in Table 5.
*** Duplex.

TABLE 5 STRESS-RUPTURE STRENGTH OF SEVERAL AUSTENITIC STAINLESS STEELS AT VARIOUS TEMPERATURES

(Tentative values)

Alloy	B&W Creep Material No.	Heat Treatment	Test Temp., F.	Stress, psi, to Cause Rupture in 1,000 hrs.	10,000 hrs.	100,000 hrs.	Duration of Longest Test, hrs.
Croloy 18-8S	304	A	1050	33,500	23,600	16,000	4,564
18-8S	304	B	1050	34,500	24,800	17,800	4,201
18-8S	304	B	1200	20,000	15,400	11,800	9,752
18-8S	304	S	1200	21,500	14,700	10,000	7,474
Croloy 18-8Cb*	283	A-1	1000	48,500	36,200	27,000	4,504
18-8Cb	300	B	1050	45,500	30,000	19,300	4,553
18-8Cb	300	S	1050	45,500	30,000	18,500	4,798
18-8Cb	300	B	1200	24,500	16,000	10,500	6,200
18-8Cb	300	S	1200	24,000	13,000	6,900	8,589
18-8Cb*	283	A-1	1350	12,500	6,700	3,600	15,150**
Croloy 18-8Ti	301	A	1050	42,000	32,500	25,500	2,707
18-8Ti	301	B	1050	40,700	27,500	17,500	3,896
18-8Ti	301	S	1050	39,500	30,500	23,300	4,469
Croloy 18-8Si	305	B	1350	9,700	6,070	3,900	5,266
18-8Si	305	S	1350	10,500	5,700	2,400	4,752
Croloy 16-13-3	302	B	1200	27,500	23,000	19,000	3,500
16-13-3	302	S	1200	28,000	22,000	17,300	3,007
16-13-3	302	B	1350	11,500	7,400	4,600	2,865
16-13-3	302	S	1350	12,300	6,950	3,700	3,137
Croloy 16-13-3Cb	303	A	1350	11,750	6,420	3,450	5,811
16-13-3Cb	303	B	1350	12,000	7,900	5,200	3,417
16-13-3Cb	303	S	1350	11,500	6,850	4,200	1,257
16-13-3Cb	303	A	1500	4,850	2,600	1,400	5,168
16-13-3Cb	303	B	1500	4,650	2,450	1,100	6,229
16-13-3Cb	303	S	1500	5,000	2,500	1,240	5,975
Croloy 25-20*	284	A-2	1350	9,600	4,300	2,200-3,100	16,700**
25-20*	284	A-2	1500	4,800	2,800	1,600	6,310
25-20*	284	A-2	1650	2,700	1,000	240	10,083
25-20*	284	A-2	1800	1,450	500	175	10,080

Heat Treatment A - 2000 F for 1/2 hr. W.Q.
A-1 - 1900 F for 2 hrs., transferred to 2000 F for 1/2 hr., W.Q.
A-2 - 1950 F for 1 hr., W.Q.
B - 2000 F for 1/2 hr., W.Q.; then 1750 F for 1 hr., A.C.
S - 2000 F for 1/2 hr., W.Q.; then 1600 F for 5 hrs., F.C.

* These tests were conducted by Allegheny Ludlum Steel Corporation in a co-operative program with B&W
** These tests have not yet ruptured.
NOTE: All tests were held 24 hr at test temperature before loading.

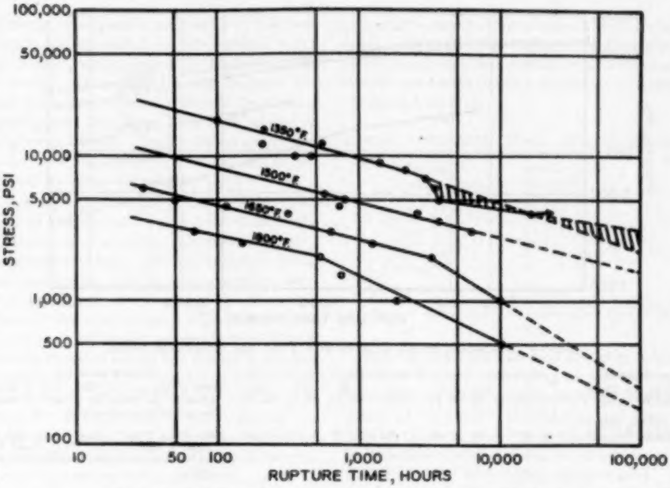

FIG. 5 STRESS-RUPTURE CURVES FOR TYPE 310 STAINLESS STEEL

Legend	C	Mn	Si	Cr	Ni	Heat-treatment
Heat No. 14156 (Allegheny Ludlum)	0.084	2.00	0.31	24.80	20.95	1950 F for 1 hr, WQ
→ Test still in progress						Held 24 hr at test temperature before loading
Dashed lines indicate extrapolation						

steels are still in progress. Creep tests are in progress also on some of these same steels and all are to be so tested in order to complement the stress-rupture data.

The test materials for which the stress values are given in these tables, were secured, in many cases, from commercial heats of material made with manufacturing practices which would or do conform with current steel-manufacturing methods. Details regarding manufacturing history, deoxidation practice, and heat-treatment have been omitted from this compilation but are available in the company's records for many of these test materials. Some of the compositions tested were of experimental nature and did not reach commercial development and utilization.

Fig. 5 is a family of stress-rupture curves for Type 310 stainless steel (25 Cr, 20 Ni) through the usual use range of 1350 to 1800 F. These data are taken from a co-operative test program now in progress on this steel between the Allegheny Ludlum Steel Corporation and The Babcock & Wilcox Tube Company. Creep tests on this particular steel are being performed at the same temperatures as for the rupture tests. The hatched area shown on the rupture curve may reflect the influence of sigma-phase precipitation at 1350 F since there was a significant change in slope after a time sufficient for sigma phase to form in the annealed metal. Rupture curves on Type 347 stainless steel, which has been used in superheaters of a number of the newer boiler installations for 1050 F total steam temperature, are given in Fig. 6. Log-log creep curves for temperatures of 1000 F and 1200 F, based on tests exceeding 10,000 hr duration, are given in Fig. 7. Some rupture-test results on austenitic stainless weld-deposited metals have been reported recently by Carpenter (22).

There are indications that the type of atmosphere surrounding the specimen during testing has some influence on the high-temperature properties of metals. This is perhaps of more significance in rupture testing than in creep testing. Some rupture tests have been made in steam atmospheres at 1200 F by Agnew (30) with rupture-strength results as great or greater than those obtained in air. Attention is now being turned to the effect of combustion-gas atmospheres and some rupture tests of that nature are in progress at Purdue University. The possible effects of various atmospheres are indicated in a recent paper by Shepard and Schalliol (31).

Aside from the early creep tests done under nitrogen atmospheres, all of our creep and rupture testing on solid specimens has been done in air atmospheres.

SUPERHEATER MATERIALS

Historical. Stainless-steel superheater tubing was first used in boiler equipment manufactured by the authors' company in 1926. The alloy tubing available at that time was a ferritic 17 per cent chromium-iron alloy which developed brittleness after cooling from the service temperature of 900–925 F. Its use was discontinued and 18-8 austenitic steel substituted. The 18-8 alloy was then used in a limited number of boiler installations and proved reasonably satisfactory although some difficulty was encountered with leaky tube seats because of differential expansion since the headers used were not stainless steel. Beginning in 1933, the company started using 5 per cent chromium, 0.5 per cent molybdenum steel in marine boilers in both headers and tubes. This steel was used to some extent in stationary boilers. Carbon-molybdenum steel began to receive attention at about that time because of its superior creep strength over carbon steel and the company began using it for moderate-temperature zones in superheaters about 1935.

During this period the company's metallurgical laboratories were active and created in the following sequence a number of high-temperature steels which currently are being used in boiler application. These were 2 per cent chromium, 0.5 per cent molybdenum steel, SA-213 Grade T-14; 9 per cent chromium, 1.5 per cent molybdenum steel[4] which was the forerunner of the present SA-213 Grade T-9. Two other steels were developed also, which since have been widely used in high-temperature

[4] U. S. Patent 2,123,144.

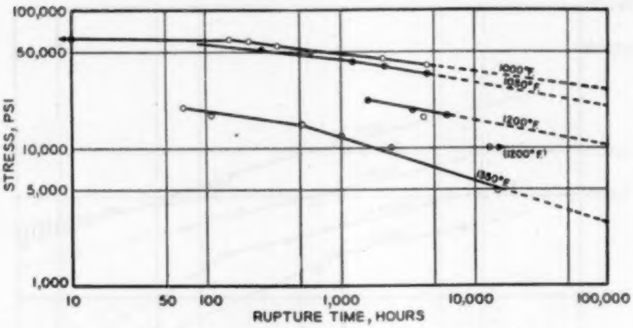

FIG. 6 STRESS-RUPTURE CURVES FOR TYPE 347 STAINLESS STEEL

Legend	C	Mn	Si	Cr	Ni	Cb	Mo	Heat-treatment
	Composition							
● Heat No. 28486 (B&W Tube Co.)	0.058	1.68	0.24	17.29	12.44	0.75	0.13	2000 F for 1/3 hr, WQ, and 1 hr at 1750 F (held for 24 hr at test temperature before loading)
○ Heat No. 25841 (B&W Tube Co.)	0.07	1.75	0.46	17.30	12.42	0.71	0.10	1900 F for 2 hr; then transferred to 2000 F for 1/3 hr, WQ (held for 24 hr at test temperature before loading)

→ Test still in progress
← Ruptured in less than 10 hr

Dashed lines indicate extrapolation

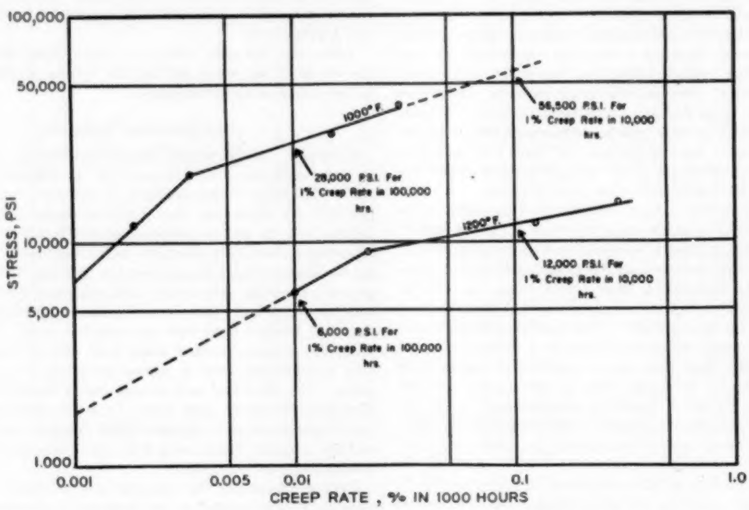

FIG. 7 CREEP CHARACTERISTICS OF CROLOY 18-8 CB AT 1000 AND 2000 F

Legend
Heat No. 14011 (B&W Tube Co.)

C	Mn	Si	Cr	Ni	Cb	Mo
Composition						
0.08	1.47	0.41	17.70	12.86	0.87	0.06

Heat-treatment
1975 F for 1/2 hr, WQ

ASTM grain size
6–7

equipment including steam superheaters, namely, $2^1/_4$ per cent chromium, 1 per cent molybdenum and 3 per cent chromium, 0.9 per cent molybdenum steels,[5] corresponding to SA-213 Grades T-22 and T-21, respectively. All the steels mentioned have had relatively wide use in petroleum-refining processes in tubular heaters and hot-oil piping, and they have been used widely as superheater elements in steam boilers. Today the company prefers steels other than the once popular 5 per cent chromium, 0.5 per cent molybdenum steel for steam-superheater service.

Except at extreme pressures, austenitic stainless-steel tubes are not required for metal temperatures below 1100 F since the lower-chromium-alloy steels offer adequate oxidation resistance both in steam and in combustion gases. Corrosion and oxidation experiences with these materials in high-temperature steam service have been described by Brister and Romer (32). Stainless-steel tubes are required in the most modern high-temperature-high-pressure boilers since a total steam temperature of 1050 F means 1100–1200 F metal temperature on the tubing in the last steam passes in the superheater. Alloys presently used for such service are of stabilized types, either TP-347 or TP-321. At the present time Type 321 is being used to an increasing extent because of the critical situation with respect to columbium supply. Both alloys are adequately stable under long-term heating so that mechanical properties are well maintained.

Temperature Limits. A considerable background of field experience with these steels has indicated that the temperature levels given in Table 6 may be used as a general guide. These limits may be modified depending upon the circumstances in a specific case and are dependent on the design pressure of the unit and on economics in arriving at the material of choice. Many superheaters today may have two or more types of steel used, beginning with carbon steel in the low-temperature zone, followed by carbon-molybdenum and then the chromium alloyed steel and even stainless for the maximum conditions.

TABLE 6 SUPERHEATER-TUBE MATERIALS TEMPERATURE LIMITS

Material[a]	ASME grade	Maximum metal[b] temp, deg F
Carbon steel (0.10% Si min)	SA-83	950
Carbon steel (0.25% Si max)	SA-192	950
Carbon steel (0.35% C max)	SA-210	950
Carbon-molybdenum steel	SA-209-T1a	975
Croloy $^1/_2$	SA-280 chemistry	975
Croloy $1^1/_4$	SA-213-T-11	1000
Croloy 2	SA-213-T-14	1080
Croloy $2^1/_4$	SA-213-T-22	1100
Croloy 3M	SA-213-T-21	1125
Croloy 9M	SA-213-T-9	1200
Croloy 18-8 Cb or Ti	SA-213-TP347-321	1400

[a] For nominal composition, see Table 1.
[b] Metal temperature of side in contact with flue gas.

Graphitization has occurred in random distribution to some extent in carbon-steel superheater tubes exposed between 850 and 950 F. It has been observed infrequently in carbon-molybdenum steel tubes of the diameters commonly used in superheaters. This is in contrast to its occurrence in steam-piping installations where its presence in chainlike form adjacent to welds has caused the power industry much concern. The smaller and more homogeneous metal in the superheater tubes and the fabricating practices employed may account for this difference in metallurgical behavior. In most cases the steelmaking technique for the carbon-molybdenum steel used in superheater tubes has involved deoxidation with 1 to $1^1/_2$ lb of aluminum per ton. This would be undesirable for carbon-molybdenum piping in the light of present experience. Since safety requirements in piping external to the boiler and in large-diameter headers are more stringent than in small superheater tubes, the temperature limits for headers and piping are somewhat more conservative for carbon and the alloy steels. Limits for these items are indicated in Table 7. Carbon-molybdenum steel has lost favor as a steam-piping material and current practice is to use a chromium-containing alloy steel to inhibit graphitization.

[5] U. S. Patent 2,182,177.

TABLE 7 TEMPERATURE LIMITS—HEADERS AND PIPES

Material	ASME grade	Maximum metal temp, deg F
Carbon steel	SA-106-B	800
Carbon steel	SA-266 2[a]	850
Croloy $^1/_2$	SA-280	950
Croloy 1	SA-315	975
Croloy 2	SA-158 P3b	1080
Croloy $2^1/_4$	SA-158 P3b[b]	1100
Croloy 3M	SA-158 P3b[c]	1100
Croloy 9M	SA-158 P-17	1200

[a] Carbon 0.30 per cent maximum.
[b] Except: Chromium 2.0–2.5—Mo 0.90–1.10 per cent.
[c] Except: Chromium 2.75–3.25—Mo 0.80–1.00 per cent.

Stainless steels may be used at higher temperatures than those stated in Table 7, depending on the stresses imposed, and normally will provide oxidation resistance in steam to 1400 F. Oxidation on the gas side is related to fuel supply, and high-sulphur fuels or those depositing vanadium-containing ash may cause depreciation of scaling resistance at temperatures beginning about 1200 F (1150 F with highly alkaline ash). Because of the high pressures involved in the present 1050 F steam units which are 1800 to 2300 psig design pressure, stainless tubes are used in the hot sections of the superheater beginning at the 1100 F temperature level.

Summary and Conclusions

For a number of years the authors' company has been evaluating steels for high-temperature steam-boiler application. The facilities of a newly installed high-temperature creep and rupture testing laboratory have been described briefly. Tests of long duration are considered as furnishing the most reliable data; this is in keeping with the long service expected from steam-boiler equipment.

The high-temperature testing of metals has been largely responsible for the improvements made in steam-generation equipment leading to present reliability and economy. Present practice is to run both creep and rupture tests on important materials and for test periods extending to at least 10,000 hr. This duration of testing is usually sufficient to permit phase changes or alterations in structure to become complete in the metal, thus lessening errors when extrapolating to 100,000 hr. Both creep and rupture testing are considered important, especially for the metals in those portions of the boiler exposed to heat input. The relationship between rupture strength and the time a metal will withstand continuous creep action and remain usable is still ill-defined. Some ability to withstand plastic deformation before rupture is believed to be an important property.

A carefully co-ordinated program of creep and rupture testing of a number of materials is in progress in the new laboratory. There are included in this program carbon, low-alloy, and stainless-steel grades, as well as cast-alloy materials and weld metals. As new data become available, they will be published as sequels to this paper and will be furnished to the Sub-Group on Stress Allowances for Ferrous Materials, Boiler Code Committee, to assist in the selection of safe working stresses for ferrous materials.

The advance of total steam temperature from the present 1050 F level to 1100 F and upward will require superior alloy tubing materials for superheaters which will withstand oxidation and offer long life at metal temperatures of 1200 to 1400 F. Under present Boiler Code regulations, austenitic stainless alloys are limited to low working stresses owing to their low strength under prolonged exposure to these temperatures. This results in in-

ordinately heavy tubing. This, in turn, causes high steam-pressure drop and greater temperature differential across the wall of the tube from the gas to the steam side. Superior alloy materials, with at least equivalent resistance toward oxidation to the presently used austenitic stainless steels, are required. These new alloys must lend themselves to production into tubing and pipe and be amenable to fabricating practices and to the welding techniques used in boiler construction. Needless to say, development work on such materials is in progress, and evaluation will be made largely by creep and rupture testing, following the practices described herein. A forecast is made that further advances in steam-generation economy and efficiency will be made in the next several years.

BIBLIOGRAPHY

1 "Steam—Its Generation and Use," thirty-sixth edition, The Babcock & Wilcox Company, New York, N. Y., 1923.

2 "High-Pressure Boilers With Reheaters," by W. H. Rowand, A. E. Raynor, and F. X. Gilg, Trans. ASME, vol. 71, 1949, p. 719.

3 "Developments in Resuperheating in Steam Power Plants," by E. E. Harris and A. O. White, Trans. ASME, vol. 71, 1949, p. 685.

4 "Reheating in Steam Turbines," by R. L. Reynolds, Trans. ASME, vol. 71, 1949, p. 701.

5 "Sur la Viscosité des Aciers aux Temperature Elevebs," by P. Chevenard, Comptes Rendus, vol. 169, 1919, p. 712.

6 "Some Experiments on the Flow of Steels at Low Red Heat, With a Note on the Scaling of Heated Steels," by J. H. S. Dickenson, *Journal of the Iron and Steel Institute*, vol. 106, 1922, p. 103.

7 "Effect of Temperature, Deformation and Rate of Loading on the Tensile Properties of Low Carbon Steel Below the Thermal Critical Range," by H. J. French, U. S. Bureau of Standards, Technical Paper, No. 219, 1922, p. 679.

8 "Methods of Test in Relation to Flow in Steels at Various Temperatures," by H. J. French, Proceedings of the American Society for Testing Materials, vol. 26, part 2, 1926, p. 7.

9 "The Tensile Properties of Metals at High Temperatures," by T. D. Lynch, N. L. Mochel, and P. G. McVetty, Proceedings of the American Society for Testing Materials, vol. 25, part 2, 1925, p. 5.

10 "Long-Time or Flow Tests of Carbon Steel at Various Temperatures With Special Reference to Stresses Below the Proportional Limit," by J. J. Kanter and L. W. Spring, Proceedings of The American Society for Testing Materials, vol. 28, part 2, 1928, p. 80.

11 "Properties of Boiler Tubing at Elevated Temperatures Determined by Expansion Tests," by A. E. White and C. L. Clark, Trans. ASME, vol. 48, 1926, p. 1075.

12 "Creep of Steel at High Temperatures," by F. H. Norton, McGraw-Hill Book Company, Inc., New York, N. Y., 1929.

13 "Working Stresses for Steel at High Temperatures," by D. S. Jacobus, Trans. ASME, vol. 52, 1930, Paper FSP-52-35, pp. 295–299.

14 "Safety Margins and Stress Levels in High-Temperature Equipment," by E. L. Robinson, Trans. ASME, vol. 73, January, 1951, pp. 89–95.

15 "B&W Installs New Equipment for Creep and Stress-Rupture Studies," *Industrial Heating*, vol. 17, June, 1950, pp. 988–994.

16 "Recommended Practice for Conducting Long-Time High Temperature Tension Tests of Metallic Materials E-22-41," American Society for Testing Materials, Standards, part 1, 1949.

17 "Report on the Strength of Wrought Steels at Elevated Temperatures," by R. F. Miller and J. J. Heger, Special Technical Publication No. 100, American Society for Testing Materials, March, 1950.

18 "Metallic Creep," by A. H. Sully, Interscience Publishers, Inc., New York, N. Y., 1949.

19 "The Creep of Metals and Alloys," by E. G. Stanford, Temple Press, Ltd., London, England, 1949.

20 "Metals at High Temperatures," by F. H. Clark, Reinhold Publishing Corporation, New York, N. Y., 1950.

21 "Properties of Metals at Elevated Temperatures," by G. V. Smith, McGraw-Hill Book Company, Inc., New York, N. Y., 1950.

22 "Some Considerations in the Joining of Dissimilar Metals for High Temperature Service," by O. R. Carpenter, N. C. Jessen, J. L. Oberg, and R. D. Wylie, Proceedings of the ASTM, vol. 50, 1950, pp. 809–857.

23 "Welds Between Dissimilar Alloys in Full-Size Steam Piping," by R. U. Blaser, F. Eberle, and J. T. Tucker, Jr., Proceedings of the ASTM, vol. 50, 1950, pp. 789–808.

24 "Correlation of Short and Long-Time Elevated Temperature Test Methods," Project 25, Appendix 2, Proceedings of the ASTM, vol. 44, 1944, p. 186.

25 "The Rupture Strength of Steels at Elevated Temperatures," by A. E. White, C. L. Clark, and R. L. Wilson, Trans. ASM, vol. 26, 1938, p. 52.

26 "Progress Report on the Study of Effects of Manufacturing Variables on the Creep Resistance of Steels," by H. C. Cross and J. G. Lowther, Appendix 5, Proceedings of the ASTM, vol. 38, Part 1, 1938, p. 149.

27 "Study of the Effects of Variables on the Creep Resistance of Steels," by H. C. Cross and J. G. Lowther, Proceedings of the ASTM, vol. 40, 1940, p. 125.

28 "Effect of Manufacturing Practice on Creep and Creep-Rupture Strength of Low-Carbon Steel," by G. V. Smith and E. J. Dulis, Proceedings of the ASTM, vol. 49, 1929, p. 584.

29 "Effect of Carbide Spheroidization Upon the Creep Strength of Carbon-Molybdenum Steel," by S. H. Weaver, Proceedings of the ASTM, vol. 41, 1941, p. 608.

30 "Stress-Rupture Characteristics of Various Steels in Steam at 1200 F," by J. T. Agnew, G. A. Hawkins, and H. L. Solberg, Trans. ASME, vol. 68, 1946, p. 309.

31 "The Effect of Environment on the Stress-Rupture Properties of Metals at Elevated Temperatures," by O. C. Shepard and W. Schalliol, Reprint No. 58, ASTM, 1950.

32 "Corrosion and Oxidation Experiences in High Pressure and High Temperature Steam Service," by P. M. Brister and J. B. Romer, Trans. of the Electrochemical Society, vol. 91, 1947, p. 655.

Discussion

J. T. Bowen.[6] The authors have presented a valuable summary of current information on creep and stress-rupture phenomena. The Appendix which deals with the current methods of their laboratory is of value to other institutions engaged in such work.

Despite the amount of creep and stress-rupture data available in the literature and the efforts of theoreticians working on related problems of plastic flow, many unanswerable questions still perplex the engineer who must design structures to operate under creep conditions. In a case of great practical interest, thick-walled cylinders for high-temperature service, the pertinent variables of material composition, fabrication methods, ambient atmosphere, and temperature distribution make the calculation of stress distribution and the prediction of deformation uncertain arts at present. Evidently recognizing the situation in the case of high-temperature steam lines, the authors have undertaken "tubular stress-rupture tests" in their laboratory. Personnel of the writer's company have concluded that equivalent tests are required to simulate the operation of tubes and vessels carrying high-temperature hydrocarbon gases.

The classic objection to such simulating tests is that it is difficult to separate the effects of the several variables. It is to be hoped that when such tests are conducted all influential variables will be noted and that the stress and deformation histories will be as complete as possible. The tests will then provide data against which future theoretical work can be checked as well as answers to immediate questions.

F. B. Foley.[7] The authors of this paper have presented a very valuable compilation of the results of their high-temperature testing of a great variety of ferrous materials comprising carbon, low-alloy, medium-alloy, and high-alloy steels, and covering both ferritic and austenitic materials. The data will prove of great usefulness to engineers engaged in designing equipment for high-temperature service for, as the authors point out, the demands of higher temperatures and higher pressures are bringing stronger materials into steam-boiler construction. Attention is also called to the necessity of increasing our knowledge concerning

[6] Research Engineer, Carbide and Carbon Chemicals Company, New York, N. Y. Jun. ASME.

[7] International Nickel Company, Bayonne, N. J.

the effect of the atmospheric conditions surrounding the metal on its resistance to flow and fracture at high temperatures, and it is believed that as time goes on, more and more attention will be given to the effect of the structure of the metal as it is affected by its thermal history, not to mention its deoxidation during melting, on its elevated-temperature strength.

The authors' company was one of the first large industrial concerns to recognize the value of accurate data concerning the behavior of steels under stress at elevated temperatures, and it is gratifying to learn of the expansion of their facilities for this type of investigations. The users of steel will look forward to a continuation of the fine type of work which has come from their efforts over many years in the past.

D. L. Newhouse.[8] The large quantity of high-temperature test data presented in this paper constitutes a very valuable addition to the literature. In particular, the long-time stress-rupture test data (over 10,000 hr in some cases), as well as the current tubular stress-rupture tests described, are of very great interest.

A comparison of the maximum metal temperatures listed for superheater-tube materials in Table 6 with those listed for headers and pipes in Table 7 shows little difference, except that slightly higher temperatures are listed for several of the alloys for superheater applications. What is the basis for requiring the use of more than 1 per cent Cr in Cr Mo steels for use in headers and pipes? Is it the high-temperature creep or rupture strength, graphitization resistance, or oxidation resistance? The data presented in this paper, as well as other published data, suggest that on the basis of high-temperature strength alone, the 1 per-cent and $1^1/_4$ per cent Cr, $^1/_2$ per cent Mo steels would be at least comparable to and perhaps stronger than the higher Cr materials up to some temperature above 1000 F. On the basis of graphitization resistance, 1 per cent Cr should provide adequate insurance, since to the writer's knowledge, no graphitization has been reported for steels containing 1 per cent chromium. Even $^1/_2$ per cent chromium appears to confer a high order of graphitization resistance, with graphitization having been reported in very small quantities only in $^1/_2$ Cr $^1/_2$ Mo castings which had been deoxidized with 2 lb of aluminum per ton (Kanter and Sticha, 1947).

In so far as oxidation is concerned, it would appear that for a given metal temperature and stress, superheater service would be much more severe than piping service, because of the atmosphere of combustion products and slag to which superheater tubes are exposed; and that, therefore, the limiting temperature could be higher for piping than for superheaters, while maintaining adequate factors of safety by proper selection of working stresses. The authors' comments on this subject would be much appreciated.

H. A. Wagner.[9] The authors indicate that simultaneous creep tests are being conducted on tubular and tensile specimens of the same material. It is assumed that the purpose is to secure a correlation between uniaxial tensile creep as determined in the laboratory, and multiaxial stress as obtained in service.

According to a paper by Buxton and Burrows,[10] one might expect the circumferential creep to be one half of the tensile creep at any given stress. This is contrary to the results we obtained at Trenton Channel.[11]

The writer is interested in the results the authors may secure. Whether circumferential creep is one half of the tensile creep, or equal to it is an important consideration in high-temperature pipe and pressure-vessel design.

A. B. Wilder.[12] Instead of conducting creep-rupture tests for 10,000 hr, would it be practical to conduct creep-rupture tests for 1000 hr with material which has been exposed for 10,000 hr without stress in an ordinary furnace? We are conducting experiments of this nature and would appreciate the authors' comments. The advantages to be gained in conducting long-time exposure tests in an ordinary furnace at the creep-testing temperature would be the possibilities of developing a large amount of 1000-hr creep-rupture data with a limited number of machines.

Not subjecting to stress the material exposed for 10,000 hr raises the question whether the stability of steels at elevated temperature is influenced appreciably by stress of the magnitude encountered in creep. We are also conducting 10,000-hr exposure tests under stress based on ASME Boiler Code allowable working stresses, and after exposure expect to determine the 1000-hr creep-rupture strength. This is a slightly different approach from 10,000-hr creep-rupture tests, and we, therefore, would appreciate comments of the authors with respect to this practice. In other words, will the 1000-hr creep-rupture properties under the conditions outlined be similar to creep-rupture results based on 10,000-hr tests?

Also, what, in the opinion of the authors, is the relationship of 1000-hr creep-rupture tests obtained at higher temperatures to 1000-hr creep-rupture tests at lower temperatures, with respect to extrapolation to 100,000 hr? Can we conduct 1000-hr creep-rupture tests at higher temperature and then predict the creep-rupture strength more accurately for 100,000 hr at lower temperatures?

Authors' Closure

The authors appreciate the discussions which this paper has evoked. This is a reflection of the importance of the need of precise knowledge of high-temperature properties of metals in the engineering of equipment to operate at elevated temperatures.

We thank Mr. Foley for his kind remarks and shall hope to make further contributions on the subject through test work in progress or planned in our new Creep Laboratory. We concur that more attention will be given to thermal treatment and deoxidation practice in the future. Perhaps further improvement in properties will come largely from these sources rather than from modifications in composition.

Mr. Bowen referred to the "Tubular Stress Rupture Tests" mentioned briefly in our paper. These tests and the equipment used have now been more adequately described in a separate paper by Messrs. Kooistra, Blaser, and Tucker at the 1951 Annual Meeting of the ASME, titled "High Temperature Stress-Rupture Testing of Tubular Specimens". It is of interest that Mr. Bowen's company is planning similar rupture tests on tubular specimens using a hydrocarbon gas mixture inside tubes rather than steam. Such a test may indicate the effects of carburization on rupture strength which is of importance in oil refining and hydrocarbon process work.

Mr. Newhouse makes comment concerning the slightly higher temperatures used in superheater tubes as compared to pipes

[8] General Electric Company, Steam Turbine Engineering Division, Schenectady, N. Y.

[9] Chief Mechanical Engineer, Mechanical Engineering Division, Engineering Department, The Detroit Edison Company, Detroit, Mich.

[10] "Formula for Pipe Thickness," by W. J. Buxton and W. R. Burrows, Trans ASME, vol. 73, 1951, pp. 575–587.

[11] "High-Temperature Steam Experience at Detroit," by R. M. Van Duzer and A. McCutchan, Trans. ASME, vol. 61, 1939, pp. 383–901.

[12] Chief Metallurgist, National Tube Company, U. S. Steel Subsidiary, Pittsburgh, Pa.

and headers of identical steels. This established practice is due mainly to the need for a greater over-all safety requirement in the larger diameter headers or pipes because of the steam volume contained therein. Failure in an individual superheater tube usually does not cause equipment damage although necessitating a boiler shutdown. Failure in a superheater header or main steam pipe might be disastrous. We agree with Mr. Newhouse that 1 per cent chromium in the steel is adequate for graphitization resistance. The use of higher chromium-content ferritic steels has been predicated on somewhat improved oxidation and slagging resistance and perhaps slightly higher creep strength in annealed steels in the range 1025 to 1100 F. Steels with 1 per cent or $1^1/_4$ in. chromium with molybdenum may be equally adequate, at least to about 1050 F, and are now being used in an effort to conserve alloying elements. Superheater service is more severe than piping service but the larger-diameter piping usually requires inordinately heavy wall thickness which is one reason for fixing limiting temperatures slightly lower than for superheater tubing of the same alloy material.

Mr. Wagner points out the importance of knowing whether circumferential creep is one half of or equal to the tensile creep. In the tubular stress-rupture tests referred to in our paper and now covered by the recent paper just mentioned, the tubular rupture results for carbon steel were nearly indentical with those obtained on solid specimens at test temperatures of 850 and 950 F. More testing is necessary to see if this relationship holds for alloy steels of both ferritic and austenitic type.

Our tubular-creep studies have not progressed to the point that we can adequately answer Mr. Wagner regarding the relationship between circumferential and tensile creep. In this connection we would like to point out that Norton[12] in reporting for the Joint ASME-ASTM Committee, summarized his observations to the effect that the time for the tubular specimens to reach an equilibrium rate of flow was an important factor in determining the relationship.

Dr. Wilder's suggestion to expose material for 10,000 hr without stress in an ordinary furnace and then conduct 1000 hr creep-rupture tests on it is worthy of consideration. Certainly such exposure at the preselected testing temperature should achieve structural equilibrium in the metal in most cases and would permit a much greater volume of rupture testing with a limited number of machines. This method would be in contrast to rupture testing to 10,000 hr or more. Whether correlation would be obtained with these methods would depend on whether or not the scaled surface was removed prior to stressing or left intact. Also, it is believed that stress tends to accelerate intergranular oxidation and at certain temperatures this might make for a wide discrepancy in results as between specimens heated 10,000 hr and then stressed 1000 hr as compared with stressing for the full 10,000 hr.

It is not believed there is any consistent relationship between 1000 hr creep-rupture tests made at the higher temperatures and those at low temperatures. The degree of safety in extrapolation to 100,000 hr from either is concerned with oxidation resistance, structural stability, and with ability to withstand deformation before incipient or total fracture. We prefer the longer-time tests as giving us the most trustworthy data and even then the extrapolation to 100,000 hr is made with some misgiving.

[12] "Creep in Tubular Pressure Vessels," Trans. ASME, F. H. Norton, vol. 61, 1939, p. 239.

On the Automatic Control of Generalized Passive Systems

By KUN LI CHIEN,[1] J. A. HRONES,[2] and J. B. RESWICK,[3] CAMBRIDGE, MASS.

The dynamic behavior of a multiple-capacity passive system is compared to that of a single-capacity system of appropriate "time constant with a finite time delay." Such a comparison indicates that the latter system reproduces the dynamic behavior of the multiple-capacity system with sufficient accuracy for most engineering purposes. This fact makes it possible to characterize such systems by a single parameter, the ratio of the time constant (L) of the single-capacity system to the delay (D). Values of the control constants for various degrees of stability are plotted against this ratio (L/D) for proportional, proportional-plus-integral, proportional-plus-integral-plus-derivative type regulators. An electronic analog computer was used in obtaining the data.

Introduction

The automatic control of machines and industrial processes is commanding wider and wider attention. The problem of arriving at a properly integrated design of the over-all regulated system is a difficult one particularly where the plant is one composed of many energy-storage reservoirs. In a recent paper the authors presented a nondimensional analysis of this problem for a single-capacity system. This paper extends the work to the more complicated and more difficult problem of the regulation of multiple-capacity systems.

Multiple-Capacity Systems

All systems are characterized by the fact that they can store energy to a greater or lesser extent. In some systems the amount of energy stored is known precisely if the value of a single variable is known. Thus, in Fig. 1, the energy stored in the system shown is known if the head H is known.

In Fig. 2 the three quantities H_1, H_2, H_3, are required to specify the energy content of that system. Fig. 1 is a single-capacity system; Fig. 2 is a three-capacity system. Both systems are represented conveniently by the simple block shown in Fig. 3(a); v is the quantity to be regulated; m is the quantity to be manipulated in order to regulate v; m_L is a load, any change of which will introduce a disturbance on the plant.

Quantities m_1, m_2, and m_3 represent possible load inputs, any change of which will produce disturbances on the system. To bracket the disturbance which the system can undergo, changes in m_1 (now to be designated m_L) and changes in desired value of the regulated quantity will be used. For multiple-capacity systems the response of the system to a step change of the input m is shown in Fig. 4. A rough approximation of this behavior can be made by considering it to be a time delay D (also called transportation lag, dead time), followed by the straight line AB, Fig. 5. A considerably better approximation is realized by con-

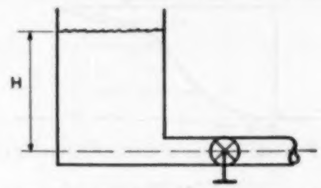

Fig. 1 Typical Single-Capacity System

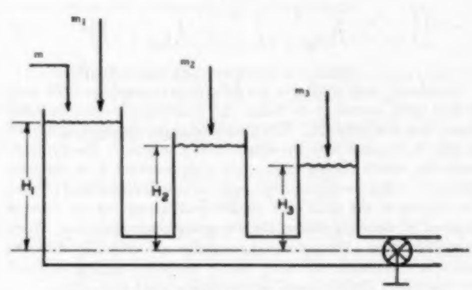

Fig. 2 Typical Three-Capacity System

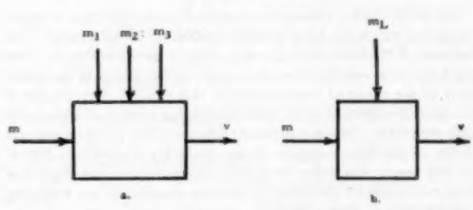

Fig. 3 Block Representation of Plant

Fig. 4 Unregulated Reaction Curve of Plant to a Step Change in Input

[1] Research Assistant, Department of Metallurgy, Massachusetts Institute of Technology.

[2] Professor, Department of Mechanical Engineering, Massachusetts Institute of Technology. Mem. ASME.

[3] Assistant Professor, Department of Mechanical Engineering, Massachusetts Institute of Technology.

Contributed by the Industrial Instruments and Regulators Division and presented at the Semi-Annual Meeting, Toronto, Canada, June 11–15, 1951, of The American Society of Mechanical Engineers.

Note: Statements and opinions advanced in papers are to be understood as individual expressions of their authors and not those of the Society. Manuscript received at ASME Headquarters, April 13, 1951. Paper No. 51—SA-29.

sidering the reaction curve to be composed of a time delay D, followed by a single exponential curve whose initial slope is the maximum slope of the actual multiple-capacity response curve,

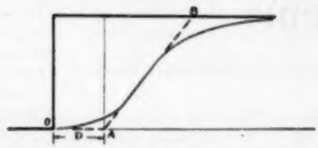

FIG. 5 APPROXIMATION BY DELAY PLUS TANGENT LINE

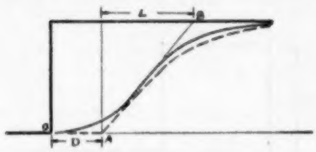

FIG. 6 APPROXIMATION BY DELAY PLUS SINGLE LAG

Fig. 6. The true response of the multiple-capacity plant is given by an equation of the following form

$$v = C\left[\left(\frac{1}{\tau_1 p + 1}\right)\left(\frac{1}{\tau_2 p + 1}\right)\cdots\cdots\left(\frac{1}{\tau_n p + 1}\right)\right]m \ldots\ldots [1]$$

$\tau_1, \tau_2, \ldots\ldots$ and τ_n are the time constants of the plant.

In general, such constants are difficult to evaluate and the analytical work necessary to design the controller is often prohibitively long and difficult. The simplified approximation, indicated in Fig. 6, requires only the single ratio r to specify the dynamic behavior, where r is the ratio of the time constant L, to the time delay D. Oldenbourg and Sartorius have calculated and plotted the values of the gain of a proportional controller for various degrees of stability, using the foregoing approximation. Such calculations for a three-element controller are extremely difficult, unless a computing aid such as an electronic analog is used. In this study, Philbrick analog computing units were used.

Representation of the Plant

The plant used in this study consists of a delay unit and a single lag unit in which the delay is approximated by 80 lag stages. The response of the delay unit to a step input is shown in Fig. 7. The lag-delay ratio r of the delay component is 0.6, which is the lower limit of the range of r considered in this study. The output of the delay component is fed into a single lag system of adjustable time constant. The unregulated response of the plant for various values of the time constant of the single lag is shown in Fig. 8. In this study the delay D is held constant and the lag-delay ratio r is varied by changing L, the time constant of the single lag component.

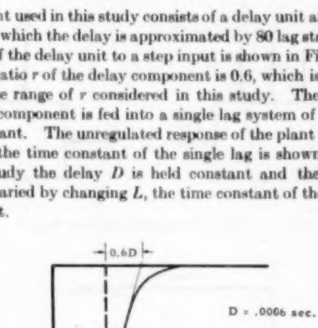

FIG. 7 CHARACTERISTIC REACTION CURVE OF DELAY COMPONENT

Criteria for "Optimum" Performance of Regulated System

No arbitrary standard for measuring optimum performance has been proposed which will meet all situations. Criteria in use are essentially of two types: One based on the transient response of the

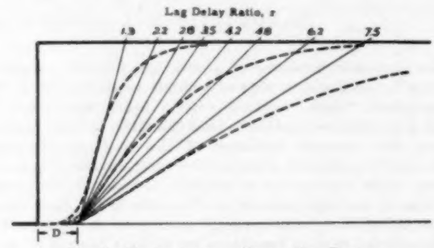

FIG. 8 CALIBRATION OF DELAY-LAG PLANT

system; the other based on the steady-state response of the system to sinusoidal disturbances over a wide frequency range. The fast type of analog employed makes the use of transient-response characteristics straightforward, simple, and rapid. In many applications this is the simplest type of disturbance to apply, as it involves a small essentially sudden change in an input quantity. The criteria selected in this study for evaluating the controller settings are as follows:

Quickest Response Without Overshoot (see Fig. 9). The regulated variable reaches its final value in the shortest possible time without overshooting that value when the system is subjected to a step change in any input quantity.

Quickest Response With 20 Per Cent Overshoot (see Fig. 10). The regulated quantity initially reaches its final value in the shortest possible time followed by an overshoot of 20 per cent of the final value when subjected to a step change in an input quantity. When the final value is zero, the overshoot is 20 per cent of the maximum excursion from zero.

The controller settings which give the foregoing results vary with the type of disturbance to which the system is subjected. (Thus the results presented show different values for a load input applied to the plant, as shown in Fig. 13, than for a change in desired value of the regulated quantity.) Fig. 11 illustrates the

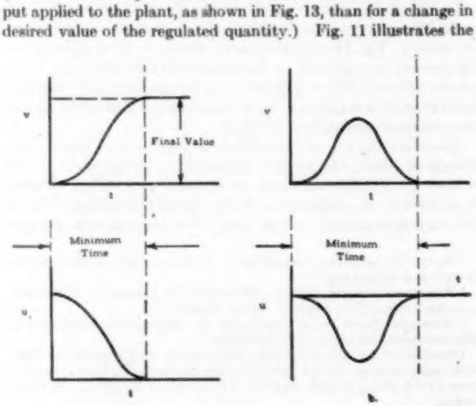

FIG. 9 QUICKEST RESPONSE WITHOUT OVERSHOOT
(a, Step change in desired value v^*. b, Step change in load, m_L.)

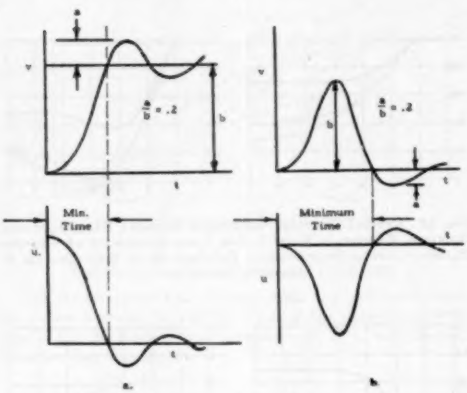

Fig. 10 Quickest Response With 20 Per Cent Overshoot
(a, Step change in desired value v^*. b, Step change in load, m_L.)

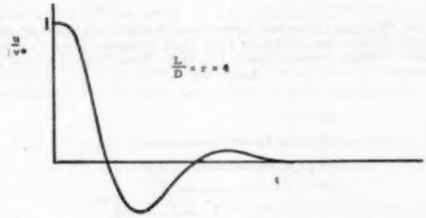

Fig. 11 Deviation Response of a System to a Step Change in Desired Value v^*, When Adjusted to Quickest Response Without Overshoot to a Step Change in Load, m_L

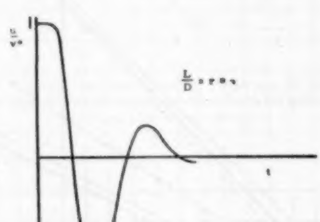

Fig. 12 Deviation Response of a System to a Step Change in Desired Value v^*, When Adjusted to Quickest Response With 20 Per Cent Overshoot to a Step Change in Load, m_L

response obtained when a "desired value change" is applied to a system designed for Quickest Response Without Overshoot under a step-load input. Fig. 12 illustrates the behavior of the system in response to a "desired value disturbance" when the controller is designed to produce Quickest Response With 20 Per Cent Overshoot when subjected to a step-load input.

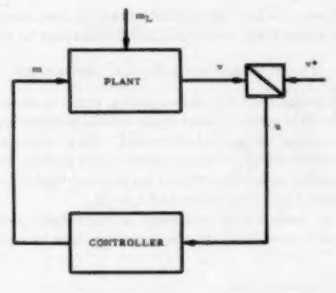

v = Regulated Variable
v^* = Desired Value
u = $v^* - v$ = Error
m = Manipulated Variable
m_L = Load

Fig. 13 Block Diagram of Controlled System

Nondimensional Symbolism

Fig. 13 is a simplified block representation of the over-all system where the symbols are defined as follows:

Nondimensional Variables

$$m = \text{manipulated quantity (controller output)} \left(\frac{\text{change in value} - \Delta m}{\text{initial value} - m_0}\right)$$

$$v = \text{regulated quantity} \left(\frac{\text{change in value} - \Delta v}{\text{initial value} - v_0}\right)$$

$$v^* = \text{desired value} \left(\frac{\text{change in value} - \Delta v^*}{\text{initial value} - v_0^*}\right)$$

$$m_L = \text{load input} \left(\frac{\text{change in value} - \Delta m_L}{\text{initial value} - m_{L0}}\right)$$

$$u = \text{deviation or error } (v^* - v)$$

$$C = \text{plant gain} = \frac{v_s}{m_s} \left(\frac{\text{final value of } v}{\text{final value of } m}\right)_{\text{unregulated Plant}}$$

$$k = \text{controller proportional constant} \left(\frac{m}{u}\right); \text{ when } D/\tau_i = \tau_d/D = 0$$

$$Ck = \text{system gain}$$

$$r = \frac{L}{D} \text{ lag-delay ratio } \left(\frac{\text{time constant of single lag}}{\text{delay time}}\right)$$

$$\frac{D}{\tau_i} = \text{integral time-constant ratio} \left(\frac{\text{delay time}}{\text{integral time constant}}\right) \text{ or (delay time} \times \text{reset rate)}$$

$$\frac{\tau_d}{D} = \text{derivative time-constant ratio} \left(\frac{\text{derivative time constant}}{\text{delay time}}\right)$$

$$\frac{t}{D} = \text{nondimensional time} \left(\frac{\text{time}}{\text{delay time}}\right)$$

The use of nondimensional terms gives a universality to the results. For any specific application where the system parameters are known, the actual controller settings can be obtained from the nondimensional plots. The basis for nondimensionalizing is arbitrary. In this case initial values of the variables are used. In many cases they are the values under normal operat-

ing conditions. Where the initial values are zero another basis such as peak operating conditions, and the like may be used.

Plant With Proportional Controller

A block diagram of the entire analog setup is shown in Fig. 14. In the first series of runs τ_d/D and D/τ_i were set to zero, thus introducing proportional control. Step changes in load m_L, and desired value v,* were applied to the system, and values of the controller gain k determined for various degrees of stability over a range of lag-delay ratios r of 1 to 10.

Values of proportional constant k have been determined, which in each case result in the following type of dynamic response:

1 Unending oscillation.
2 Quickest response with twenty per cent overshoot.
3 Quickest response without overshoot.

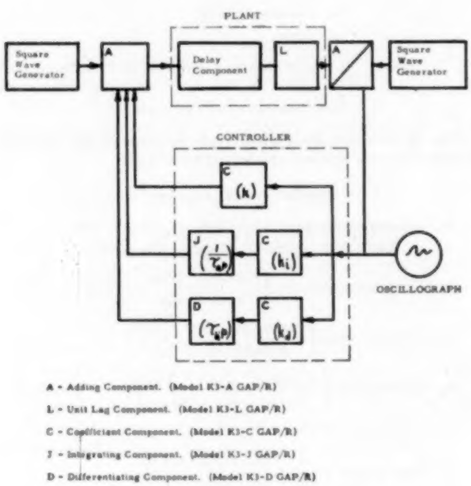

Fig. 14 Block Diagram of Analog Setup

Some transient responses for various values of r for cases 2 and 3 are shown in Figs. 15 and 16 for load and desired-value disturbances. The results are summarized in Fig. 17 where proportional constant times plant gain kC, is plotted against lag-delay ratio for the three degrees of stability listed. The suggested "optimum" values of k of Ziegler and Nichols are also plotted. Their values correspond to an overshoot of approximately 40 per cent. The calculated results of Oldenbourg and Sartorius are also plotted and check closely the results of the analog.

Check System

To check the validity of the simulation of an n-capacity system with a time delay and a single-capacity system, a 7-lag system was studied. The various time constants of this electronic system were varied giving the reaction curves shown in Fig. 18. The system was then placed under proportional control, and the results are shown in Fig. 17. It will be noted that the delay component — single lag analog approximation gives results closer to the actual 7-lag system than the mathematical analysis. This is due to the fact that the delay component does not give the sharp time delay that is obtained mathematically.

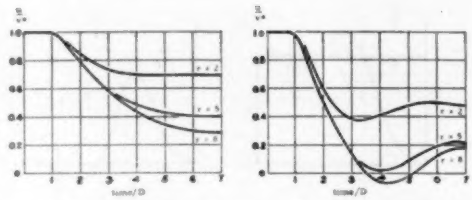

Fig. 15 Typical Quickest Responses Without Overshoot and Quickest Responses With 20 Per Cent Overshoot of Various Plants r Under Proportional Control With Step Change in Desired Value, v*

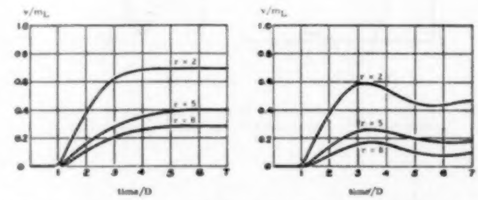

Fig. 16 Typical Quickest Responses Without Overshoot and Quickest Responses With 20 Per Cent Overshoot of Various Plants r Under Proportional Control With Step Change in Load, m_L

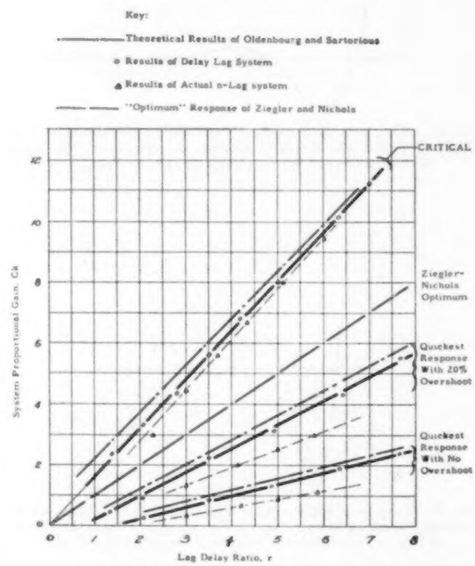

Fig. 17 Relation of Proportional Constant Times Plant Gain (Ck) Versus r for Different Systems Under Proportional Control

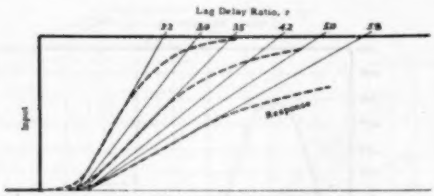

FIG. 18 CALIBRATION OF 7-LAG SYSTEM

PROPORTIONAL-PLUS-INTEGRAL CONTROLLER

With the derivative time constant ratio τ_d/D still set at zero, the system response for various values of the proportional constant k and the integral time-constant ratio D/τ_i were studied. The controller equation is

$$m = \left(k + \frac{1}{\tau_i p}\right) u \ldots\ldots\ldots\ldots\ldots\ldots [2]$$

In Fig. 19 values of Ck are plotted against the delay ratio r for values of the ratio CD/τ_i from 0 to 3 for the case of unending oscillation. Values of Ck and r which determine a point in the region to the left and below the lines of constant CD/τ_i result in unstable operation. Values of Ck and r which establish a point on the other side of the lines of constant CD/τ_i result in stable operation. In Figs. 20(a) and 21(a), the transient behavior of the system with controller constants set to give "quickest response

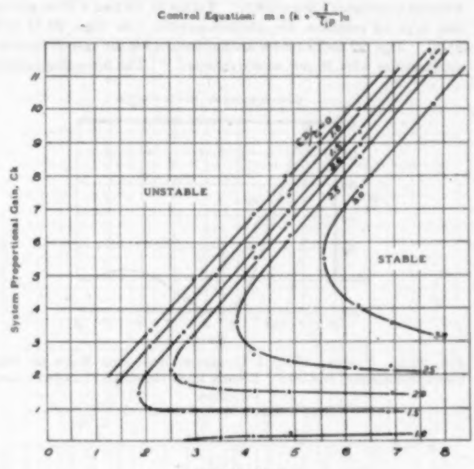

FIG. 19 Ck VERSUS r FOR CRITICAL RESPONSE WITH PROPORTIONAL-PLUS-INTEGRAL CONTROL

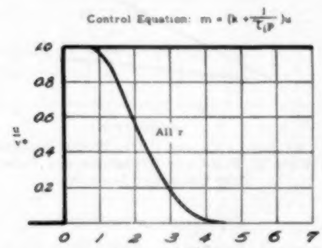

FIG. 20(a) TYPICAL UNIQUE QUICKEST RESPONSE WITHOUT OVERSHOOT FOR ALL r UNDER PROPORTIONAL-PLUS-INTEGRAL CONTROL
(Step change in desired value, v^*.)

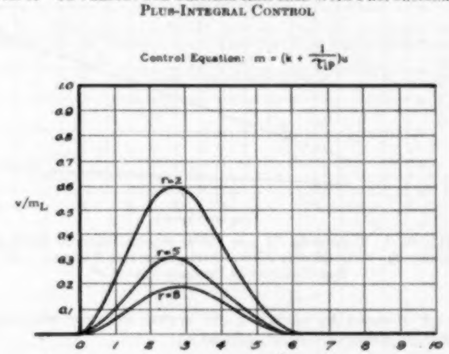

FIG. 21(a) TYPICAL QUICKEST RESPONSES WITHOUT OVERSHOOT FOR SYSTEMS UNDER PROPORTIONAL CONTROL
(Step change in load, m_L.)

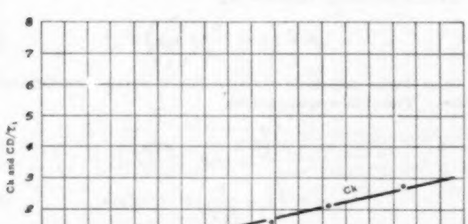

FIG. 20(b) VALUES OF Ck AND CD/τ_i WHICH PRODUCE QUICKEST RESPONSE WITHOUT OVERSHOOT FOR VARIOUS r WITH STEP CHANGE IN DESIRED VALUES, v^*

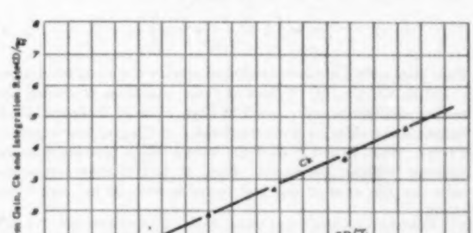

FIG. 21(b) VALUES OF Ck AND CD/τ_i WHICH PRODUCE QUICKEST RESPONSE WITHOUT OVERSHOOT FOR VARIOUS r WITH STEP CHANGE IN LOAD, m_L

without overshoot" are shown. Values of Ck and CD/τ_i giving this type of response are plotted against r in Figs. 20(b) and 21(b). Figs. 22 and 23 show similar results for the case of "quickest response with 20 per cent overshoot." The foregoing results

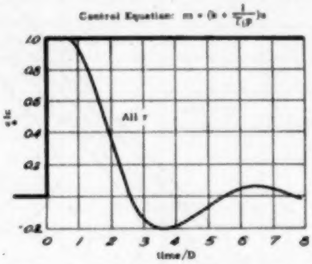

Fig. 22(a) Typical Unique Quickest Response With 20 Per Cent Overshoot for All r Under Proportional-Plus-Integral Control
(Step change in desired value, v^*.)

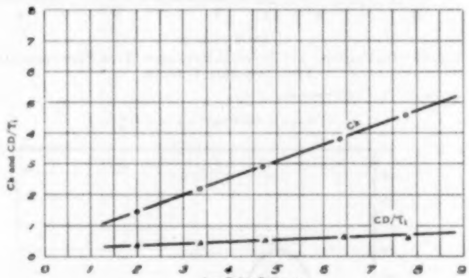

Fig. 22(b) Values of Ck and CD/τ_i Which Produce Quickest Response With 20 Per Cent Overshoot for Various r With Step Change in Desired Value, v^*

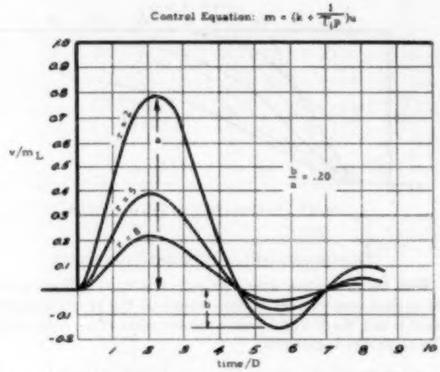

Fig. 23(a) Typical Quickest Responses With 20 Per Cent Overshoot for Systems Under Proportional Control
(Step change in load, m_L.)

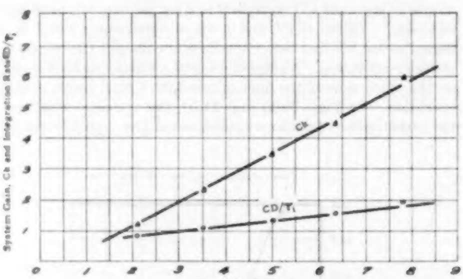

Fig. 23(b) Values of Ck and CD/τ_i Which Produce Quickest Response With 20 Per Cent Overshoot for Various r With Step Change in Load, m_L

were obtained by observing the system behavior after step changes in desired value v^* and load m_L.

Proportional-Plus-Integral-Plus-Derivative Controller

When a derivative component is introduced into the controller the controller equation is

$$m = \left(k + \frac{1}{\tau_i p} + \tau_d p\right) u \qquad [3]$$

Four parameters are now needed to specify the complete system r, CD/τ_i, Ck, $C\tau_d/D$. Values of these quantities producing unending oscillations are plotted in Figs. 24 to 27, inclusive. Each figure gives results for a constant value of integral time constant CD/τ_i. Figs. 28 and 29 show the values which produce quickest response without overshoot. Figs. 30 and 31 show similar results for the case of quickest response with 20 per cent overshoot.

Discussion of Results

In the ranges of r investigated, plots of the controller constants versus the ratio r were straight lines. Therefore the results may be summarized by the simple relationships listed in Table 1.

For simplicity of the analog setup, the control equation was taken in the form of Equation [3]

$$m = \left(k + \frac{1}{\tau_i p} + \tau_d p\right) u \qquad [3]$$

Other forms may more closely represent certain actual controllers. Two of these are as follows

$$m = k'\left(1 + \frac{1}{\tau_i p} + \tau_d' p\right) u \qquad [4]$$

$$m = k''\left(1 + \frac{1}{\tau_i'' p}\right)(1 + \tau_d'' p)u \qquad [5]$$

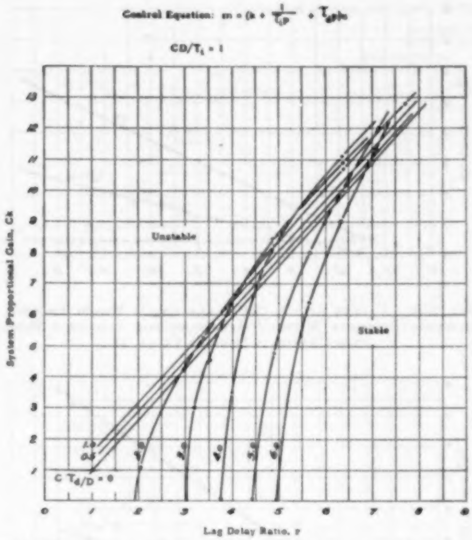

FIG. 24 RELATION OF Ck, $C\tau_d/D$, AND r FOR CRITICAL RESPONSE FOR SYSTEM UNDER PROPORTIONAL-PLUS-INTEGRAL-PLUS-DERIVATIVE CONTROL

(CD/τ_i held constant in each plot.)

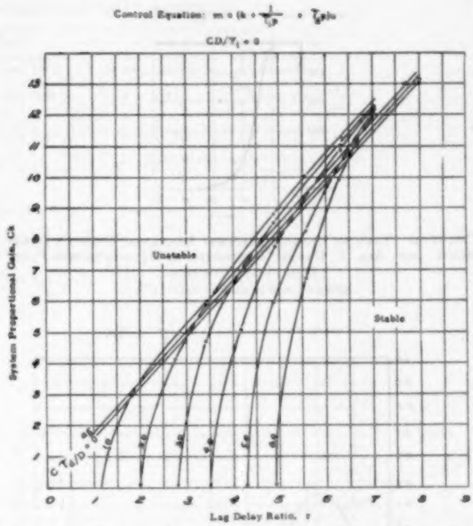

FIG. 25 RELATION OF Ck, $C\tau_d/D$, AND r FOR CRITICAL RESPONSE FOR SYSTEM UNDER PROPORTIONAL-PLUS-INTEGRAL-PLUS-DERIVATIVE CONTROL

(CD/τ_i held constant in each plot.)

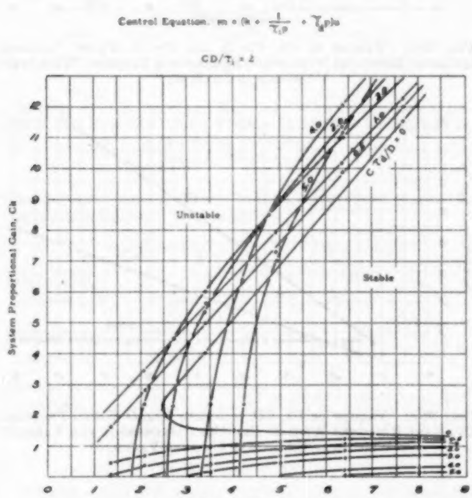

FIG. 26 RELATION OF Ck, $C\tau_d/D$, AND r FOR CRITICAL RESPONSE FOR SYSTEM UNDER PROPORTIONAL-PLUS-INTEGRAL-PLUS-DERIVATIVE CONTROL

(CD/τ_i held constant in each plot.)

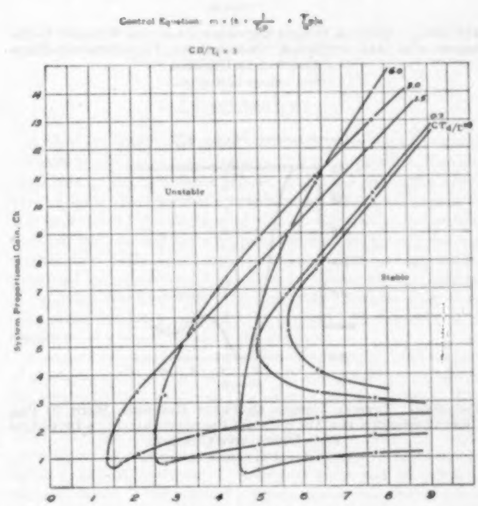

FIG. 27 RELATION OF Ck, $C\tau_d/D$, AND r FOR CRITICAL RESPONSE FOR SYSTEM UNDER PROPORTIONAL-PLUS-INTEGRAL-PLUS-DERIVATIVE CONTROL

(CD/τ_i held constant in each plot.)

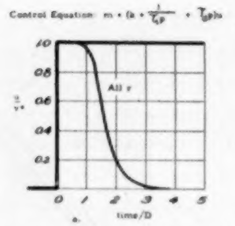

FIG. 28(a) TYPICAL UNIQUE QUICKEST RESPONSE WITHOUT OVERSHOOT FOR ALL r UNDER PROPORTIONAL-PLUS-INTEGRAL-PLUS-DERIVATIVE CONTROL

(Step change in desired value, v^*.)

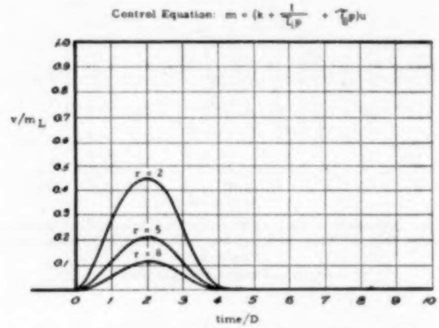

FIG. 29(a) TYPICAL UNIQUE QUICKEST RESPONSE WITHOUT OVERSHOOT FOR ALL r UNDER PROPORTIONAL-PLUS-INTEGRAL-PLUS-DERIVATIVE CONTROL

(Step change in load, m_L.)

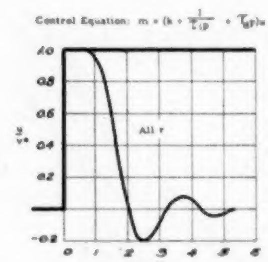

FIG. 30(a) TYPICAL UNIQUE QUICKEST RESPONSE WITH 20 PER CENT OVERSHOOT FOR ALL r UNDER PROPORTIONAL-PLUS-INTEGRAL-PLUS-DERIVATIVE CONTROL

(Step change in desired value, v^*.)

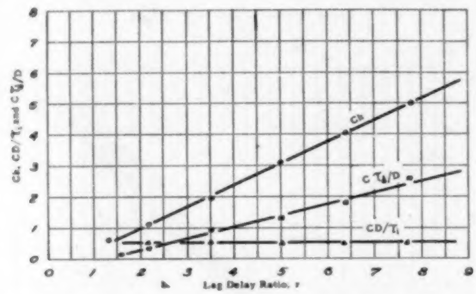

FIG. 28(b) VALUES OF Ck, CD/τ_i AND $C\tau_d/D$ WHICH PRODUCE QUICKEST RESPONSE WITHOUT OVERSHOOT FOR VARIOUS r WITH STEP CHANGE IN DESIRED VALUE, v^*

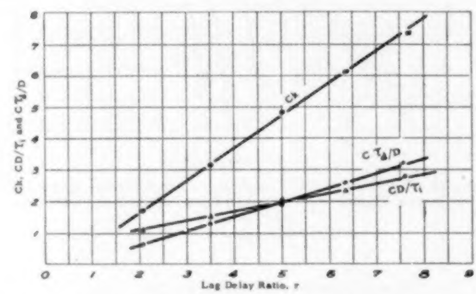

FIG. 29(b) VALUES OF Ck, CD/τ_i AND $C\tau_d/D$ WHICH PRODUCE QUICKEST RESPONSE WITHOUT OVERSHOOT FOR VARIOUS r WITH STEP CHANGE IN LOAD, m_L

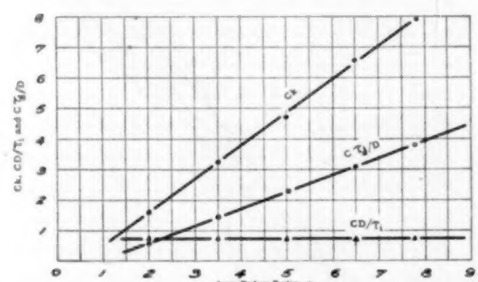

FIG. 30(b) VALUES OF Ck, CD/τ_i D AND $C\tau_d/D$ WHICH PRODUCE QUICKEST RESPONSE WITH 20 PER CENT OVERSHOOT FOR VARIOUS r WITH STEP CHANGE IN DESIRED VALUE, v^*

TABLE 1 RELATIONSHIPS FOR VARIOUS TYPES OF CONTROLS

Type of control	Quickest response without overshoot: Step change in desired value (v^*)	Quickest response without overshoot: Step change in load (m_L)	Quickest response with 20 per cent overshoot: Step change in desired value (v^*)	Quickest response with 20 per cent overshoot: Step change in load (m_L)
Proportional control $m = ku$	$k = 0.3 \frac{r}{C}$	$k = 0.3 \frac{r}{C}$	$k = 0.7 \frac{r}{C}$	$k = 0.7 \frac{r}{C}$
Proportional-plus-integral control	$k = 0.35 \frac{r}{C}$	$k = 0.60 \frac{r}{C}$	$k = 0.6 \frac{r}{C}$	$k = 0.7 \frac{r}{C}$
$m = ku + \frac{1}{\tau_i} \int u\,dt$	$\frac{D}{\tau_i} = 0.30 \frac{1}{C}$	$\frac{D}{\tau_i} = 0.15 \frac{r}{C}$	$\frac{D}{\tau_i} = 0.6 \frac{1}{C}$	$\frac{D}{\tau_i} = 0.3r$
Proportional-plus-integral-plus-derivative control	$k = 0.6 \frac{r}{C}$	$k = 0.95 \frac{r}{C}$	$k = 0.95 \frac{r}{C}$	$k = 1.2 \frac{r}{C}$
$m = ku + \frac{1}{\tau_i} \int u\,dt + \tau_d \frac{du}{dt}$	$\frac{D}{\tau_i} = 0.6 \frac{1}{C}$	$\frac{D}{\tau_i} = 0.4 \frac{r}{C}$	$\frac{D}{\tau_i} = 0.7 \frac{1}{C}$	$\frac{D}{\tau_i} = 0.6 \frac{r}{C}$
	$\frac{\tau_d}{D} = 0.3 \frac{r}{C}$	$\frac{\tau_d}{D} = 0.4 \frac{r}{C}$	$\frac{\tau_d}{D} = 0.45 \frac{r}{C}$	$\frac{\tau_d}{D} = 0.5 \frac{r}{C}$

D = delay time
C = plant gain

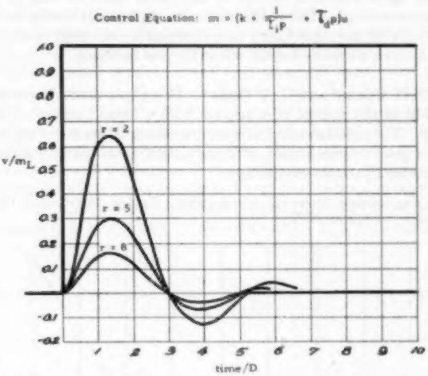

FIG. 31(a) TYPICAL QUICKEST RESPONSE WITH 20 PER CENT OVERSHOOT FOR SYSTEMS UNDER PROPORTIONAL-PLUS-INTEGRAL-PLUS-DERIVATIVE CONTROL
(Step change in load, m_L.)

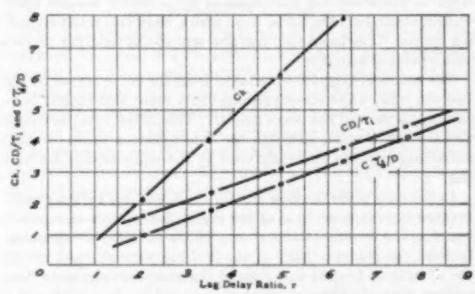

FIG. 31(b) VALUES OF Ck, CD/τ_i AND $C\tau_d/D$ WHICH PRODUCE QUICKEST RESPONSE WITH 20 PER CENT OVERSHOOT FOR VARIOUS r WITH STEP CHANGE IN LOAD, m_L

The correspondence of the coefficients in Equations [4] and [5] with those of Equation [3] is as follows

	Equation [4]	Equation [5]
Proportional constant	$k' = k$	$k'' = \frac{k}{2} + \sqrt{\left(\frac{k}{2}\right)^2 - \frac{\tau_d}{\tau_i}}$
Integral time constant	$\tau_i' = k\tau_i$	$\tau_i'' = \left(\frac{k}{2} + \sqrt{\left(\frac{k}{2}\right)^2 - \frac{\tau_d}{\tau_i}}\right)\tau_i$
Derivative time constant	$\tau_d' = \frac{\tau_d}{k}$	$\tau_d'' = \left(\frac{1}{\frac{k}{2} + \sqrt{\left(\frac{k}{2}\right)^2 - \frac{\tau_d}{\tau_i}}}\right)\tau_d$

REFERENCES

"The Dynamics of Automatic Controls," by R. C. Oldenbourg and H. Sartorius, translated and edited by H. C. Mason, and published by the ASME, February, 1948.

"Optimum Settings for Automatic Controllers and Process Lags in Automatic-Control Circuits," by J. G. Ziegler and N. B. Nichols, Trans. ASME, vol. 64, 1942, pp. 759–765.

"Time Lag in a Control System," by D. R. Hartree, A. Porter, A. Callender, and A. B. Stevenson, Proceedings of the Royal Society of London, series A, vol. 161, 1937, pp. 460–476.

"A Graphical Analysis of Controller Response," by Yasundo Takahashi, Published in Japan, September, 1949.

Discussion

A. R. CATHERON.[4] An opportunity to try out the procedures outlined in this paper was accepted with great pleasure, because of interest in the techniques presented and the possibility of review of some allied tests and conclusions. The development of this approach to the problem of control adjustment determination had been carried out with an electronic analog representing a generalized control unit, and equipment available to the writer presented the possibility of using the technique for the settings of an actual control system with a process of variable characteristics under relatively controlled conditions. This discussion is in the nature of a report on the results obtained.

Such a process has been in operation since early in 1949 as part of a program of study of the control of rate of flow of liquid and the various specific problems that arise in this connection. The system consists of a 2-in. water-flow line of maximum length of 140 ft, through which the water can be driven either by direct pumping or by a static pressure head. The line length can be reduced, and the positions of the control valve and the primary element varied. For control studies, upsets may be imposed upon the system either by changing the control-point setting of the controller or by changing the load through alternately bypassing a restriction at the head of the line, or bleeding the line from a point just downstream of the restriction. The control equipment is operated pneumatically.

To obtain the data necessary to define the process for evaluation, i.e., figures for D, L, and C, the controller output connec-

[4] Research Engineer, The Foxboro Company, Foxboro, Mass.

TABLE 2 RESULTS OF TESTS

Type of upset	r	Per cent proportioning band / sec reset time: Computed	From curve	By operation	Seconds, $L + D$	Seconds recovery time in operation
Control point	1.45	287/0.3	321/0.3	300/0.3	0.44	2
Load	1.74	162/4.6	240/2.0	200/1.6	3.2	4
Load	2.71	98/34	118/23	150/24	31.5	42
Control point	2.71	169/27	178/25	250/24	31.5	42
Control point	3.66	117/51	115/58	100/55	56	60
Load	3.66	68/48	75/40	80/35	56	60
Control point	3.65	132/8.5	129/9.7	100/10	9.2	11 1/2
Control point	4.20	114/9.4	120/11.2	100/10	9.9	11 1/2
Load	4.52	62/7.6	65/7.1	50/8.1	10.5	13 1/2
Load	5.16	61/7.2	62/7.2	50/8.1	11.1	13 1/2
Load	5.71	49/2.8	49/3.0	40/2.3	4.7	6
Control point	5.71	84/4.7	86/6.9	50/3.9	4.7	6

tion was broken, and a pair of tanks attached, so arranged that predetermined pressures could be set up in each and applied in turn to the control system by an air switch in order to form a step upset. At the other end of the system the measuring element of the controller was replaced by a similar bellows operating a strain bar, the signal from which went into a fast recording system. The input step was also sent to the recorder to provide a point of zero time.

The values of D and L were taken from the curve traced by the fast recorder, while static readings from input and output pressure gages showed the plant gain C. This latter value averaged 1.68 for this system, although the determination made for each individual run was generally used in the computation for that run.

In the tests made the flow system itself was not varied, chiefly because the response time of the liquid flow system is so much less than the response times of most of the auxiliary components. Instead, the characteristics of the problem were changed by the use of various lengths and sizes of pneumatic transmission line, various sizes of valve-operating motor, and by the addition of a high-volume repeater relay to the valve motor. This permitted variation of r through a range from 1.45 to 5.71. The response speed of the system, as arbitrarily represented by the sum of L and D, also varied (but not necessarily in coincidence with r) from 0.44 sec to 56 sec. After D, L, and C were determined for a given arrangement, the controller was put back into the system and its adjustments varied until the most rapid aperiodic recovery possible was obtained. Since the tests were made in the presence of "noise," or random variation in the flow too rapid for the controller to catch, the precise determination of 20 per cent overshoots would be extremely difficult. For this reason, and because the aperiodic recovery had been used entirely in all other test work done on the flow system, it was selected in this case. Upsets were generally held to 10 per cent of scale, uncontrolled, and made by either load or control-point variation. The recoveries were recorded as seen by the primary element, not by the controller. All tests were made at the same control-point setting or range.

A comparison of the settings determined by study of the system response with those obtained in actual operation indicates that the procedure outlined in the paper has given safe and usually conservative settings consistently. There was little to choose between values obtained by computation and from the curves given, with the exception that the curves appeared to be the more accurate at the lower values of r. Table 2 of this discussion summarizes the results obtained, with the proportioning bands expressed in per cent ($= 100/k$) and reset times in seconds per repeat. No tests were made with a three-element controller. Since the controller that was used follows Equation [4] of the paper (reduced to $m = k' [1 - 1/(r_r p)]u$, for there is no derivative term), the computed settings have been adjusted accordingly.

As a matter of possible interest, it may be noted that there seems to be a direct relationship between $L + D$ and the time required for an aperiodic recovery, the latter being approximately $1^1/_4$ times the former, except in the case of $r = 1.45$ and $L + D = 0.44$.

To sum up, the curves indicate that the technique is at least fully applicable to a system of the stated type working in the ranges covered. The writer wishes to express his thanks to the authors for the opportunity to review and try out their work, and to his own company for the use of the test facilities.

G. H. COHEN[5] AND G. A. COON.[5] This paper makes a valuable study of the control of a process with a large number of time lags. The reaction curve obtained by using 80 stages of lag may be a good representation of many actual processes and as such provides a basis for comparison.

[5] Engineering Research Department, Taylor Instrument Companies, Rochester, N. Y.

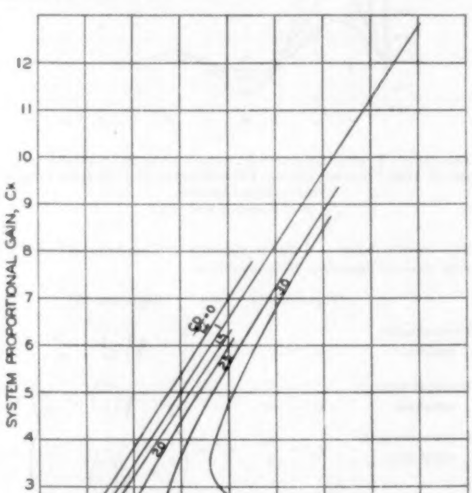

FIG. 32 RESULTS COMPUTED FOR PROPORTIONAL-PLUS-RESET CONTROL

A simpler approximation is the assumption that the reaction curve may be represented by a distance-velocity lag and a single time constant. For this case with proportional-plus-reset-plus-derivative control the critical curves corresponding to Figs. 17, 19, 24, 25, 26, and 27 of the paper, are given by the equations

$$Ck = \tau\omega \sin\omega - \cos\omega$$

$$\frac{CD}{\tau_i} = \omega^2\tau\cos\omega + \omega\sin\omega + \omega^2\tau\frac{C\tau_D}{D}$$

where

$$\omega = \frac{2\pi D}{P}$$

$$P = \text{period in seconds}$$

and all other terms are as defined in the paper.

It is obvious that the calculations are not at all difficult and can be obtained, using a desk calculator, in a few hours.

The computed results for the case of proportional-plus-reset control are shown in Fig. 32 of this discussion, which can be compared to Fig. 19 in the paper. It can be seen that the errors involved in using the delay unit can be as much as 55 per cent variation from the theoretical results. Since the delay unit imposes continuous derivatives while the theoretical simplified process characteristic has a discontinuity in first derivative at time $t = D$, it cannot be expected that the results should agree when integration is introduced in the controller. If a two-capacity process with dead period lag were used, then the problem of a discontinuity in derivative would be removed.

A paper to be published by the writers will discuss the problem of time delay and control, presenting computed curves for various degrees of stability in terms of the control parameters.

In determining the coefficients corresponding to Equation [5], the paper indicates only a positive sign before the radical. It is possible to have two values of k'', τ_i'', and τ_d'' so that the negative sign is also permissible. This has appeared in practice on a commercial controller, and it can be shown that these double-valued functions are the determining factors which allow this type of controller to be used on the start-up of batch processes.[8]

The analog computer is of great advantage in determining the transient-response curves, since the calculation of the response curves requires tedious computation. The authors should be commended for applying this method of analysis to the problem of retarded control.

Authors' Closure

The observations of Mr. Catheron on the applications of the results of this paper to a pneumatic system are of great interest to the authors. The correlation with analog data is good. It is interesting to note the performance of actual system is more closely predicted from analog results than it is by mathematically derived results. This is true because no real physical system exhibits the discontinuities existing in the mathematical presentation of Gohen and Coon. The authors express their appreciation of the contributions of the discussers to this paper.

[8] "A New Concept of Automatic Control," by R. E. Clarridge, *Instruments*, vol. 23, 1950, p. 1248.

Supervisory Instruments for Power-Generating Equipment—Application and Interpretation of Records

By E. Y. STEWART[1] and J. H. REYNOLDS, JR.,[2] SCHENECTADY, N. Y.

The proper application and use of turbine supervisory instruments is becoming more important owing to centralization of controls at remote points from the power-generating equipment and also the growing trend of power companies to quick-start their machines. Equipment is available to record turbine conditions in terms of shell and differential expansion, speed and camshaft position, bearing vibration, and shaft eccentricity. A description of shell and differential-expansion recording equipment is included. The value of the instruments depends upon the proper interpretation of the records. A feature of the paper is a discussion of a number of case examples in which mechanical trouble in the turbine or generator was detected by the instruments.

Introduction

A NUMBER of years ago the authors' company developed a line of turbine supervisory instruments for use as telemetered recording instruments to meet the demand for protection and supervision of remote outdoor operation of large steam-turbine generator sets.[3] The instruments as originally developed measure and record turbine conditions in terms of shaft eccentricity, bearing vibration and shell expansion, and also detect interference or rubbing of rotating parts.

Since their development, turbine supervisory instruments were never used as originally intended but were, however, used to good advantage in providing the operator with an indication and a permanent record of the mechanical performance of the turbine generator throughout the starting period and subsequent running time.

The records obtained indicate to the operators the current conditions and permit all interested individuals to review the past operation of the machine and plan future operating methods to be used.

The trend in the operation of power stations in recent years has been to centralize power-station controls in a central control room at a point remote from the turbine. Thus it follows that the supervision, which is so necessary while starting the machines, and during their running period, is substantially reduced. Consequently it is imperative that adequate instrumentation be provided to indicate to the operators the condition of the unit. In conjunction with this there is also a growing trend for the power companies to make quick starts of their machines.[4]

This stems from the large load drop-off at night, in which the less efficient units are shut down and quick-started in the morning to satisfy the rapid increase in load demand. The authors' company has recognized this trend,[5] and studies to date have indicated that more comprehensive instrumentation is becoming essential in order to keep track of the rapidly changing conditions during this period. Knowledge of the over-all mechanical condition of the turbine-generator set as portrayed by the turbine supervisory instruments is invaluable to the turbine operator during quick starts.

Through experience with the instruments, we have increased greatly the ability to analyze the records and detect some of the more typical troubles that might occur. Examples of this will be described later in the paper. In several cases when reliability of the instruments was questioned because of the unusual records obtained, analysis showed trouble had developed in the machine.

Supervisory Instruments

Fig. 1 illustrates a typical panel arrangement of a complete set of supervisory instruments. The equipment consists essentially of a strip-chart recorder, electronic power units, and suitable detectors mounted on the turbine generator.

The most important requirement and also the most difficult problem that had to be surmounted in the development of the instruments was to design electronic equipment having a reliability comparable to that of steam turbines. Consequently the electronic design was purposely made very conservative, and improvements were included from time to time as the art of electronics advanced. As an added feature in maintaining reliability each equipment has a built-in test circuit, consisting of test switches and a small test instrument. Through this the various electronic circuits can be checked to locate any difficulty that might develop, such as deterioration of tubes, detector grounds, component failures, and so forth. In conjunction with this, each equipment has a one-point built-in calibration check in which the over-all calibration may be maintained.

At the present time these instruments measure turbine conditions in terms of shell and differential expansion, speed and camshaft position, bearing vibration, and shaft eccentricity.

The shell and differential-expansion recorder was added to the turbine supervisory-instrument line in 1945, having been used previously for a number of years in engineering investigations. The equipment consists of a strip-chart recorder of the inkless type, a power unit, and two detector units mounted on the turbine, which are connected alternately to the measuring circuit through a time switch.

---

[1] Development Engineer, General Engineering Laboratory, General Electric Company.

[2] Service Engineer, Service Engineering Division, Turbine Section, General Electric Company.

[3] "Turbine Supervisory Instruments and Records," by J. L. Roberts and C. D. Greentree, Trans. ASME, vol. 58, 1936, pp. 607–614.

Contributed by the Power and Industrial Instruments and Regulators Division and presented at the Semi-Annual Meeting, Toronto, Ont., Can., June 11–15, 1951, of The American Society of Mechanical Engineers.

 Manuscript received at ASME Headquarters, April 24, 1951. Paper No. 51—SA-49.

[4] "Quick Starting of High-Pressure Steam-Turbine Units," by J. C. Falkner, R. S. Williams, and R. H. Hare, Trans. ASME, vol. 70, 1948, pp. 201–209.

[5] "Operating Characteristics of the 100,000-Kw Essex Turbine Generator," by Stanford Neal and Vinal S. Renton, Trans. ASME, vol. 72, 1950, pp. 267–290.

Fig. 1 Turbine Supervisory-Instrument Panel

In order to differentiate between the two readings on the chart paper, the time switch is so adjusted that the differential-expansion detector is connected to the measuring circuit for 2 min and 40 sec, thus recording a dash. Then the shell-expansion detector is connected to the circuit and is recorded for 20 sec, thus making a dot. The complete cycle is finished in 3 min and is then repeated. The differential expansion appears as a very nearly continuous line, while the shell expansion is a series of dots. By connecting these points a continuous curve may be drawn.

Shell-Expansion Detector. The shell-expansion detector consists of two pairs of stationary coils on laminated cores with a movable armature between them. This armature is linked by a variable-ratio lever to a contact rod projecting from one end of the detector. Motion of the contact rod moves the armature between the coils, changing their impedance. The detector is mounted on the front end standard and measures the axial motion of the shell with reference to the foundation, Fig. 2.

In our turbines, the turbine casing is keyed at the rear or exhaust section, and axial expansion is always forward, away from the generator. The scale on the recorder reads 0 to 250 mils full scale. To obtain total shell expansion, multiply the reading obtained on the recorder by the multiplier number marked on the scale in the space provided.

Differential-Expansion Detector. The differential-expansion detector consists of two pairs of stationary coils on laminated cores, mounted on the shell in such a position that the bull gear or special ring on the shaft acts as an armature between them. The difference in axial motion between the shaft on which the bull gear or special ring is mounted and the shell changes the air gap, thus varying the impedance of the coils, Fig. 2. The total air gap between the coils is always 500 mils, and the scale of the recording instrument reads forward clearance from 0 to 500 mils full scale. The division of the gap, that is, the gap between the forward or turbine-end coil and the bull gear or special ring, and the gap between the back or generator-end coil and bull gear or special ring, will vary, depending on the design of the turbine. The reading on the recording instrument of differential expansion is in effect a measure of the clearance between the rotating and stationary elements in the turbine.

In order to warn the operator when the clearances in the turbine have been closed and that further reduction will mean rubbing will take place, red danger bands have been placed on the recorder scale. One band extends from zero to some value short of mid-scale. The other band extends from some point above mid-scale to full scale. How far these bands extend toward mid-scale depends upon the design of the machine and what the internal clearances are. If the pen on the recorder just touches the red area in either direction from center, it means that if there is any further movement into the red area a rub will develop.

To aid the operator further a small green mark is placed on the scale at a point denoting the cold-gap setting between the turbine-end coil and bull gear or special ring. Therefore the space between this mark and the start of the red bands at either end of the scale is the amount of normal clearance available between the stationary and rotating elements inside the machine. Consequently any movement of the pen in either direction from this mark will give the operator a clear idea of how fast the clearances are being closed or opened. An example of the scale is shown in Fig. 3. The red bands and green mark are indicated.

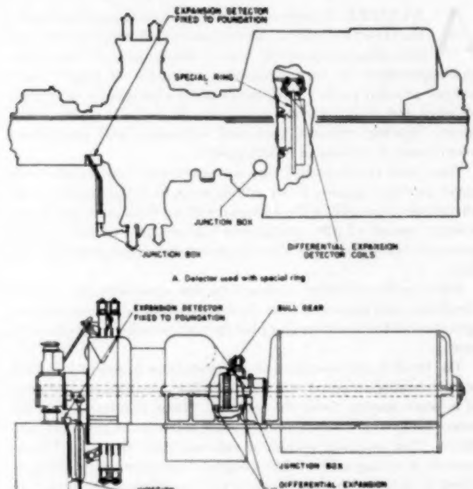

Fig. 2 Outline of Two Typical Turbine-Generator Sets Showing Physical Location of Shell and Differential-Expansion Detectors

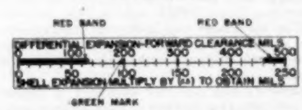

Fig. 3 Recorder Scale for Shell and Differential-Expansion Recorder

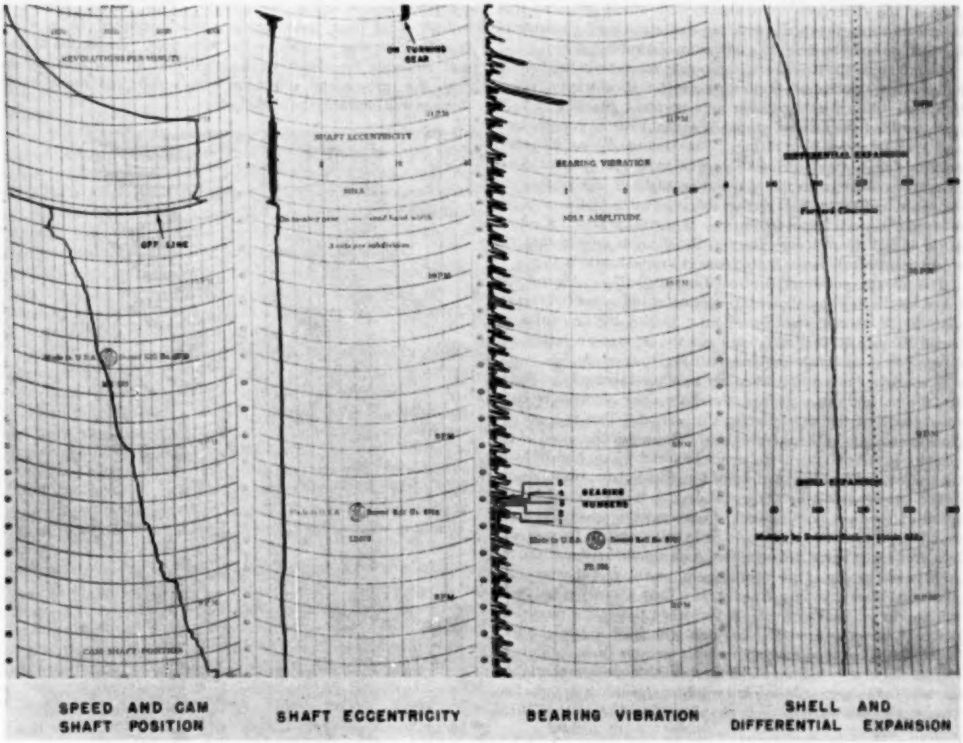

FIG. 4 UNLOADING RECORDS OF A 35,000-KW 3600-RPM HIGH-PRESSURE ELEMENT OF A 125,000-KW CROSS-COMPOUND UNIT

SCALES USED IN INSTRUMENTS

Previous papers have been written,[5,6] in which the operation of the speed and camshaft position, bearing vibration, and shaft-eccentricity recording equipment were completely described. In order to aid in the interpretation of the records which will be described later, a brief review of the various scales used in the instruments and a few of the salient points are now given.

The speed and camshaft-position recorder chart, Fig. 4, is marked with two sets of values; (1) speed in revolutions per minute, (2) camshaft position in per cent open.

If the machine is being brought up to speed, the record made is referred to the speed scale. After the machine is brought to synchronism and placed on the line, it is no longer necessary to measure speed because the speed is determined by the system frequency. Upon closing the line breaker, the recorder is transferred automatically to the measurement of camshaft position. The load on the machine is then indicated by the per cent rotation of the camshaft. Opening of the line breaker for any reason will return the recorder automatically to speed indication.

The bearing-vibration scale, Fig. 4, is logarithmic to enable accurate reading of the low vibrations and still enable vibrations as high as 15 mils to be recorded on the same scale. A time switch is provided so that up to five detectors can be recorded in sequence. A short pause is provided between the end of the last bearing recorded and the start of a new cycle, thus giving a reference point to pick off which bearings are being recorded.

The shaft-eccentricity scale, Fig. 4, is linear and consists of two scales—one for turning-gear operation, and the other for steam operation. When the machine is on turning gear the measurement of eccentricity is the width of the band drawn on the chart regardless of its position on the chart. If the machine is taken off turning gear and rolled by steam, the scale is transferred automatically by a switch operated by the turning-gear mechanism on the turbine so that the measurement of eccentricity is from 0 left to 15 mils full scale right, on the chart.

The shell and differential-expansion recorder chart, Fig. 4, is linear and marked with two sets of values, explanation of which has already been given.

RECORD ANALYSIS

Since the value of these instruments depends upon the ability to analyze the records obtained, there are herein described a number of interesting cases in which the instrument warned of impending trouble.

Fig. 4 shows a set of records taken from a 35,000-kw 3600-rpm high-pressure element of a 125,000 cross-compound turbine-generator unit during a shutdown. Of particular interest is the

[6] "Application of Turbine Supervisory Instruments to Power Generating Equipment," by J. L. Roberts and H. M. Dimond, Trans. ASME, vol. 65, 1943, pp. 803–809.

slope of the differential-expansion record which indicated that the clearance between the rotating and stationary elements of the turbine had decreased to a minimum allowable value.

At 7:30 p.m. the machine was carrying very nearly full load as indicated by the camshaft-position chart. Eccentricity, vibration, and differential expansion were normal. Starting at 7:33 p.m., the load was reduced gradually so that by 9:45 p.m. the load was down to about $^1/_3$ of rating. The eccentricity and vibration records were normal during this period, and the differential-expansion recorder indicated that only a slight change of forward clearance had taken place during this interval. At this time the forward clearance began to decrease at a greater rate. A record of the initial steam temperature at the throttle showed that the steam temperature began to decrease at a rapid rate at 9:45 p.m.

The unloading cycle was continued and at 10:27 p.m. the unit was taken off the line and allowed to operate at full speed (3600 rpm) until 10:58 when it was tripped out. During the unloading interval (9:45 p.m. to 10:27 p.m.) and the no-load operation, the forward clearance of the turbine continued to decrease.

It should be noted that when the unit was taken off the line at 10:27 p.m., and run at no load, the eccentricity recorder traced a small band on the chart during this period. This is a normal phenomenon on 3600-rpm machines. Whenever the speed of the machine is just off system frequency or speed (either high or low), the recorder will trace a small band which is explained as follows:

The frequency of the shaft eccentricity is determined by the speed of rotation of the shaft. Consequently, when this rotational speed is a little above or a little below system frequency, a beat frequency exists between the shaft eccentricity and the 60-cycle power supply of the recording equipment, and the recording pen will follow this beat frequency. Thus a small inked band will appear on the chart. However, when the unit is phased-in, the beat becomes zero and the pen will draw a straight line. When the speed becomes appreciably greater or less than the system frequency, the recording mechanism no longer can follow the beat frequency, and the band will converge into a straight line. This was shown when the unit was allowed to decelerate at 10:58 p.m.

The differential-expansion slope appeared to increase at a greater rate when the unit was taken off the line and run at no load. At 11:40 p.m. the unit came to rest and was placed on turning gear. Differential expansion at this time was 90 mils. The red danger band on this particular unit ended at 84 mils.

If the differential expansion had decreased any further rubbing would have taken place. Although the operation in this instance was satisfactory, we believe that the differential expansion would not have reached such a low value if the machine had been allowed to decelerate when it was taken off the line.

Fig. 5 shows the vibration and eccentricity records from a 60,000-kw, 3600-rpm noncondensing machine in which the generator rotating-element field coils failed to ground. Referring to the records from 3:00 a.m. to 7:28 a.m. the record indicates the machine was normal while carrying full load. During this period the shaft eccentricity was steady at a value of $4^3/_4$ mils, and the bearing vibration was constant with the number 4, or generator-end bearing, at 1.2 mils. At 7:30 a.m. the shaft eccentricity increased very rapidly to 7 mils and oscillated. At the same time the bearing vibration increased to about 2 mils at No. 1 bearing. The shaft eccentricity showed rapidly varying values until 7:42 a.m., at which time the eccentricity leveled off at 12 mils. The bearing vibration in the meantime was steadily increasing. At 8:36 a.m. the shaft eccentricity dipped rapidly and then went to 14 mils. At the same time the bearing vibration increased still further. Between 8:30 a.m. and 8:45 a.m. the unit vibrated so violently that it was taken off the line.

The unusual records were caused by a field coil on the generator rotor failing to ground. This failure developed a high local heat concentration which resulted in a shaft bow that became steadily worse with time. Inspection of the unit following the shutdown disclosed that all the bearings on both the turbine and generator were wiped, and considerable damage was found on the oil deflectors.

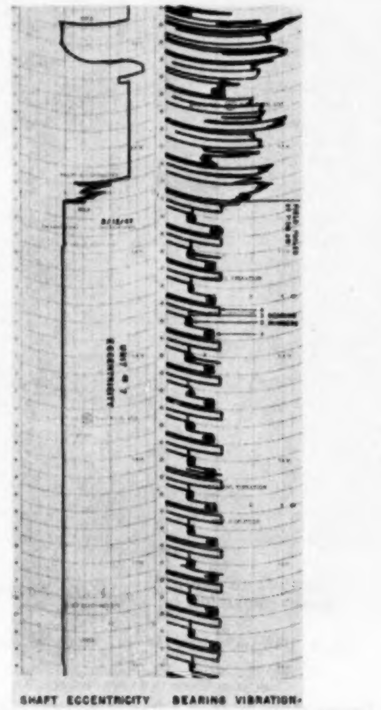

Fig. 5 Eccentricity and Vibration Records Taken From a 60,000-Kw 3600-Rpm Noncondensing Turbine Generator During a Field Failure

The mechanical damage could have been minimized if the unit had been taken off the line at 7:28 a.m. when both the eccentricity and vibration recorder indicated an unusual operating condition instead of allowing it to continue.

Figs. 6(*a* and *b*) show an initial start-up of a 125,000-kw cross-compound turbine generator, consisting of a 35,000-kw 3600-rpm high-pressure unit, Fig. 6(*a*), and a 90,000-kw 1800-rpm low-pressure unit, Fig. 6(*b*). It should be noted that the generators of all cross-compound units of this design are tied in electrically while on turning gear so that when the unit is rolled on steam, the speed of the low-pressure unit is always $^1/_2$ of the high-pressure unit. The charts as shown started at 12 noon at which time both units were on turning gear.

At 12:14 p.m., the unit was rolled. Speed on the high-pressure unit was increased to 500 rpm, Fig. 6(*a*), and was held at that value until 12:23 p.m. at which time it was increased rapidly to 1000 rpm at 12:29 p.m. At this time the eccentricity started to increase gradually. At 12:30 p.m. the speed was again increased, obtaining 1300 rpm at 12:36 p.m. During this interval the ec-

centricity in the high-pressure unit increased rapidly from 1 to 9 mils. The bearing-vibration recorder showed vibrations that are considered excessive for this type unit in this speed range.

At 12:36 p.m., the stop valve was tripped, and the unit coasted to rest. During the deceleration period, the eccentricity increased and went off scale, and the vibration on the unit was excessive.

In Fig. 6(*b*) the records of the low-pressure unit during this period indicated normal operation. Proper interpretation of the record of the high-pressure unit, Fig. 6(*a*), at 12:30 p.m. indicated that the unit had developed a rub. At this time the speed either should have been held constant or decreased, depending upon whether the shaft eccentricity remained constant or increased, thus preventing possible mechanical damage due to rubs.

When the unit had decelerated to rest it was placed on turning gear, and the record indicates a shaft eccentricity of 10 mils. Turning-gear operation for 1 hr 40 min was required to reduce the shaft eccentricity to its original value.

At 2:25 p.m. the unit again was started. The speed of the high-pressure unit Fig. 6(*a*) was increased to approximately 350 rpm (175 rpm for the low-pressure unit). The records of the high-pressure unit indicated normal operation. At 2:32 p.m. the shaft eccentricity on the low-pressure machine Fig. 6(*b*), started to increase as the speed had been increased to 250 rpm. Noting this increase, the operator held constant speed around 150 to 250 rpm until the shaft eccentricity decreased to its original value. This required about 1 hr 50 min of time. Then, as the shaft eccentricity on both units was normal, the unit was brought gradually to speed.

The records for the second start-up indicate that a small rub had developed in the low-pressure unit. This fact was recognized, and the speed was held constant until the rub cleared itself and the shaft eccentricity decreased to normal. Then the usual start-up procedure was followed in bringing the unit up to speed without further difficulty.

Fig. 7 shows the records obtained during a start-up of a 60,000-kw 3600-rpm reheat machine, in which a rub developed. The unit was rolled on steam at 4:12 p.m. and speed was increased to approximately 1900 rpm. At this speed the eccentricity started to increase, and the speed was held constant in order to determine if the eccentricity would increase further or decrease. The shaft eccentricity reached a value of 2.8 mils and started to decrease. However, the bearing vibration continued to increase so that at approximately 4:47 p.m. the unit was tripped out. As the unit decelerated, the shaft eccentricity decreased to about 1.5 mils and then increased rapidly to nearly full scale. The vibration still continued to increase. The machine was placed on turning gear when the unit came to rest, and the turning-gear record indicated a 7-mil shaft runout.

In analyzing the records, it was noted that a rub developed at 4:42 p.m., at which time the eccentricity was 2.8 mils, thus causing the shaft curvature to reverse itself. As the rub progressed, the shaft eccentricity decreased to a minimum value and then increased rapidly.

Fig. 8 shows the eccentricity, vibration, and speed and camshaft-position records of a 100,000-kw 3600-rpm tandem-compound machine during a bucket failure. In this particular installation two eccentricity-detector coils were installed 90 deg apart around the circumference of the shaft at the front end of the machine instead of the usual one. This was a special installation which was made for the express purpose of determining the approximate direction of the major axis of the shaft-vibration ellipse. The two coils are connected to the measuring circuit through a time switch one after the other. As can be seen from the eccentricity record, the time that one detector is being recorded is shorter than the other. Consequently, it is easier to identify them.

The spikes or sudden surges of the pen part way up the scale are due to the switching of the measuring circuit from one detector to the other and can be disregarded.

At 12:05 p.m. the load was increased from 65 per cent to about 90 per cent load by 12:20 p.m. This load was held constant for about 2 hr. The records indicate that during this period conditions were normal.

At approximately 2:56 p.m. both the shaft eccentricity and bearing vibration increased sharply. Eccentricity increased from approximately 1 to $5^1/_2$ mils, vibration from 0.3 mil to 1 mil. The operators immediately recognized that there was an unusual condition present and made arrangements with the system to pick up the approximate 100,000-kw load this unit was carrying so that a shutdown could be made.

At approximately 3:08 p.m. unloading was started, and at 3:58 p.m. the unit was taken off the line. During the unloading period the bearing vibration continued to increase. When the unit was shut down, inspection revealed that a bucket failure had occurred with a minimum amount of damage. It is believed that the damage was minimized by the prompt action of the operators in shutting the machine down after observing the abnormal records. Longer operation of the machine might have resulted in further damage.

Fig. 9 shows the eccentricity, vibration, speed, camshaft position, and shell- and differential-expansion records from a 100,000-kw 3600-rpm tandem-compound turbine generator during a thrust-bearing failure.

At the time the thrust failed, a second boiler was being placed on the line to take care of an anticipated load increase. It is believed that the turbine received a slug of water when the second boiler was cut in which caused the thrust to fail.

Examination of the records indicates that operation was normal up to about 1:32 p.m., at which time the camshaft-position recorder indicated that the load was increased. At this time the eccentricity recorder immediately went off scale. The differential-expansion recorder indicated that the turbine rotor moved toward the generator 50 mils with respect to the turbine shell. This was immediately followed by alarms from the thrust thermoalarm relay and high discharge thrust oil-temperature alarm. After 3 min the unit was tripped off the line while carrying approximately 80,000-kw load.

It is to be noted that the vibration did not increase during this interval, since the rotor did not go down stream enough to rub the stationary elements.

Further examination of the records after the trip-out indicates that the rotor continued to move toward the generator during the deceleration interval. It can be seen in this case that the turbine supervisory instruments immediately indicated the trouble and analysis of the eccentricity and differential-expansion records obviously showed that there was a thrust-bearing failure.

Figs. 10(*a*, *b*, and *c*), illustrate several eccentricity records made over a period of years, showing an increase in eccentricity caused by a loose thrust sleeve. These records were made on a 39,400-kw, 3600-rpm high-pressure element of a cross-compound unit. Fig. 10(*a*) shows the eccentricity record of the unit on load in July, 1945. Figs. 10(*b* and *c*) show the eccentricity record of the same unit during starting and loading in 1948. It should be noted that the shaft eccentricity in Fig. 10(*b*) (March, 1948), is the same as that in Fig. 10(*a*) (July, 1945). The eccentricity record in Fig. 10(*c*) (April, 1948), indicates that the shaft eccentricity had increased quite considerably over that shown in the previous records.

Owing to the increase in eccentricity the unit was shut down and investigation revealed a loose thrust sleeve. Continued op-

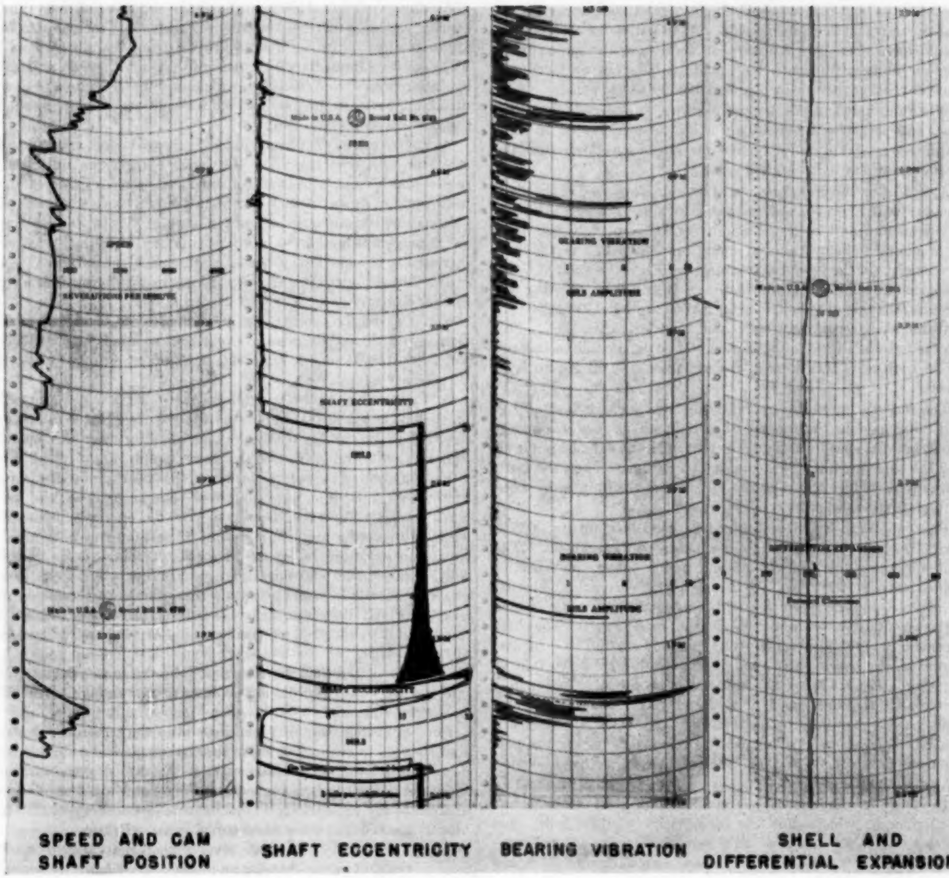

(a), 35,000-Kw 3600-Rpm High-Pressure Element

FIG. 6 RECORDS TAKEN FROM A 125,000-KW CROSS-COMPOUND

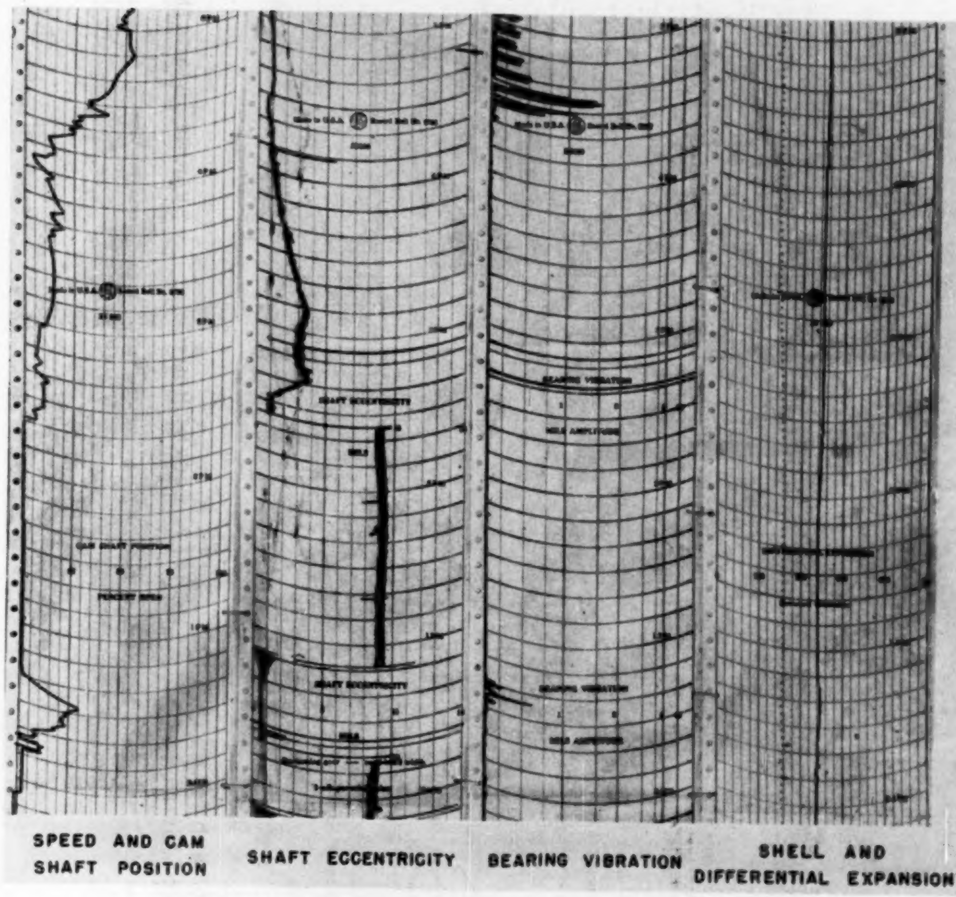

(*b*), 90,000-Kw 1800-Rpm Low-Pressure Element

Turbine-Generator Unit During Its Initial Start-Up

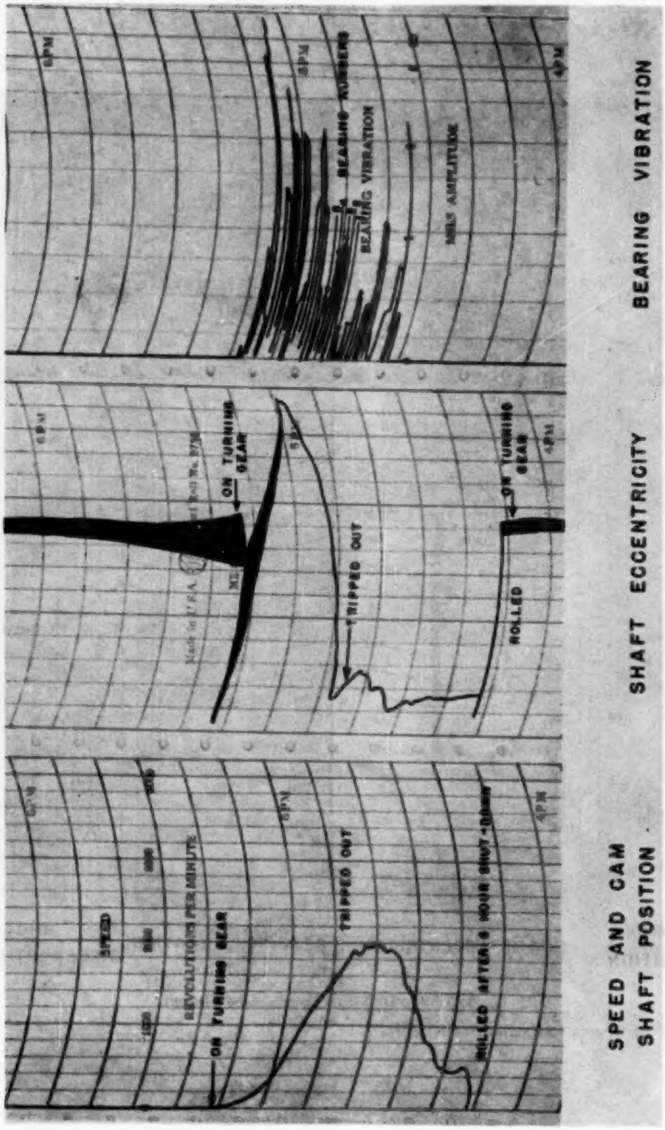

FIG. 7 START-UP RECORDS TAKEN FROM A 60,000-KW 3600-RPM REHEAT TURBINE-GENERATOR UNIT

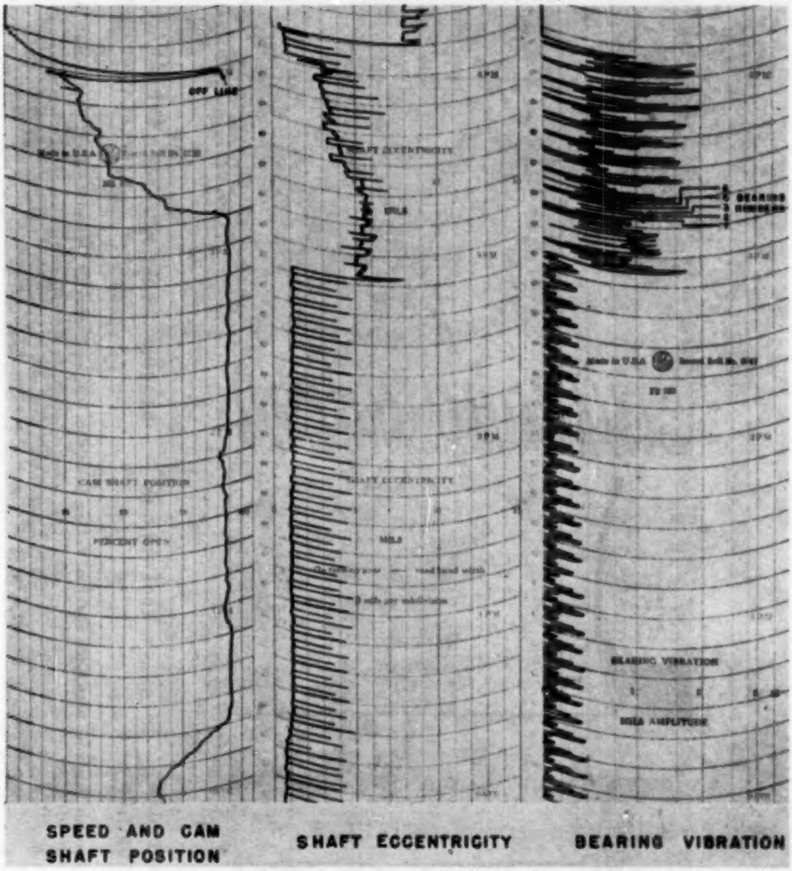

Fig. 8 Records Taken From a 100,000-Kw 3600-Rpm Tandem-Compound Turbine Generator in Which Buckets Failed

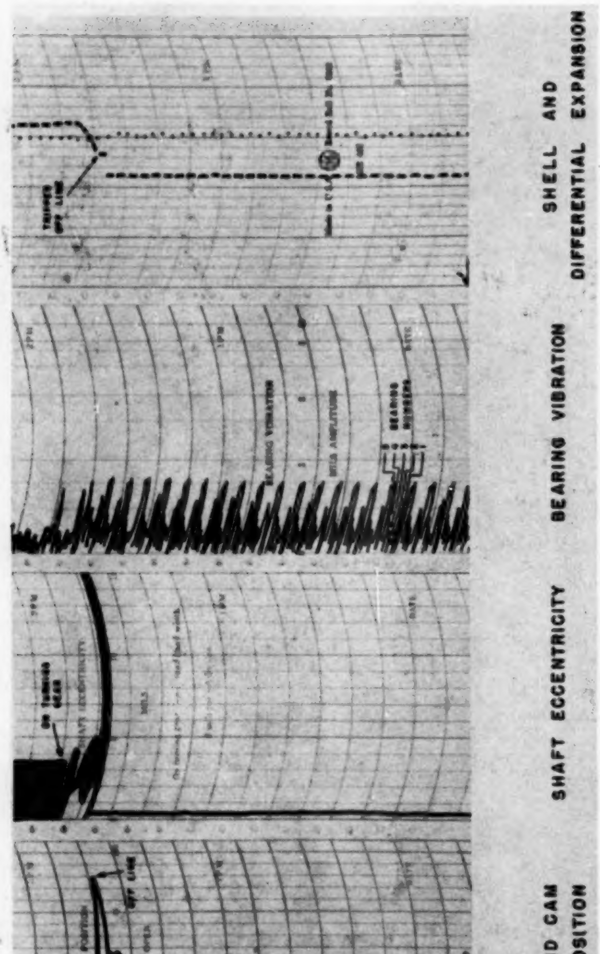

Fig. 9 Records Taken on 100,000-Kw 3600-Rpm Tandem-Compound Turbine Generator During a Thrust-Bearing Failure

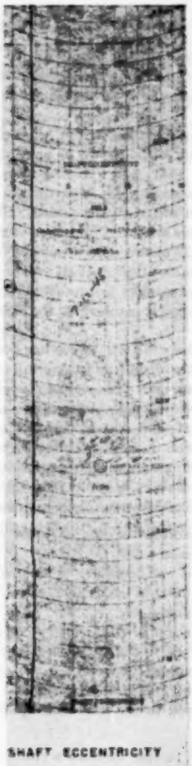

(a), July, 1945

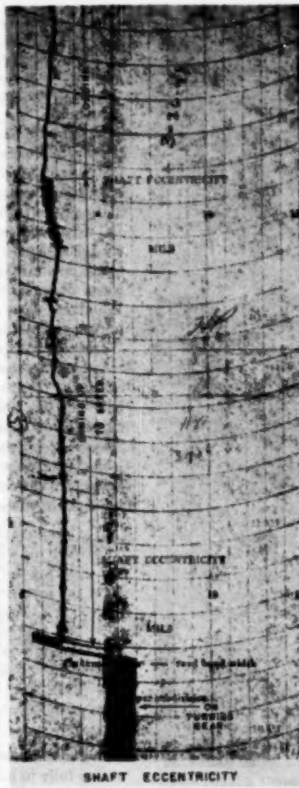

(b), March, 1948

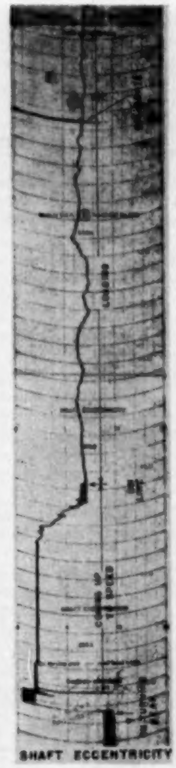

(c), April, 1948

Fig. 10 Eccentricity Record Taken From a 39,400-Kw 3600-Rpm High-Pressure Element of a Cross-Compound Unit With a Loose Thrust Sleeve

eration under these conditions might have resulted in a thrust-bearing failure.

Fig. 11 shows another instance of high shaft eccentricity which, after investigation, was found to be due to a loose thrust sleeve. This record was made on a duplicate machine of those shown in Fig. 10.

The record shows a different eccentricity pattern in that it increased with load whereas in Fig. 10(c), it can be seen that the eccentricity increased during the starting period and remained constant during the loading cycle. As in the previous case, continual operation with a loose thrust sleeve might have resulted in a thrust failure.

In turbines built by the authors' company shaft eccentricity is measured from the thrust sleeve. This sleeve is concentric with and a close fit with the shaft at the governor end of the turbine. It holds the thrust runner tightly against the shaft shoulder by means of a shaft nut. Therefore, if the thrust runner becomes loose it will work against the sleeve which, in turn, will cause an increase in eccentricity reading. There have been two cases where this has occurred and the trouble was detected and corrected before any damage resulted. This is borne out by the records shown in Figs. 10 and 11.

Conclusions

The shell- and differential-expansion recording equipment records in alternate sequence the amount of forward expansion of the turbine shell or outer casing, and the differential expansion between the shell and turbine rotor. The measurement of differential expansion not only provides an index as to the operating clearances between rotating and stationary elements but provides extremely valuable information for setting up proper starting and operating procedures on the higher-temperature machines.

The speed and camshaft-position recording equipment records the speed when starting up and shutting down the turbine and also gives a measure of the load that the machine is carrying in terms of per cent rotation of the camshaft. This instrument is valuable in analyzing events which take place when the line breaker of the generator opens due to system disturbances.

Bearing-vibration recording equipment records the amount of vibration on each of the main bearings of the turbine generator in

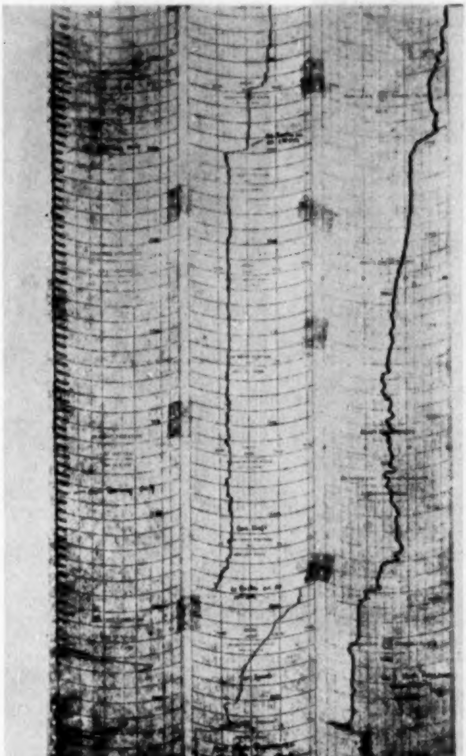

FIG. 11 ECCENTRICITY RECORD TAKEN FROM A 39,400-KW 3600-RPM HIGH-PRESSURE ELEMENT OF A CROSS-COMPOUND UNIT WITH A LOOSE THRUST SLEEVE

sequence. This equipment detects immediately disturbances which cause high vibration and also detects gradual long-time changes in vibration due to misalignment, and so forth.[8]

Shaft-eccentricity recording equipment detects and records once per revolution shaft bow, the causes for which have been covered in a previous paper.[3] However, it is extremely helpful in detecting a loose thrust sleeve or runner which would not otherwise be detected by any other means until actual failure occurred.

A complete set of turbine supervisory instruments is valuable since only a study of all records made by the recorders will give an over-all picture of the operating characteristics of the turbine generator at any particular time. Since the records for any particular machine are peculiar to that unit, normal operating records and records of unusual conditions in the machine should be used by the operators as a guide in operating, detecting unusual conditions, and in the training of operating personnel.

The interest that has been evidenced in the quick-starting of turbine generators makes the use of turbine supervisory instruments essential in order to keep track of the rapidly changing conditions.

Discussion

T. T. FRANKENBERG.[7] The authors are to be congratulated on presenting a paper of unique timeliness due to the trend for remote operation of many new turbines and the quick-starting of older units.

No turbine has been installed on the American Gas and Electric System since 1935, without two or more of the supervisory instruments. Until 1941 only bearing-vibration and shaft-eccentricity recorders were used. Starting in 1942, the speed and camshaft-position recorder was added. Shell and differential expansion recorders were not added as standard until 1949, though an earlier model of this device was given trials and is still in use on a machine started during 1941. At present, 1575 megawatts of generating capability is protected with these devices. Equal or greater coverage is planned for the 1250 megawatts now under construction.

In spite of this widespread use, there has been a considerable reluctance on the part of operators to give full regard to the indication of these instruments. Several of the authors' examples bear out this point, showing that immediate recognition of the trouble (and appropriate action) would have minimized the damage or at least the period during which the turbine was placed in jeopardy by continued operation. The reason for such reluctance and the resultant hesitation is to be found at least in part in some of the early difficulties with this equipment. For example:

1 Certain cam-operated selector switches created open circuits when the wires became disarranged.

2 During the war it was necessary to make a circuit change in all of the eccentricity units to lessen their sensitivity to defects in the vacuum tubes then available.

3 The field installation of the primary elements was not always carefully performed so that wear and bearing heat lessened or eliminated their useful life.

4 Finally, a number of minor mechanical failures in electrical components added to the time this equipment was out of service.

An equal handicap to the operator's confidence was the inability fully to interpret those readings which he did have.

A great deal of educational work remains to be done before the turbine supervisory instruments will be providing the operator with all of the information of which they are capable. This paper should help considerably in the education of the top level of operating plant personnel. The magnitude of the remaining job, however, is indicated by the following comparison: In order to interpret the indications of these instruments to a highly intelligent group which should be skilled in making engineering deductions, it was necessary to line up carefully the time co-ordinates of the charts and then use an average of 250 words of explanation to point out the trouble. Now consider the typical operator in the midst of some fast developing difficulty (who has many other responsibilities), and expect him to make a correct decision affecting four or five million dollars' worth of turbine-generator equipment. The case for more education and clearer presentation of the story is complete.

The necessity to correlate the readings of three and in some cases four charts has led to inquiry into the possibility of combining these various records on a single chart. To date the lack of unanimity on the part of users as to which records should be provided has encouraged the manufacturer to treat them as entirely separate units. It is our experience that all records are needed to interpret troubles adequately, and that presentation on a single chart would eliminate faulty time settings between charts,

[7] Assistant Mechanical Engineer, American Gas and Electric Service Corporation, New York, N. Y. Mem. ASME.

conserve panel space, and, most important, save time for the operator when making comparisons during unusual operating conditions. Since the average size of turbine purchased by utilities has increased rapidly since World War II (see Table 1, herewith), the cost of one additional record may be as little as 0.25 per cent or even 0.10 per cent of the total cost. This should encourage users to accept the full complement of instruments for the protection of their equipment.

TABLE 1 AVERAGE SIZE OF UTILITY TURBINES ON SHIPPING SCHEDULE OF ONE MANUFACTURER

Year	Average size, kw
1946	29800
1947	35000
1948	42200
1949	51600
1950	54800
1951	57600
1952	71300
1953	77300

H. Weisberg.[8] The justification for the supervisory instruments described by the authors is self-evident when we consider that the total installed cost is less than $20,000, and that these instruments are used to safeguard the operation of a machine which may cost as much as $4,000,000, and be part of a $30,000,000 installation. The outage of these large units results in a daily loss up to $10,000. Detection of abnormal operating conditions which would avoid 2 days' outage in the life of a machine would pay for the total cost of the instruments.

It is suggested that development of additional instruments which will indicate the operating condition of the machine would be well justified. In particular, more information on the operation of the thrust bearing, indicating perhaps the direction and amount of the thrust load, would be of considerable value for a continuous check of the condition of the blade path.

[8] Mechanical Engineer, Electric Engineering Department, Public Service Electric and Gas Company, Newark, N. J. Mem. ASME.

Authors' Closure

The authors would like to thank the discussers for their interest in the paper and for the various points that were brought out. These discussions have emphasized the authors' contention that turbine supervisory instruments are a valuable adjunct in turbine-generator operation. Several points have been brought up, however, that require further explanation.

Some difficulty was experienced with the instruments early in their history as indicated in T. T. Frankenberg's discussion. These difficulties have since been rectified by design changes. Drawing upon our long field experience with the instruments, a complete redesign has been made within the last year of all four instruments that make up the turbine supervisory group. Our objective in the redesign was to make them more reliable and rugged and easier to service.

The authors agree that educating the turbine operators in the interpretation of the records made by the instruments is a real problem. Recognizing a need for educational work, the authors' company held a supervisory-instrument symposium early in 1950, which was attended by results engineers from interested power companies and our own district service men. Not only was the operation and maintenance discussed but those attending actually tested and calibrated the instruments. During this period, a lecture with illustrations was given devoted entirely to record analysis.

Recording simultaneously all four instrument readings on one piece of paper is a desirable objective, yet no practical solution has been found.

H. Weisberg's suggestion of an instrument to measure the direction and thrust load is a good one. The differential-expansion recorder can be used to indicate and record thrust direction, provided the detectors are located forward of the thrust bearing. Such an application was used some years ago. At the present time a study is being made of the possibility of developing an instrument to measure thrust load.

Field Inspection of Boiler Tubes With Ultrasonic Reflectoscope

By J. A. Tash,[1] Pittsburgh, Pa.

Details are given of the ultrasonic reflectoscope and its use in detecting defective small-diameter tubing. By means of the ultrasonic shear-wave method and the reflectoscope, 90 sections of defective tubing, representing over 1500 ft, were detected and replaced in the convection-superheater outlet section of two boilers.

Introduction

Repeated failures of defective superheater tubes seriously threatened the continued safe operation of two new boilers. To forestall further forced outages it was imperative that the defective tubes be found and removed. Of the several nondestructive inspection methods considered, the ultrasonic shear-wave method and the "reflectoscope" looked most promising and eventually were successfully used in the field inspection of the tubes. By this means 90 tube sections, representing over 1500 ft of defective tubing, were detected and replaced.

Nature of Failures and Defects

The first tube failure occurred after about 1200 hr of service in the convection-superheater outlet section of the No. 4 boiler, on March 15, 1950. This was followed by additional ruptures of tubes, one at a time and in the same region, on April 20, May 1, May 6, and May 19. Examination of one failed tube after another showed that the ruptures developed along one or more longitudinal seams that originated at the inner surface and penetrated 75 to 90 per cent of the tube wall. In the region of the failure the seams were quite evident, Fig. 1. However, in adjacent undeformed regions or in unfailed tubes the seams were not readily found or followed on either the tube cross section or the inner surface. The usual method of determining the presence of seams consisted of cutting a series of rings which were then deformed along several diameters by squeezing in a vise. This would cause the seam to open and become visible. The appearance of such seams in a polished cross section and in the section after a slight amount of deformation is shown in Fig. 2. It is to be noted that the amount of residual metal near the outer surface is very small but was still sufficient to pass all routine inspections and cold hydrostatic tests.

Fig. 3 shows the comparative appearance between seams and the usual scratches and draw marks on the inner surface. The seams are delineated and appear in the illustration only because of some special manipulation. The seams located by the polished cross section of Fig. 2 were not photographed successfully until the section was washed with water, quickly dried, and photographed while some moisture was still present in the crevices.

The seam pattern varied. Some tubes had one, some more than one seam. In one tube from which a wall section $1^1/_4$ in. wide and 20 in. long was blown out, six different seams were evident. Similarly, some seams were long, some short, some interrupted, some overlapping; in several cases the seams extended the full length of the tube.

The seams did not penetrate the tube wall radially but instead, as visible in Fig. 2, followed a regular curve, the direction

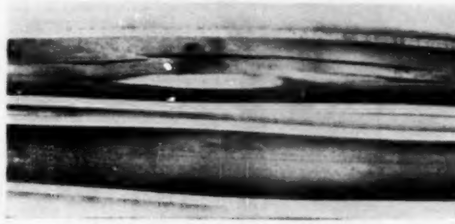

Fig. 1 5 Cr-Mo-Ti Superheater Tube That Ruptured in Service Because of Longitudinal Seams

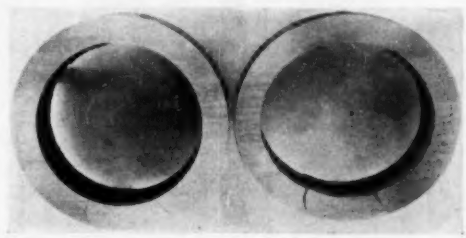

(a) (b)

Fig. 2 Cross Sections of Defective 2-In-OD Tube

(a, Showing pronounced curvature of seams. b, Appearance after a slight amount of deformation.)

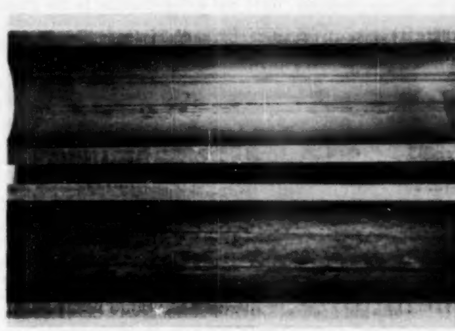

Fig. 3 Comparative Appearance of Seams and Draw Marks on Inner Surface

(Lower sections of seams are delineated by residual moisture in crevices.)

---

[1] Chief Chemist, Duquesne Light Company.

Contributed by the Power and Industrial Instruments and Regulators Divisions and presented at the Semi-Annual Meeting, Toronto, Ont., Can., June 11–15, 1951, of The American Society of Mechanical Engineers.

 Manuscript received at ASME Headquarters, May 8, 1951. Paper No. 51—SA-48.

of curvature being the same for all the seams of any one tube. Microscopic examination revealed that even though the seams were tight, they contained nonmetallic inclusions and frequently terminated in an enlarged smoothly rounded end, as visible in micrograph, Fig. 4. The faces of the crevice were parallel and

Fig. 4 Micrograph of Seam, Showing Parallelism of Faces as Though Originally a Rupture; × 50

dovetailed with each other almost exactly as if resulting from a brittle rupture; however, there was a discontinuity in the grain structure across the seam as though the tube were annealed subsequent to crack formation. As a rule, branch cracks and fissuring were absent except near ruptures or in cold-bent sections of tube.

History and Location of Defective Tubes

While the tubes of No. 4 boiler were failing with disconcerting regularity, the adjacent No. 5 boiler was being prepared for initial service. These were identical units each rated at 600,000 lb per hr, 900 psi, 900 F.

A review of manufacturing and fabricating history failed to disclose any information that would help to discriminate between good and bad tubing.

The chrome-moly superheater tubes for these boilers were manufactured by conventional piercing and drawing operations from an alloy containing 5 per cent chromium, $^1/_2$ per cent molybdenum, and stabilized with titanium, conforming to chemical and physical requirements of ASTM A-213, Grade T-16. They were shipped to and stored in the fabricating plant as two lots, one 2 in-OD × 0.220-in. wall, and the other, 2 in-OD × 0.200-in. wall; some were 22 ft long, some were 24 ft. Altogether, there were 2300 pieces which were cut, bent, and welded as necessary, and installed as preformed sections in the wall of the radiant superheater and in the last one and one-half loops of the prefabricated elements of the convection superheater. The sections were joined in the field by manual electric-arc welding using a 25 per cent chromium, 20 per cent nickel,d-c electrode.

In terms of footage the tubes were equally distributed between the radiant and convection superheater. Most tubes as indicated in the boiler cross section, Fig. 5, were in the vertical position. Those in the radiant superheater are tangent tubes forming the rear wall of the superheater furnace, and have perhaps three fourths of the tube surface exposed for examination. This is markedly reduced as the tubes enter the ashpit slope where only one side is visible. In the convection superheater the tube rows are on 3-in. centers in both directions so that only the outermost two rows, which consist of the last pass of staggered adjacent elements, can be examined visually with any degree of accuracy.

Inspection Methods—Magnetic Particle

The primary considerations in the search for an inspection method were ability to distinguish between good and bad tubing and adaptability to the anticipated working conditions in the confined spaces of the boiler. In view of the nearly 10 miles of unfavorably oriented and notably inaccessible tubing involved, speed was an important factor; however, we were willing to sacrifice speed provided the other requirements were met.

The possibilities of the magnetic-particle method of inspection were investigated even though the method promised at best only a 50 per cent coverage. A few experiments with currents of 400 to 2000 amperes flowing through a section of tube about 5 ft long proved that a fair indication of the subsurface defects was secured only when the depth of seam exceeded 70 per cent of the tube wall. Low amperages failed to yield satisfactory indications when the tube axis was vertical, while higher values of current tended to show more false indications at scratches resulting from the cleaning by wire-brushing. Because of these indifferent results as well as the manifold unsolved problems of securing an adequate current density in the section being examined in the boiler, and the handling and positioning of electrodes, the experiments were discontinued in the hope that a more sensitive and adaptable method might be found.

Inspection Methods—Ultrasonic

The ultrasonic "reflectoscope" was the next inspection method investigated and, as evident from the title of this paper, was successful. Since its introduction during the late war, considerable data have been accumulated on the use and application of the longitudinal wave in detecting deep-seated defects in a wide range of forged and rolled products. More recently there has been a rapid expansion in the use of the shear-wave technique. The latter scheme has proved effective for locating root cracks and longitudinal bead cracks in welds and had been reported successful in the detection of longitudinal seams and defects in pipe.[2]

The basic principles of ultrasonic inspection by both the longitudinal- and the shear-wave methods are the same and have been described in detail in previous papers.[2,3,4,5] The material being examined must be homogeneous and be able to transmit a mechanical vibration such as a sound wave, meaning that it has a high modulus of elasticity.

The ultrasonic reflectoscope consists of three essential units, a pulse generator, an oscilloscope, and a searching unit. The last consists of an X-cut quartz crystal which acts as the transducer between electrical oscillations and mechanical (ultrasonic) vibrations. The pulse generator produces bursts of electrical oscillations which are fed by coaxial cable to the quartz crystal and

[2] "Ultrasonic Flaw Detection in Pipes by Means of Shear Waves," by C. D. Moriarty, Trans. ASME, vol. 73, 1951, pp. 225–235.

[3] "Supersonic Flaw Detector," by R. B. Delano, Jr., *Electronics*, vol. 19, January, 1946, p. 132.

[4] "The Supersonic Reflectoscope for Interior Inspection," by F. A. Firestone, *Metal Progress*, vol. 45, 1945, p. 505.

[5] "Symposium on Ultrasonic Testing," ASTM Special Technical Publication 101 (1951), American Society for Testing Materials.

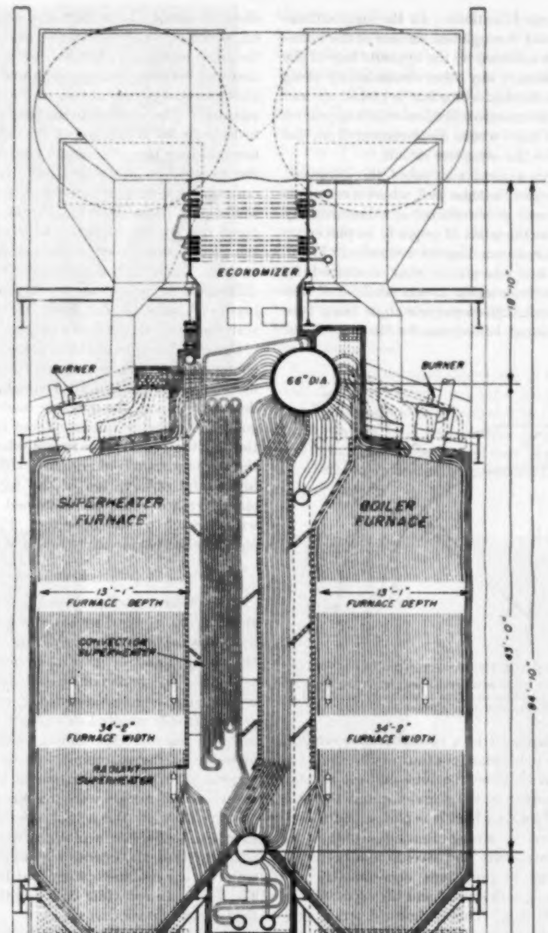

Fig. 5 Cross Section of Boiler

(Defective tubing was located in radiant superheater which forms rear wall of superheater furnace and in last 1½ loops of convection superheater.)

there converted into ultrasonic vibrations. In the longitudinal-wave method these are directed through one surface of the material as narrow beams that are reflected by the opposite face of the material or by a crack, inclusion, or any other discontinuity along the path. The reflected mechanical vibration is picked up and converted by the quartz into electrical oscillations which appear on the oscilloscope screen as a "pip" whose displacement from the origin varies with the time for the complete circuit.

In the shear-wave technique as used with tubes, the ultrasonic beam is projected at an angle into the tube wall, where it rebounds between inner and outer surfaces until reflected at a discontinuity in the metal, or comes back to the point of origin to be picked up by the searching unit. This is shown diagrammatically in Fig. 6. The successful procedure was essentially that described by Moriarty.[3] After some experimentation it was established that the smaller $^1/_2$-in-square crystal, 2.25-megacycle angle beam type was better than the conventional 1-in-square for the size of our tubing.

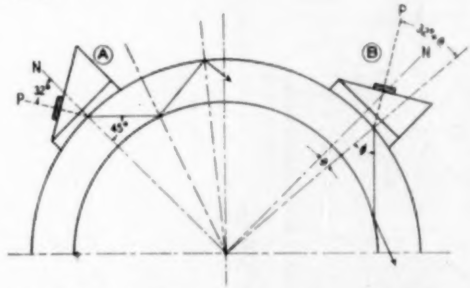

Fig. 6 Manner of Shear-Wave Propagation in Tube Wall
(A, At 45 deg to outer surface when wave is centered properly. B, At much larger angle at reduced sensitivity when incident sonic wave makes angle greater than 32 deg with tube surface.)

The searching unit was mounted in a special plastic adapter which was shaped to fit the cylindrical contour of the tube and served to preserve alignment between the tube and the crystal. The quartz crystal is so oriented in the searching unit that the angle between the plane surface on which it is placed and the resultant shear wave is approximately 45 deg. Refraction of the sonic beam at the interface between lucite and steel accounts for approximately a 13-deg change in direction; consequently, the angle between the face of the quartz crystal and the surface being examined is approximately 32 deg. This is shown diagrammatically in Fig. 6, position A, where the angle is measured between the plane of the crystal and the plane tangent to the tube. This angle is geometrically equivalent to the angle between the normal to the tangent plane (N) and the normal to the crystal plane (P).

For large crystals and large-diameter tubes, the location of the crystal with respect to the point of tangency is not critical; however, with the smaller searching unit and tubes of smaller diameter, it is important that the mid-point of the ultrasonic beam strike the tube surface very near the point of tangency. When, as in Fig. 6, position B, the point of entry of the sonic beam is displaced slightly so that the incident angle is other than 32 deg, the resultant shear wave has reduced intensity and sensitivity and may be misdirected so as to miss the inner tube wall completely. For the 2-in. tubing, the point for grinding the lucite adapter was determined with sufficient accuracy by sighting. Final adjustment of the searching unit in the adapter was made by observing the magnitude of the indication produced while exploring a short section of defective tubing.

For inspection purposes, the tube to be examined was wiped clean to remove loose dust and copiously brushed with SAE 30 oil, which acted as a lubricant, obviated minor surface irregularities or deposits, and provided continuity of sonic-wave-conducting material between the searching unit and the tube. Oil was used also to insure sonic contact of the searching unit with the lucite adapter. The composite searching unit was rocked back and forth over 90 to 120 deg of the tube circumference while slowly moved along the tube lengthwise; the pattern was analogous to the weave used in arc welding. In the examination of tubular material as distinguished from examination of plates, where the sound path has a finite length, the presence of a defect is recognized not by the existence of a pip but by its movement across the oscilloscope screen as the searching unit is moved circumferentially. It is by this movement that a pip due to a defect is differentiated from those due to interference and from the standing-wave patterns that flash on the screen solely because the searching unit moves over a relatively rough surface.

Some of the tube sections removed from the boiler during the epidemic of failures were used to test the ultrasonic shear-wave method in the shop. After standardizing on a short section of defective tubing, the operator readily differentiated between the good and defective pieces offered for examination. The indication on the oscilloscope screen was positive; the beginning and the end of a seam could be fixed within $^1/_4$ in. There was no need for careful observation of the tube surface. The entire tube circumference could be examined provided one quadrant was within reach of the operator. Furthermore, the method was equally effective for any position of the tube.

Field Inspection

There were several problems, however, that related to the use of the method in the furnace and gas passes of the boiler. The footing was not as secure, the tubes were not always straight, and the arrangement of instrument and searching unit not as convenient. The maximum length of cable between the exploring crystal and the pulse-generating unit was established at 12 ft; a greater length resulted in reduced sensitivity. Furthermore, in order to interpret the findings reliably, it is necessary that the operator of the searching unit be able to see the oscilloscope screen. The tubes of the radiant wall and the convection-superheater outlet section were examined by taking the unit into the furnace through the ashpit door and operating either from a swinging scaffold or a platform built on needle beams. In the outlet section, the operator was in the gas passes, Fig. 7(*b*), and watched the oscilloscope located beyond the tubes at his right, Fig. 7(*a*). It was while exploring the tubes of this region that the field standardization was made.

The first group of tubes were examined with extra care and constant reference to the short section of defective tubing which served as a check on instrument operation. The indications were classified as being major, medium, and minor, and their exact locations along the tubes were recorded. These tubes were removed in their entirety, cut up, and examined visually and tested for seams by deformation in a vise. In this manner it was established that all major indications were cause for removal and that minor indications invariably were due to score marks on the inner surface. The number of medium indications was small, and nothing was found wrong with the tubes examined, although score marks were present. During the course of the field inspection there were a few tubes which gave a stationary pip comparable in size to that of a major indication. When these tubes were cut and examined, no defects of any kind could be found; however, many deep draw marks were found scattered around the tube circumference.

The inspection of the radiant wall was conducted from a swinging scaffold, Fig. 8. Defective sections of tubing were found in

(a) (b)

FIG. 7 ULTRASONIC INSPECTION OF OUTLET SECTION OF CONVECTION SUPERHEATER

(Operator was located in gas passes and watched reflectoscope placed on platform on opposite side of tube bank.)

blowers and their supports. Typical working conditions at different elevations are shown in Figs. 9 and 10. In Fig. 9 the reflectoscope was turned to face the camera so as to be recognized; normally, the oscilloscope was turned toward the operator as in Fig. 10. The latter view shows the reflectoscope enclosed in a special "homemade" protective shield which was necessary because of the incongruity between the size of the access doors and the size of the instrument case.

Most of the troubles experienced were associated with the working conditions. Constant flexure of the cable adjacent to the exploring unit and the severe use of the searching unit itself caused several failures of the conducting wire. A more rugged type of construction for both the crystal holder and the cable connector would be an advantage for this type of work. The abrasive action of the tube surfaces on the lucite adapter caused it to wear rapidly and to require frequent regrinding and replacement. However, in no instance did the severity of the trouble rise above the nuisance level.

Since this initial field experience in the ultrasonic inspection of small-diameter tubing, one tube manufacturer has further developed the method and applied it to the mill inspection of tubing as small as 1 in. OD. A corresponding growth of the method as a power-plant maintenance tool may be expected as more engineers and operators investigate its possibilities in solving routine operating problems.

FIG. 8 OPERATION OF REFLECTOSCOPE FROM SWINGING SCAFFOLD DURING INSPECTION OF RADIANT WALL

FIG. 9 INSPECTION OF LAST PASS OF CONVECTION SUPERHEATER JUST UNDER ONE OF THE "KICKER" BAFFLES

FIG. 10 INSPECTION OF SAME REGION AS SHOWN IN FIG. 9, BUT AT DIFFERENT ELEVATION SHOWING REFLECTOSCOPE ENCLOSED IN SPECIAL PROTECTIVE SHIELD FOR ADMITTANCE TO FURNACE

both boilers near the roof, midway in the wall and in the ashpit slope.

The inspection of the last pass of the convection superheater was a test of both men and equipment. There were only about 20 in. of working space between the face of the tubes examined and the refractory baffle hung on the generating tubes. Vertically, the space was divided by "kicker baffles," and by soot

CONCLUSION

The ultrasonic reflectoscope was investigated and found to be a practical tool for the field inspection of small-diameter tubing. Through its use in the furnace and gas passes of two boilers, the 2-in-OD chrome-moly superheater tubes having defects of manufacturing origin were identified successfully. The replacement of these tubes alleviated a serious operating condition.

Discussion

J. H. Eddy, Jr.[6] In reviewing Mr. Tash's paper it is felt that certain statements should be clarified from a practical standpoint. Having supervised and performed the actual reflectoscoping operation of the boilers, on which this paper is based, the writer offers the following comments:

In the plastic adapter, Plexiglas, not lucite, was used for it seemed to give better results, especially in obtaining the correct angle of refraction.

In the use of the plastic adapter it was found that if the thickness was greater than $^3/_{32}$ in. at the tangent point, the response was damped almost to the point where interpretation of the picture on the oscilloscope screen was impossible. The contour of the working face of the plastic adapter must be in perfect alignment and centered with respect to the searching head and crystal.

If any air bubbles are present between either the plastic adapter and the searching unit, or the boiler tube and the adapter face, false indications might readily result. This was especially troublesome when the plastic was worn down by continuous usage to less than $^1/_{32}$ in., and the adapter piece would readily flex or bend allowing the bubbles to form. However, with careful manipulation, the best indications were obtained with the adapter at minimum thickness.

The main failures occurred in the connecting wire in the searching unit itself. Continued usage seemed to cause the soldered connection of the wire to the back of the crystal to break loose. The construction of the searching unit had to be flexible enough to assemble and repair when necessary. It is believed the design has been improved to eliminate such failures. The continuous presence of fly ash and dust in the boiler made it necessary to completely clean the connecting wire from the searching head to the instrument at least two or three times a day to minimize breakdowns.

It is imperative to have a test specimen available so that the reflectoscope may be frequently adjusted and calibrated. In this manner false indications can be eliminated and any breakdown of the equipment detected.

Operating the reflectoscope at the maximum speed resulted in the removal of ninety tubes from these boilers. Sixty per cent of the tubes removed were checked by other means and of these, ninety per cent were found to be defective.

[6] Service Department, Foster Wheeler Corporation, New York, N. Y.

Author's Closure

Mr. Eddy's explanatory remarks and the correction on the brand of plastic used are appreciated. Lucite and plexiglas are both clear thermoplastic materials of the methacrylate type and for most uses are interchangeable; however, in our testing the plexiglas was the superior ultrasonic coupling material. Whether this superiority of plexiglas is characteristic of the material or of the particular pieces tried has not been determined.

Each new application of ultrasonic testing is essentially a modification of a previously established testing procedure. Consequently, in the interest of brevity, many details and principles of our testing procedure were omitted from this paper since they have been adequately covered in the publications of the footnotes. In any application of ultrasonic testing judicious experimentation is generally more fruitful than theoretical computations; for, as Hasting and Carter stated (footnote 5, p. 36), "regardless of the means of detection employed, the interpretation of test results is primarily based upon a knowledge of the basic theory regarding ultrasonics and a certain amount of actual experience." The necessary experience is acquired only by trial and error testing and comparison of samples with and without known defects.

Methods of Reducing Dust Emission From a Spreader-Stoker-Fired Boiler Furnace

By W. C. HOLTON[1] and R. B. ENGDAHL,[2] COLUMBUS, OHIO

Forty-seven tests were made on a continuous-ash-discharge spreader-stoker-fired boiler to determine means of reducing dust emission. In addition to burning rate, variables investigated were the amount of overfire air, the use of air, steam, and steam-air jets, the location of steam jets, the degree of reinjection used, and coal size. These tests showed that the use of overfire-jet turbulence decreased smoke density, carbon loss, and dust emission from the furnace. It was found that steam jets located low in the rear wall gave the lowest dust emission. Reinjection of all collected cinder decreased carbon loss to one fourth of its value without reinjection, but doubled the dust-loading of the stack gases. The use of double-screened coal was found to reduce dust emission appreciably.

This project was organized by Bituminous Coal Research, Inc., which obtained the participation of the American Engineering Company, Combustion Engineering-Superheater, Inc., Detroit Stoker Company, Hoffman Combustion Engineering Company, Iron Fireman Manufacturing Company, Riley Stoker Corporation, and Westinghouse Electric Corporation. The project was also supported by the General Motors Corporation which furnished the test site, special test facilities, and the coals used.

PLANT operators have been quick to recognize the ability of the spreader stoker to burn coals of a wide range of size and type, to respond quickly to load changes, to operate easily, and to require a minimum of maintenance, even when operating at high burning rates. The design permits ready synchronization with most types of boilers to meet widely different plant-space conditions. Because of these advantages, the number of spreaders installed has increased greatly in the past few years. At the same time that spreader-stoker installations have become more common, increased attention has been directed toward the subject of air pollution. Public demands for the abatement of smoke and dust nuisance, regardless of the source, have often been directed toward suspension-burning devices, such as the spreader.

Little factual information was available on the amount and methods of reducing the carry-over from spreader-stoker-fired boilers. To obtain the desired information, a Spreader Stoker Research Committee was formed in 1948, by the sponsors named in the "abstract," to develop and conduct a program of research. After considering a number of possible test locations, the boiler plant of the Brown-Lipe-Chapin Division of General Motors Corporation in Elyria, Ohio, was chosen as the most suitable test site. Battelle was asked to conduct the tests and analyze the results.

[1] Battelle Memorial Institute.

[2] Supervisor, Battelle Memorial Institute. Mem. ASME.

Contributed by the Fuels and Power Divisions and presented at the Semi-Annual Meeting, Toronto, Ont., Can., June 11–15, 1951, of The American Society of Mechanical Engineers.

Note: Statements and opinions advanced in papers are to be understood as individual expressions of their authors and not those of the Society. Manuscript received at ASME Headquarters, March 2, 1951. Paper No. 51—SA-20.

Objectives of Spreader-Stoker Research Program

The original objectives of the program were to obtain factual information on the amount of, and methods of reducing, cinder and fly-ash carry-over from spreader-stoker-fired boiler furnaces. To obtain these objectives, the effect on dust emission of the following factors was to be investigated:

1. Overfire air and cinder reinjection, singly or combined.
2. Percentage of overfire air.
3. Steam jets.
4. Steam-air jets.
5. Location of steam jets.
6. Partial and total reinjection.
7. Coal size.

Test Plan

The first step was to determine the dust loading obtained when operating without overfire-air jets or cinder reinjection, in order to obtain a base point to use in future work. Tests were then run under normal operating conditions, that is, using 5 per cent overfire air with total cinder return. These results, which were representative of good operating practice in the test plant, gave other base points for comparison.

Other tests were planned to determine what other operating variables might be changed to reduce dust emission. Other criteria used in evaluating test results were smoke density, carbon loss, and the percentage of CO_2 in the flue gas. The additional tests were planned around the investigation of the seven operating variables previously outlined.

Apparatus

Plant Equipment. Fig. 1 shows a side elevation of the test plant. The boiler is a Wickes 60,000-lb per hr four-drum bent-tube unit, which was erected in 1946. Three sides of the furnace are water-cooled. No superheater, air heater, or economizer is provided. All tubes are $3^1/_4$ in. OD; waterwall tubes are 9 in. on centers, and bridge-wall tubes 6 in. on centers. This unit is fired by a Detroit Rotograte (continuous-ash-discharge) spreader stoker consisting of three feeders and a grate 10 ft $1^1/_2$ in. wide and 14 ft 8 in. between centers of the grate sprockets. The area of grate inside the furnace proper was taken as 131.25 sq ft, and the furnace volume as 2600 cu ft; total furnace volume is 2900 cu ft.

Primary air is furnished by a No. 360 American Blower forced-draft fan driven by a 28-hp Elliott turbine. Cooling air, which is admitted to the furnace under the stoker feeders, is taken off the primary-air duct. Overfire air is supplied to the furnace by a Buffalo Forge Type 6-E blower with a $7^1/_2$-hp motor operating at 3600 rpm. This air is admitted to the furnace through three jets and two reinjection nozzles located in the rear wall, all five jets being 18 in. from the grate and pointed down toward the imaginary intersection of the front wall with the grate. Five overfire jets are also located 18 in. from the grate in the front wall, but are pointed in a horizontal plane. This front-wall overfire air is automatically varied with load by a mechanical linkage to the fuel-feed control.

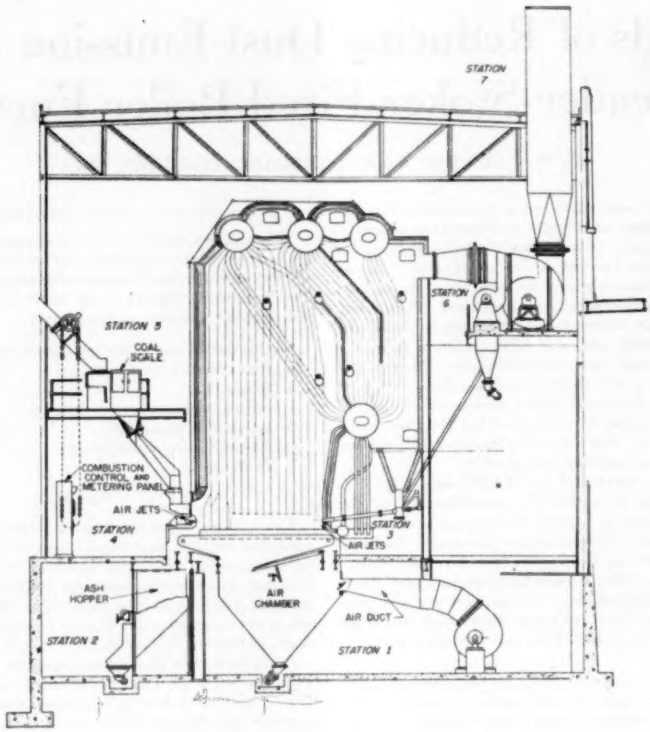

FIG. 1 SIDE ELEVATION OF BOILER TEST PLANT

A Sturtevant fly-ash-separating induced-draft fan provides a measure of dust collection as well as induced draft. The main purpose of the collector section of this fan is to protect the impeller rather than to reduce stack emission. The fan is powered by an Elliott turbine, and the secondary (blowdown) fan is powered by an electric motor. Cinder from the collector hopper is normally piped to the boiler hoppers, where it is aspirated with the boiler cinder into the furnace. No rotary valves or other sealing devices are used between the collector hopper and the boiler hoppers. A stub stack is mounted directly on the outlet of the induced-draft fan.

Instrumentation of the boiler and furnace consists of a Bailey steam flowmeter, draft gages, and combustion control.

Coal is dumped into a track hopper under a railroad siding which discharges to an apron conveyer and then to a vertical bucket elevator. Coal may be placed by a scraper conveyer into one of two coal silos (each of which has a live storage capacity of 45 tons, and dead storage capacity of 305 tons), or may be chuted into yard storage. A reclaim apron conveyer moves coal from the reclaim hoppers, into which it is pushed by a bulldozer, into the vertical elevator. Coal flows by gravity from live storage to an automatic Stock coal scales and through a Stock coal chute to the stoker hoppers.

Ash disposal is effected by a United Conveyer "Nuveyor" system which is piped to the collector hopper, grate ash hopper, and undergrate (siftings) hopper. Ash is discharged into a 50-ton silo.

The output of the boilers is normally used to supply process steam and heating load, and to drive a large air compressor. Because much of the process steam is lost and, consequently, a large amount of make-up must be supplied, the plant uses a 240,000 lb per hr water-treatment system.

Test Equipment. Sufficient additional instrumentation was installed in the test plant to obtain complete information on rates of air flow and cinder and ash collection. Primary-air flow was determined by readings of Kiel tubes, which measured impact pressure, coupled with a piezometer ring for measurement of static pressure. The differential pressure was read on an inclined manometer, and the static pressure by means of a vertical water column. The temperature of the primary air was read from a thermometer inserted in an oil-filled well which was welded into the duct. The amounts of high-pressure (overfire) and cooling air were determined from readings of the differential pressure between piezometer rings and impact tubes with which the ducts were traversed. As in the primary-air duct, temperatures of the air in the duct were recorded. Wet and dry-bulb thermometers were placed at the inlet to the high-pressure blower (or the forced-draft fan, when overfire air was not used) to determine the room temperature and the amount of moisture in the air. All readings used in obtaining air-flow rates were taken hourly. A check on the total air-flow rate was furnished both

by the Pitot tube used in dust sampling and by the gas-flow rate calculated from the Orsat analysis of the flue gas.

Refuse discharged from the traveling grate was removed from the hopper hourly, was weighed, sampled, and then dumped into the ash-conveyer system. This was done hourly during the test, except when the rate of flow was heavy, in which case the hoppers were cleaned every 30 min. The hopper doors were kept closed as much as possible to avoid undue disturbance to the furnace draft. The small amount of ash that sifted through the grate was removed from the undergrate (windbox) hopper as soon as possible after each test. When it was established that this weight of ash was negligible, no more weights were recorded.

In addition to recording the usual pressures and drafts from the instruments on the main control board, the grate speed was recorded during two series of tests. Feedwater temperature was also recorded for use in calculations. Quality of the steam was not measured; saturation was assumed in the calculations. The steam-flow rate was calculated from the readings of the meter integrator for all but the last 18 tests, in which the curves were integrated manually.

Cinder from the boiler hoppers was removed periodically during each test (except in eleven tests); it was weighed, sampled, and either returned to the furnace or discarded, according to the conditions of the test. The cinders were returned either by steam or by air ejectors, which aspirated the material first from barrels on the floor, but later from hopper-bottomed barrels placed overhead on a temporary platform erected below the collector hopper. Barrels of cinder first were hoisted with a block and tackle but later by an electric hoist. Boiler cinder to be discarded was dumped into the ash-conveyer system.

The weight rate of coal flow was obtained directly from the dump counter on the Stock scales by taking readings every half-hour. Samples of coal for chemical and size analyses were taken by passing a scoop across the conveyer belt while coal was being fed into the scale hopper. The scales were calibrated at frequent intervals to insure accurate weight measurements.

Cinder from the dust-collector hopper was first removed through a double-valved lock-hopper arrangement which prevented flow of air into the collector. This material was weighed, sampled, and returned to the furnace or discarded, according to the test conditions. At first, reinjection was accomplished by air or steam-jet ejectors drawing the cinders from barrels on the floor. Difficulties with this system led to the construction of a temporary platform below the collector. The lock hopper was moved to this location, and the collector cinder, after being weighed, was removed from the hopper-bottomed barrel by gravity and the ejector suction. For the last tests, the lock hopper was replaced by an arrangement which made it possible to collect cinder in one barrel while reinjecting the material from another. In this way the barrels were alternated to give a steady flow of cinder when reinjecting. Slide gate valves were used at both the inlet and outlet of the open barrels. The operators were careful to see that no air leaked into the collector hopper through an open valve or into the ejector suction through the empty barrel.

At another test station, adjacent to the induced-draft fan, the Orsat equipment, smoke recorder, and temperature recorder were located. Gas-sampling lines from each of the two ducts leading to the induced-draft fan were brought to the Orsat, connected to a manifold, and gas samples were withdrawn by means of an air aspirator. A photoelectric smoke meter connected to a recording potentiometer, calibrated in Ringelmann numbers, was used. Six chromel-alumel thermocouples were placed in each of the offtake ducts at approximately the centers of equal areas. The thermocouple wires were led to a 12-point recording potentiometer.

Dust emission from the stack was obtained by traversing the stack, using equipment and procedure as outlined in the ASME "Test Code for Dust Separating Apparatus." The apparatus consisted of a Pitot tube, sampling tube with various sizes of nozzles for use at varying stack-gas-flow rates, a small cyclone separator for removal of coarse particles, a can to hold the bag used to retain the finer dust particles, blowers (or ejectors) to furnish suction, and the necessary barometer and gages. The flow rate of gas withdrawn from the stack was measured with a Venturi. In most cases, it was necessary to restrict sampling time to 8 min for each point of the 10-point traverse (in one direction) in order to obtain sufficient points during the test for an accurate determination of dust concentration. Wherever possible, two complete traverses of the stack were made during the course of each test. Sampling points were chosen as centers of equal areas, each representing one tenth the stack area.

Test Procedure

The boiler-plant operators were given instructions to bring the steam output of the boiler up to the load at which the test was to be run, about 2 hr before the start of the test. For low-load tests, two boilers were carried on the line, with the boiler on test being held at fixed output and the plant-load fluctuations being carried by the second boiler. For tests at full load, only one boiler was used. Excess steam was vented to the atmosphere during full-load tests when the plant load was low. In all cases, the boiler was operated at test conditions for a period sufficiently long to allow for stabilization of bed conditions, temperatures, and steam output before the actual test was begun. This included the operation of the reinjection system before tests which were to be run under this condition.

Ideally, the length of run preliminary to any test should have been determined by the length of time required for the grate to discharge all the fuel bed which had been built up prior to the test. In the case of the low-load tests, this time would have been prohibitive in view of the 8-hr duration of some of the tests. Consequently, the preliminary run usually did not exceed 2 hr in length. During the period before each test, the stoker settings, overfire-jet pressures, and grate speed necessary for best operation were established. The operators attempted to operate for the duration of the test without changing these settings, in order to assure operation at steady state.

Nearly half the tests were run for an 8-hr period. The remaining tests lasted 4 hr.

Calculations

Although samples of coal were taken during each test, only one ultimate analysis was made for each group of tests with a given coal. This analysis was made of a composite sample which was made up of portions taken during the individual tests. Because coal samples were analyzed for ash and moisture content for each test, it was possible to calculate an ultimate analysis for each test in a given group. Heat-balance calculations were then made using the calculated ultimate analysis.

The general form of the calculations was that of the short form presented in the ASME "Test Code for Stationary Steam-Generating Units." Radiation loss was taken from the ABMA Radiation Loss Chart presented in this test code.

Emission of dust from the stack was determined by withdrawing a sample of stack gas and dust at a rate of flow equal to that in the stack at the sampling point. This was accomplished by calculating the Venturi differential using the Pitot-tube differential and the ratios of static pressures and absolute temperatures at the stack and Venturi. The flow rate of stack gas was calculated from the measured Pitot differentials across the traverse. The weight of (dried) dust collected, multiplied by the ratio of areas of the stack and sampling nozzle, using a time-conversion

factor, gave the dust emission from the stack in pounds per hour at test conditions.

In order to compare dust emissions obtained from a group of tests, it was necessary to express dust loading in terms of standard conditions. For this work, standard conditions were taken as being 50 per cent excess air and 500 F, as recommended in the ASME "Example Sections for a Smoke Regulation Ordinance," 1949. The conversion from test conditions to standard conditions was made by assuming the weight rate of flow of stack dust to be constant.

Dust loadings were also calculated at the furnace outlet and boiler outlet. The furnace outlet was taken as any location in the first pass of tubes, i.e., a point before the boiler hoppers. The term, as used in this report, is synonymous with collector inlet. No attempt was made to obtain accurate dust loadings at these points directly because of the extreme difficulty of sampling in turbulent gas streams. The dust loading at the boiler outlet was obtained by adding the weight rate of flow of stack dust to that of cinder from the collector (which addition gives the weight rate of flow of cinder at the boiler outlet) and dividing this sum by the weight rate of flow of stack gas (adjusted to standard conditions). The rate of flow of dust at the furnace outlet was assumed to be the sum of the weight rate of flow at the boiler outlet and the weight rate of flow of cinder from the boiler hoppers. This total was then divided by the (adjusted) weight rate of flow of stack gas to obtain the furnace-outlet dust loading.

Test Results

The detailed results of the most important tests and the comparisons drawn in evaluating these results are presented below. These are subdivided to facilitate discussion and to emphasize the effect of the major changes in imposed operating conditions.

Effect of Overfire Air With and Without Reinjection at Various Load Conditions. Fig. 2 shows the variation of smoke, CO_2, carbon loss in per cent of the heating value of the coal, and dust-loading at the furnace outlet as a function of burning rate for the following conditions:

1 No overfire-air jets and no reinjection.
2 No overfire-air jets with reinjection.
3 Overfire-air jets without reinjection.
4 Overfire-air jets with reinjection.

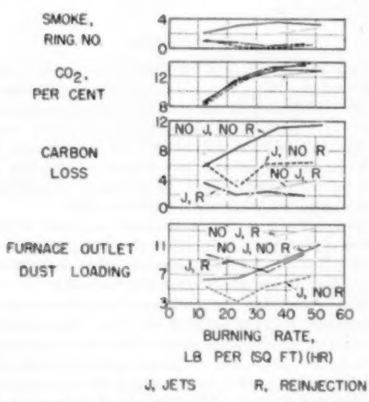

Fig. 2 Evaluation of Comparative Degrees of Reinjection for Tests With and Without Reinjection at Several Loads

(Carbon loss reported in per cent of available heat in coal. Dust loading is in lb dust per 1000 lb gas, adjusted to standard conditions.)

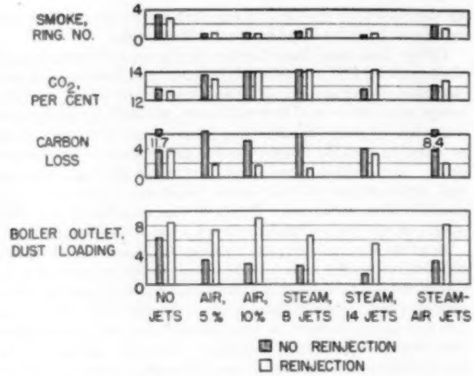

Fig. 3 Comparison of Results Obtained From Full-Load Tests With Several Types of Overfire Jets, With and Without Reinjection

(Steam-air jets located 68 in. from grate in front wall. All other jets 18 in. from grate in front and rear walls. Carbon loss reported in per cent of available heat in coal. Dust loading is in lb dust per 1000 lb gas, adjusted to standard conditions.)

From this plot the following observations may be made:

1 Overfire-air jets reduced smoke density to No. 1 Ringelmann, or less, even when operating with total reinjection.

2 Overfire-air jets, either alone or with cinder reinjection, do not increase the percentage of CO_2 in the flue gas significantly.

3 Carbon loss found when operating without jets or reinjection is decreased by one half when jets alone are used, and is again cut by one half when all collected cinder is returned to the furnace.

4 The lowest dust loading at the furnace outlet was obtained when using overfire air but no reinjection, as would be expected. Above one-half load, the dust loading for tests with both overfire air and cinder reinjection was lower than that calculated for tests with neither jets nor injection.

Thus it is seen that the use of overfire-air jets improves boiler performance by reducing smoke emission, decreasing carbon loss, and reducing dust loading (when operating above one-half load).

Effect of Various Types of Jets at One Location With and Without Reinjection. Fig. 3 presents the results of full-load tests run with one coal, both with and without total cinder return, with the following arrangements for providing turbulence (all but the steam-air jets were located the same distance from the grate in both front and rear walls, and were parallel to the side walls):

1 No jets.
2 Overfire-air jets supplying 5 per cent of the total air.
3 Overfire-air jets supplying 10 per cent of the total air.
4 Four steam-air jets in the front wall, 68 in. from the grate, pointed downward.
5 Eight steam jets, in the same location as the air jets.
6 Fourteen steam jets at the same elevation as the air jets, but more closely spaced.

The major conclusions which can be drawn from these data are as follows:

1 As long as some form of turbulence is provided, neither the type of jets used nor the addition of cinder reinjection affects smoke density materially. The steam-air jets used were less successful in reducing smoke than other jets tested. It is thought

that this poor performance should be attributed to improper location of the jets.

2 The CO_2 content of the flue gas does not vary significantly for these conditions.

3 Steam jets were responsible for the lowest values of carbon loss obtained; the eight jets gave less loss for total reinjection, but the fourteen jets resulted in the lowest value for the tests without reinjection.

4 The fourteen steam jets gave the lowest dust loadings at the boiler outlet, both with and without reinjection.

Although these results indicate that steam jets are more effective than air jets in reducing carbon loss and dust emission, it should be noted that this steam cost from 5 to 7 times as much as the overfire air.

Comparison of Results Obtained With Various Degrees of Reinjection. Fig. 4 presents an evaluation of tests conducted with no reinjection, partial reinjection (that is, cinder return from the boiler hoppers only), and total reinjection. It will be noted that

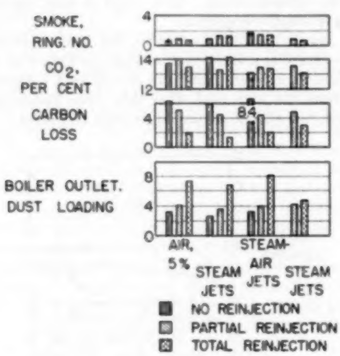

FIG. 4 EVALUATION OF COMPARATIVE DEGREES OF REINJECTION FOR FULL-LOAD TESTS

(Carbon loss reported in per cent of available heat in coal. Dust loading is in lb dust per 1000 lb gas, adjusted to standard conditions.)

these data are from tests using steam, air, and steam-air jets, and that two sizes of Ohio Pittsburgh No. 8 coal were used.

This figure brings out the following conclusions:

1 The degree of reinjection does not affect smoke density.

2 These tests show no appreciable variation in the percentage of CO_2 in the flue gas.

3 Returning cinder from the boiler hoppers to the furnace decreases carbon loss 2.3 to 4.1 percentage points. Reinjection of all cinder collected (both in boiler and collector hoppers) gives a further decrease of 2.1 to 2.8 percentage points.

4 When compared to the dust-loading obtained under conditions of no reinjection, partial reinjection increases dust loading at the "boiler outlet" 20 to 40 per cent, but total reinjection increases this loading by 125 to 155 per cent. If comparisons are based upon dust loading at the "stack," partial reinjection increases loading 20 to 90 per cent, and total reinjection increases the dust loading 60 to 160 per cent.

If the absence of restrictive smoke ordinances or the use of a high-efficiency dust collector permits a plant to operate with total reinjection, valuable savings in fuel result.

Effect of Number of Steam Jets. Fig. 5 shows the effect of using eight versus fourteen steam jets, all at the same elevation. Five jets were used in the front wall on all tests. Results are presented for two sizes of washed Ohio Pittsburgh No. 8 coal,

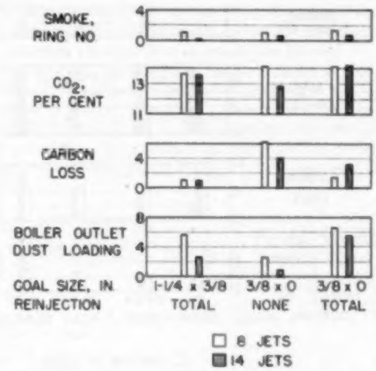

FIG. 5 COMPARISON OF TEST RESULTS SHOWING EFFECT OF NUMBER OF JETS

(Carbon loss reported in per cent of available heat in coal. Dust loading is in lb dust per 1000 lb gas, adjusted to standard conditions.)

operating with and without cinder return. These results show:

1 Increasing the number of jets from eight to fourteen has little practical effect on smoke density.

2 With one exception, the values of CO_2 reported are quite similar. It is thought that the lowest value (12.9 per cent) should be attributed to general test conditions rather than to the number of jets used.

3 No clear trend in carbon loss can be credited to increasing the number of jets.

4 Increasing the number of jets decreased the dust loading at the boiler outlet by 17 to 53 per cent.

In general, increasing the number of steam jets used improved boiler performance.

Effect of Jet Location. Fig. 6 presents the results of tests at one fifth and at full loads using four locations of steam jets. All tests were run without reinjection using Ohio Pittsburgh No. 8 coal, $^3/_8 \times 0$ in. Five front-wall jets, 18 in. from the grate, were used in all tests. This was done primarily to cool the air nozzles in which the jets were placed. The front-wall jets have little added effect on smoke density. From this plot the following observations may be made:

1 Jet location has little effect on smoke density.

2 The percentage of CO_2 in the flue gas does not appear to be a function of the jet location.

3 The lowest carbon loss was obtained when using jets low in the rear wall.

4 Placing jets low in the rear wall contributed to low dust loading at the furnace outlet.

With respect both to carbon loss and dust loading, the results of the full-load tests with jets in the rear wall at 18 or $28^1/_4$ in. from the grate are quite similar. Had the second full-load test at the 18-in. location not been run, the results would have indicated the optimum location to be $28^1/_4$ in. Because the second full-load test at the 18-in. location gave the best results, it is concluded that either location would probably be equally satisfactory.

The results of the test at one-fifth load with jets at 18 in. are not considered in this discussion. In this test, the rate of flow of cinder from the collector was abnormally high. This was reflected in the dust loading at the furnace outlet, which seems to be too high to be reliable.

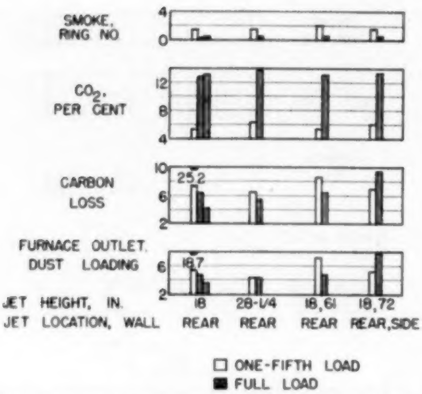

Fig. 6 Comparison of Results Obtained From One-Fifth and Full-Load Tests Without Reinjection, Using Several Jet Locations

(Front-wall jets 18 in. from grate used on all tests. Carbon loss reported in per cent of available heat in coal. Dust loading is in lb dust per 1000 lb gas, adjusted to standard conditions.)

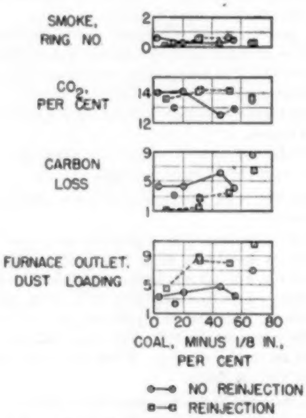

Fig. 7 Effect of Coal Size on Results of Full-Load Tests With and Without Reinjection

Carbon loss reported in per cent of available heat in coal. Dust loading is in lb dust per 1000 lb gas, adjusted to standard conditions.)

These results indicate that low rear-wall jets were the most effective tested with regard to carbon loss and dust emission.

Effect of Coal Size. Fig. 7 is a plot of smoke density, CO_2, carbon loss, and dust loading as a function of coal size for tests with and without reinjection. All tests plotted were run at full load. The points not connected were obtained with either Illinois or West Virginia coal, characteristics of which are different from those of the Ohio Pittsburgh No. 8 coal which was used in the other tests plotted. For these tests, nine steam jets in the rear wall and five steam jets in the front wall, all 18 in. from the grate, were used.

The following conclusions may be drawn from a consideration of the results of tests run "without reinjection:"

1 Smoke density is not affected by coal size.

2 Coarse coal gave higher values of CO_2 than were found with coal containing larger percentages of minus $^1/_8$-in. material.

3 Carbon loss is not greatly affected by coal size.

4 The dust-loading at the furnace outlet increased slightly with increasing amounts of minus $^1/_8$-in. coal.

The tests run with reinjection show the following:

1 Coal size has little effect on smoke density.

2 The percentage of CO_2 in the flue gas did not vary significantly for the coals tested.

3 A very definite trend toward lower carbon loss was noted when using coals containing only 30 to 50 per cent of material passing a $^1/_8$-in. screen.

4 The use of coarse coal results in low dust loadings at the furnace outlet when operating with total reinjection.

The most important over-all conclusion which may be drawn is that the use of coal containing a small percentage of minus $^1/_8$-in. material contributes to low carbon loss and low dust loadings at the furnace outlet. This trend is most marked when operating with total reinjection.

Fig. 8 shows the dust loading at the furnace outlet, boiler outlet, and stack as a function of coal size for tests with and without reinjection, all tests being run at full load. Again, the results of tests run with coal other than Ohio Pittsburgh No. 8 are plotted, but are not connected to other test points.

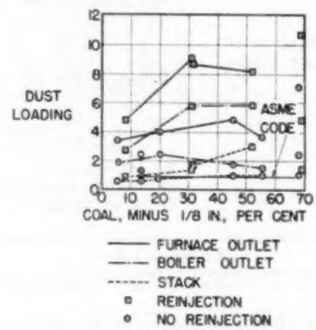

Fig. 8 Dust Loading at Furnace Outlet, Boiler Outlet, and Stack, Expressed as a Function of Coal Size for Tests With and Without Reinjection

(Dust loading is in lb dust per 1000 lb gas, adjusted to standard conditions.)

This figure is included to show the effect of the dust collection of the boiler hoppers and the induced-draft-fan collector, as well as the effect of coal size, on dust loading at various points. It will be noted that the curves for emission at the furnace outlet are quite steep, whereas the slope decreases for the boiler outlet. At the stack, the results for the tests without reinjection plot nearly on a straight line.

Summary

The most significant results of these tests are as follows:

1 Jet turbulence, whether provided by steam or by air, is needed to assure low smoke densities required by municipal ordinances. The use of overfire jets also reduces the carbon loss and dust emission from the furnace. The lowest dust emission was obtained when 14 steam jets (nine jets low in the rear wall, plus five jets in the front wall) were used. This condition also gave the lowest carbon losses for the tests without reinjection, but the test with eight steam jets (three jets low in the rear wall,

plus five jets in the front wall) showed the lowest carbon loss for the tests with total cinder reinjection.

2 Reinjection of cinder from the boiler hoppers decreased carbon loss 2.3 to 4.1 percentage points, while increasing dust loading from 20 to 40 per cent. Returning all the collected cinder (from both boiler and collector hoppers) to the furnace gave a further decrease in carbon loss of 2.1 to 2.8 percentage points at the expense of an increase in dust loading of 125 to 155 per cent.

3 The use of coal containing a small percentage of minus $^1/_8$-in. material resulted in lower values of carbon loss and dust loading at the furnace outlet than were found with finer coal. This decrease was not so great at either the boiler outlet or the stack. In no case was the dust loading at the boiler outlet reduced enough by burning double-screened coal to enable the plant to meet the proposed smoke ordinances without the use of a collector. Coal size had a negligible effect on smoke density. Oil treatment of coal had no appreciable effect on dust emission.

Acknowledgments

The authors wish to give recognition to the efforts of W. S. Major, formerly BCR Development Engineer, who not only conceived this investigation, but also supplied much of its initial impetus. The generosity and co-operation of the General Motors Corporation, H. F. Rech, Director of the Power Section, in making the test plant available and in providing the coal used for the tests, contributed in large measure to the success of the investigation. The interest and helpfulness of R. F. Hanson of the General Motors Power Section, and of G. S. Cole, H. B. Wilson, and H. E. Esch, of the Elyria plant, are also gratefully recognized. The work of H. M. Carlson, formerly of Battelle, who supervised the test crew for the first half of the tests, provided a good pattern for the remainder of the tests.

The financial support of the member companies of the Spreader Stoker Research Committee and of Bituminous Coal Research, Inc., which made this work possible is also gratefully recognized.

The members of the Spreader Stoker Research Committee themselves contributed valuable advice in planning the test program and helped greatly in the evaluation of the test results.

Also, acknowledgment should be made of the co-operation of those member companies of the Spreader Stoker Research Committee who provided men for the test crews. This group of men, who remain anonymous because of space limitations, includes the Battelle staff members who assisted in the performance of the tests.

Appendix

Physical and Chemical Characteristics of Coals Tested

Table 1 presents the description of the coal (mine, seam, and nominal size), the size consist (as expressed by the percentage minus $^1/_4$ and minus $^1/_8$ in.), and the ultimate analysis of each of the coals used in the tests. Proximate analyses included were furnished by the mines and were adjusted to the values of ash and moisture found by the ultimate analyses.

Physical Characteristics of Emitted Solids

Size Consist. Samples of cinders and dust taken from the boiler hoppers, collector hoppers, and stack were screened after each test. Using the resulting data plus the weight rate of flow at each of the sampling locations, it was possible to calculate the probable size consist of cinders which would be carried in the flue gas at the furnace outlet and at the boiler outlet. Examination of these analyses showed a wide spread in size consist and a lack of correlation of screen sizing to operating conditions. Thorough evaluation of the results was complicated by the lack of check-test results which would have established the degree of reproducibility of the data. Considering the normal spread in results of screen sizing of identical samples, no clear effect of any of the operating variables on size consist can be seen.

Table 2 presents, for reference, the size consist of cinders collected from full-load tests with total reinjection, in which several forms of jet turbulence were used. These data show the narrow range of percentages noted in the foregoing. Approximately 88 and 99 per cent of the cinders from the boiler hoppers and the collector, respectively, passed through a U. S. standard 20-mesh (0.0331-in.) sieve.

TABLE 2 SIZE CONSIST AND COMBUSTIBLE CONTENT OF CINDERS COLLECTED FROM BOILER AND COLLECTOR HOPPERS DURING FULL-LOAD TESTS WITH TOTAL REINJECTION USING SEVERAL FORMS OF TURBULENCE

	Per cent under U. S. standard screen, mesh				Per cent combustible
	60	100	200	325	
Sample from boiler hoppers					
Turbulence, by means of:					
5 per cent air	9.2	3.2	1.6	0.6	59.7
10 per cent air	20.6	8.0	2.3	1.5	62.3
8 steam jets	18.3	5.0	1.3	1.1	72.4
14 steam jets	7.8	3.2	1.7	1.3	49.6
Sample from collector hoppers					
Turbulence, by means of:					
5 per cent air	65.2	48.8	29.2	16.4	41.9
10 per cent air	73.7	60.0	30.1	19.1	24.7
8 steam jets	79.3	63.5	32.5	19.2	32.6
14 steam jets	81.2	62.4	31.0	14.8	65.7

TABLE 3 SIZE CONSIST AND COMBUSTIBLE CONTENT OF CINDERS AND DUST IN FLUE GAS AT SEVERAL LOCATIONS IN INSTALLATION FOR FULL-LOAD TESTS WITH REINJECTION USING SEVERAL FORMS OF TURBULENCE

	Per cent under U. S. standard screen, mesh				Per cent combustible
	60	100	200	325	
Sample from furnace outlet[a]					
Turbulence, by means of:					
5 per cent air	57.4	45.9	33.1	30.5	44.6
10 per cent air	64.5	53.0	33.1	25.3	34.4
8 steam jets	60.7	48.0	30.6	22.8	46.6
14 steam jets	65.8	57.3	42.3	30.5	55.7
Sample from boiler outlet[b]					
Turbulence, by means of:					
5 per cent air	72.3	59.1	42.9	26.7	39.9
10 per cent air	78.8	67.7	43.3	33.1	25.3
8 steam jets	83.8	71.4	46.5	34.6	32.8
14 steam jets	80.9	79.6	59.0	42.6	58.0
Sample from stack					
Turbulence, by means of:					
5 per cent air	98.8	97.4	93.8	65.0	32.2
10 per cent air	99.7	99.4	97.7	92.2	27.8
8 steam jets	99.7	99.3	96.4	89.3	34.3
14 steam jets	98.2	95.9	85.5	68.9	50.7

[a] Calculated from size consist and rate of flow of cinders from boiler hoppers, collector hoppers, and stack.
[b] Calculated from size consist and rate of flow of cinders from collector hoppers and stack.

Table 3 shows the size consist of cinders and dust carried in the flue gas at several locations in the installation. The data for the furnace-outlet and boiler-outlet locations were calculated, but those for the stack were obtained by screening the sample obtained with the dust-sampling apparatus. No significant trend can be observed from these results. About 96 and 99 per cent of the cinders at the furnace outlet and boiler outlet, respectively, passed through a U. S. standard 20-mesh sieve.

Although the data presented are of general interest, greater attention has been focused on the subsieve size consist of cinders. This information is of considerable importance to anyone interested in the design of equipment for dust collection. In order to extend the applicability of these data, subsieve-size analyses were made, using samples collected from ten tests. Portions of the material removed from the dust collector and from the stack were combined in weight ratios determined from the calculated collector efficiency. The infrasizer was used to determine the size consist.

The results of this analysis showed a surprising uniformity of

TABLE 1 ANALYSES OF COALS TESTED

Number of tests	10	8	5	10	1	2	1	2	2	1	1	1	2	1
Coal description:														
Mine	A								B	C		D	E	F
Seam	Ohio Pittsburgh No. 8											Miller "B"	Island Creek	Illinois No. 5[a]
Nominal size, in.	3/8 x 0				3/4 x 0		1-1/4 x 3/8		1/2 x 0	1-1/2 x 0		1-1/4 x 0	1/4 x 0	3/4 x 0
Average per cent:														
Minus 1/4 in.	68.7	67.9	64.9	65.9	70.8	52.9	7.7	10.8	73.0	42.9	36.3	73.3	95.4	30.4
Minus 1/8 in.	43.0	41.9	41.7	43.3	13.3	35.4	3.7	5.5	48.9	26.3	20.0	51.2	68.0	13.5
Treatment	Washed								None					Washed
Ultimate analysis of composite sample, per cent by weight:														
C	71.3	71.0	67.5	71.0	72.5	71.6	71.7	71.6	64.0	68.7	67.7	80.1	76.4	67.0
H_2	5.0	4.7	4.5	5.1	5.0	4.9	4.9	4.9	5.4	4.7	4.7	4.6	5.1	4.5
N_2 (by difference)	1.2	1.2	1.0	1.2	1.2	1.2	1.4	1.2	1.0	1.1	1.0	1.4	1.1	1.1
O_2	4.4	7.4	8.3	6.9	7.2	7.5	7.7	8.0	5.6	7.4	7.2	1.9	6.2	7.0
S	2.6	1.8	2.0	2.3	1.9	2.2	1.7	2.6	3.2	2.7	2.3	2.6	1.2	2.0
Ash	8.9	8.2	8.4	8.7	7.1	7.8	7.9	8.2	13.8	10.3	9.8	7.3	6.9	9.6
Moisture	6.6	5.7	8.3	4.8	5.1	4.8	4.7	3.5	7.0	5.1	7.3	2.1	3.1	8.8
Heat content of coal as fired, Btu per lb	12,810	13,500	12,120	12.740	12,950	12,930	12,910	12,960	11,660	12,510	12,190	14,170	13,670	11,830
Proximate analysis of typical sample, per cent by weight:														
Moisture	6.6	5.7	8.3	4.8	4.1	4.8	4.7	3.5	7.0	5.1	7.3	2.1	3.1	8.8
Volatile matter	35.2	36.1	34.9	35.8	36.9	36.2	36.9	36.6	34.9	36.6	35.6	22.3	37.8	32.0
Fixed carbon	49.3	50.0	48.4	50.7	51.3	51.2	50.5	51.7	44.3	48.0	47.3	68.3	52.2	49.6
Ash	8.9	8.2	8.4	8.7	7.7	7.8	7.9	8.2	13.8	10.3	9.8	7.3	6.9	9.6
Sulfur	2.6	2.7	2.8	2.7	2.8	2.8	2.8	2.6	3.2	2.8	2.9	2.3	1.3	1.3
Ash-softening temperature, F	2,230	2,230	2,230	2,230	2,230	2,230	2,230	2,230	2,100	2,450	2,450	2,400	2,350	2,350
Analysis of samples from each test, per cent by weight:														
Moisture: Maximum	7.8	8.4	8.0	4.9	-[b]	5.8	-[b]	3.6	-[c]	-[b]	-[b]	-[b]	3.7	-[b]
Minimum	4.9	4.0	7.1	3.6	-[b]	4.7	-[b]	3.2	-[c]	-[b]	-[b]	-[b]	2.7	-[b]
Average	6.6	6.5	7.6	4.3	-[b]	5.1	-[b]	3.4	-[c]	-[b]	-[b]	-[b]	3.2	-[b]
Ash: Maximum	11.9	9.8	9.2	10.5	-[b]	8.0	-[b]	9.0	-[c]	-[b]	-[b]	-[b]	7.5	-[b]
Minimum	6.6	7.7	8.4	8.2	-[b]	7.9	-[b]	8.5	-[c]	-[b]	-[b]	-[b]	7.3	-[b]
Average	8.9	8.5	8.7	9.3	-[b]	8.0	-[b]	8.8	-[c]	-[b]	-[b]	-[b]	7.4	-[b]
Free-swelling index	2	2-1/2	3	5	-[d]	4-1/2	3	5-1/2	4	3-1/2	4-1/2	9	7	1-1/2
Fe_2O_3, per cent:														
In coal	1.3	2.0	1.7	2.1	-[d]	1.8	1.7	2.2	3.1	3.2	2.2	2.8	0.7	1.8
In ash	14.6	24.4	20.3	24.1	-[d]	23.1	21.5	26.9	22.5	31.1	30.2	38.4	22.6	18.8

[a] Saline County.

[b] Only one test run with this coal.

[c] Only one sample analyzed.

[d] Not determined.

TABLE 4 TYPICAL SUBSIEVE ANALYSIS OF BOILER-OUTLET CINDER FROM A FULL-LOAD TEST WITH TOTAL REINJECTION

Average particle size, microns	Undersize, per cent by weight	Terminal velocity, fpm[a]
10	16	0.8
15	19	1.2
20	21	1.7
30	26	2.5
40	30	3.3
50[b]	33	4.2

[a] Measured in air at room temperature.
[b] 44 microns = 325 mesh.

material representing the boiler-outlet dust from full-load tests with total reinjection, using several coals. Table 4 shows a typical size consist.

Bulk Density. Determination of the apparent bulk density of samples of cinder collected from the boiler hoppers and collector hoppers was made for 16 tests. These results showed that the rate of gas flow (as indicated by the operating load of the boiler) was the major variable affecting bulk density.

TABLE 5 RANGE OF BULK DENSITIES OF CINDERS FROM TWO LOCATIONS

	Apparent bulk density, lb per cu ft	
Operating load	One fifth	Full
Sample from:		
Boiler hoppers	5.3–7.0	13.0–16.5
Collector hopper	6.7–8.0	14.4–25.3

Table 5 shows the range of results obtained.

Specific Gravity. The true specific gravity of a typical stack dust (containing 32 per cent combustible) was determined (by a picnometer) as being 2.25.

Discussion

W. S. Blundin.[3] During past years there has been a gradual increase in boiler ratings with a corresponding increase in flue-gas velocities through the boilers. In the case of some solid-fuel-fired boilers, velocities have been high enough to cause erosion and failure of pressure parts by the scrubbing action of particles of ash or cinders entrained in the flue gases. This erosion has not been confined to one fuel or type of firing equipment, but it has been more prevalent with spreader stoker-firing because of the comparatively large quantities of relatively heavy cinders entrained in the flue gases with this type of firing.

[3] Staff Engineer, The Babcock & Wilcox Company, New York, N. Y.

The scrubbing action of entrained cinders has had the beneficial effect of tending to keep heating surfaces clean. Our experience has been that fouling difficulties are less with spreader stoker-firing than with other types of coal-firing equipment. That the scrubbing action is largely responsible for the ease of cleaning has been demonstrated on units having the dust collector located ahead of the economizer. Cleaning requirements on the economizer of such jobs are comparable to those for pulverized-coal-fired units.

There have been a number of modifications in boiler design directed toward the elimination of erosion. Among these are the following:

1 Keeping gas velocities below that at which erosion will occur.

Experience indicates that for any combination of ash or cinder type and concentration, there is some critical velocity below which erosion trouble will not occur. Other things being equal, the critical gas velocity with spreader stoker-firing is approximately 25 per cent lower than that for pulverized coal-firing.

2 Use of single gas-pass boiler.

Erosion has been most severe at gas turns and other places where the gas-flow pattern is such as to concentrate the cinders. The single-pass boiler design minimizes the possibility of cinder concentration. A typical single-pass boiler is shown in Fig. 9 of this discussion.

3 Use of cinder-catcher baffle.

Baffle plates are sometimes placed at the boiler outlet to serve as a skimmer and remove the coarser material from the gas stream and thus reduce the dust load to the other heat traps in the boiler circuit. The coarse particles are removed due to a change in direction and velocity as the gas stream flows around the baffle.

For boilers with baffles which concentrate the ash, a "cinder catcher" or baffle slot has been designed. This design is shown in Fig. 10 herewith, applied to a Stirling boiler; it allows the con-

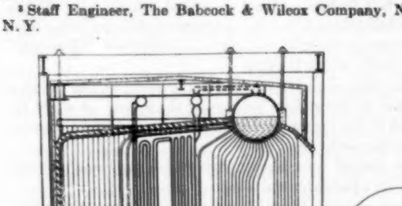

Fig. 9 Typical Single-Pass Boiler

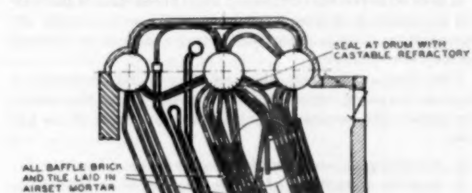

Fig. 10 Cinder Catcher or Baffle Slot

centrated stream of ash to discharge into a relatively dead zone. It then can disperse prior to being picked up by the gas stream after its flow has fairly well straightened out.

4 Baffle construction.

Baffles in boilers fired by abrasive fuels are made as gas-tight as possible. All tile and brick are laid in airset mortar. Tight baffles are particularly important when the draft differential across the baffle exceeds $^1/_2$ in. with pulverized coal, or $^1/_4$ in. with a spreader stoker. These differentials will produce leakage velocities equal to the critical velocities.

5 Elimination of lanes.

Lanes or open spaces along the walls at the outside of a tube bank are kept to a minimum.

The data presented in the paper indicate that cinder return is desirable from an efficiency standpoint; however, it materially increases the dust loading in the boiler bank and is certainly not in the direction of minimizing erosion problems.

Fig. 8 of the paper, giving dust loadings at various points in the unit, shows that with reinjection from both the boiler hoppers and dust collector, the dust loading leaving the collector is above the ASME proposed ordinance. Where compliance with the ASME limit is required, it appears that cinders from the dust collector would have to be rejected at some loss in efficiency, or else a second collector would have to be installed following the first.

It is believed that the work done in the use of overfire air jets to reduce the dust loading of gases from spreader stokers as described in the paper is a significant step in overcoming the most important outstanding problem in connection with spreader-stoker-firing.

It is noted that steam jets were found to be more effective than air jets. We would like to ask the authors if any conclusion has been reached as to why this should be so.

H. D. Fisher.[4] A project of this kind would be a heavy burden on any single manufacturer, and it is an outstanding example of co-operation between competitors that such a research could be organized to establish principles of operation and secure design data for improving the performance of their equipment.

It is to be hoped that ultimately more of the data of the tests will be published, because analyses of such a series of tests will throw light on other problems than those for the solution of which the tests were planned.

Three phases of the tests, which are of considerable interest in a study of the paper, are omitted and it is hoped that the authors can supply this supplementary information. These are as follows:

1 Percentages of combustible in ashpit refuse.

2 Relative percentages of refuse disposed of in (*a*) ashpit; (*b*) stack losses; and, with recirculation, corresponding amounts of fly ash recirculated from boiler hoppers and cinder catcher, these figures being stated in terms of ash and combustible content. Certain deductions can be made from Fig. 8 of the paper, but the exact applicability of the data is a little obscure.

3 Heat balances for the tests, particularly as to "unaccounted for" items. While the furnace volume is apparently adequate for complete combustion of gases, a low and relatively uniform value of these items for the various tests would be a desirable confirmation that this is the case.

The writer designed and put into operation on March 1, 1950, a spreader-stoker-fired unit, which, although he had no knowledge of the Elyria unit, is strikingly similar.

This unit consists of a 60,000-lb per hr, 24-hr-rating; 75,000-lb per hr, 4-hr-rating, Bigelow three-drum bent-tube boiler. The boiler proper has 8584 sq ft of heating surface, the furnace 562 sq ft in two side waterwalls, which consist of $3^1/_2$-in. tubes on $9^3/_8$-in. centers, set tangent to the refractory walls of the setting. Front wall and bridge wall are not water cooled. The boiler has a Foster Wheeler intertube superheater, containing 487 sq ft of surface in $1^1/_2$-in. tubes.

The boiler is fired with a Detroit spreader-type stoker with power-operated dump grates 12 ft 6 in. wide, 13 ft 7 in. long, of 170 sq ft area. The stoker is normally driven by a motor but has a steam turbine as an emergency drive. Furnace volume is 3425 cu ft.

Forced draft is furnished by an American Blower Company Series 82, No. 300 DIDW fan, 27,000 cfm at 3-in. static and 70 F, at 1170 rpm with inlet vane control. Overfire air at the front of the boiler from this fan is introduced through openings in the piers between and beside the doors just below the feeders.

Air for cinder reinjection is supplied by a high-pressure motor-driven fan, there being four reinjection nozzles from the boiler cinder hoppers and two from the ash-collector hoppers.

The unit is equipped with a Thermix tubular dust collector, Design 6HC-No. 2-190, and a Thermix induced-draft fan and stack, Type 1 Design KWS No. 135, 70,000 cfm at 4.98 in. static and 600 F, at 875 rpm. Fan control is by louver dampers in the inlet ducts.

The fans have duplex motor and turbine drive at opposite ends of the fan shaft.

Operating conditions are 190 psig, 490 F steam, 250 F feedwater, which is heated by the exhaust of the auxiliaries in an Elliott deaerating heater.

The unit is equipped with Leeds and Northrup metering-type combustion control, including damper position indicators, steam flow-air flowmeter, draft gages, and so forth.

Coal is, as in the Elyria unit, dumped from cars into a track hopper, transferred by an apron conveyer to a bucket elevator from which a scraper conveyer distributes it to three silos, one for each of the old boiler units in the plant and one for the new boiler. Each silo has 150 tons active capacity, this being secured by the use of long belt Richardson coal scales which draw from the silo outside the building and feed the weighing mechanism of the scale which is located at the inner end above a Richardson "Monorate" distributor to the stoker hoppers.

Emergency chutes enable the coal in the upper half of the silos to be supplied to the stokers by-passing the scales. A slight rearrangement of the former coal-handling system permits transfer of coal from one silo to another.

Ashes are sluiced to a lagoon from which they are removed periodically by a bulldozer and trucks.

Fuel is high-volatile West Virginia coal of 30 to 35 per cent volatile, 8 to 10 per cent ash, 2300 to 2500 F ash-softening temperature.

The boiler is usually operated between 65,000 and 75,000 lb per hr capacity continuously 24 hr per day 7 days per week except for 8-hr interruptions of process work about every week or 10 days. Operation has been very satisfactory, the only observed difficulty being a polishing of the tubes and the boiler drum, where the gases pass over the top of the baffle just back of the superheater. On some of these tubes the mill scale has been removed but no measurable erosion of the tubes has taken place.

A similar but less complete polishing of the tubes can be observed at turning points in the gas passages in the rear passes of the boiler.

Velocity of the gases through the superheater and over the top of the first baffle is about 43 to 45 fps at a capacity of 75,000 lb per hr, 33 to 34 fps at 60,000 lb per hr. It is very credibly reported

[4] Consulting Engineer, Westcott & Mapes, Inc., New Haven, Conn. Mem. ASME.

that gas velocities of 38 to 40 fps will give no difficulties with erosion of tubes except with anthracite ash which is highly abrasive.

It is planned to remove the horizontal portion at the top of the front baffle which will reduce gas velocities at this point to 31 to 34 fps at 75,000 lb per hr and 24 to 26 fps at 60,000 lb per hr, in order to increase the margin of safety against erosion. A slight drop in superheat may result but this will not be an operating detriment.

The authors' comments on their experience with the test boiler in this phase of operations will be of interest.

In an endeavor to obtain additional data on this point, weighed and micrometered tube samples were exposed for a number of weeks on top of the front baffle shelf and in front of the boiler drum, but no measurable change in weight or dimensions could be detected, although they began to show a satiny surface.

Samples of fly ash from boiler hoppers and dust-collector hoppers show somewhat lower combustile than in the Elyria tests, the analyses being as follows:

Constituent	Boiler hoppers	Dust-collector hoppers
Combustible.....	38.4	27.6
Noncombustible..	61.6	72.4

Some difficulties have been encountered with clinker bridging over a dump-grate section and requiring barring to break it down when grates are dumped. This clinkering condition has apparently been lessened by an increase in air pressure at the front overfire air jets and it would be interesting to have the authors' comments as to what correlation if any had been observed between clinkering on the grates and the various air and steam-jet arrangements; also, whether any difference was observed in clinker formation with and without reinjection of fly ash.

R. W. GAUSMANN.[5] This paper appears to be the first to give authentic information on the dust concentrations at the furnace outlet, taking into consideration such variables as percentage of overfire air and type and size of the coal being burned. This information should assist both operators and designers in limiting the amount of fly ash produced by spreader-stoker-fired boilers and also should serve as a landmark for any future developments in furnace design made to limit fly-ash emission.

From the viewpoint of operators of spreader stokers, it is regretted that the scope of this project was not broadened to include the fly-ash emission from the stack. From the operator's viewpoint it is necessary to obtain acceptable efficiency of the unit as a whole while still maintaining fly-ash emission within limits imposed by regulatory bodies. Not only must the fly-ash emission from the furnace itself be considered but also means of collecting the fly ash before it is allowed to escape from the stack.

From Fig. 8 of the paper it is evident that with most coals it is not possible to keep dust emission from the stack within the ASME Code, with total reinjection of fly ash from a moderately efficient collector. Tests made elsewhere indicate that it is also impossible to keep within the ASME Code limitations with a high-efficiency mechanical collector when total reinjection of the collected dust is practiced. In order to live within the limitations of such a code, it is therefore necessary to discard the combustible rich dust caught by the collector, resulting in an increase in coal cost of around 3 per cent, as well as a much higher ash-disposal cost. An economical solution to this problem is urgently needed.

Table 3 in the Appendix of the paper presents some very interesting data which are particularly significant if two-stage collection of the fly ash is being considered. Tests generally indicate that the bulk of the combustible in fly ash is concentrated in the coarser fractions of the fly ash. Hence it might be presumed that a lower or moderately efficient collector would tend to remove most of the combustible matter. Table 3 indicates that this presumption is not valid. A possible reason for the failure of the collector to classify dust by combustible content is that the combustible matter is present mainly in the form of coke breeze of low specific gravity which is not removed easily by a low-efficiency collector.

In view of the many demonstrated advantages of spreader stokers in certain fields it is believed that further research is warranted in order to obtain a low over-all carbon loss, together with stack emission within reasonable code limitations.

[5] Director of Plant Research, Indianapolis Power & Light Company, Indianapolis, Ind. Mem. ASME.

B. MEYER.[6] The writer's company, which manufactures a low-head boiler, Type V-I., in sizes from 100 hp to 550 hp, has encountered special problems in operating spreader stokers that do not seem to occur in the larger boilers.

The following steps have been found to be necessary for smokeless combustion:

1 Completely automatic combustion controls. The supply of air must follow the coal feed very closely.

2 Adequate meters and instruments including a CO_2 indicator or recorder.

3 Correct coal sizing. Small sizes can be used in the summer but excess fines pick up too much water in the winter.

4 High-pressure overfire air and cinder-return jets. At least 10-in. SP must be used with jets preferably in the bridge wall.

5 Reasonable CO_2. CO_2 above 12.5 per cent at the boiler outlet seems to produce very smoky conditions.

6 Adequate furnace height. The actual height to which the fines or ash must rise before passing over the bridge wall seems as important as the Btu release rate per cubic foot.

7 Low furnace draft. This should not exceed 0.05 in. to avoid high velocities in the furnace.

8 Reduced stoker area for reduced loads. When operating with dumping grates at 1/3 load or less, part of the grate surface should be covered to approach the best grate load which is around 30 lb per sq ft per hr.

9 A dust collector is always needed.

10 When burning high-moisture coals like lignite, it may be necessary to raise the furnace temperature by covering some of the waterwalls with plastic refractory.

11 Highly skilled, experienced, and attentive operators are required. Considerable experimentation with different coals and firing methods are necessary before optimum combustion conditions are produced.

The foregoing points will suggest other variables which might be studied to improve the operation of small spreader-stoker installations.

D. J. MOSSHART.[7] In 1950 our company conducted a number of tests of a traveling-grate spreader stoker of its own manufacture in one of its own plants. In most significant phases, the tests were similar in nature to those reported in the paper, but were made with fuels considerably inferior to those used at Elyria. The results obtained and conclusions drawn were quite similar, although no work whatever was done with steam jets.

We regard it as unfortunate that so much of the work done at Elyria was based on the use of steam rather than air jets, since economic considerations practically rule out steam jets in most cases. In our more limited work, we found that carbon loss and

[6] John Inglis Company, Limited, Toronto, Ontario, Canada.

[7] Engineering Manager, Stoker Department, Westinghouse Electric Corporation, South Philadelphia Works, South Philadelphia, Pa. Mem. ASME.

dust loading were reduced (at constant excess air) by reducing air flow through the grate and increasing overfire air to an extent just short of causing formation of clinkers of a nature to impede flow of air through the fire bed.

However, our work indicated, as does this paper, that the effects obtainable on dust loading by development of overfire jets, selection of fuel sizing, and so forth, are relatively minor and uncertain, and that the only certain method of assuring tolerable dust loading in the stack gas is to install a high-efficiency dust collector or to use a different type of stoker.

Further, it is evident that satisfactorily low fly-carbon losses cannot be assured for all fuels without return to the furnace of the material caught in the collector. Available data indicate that fly-carbon losses increase with rank of coal, and the low losses found with low-rank coals without return from the collector are no indication of performance with coals of higher rank.

Thus there arises a "penny or cake" problem. There is good reason to expect that satisfactory fractions of the penny of low dust loading and the cake of low carbon loss may be obtained by return of collector-caught dust to the furnace with periodic "purging" of the gas stream by diversion of the dust to waste for very short periods of time. This operation is readily established with automatically operated dust valves which direct the flow of dust alternately to the furnace and to the ash-handling system.

Our company is now equipping several installations with such systems and intends to conduct and report tests establishing comparative performance.

Authors' Closure

Mr. Blundin's comments on the scrubbing action of entrained cinders and their effect of maintaining clean tube surfaces are a valuable addition to the test work reported. It might also be added that in boilers having baffles which are substantially vertical and having no natural "pockets" to collect fly ash, this scrubbing action has been used to advantage by removing the soot blowers. The consequent reduction in daily operating labor, to say nothing of the reduced first cost of the entire boiler furnace, reduction in steam demand for these auxiliaries, and the elimination of a maintenance problem, is a valuable feature of the spreader stoker. It is recognized that there will be increased erosion from operating with cinder reinjection, but comprehensive data are not available n this point. No measurements of this effect were made during the tests at Elyria. The use of a "cinder catcher" or baffle slot would doubtless be helpful in reducing erosion. However, as Mr. Blundin implies, such a modification works to the advantage of reducing erosion at the expense of increasing dust loading into the collector. In one installation using a baffle slot, it was learned that a negligible amount of cinders were caught in the boiler hoppers with a resultant overloading of the collector. Thus a balance must be struck between factors of erosion and the loading of the dust collector, giving consideration also to the amount of dust emission from the stack.

Mr. Mosshart regards the use of steam jets during many of the tests as "unfortunate". These jets were used at the direction of the Spreader Stoker Research Committee, of which Mr. Mosshart was a member, primarily because tests showed that the steam jets were slightly more effective than air jets in reducing dust emission. Secondarily, steam was chosen to simplify changes in jet arrangements. It was recognized, and pointed out in the text of the paper, that the use of steam jets in regular full-time operation is not practical. In reply to Mr. Blundin's question on this subject, it should be noted that only a slight reduction in dust emission was obtained when using steam jets over that found when jets of air were used. Furthermore, the greater amount of turbulence produced by the smaller jets of higher-velocity steam may have caused a greater amount of mixing of hot furnace gases with the reinjected cinders than was produced by the larger but lower-velocity jets of air.

Space did not permit inclusion of the complete information of the type requested by Mr. Fisher. The authors hope that it can be published later. As noted previously, no measurements of erosion or calculations of gas velocities in the furnace were made during the tests. Thus comparisons with the data presented by Mr. Fisher cannot be made. With regard to clinker formation, it may be noted that no clinkers large enough to require manual removal were formed during any of the tests. When jets high in the side walls of the boiler were used, small accumulations of extremely light clinker were found which were attributed to the action of these jets on the reinjected cinder.

Mr. Gausmann has raised an interesting point in attempting to use the data reported to justify two-stage collection of cinders. It is thought that the test data do not show this to be advisable because of the relatively low efficiency of the dust collector used.

The ten points which Mr. Meyer lists are certainly important for any spreader-fired boilers. It might be pointed out that current practice favors the use of oxygen recorders rather than CO_2 recorders as control instruments. This is done not only because of the easier maintenance of the oxygen recorder but also because the oxygen content of flue gas is more sensitive to changes in operating conditions than is the CO_2 content. Admittedly, much work needs to be done to obtain more fundamental data on the operation of the popular low-head boilers.

The "gas-producer action" which Mr. Mosshart achieves by reducing undergrate air flow while holding excess air constant is an interesting deviation from conventional spreader-stoker operation. It is questionable, however, that primary-air flow can be reduced enough to take full advantage of this action without encountering grate temperatures which are excessively high.

The authors note with interest Mr. Mosshart's description of reinjection with "purging" of the gas stream by discarding a portion of the collected cinders. Although experience previously has indicated that the automatically operated dust valves will require considerable maintenance in order to prevent leakage of air and cinders, the development of the idea is still interesting. A report of the tests on this system would be most welcome.

In conclusion, the authors wish to call attention to Mr. Fisher's commendation of the spreader-stoker manufacturers who co-operated in undertaking this test program. Research of this type and of this magnitude is obviously beyond reach of any single manufacturer, and problems such as these can be attacked and solved only by co-operative action for mutual benefit of all participants. The needed fundamental work cited by Mr. Meyer is an example of the need for such group activity. It is hoped that these and similar problems in this field can be solved by combining research appropriations from the many interested companies into an amount sufficient to obtain fundamental data which cannot be obtained otherwise.

A New Method for Determining the Static Temperature of High-Velocity Gas Streams

By J. A. Clark[1] and W. M. Rohsenow,[2] Cambridge, Mass.

The general problem of measuring the static temperature of gases flowing at high and low temperatures and at low and high velocities is reviewed. Thermodynamic methods are discussed and a new method is presented with experimental results. This proposed temperature-measuring method has several important and desirable features: (*a*) The calculated static temperature is practically independent of gas composition in so far as composition is characterized by the specific-heat ratio *k*; (*b*) like the thermocouple, the temperature determined by this method is a "point" value, not a mean value at the flow cross section where the measurements are made; (*c*) unlike the thermocouple, the method improves in accuracy as both the gas temperature and velocity are increased; and (*d*) the instrument required is relatively simple to build, is not subject to the effects of corrosion, and is extremely rugged when installed. The instrument requires no special handling and can be installed conveniently and easily in ducts of any shape or in a stream of unconfined gas.

Nomenclature

The following nomenclature is used in the paper:

A = area, sq ft
c = sound velocity, fps
C_1, C_2, C_3, C_4 = numerical constants
c_p = specific heat at constant pressure, Btu/lbm-deg F
c_v = specific heat at constant volume, Btu/lbm-deg F
f = fuel/air ratio, w_f/w_a, dimensionless
g_0 = conversion factor, 32.2 lbm-ft/lbf-sec²
G = mass velocity, lbm/sec-ft²
J = $\bar{V}_m/\bar{V}$, see Equation [18]
k = specific-heat ratio c_p/c_v, dimensionless
K = flow coefficient, dimensionless
M = Mach number, dimensionless
P = static pressure, lbf/ft²
P_0 = stagnation pressure, lbf/ft²
P_w = wall static pressure, lbf/ft²
ΔP = $P_0 - P_1$, lbf/ft²
R = gas constant, (ft lbf)/(lbm deg R)
S = series (Equation [13]), dimensionless
T = absolute temperature, deg F abs (deg R)
T_0 = stagnation temperature, deg F abs (deg R)

$$\%\Delta T_1 = \frac{T_1 - T_{k=1.33}}{T_1}(100);\ \text{also}\ \frac{T_{\text{probe}} - T_{\text{thermocouple}}}{T_{\text{thermocouple}}}(100)$$

T_{CL} = center-line value of absolute temperature, deg R
V = flow velocity, fps
V_{CL} = center-line value of flow velocity, fps
W = mass flow, lbm/sec
W_a = mass flow of air, lbm/sec
W_f = mass flow of fuel, lbm/sec
ρ = weight density, lbm/ft³
ϵ = $P_B - P_A$ inherent instrument error, in. of water

A bar over any symbol refers to an average value.

Stations:

1 = any arbitrarily selected point in a flow field
2 = entrance combustion chamber
2′ = location of fuel injection
3 = exit combustion chamber
A = point immediately preceding probe entrance
B = point immediately inside probe entrance

Introduction

One of the many important technical problems arising from the development of modern propulsion systems has been the measurement of the static temperature of the high-velocity high-temperature exhaust gases. The static temperature is mentioned here as opposed to the stagnation or total temperature as it is the static temperature which along with static pressure defines the thermodynamic state of the gas. The static temperature of flowing gases is often described as that temperature which would be indicated by a thermometer if it were to move in thermal equilibrium with the gas stream at zero relative velocity and zero external heat transfer.

This paper describes a device for determining the static temperature of high-velocity gases flowing subsonically and at any level of temperature. Experimental work has been carried out during the past year on flowing air at low temperatures and low Mach numbers, and with combustion products at approximately 1500 F, yielding promising results which are reported herein. At present, experimentation is being continued extending to higher temperatures and velocities using combustion products as gases.

Gas temperatures which have to be measured by the industry range from about 1400 F for turbojet engines to more than 8000 F for rockets. Afterburning in standard turbojet and turboprop installations will produce gas temperatures in excess of 3500 F. Ramjet engines operating at high flight Mach numbers can be expected to have exhaust-gas temperatures as high as 5000 F.

The problems in temperature measurements of gas streams may be grouped into three ranges of temperature and three ranges of Mach numbers (Table 1).

The problems of class 1 (*a*) have been treated adequately by the Bureau of Standards in reference (1),[3] the problems of class

---

[1] Instructor, Mechanical Engineering, Massachusetts Institute of Technology. Jun. ASME.

[2] Assistant Professor, Mechanical Engineering, Massachusetts Institute of Technology. Jun. ASME.

Contributed by the Heat Transfer Division and presented at the Semi-Annual Meeting, Toronto, Ont., Can., June 11–15, 1951, of The American Society of Mechanical Engineers.

Note: Statements and opinions advanced in papers are to be understood as individual expressions of their authors and not those of the Society. Manuscript received at ASME Headquarters, April 12, 1951. Paper No. 51—SA-33.

[3] Numbers in parentheses refer to the Bibliography at the end of the paper.

TABLE 1 RANGES OF TEMPERATURE AND MACH NUMBERS

1	Room temperature	
	(a) Mach No. range	0–0.25
	(b) Mach No. range	0.25–1.0
	(c) Mach No. range	above-1.0
2	Temperature range 60 F–3000 F	
	(a) Mach No. range	0–0.25
	(b) Mach No. range	0.25–1.0
	(c) Mach No. range	above-1.0
3	Temperature range above 3000 F	
	(a) Mach No. range	0–0.25
	(b) Mach No. range	0.25–1.0
	(c) Mach No. range	above-1.0

1 (*b*) have been studied by Hottel and Kalitinsky (2), and the problems of class 1(*c*) are at present under investigation by many groups. The methods of applying pyrometry to the remaining classes are not so well defined. Measurement of temperatures in class 2 (*a*) may be made with thermocouples or resistance thermometers (shielded or unshielded), and the radiation errors may be approximated as shown in references (3) and (4).

A review of flame-temperature-measuring methods is presented in reference (5) by B. Pugh. At high temperatures the sodium line-reversal method has become the most widely used method of measuring temperatures. In some cases this method does not permit the measurement of temperature at a "point" in the gas stream and, as Pugh illustrates, various experimenters have obtained widely differing results with this method, particularly in the rich and lean fuel-air mixtures.

Thermodynamic Methods

The major contributions to the unclassified literature on thermodynamic methods of gas-temperature measurement are those of the Fairchild Instrument Company (6), W. A. Wildhack (11), R. S. Cesaro, et al (12), and P. L. Blackshear, Jr. (13). A method similar to those of references (11) and (13) is given in reference (14) with no experimental results. These methods will be discussed briefly.

The Fairchild instrument consists of a probe immersed in the gas stream whose temperature is to be determined, Fig. 1. Gas

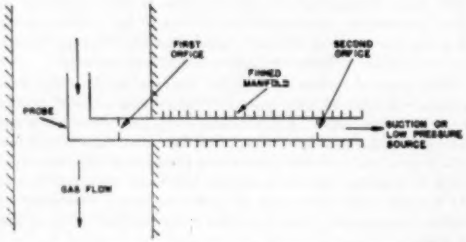

Fig. 1 Schematic Diagram of Fairchild Instrument

samples are drawn through this probe and into a manifold which is fitted with two consecutive flow-measuring orifices, the orifices being separated by a sufficient length of manifold tube to allow for cooling of the gas sample. Cooling is required in order that the temperature of the gas may be measured by a thermocouple at the second orifice. The Fairchild method is based upon the fact that the mass flow rate of a compressible fluid across an orifice can be written as a function of the density of the fluid before the orifice. By equating the mass rate of flow at the first and second orifices, it is shown how the density and thus the thermodynamic (absolute) temperature of the gas before the first orifice can be determined from the orifice pressure drops, and the gas temperature measured at the second orifice. As mentioned in reference (8), an arrangement very similar to this was proposed by H. Schmick (7) in Germany about 20 years ago, and Schmick reports that his method is an outgrowth of a suggestion of a German inventor as early as 1893.

The Fairchild instrument measures the static temperature of the gas at the first orifice. For gas flows at low velocities this temperature probably will be fairly representative of the static temperature of the gas stream whose temperature is being measured. In high-velocity gas streams the temperature indicated by the instrument will be different from the static temperature of the free stream, probably being somewhere between free-stream static and stagnation (total) temperature, depending upon the rate of flow into the probe and the degree to which the flow is adiabatic. For the particular instrument described (6), it is seen that its geometry limits its application to gas streams with Mach numbers less than 0.09 if the temperature it records is to be identical with the static temperature of the free stream. The determination of temperature with this instrument also depends upon the constancy of orifice flow coefficients and flow areas, something which may be difficult to achieve for all conditions of operation. The Fairchild method is probably valid for cases 1(*a*) and 2(*a*) of Table 1.

Improvements in the basic scheme of Fairchild, involving two consecutive flow-measuring elements, have been made independently by Wildhack (11), Blackshear (13), and the United Aircraft Corporation Research Department (14). These improvements, all fundamentally the same, consist of obtaining and maintaining sonic (critical) flow at each flow-measuring element, nozzle, or orifice. The instruments reported by these investigations all measure stagnation gas temperature at the throat (or point of minimum flow passage) of the first flow-measuring device, and the temperature determined, like the Fairchild instrument, depends upon the constancy of orifice area ratios and flow coefficients and to a lesser extent upon gas composition. Stagnation pressure must be measured or determined at the throat of each flow-measuring element.

Blackshear is the only one who reports experimental data, having compared his results with temperatures measured by suction pyrometer up to approximately 1200 R and with the sodium D-line reversal method from 3400 to 4000 R. Good agreement is reported in the range tested. Curiously, the results from the sodium D-line method, which measures static temperature, exceed those of the probe which measures stagnation, or total temperature. Wildhack reports the use of critical flow nozzles of 0.0135 in. diam, indicating how small these pneumatic temperature-measuring instruments can be made.

Cesaro, et al. (12) report a method for determining the average stagnation temperature of flowing gases in a particular system, and tested the method in a system consisting of a circular duct preceded by a combustion chamber. The average stagnation temperature at the discharge of the combustion chamber is written as a function of the average stagnation temperature at the inlet, the fuel/air ratio, pressure ratio across the combustion chamber, flow-area ratio, and the ratio of the difference between the stagnation and static pressures at the inlet and outlet. This method is more involved than any of the others and is not a "temperature meter" since it must be calibrated to the system on which it is to be used.

Another Thermodynamic Method. The methods of steady one-dimensional compressible flow can be used to derive an expression for the thermodynamic static temperature of a flowing gas in terms of upstream properties (8). Since such an expression is most useful for the determination of temperatures which fall in the classifications *b* and *c* of classes 1, 2, and 3 of Table 1, it shall be derived here for a combustion chamber, Fig. 2, in which combustion occurs at constant area. This configuration represents a

common design. For subsonic combustion high-pressure air enters the combustion chamber at station 2 and mixes with uniformly injected fuel at station 2′. Combustion occurs between stations 2′ and 3, the combustion products leaving at 3 with a higher temperature and velocity.

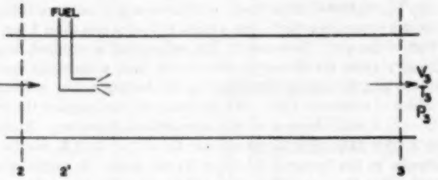

Fig. 2 Constant-Area Combustion Chamber

Assuming the effects of wall friction and fuel injection to be small as compared with other effects and that the combustion chamber is a constant-area tube, the momentum equation may be written between stations 2 and 3 as

$$(P_2 - P_3)\,A = \frac{W_2}{g_0}\,[(1+f)\,V_3 - V_2] \quad \text{[1]}$$

For a gas whose equation of state can be given accurately by $P = \rho RT$, Equation [1] may be combined with the relation $W_2(1+f) = A\rho_3 V_3$ to obtain

$$T_3 = \frac{P_3}{P_2}\frac{R_2}{R_3}\frac{T_2}{(1+f)^2}\left\{\frac{g_0 R_2 T_2}{V_2^2}\left[1 - \frac{P_3}{P_2}\right] + 1\right\} \quad \text{[2]}$$

Here Equation [2] relates the static temperature of the exhaust gases (at any velocity or level of temperature) at the combustion-chamber exit to the air properties at the inlet, the static pressure at the inlet, the static pressure at the exit, and the fuel/air ratio. Presumably, it is possible to measure these and thus determine T_3.

This equation is based on the assumption of one-dimensional flow, but it may be used for average values of the properties if the temperature and velocity variations across the cross section are not great. If these variations are great but are known, a modified form of Equation [2] (see Appendix) may be employed to find the average value of T_3.

Whether Equation [2] is adequate for the measurement of the temperature of high-velocity gases depends upon the required accuracy of the measurement as compared to the errors introduced by the assumptions underlying its derivation. At best the resulting temperature is a mean value applicable only for combustion at constant area. However, the measurements required are those which are usually made on a test stand combustion chamber, and thus no special device nor extra equipment is required in such instances. Also, the only measurement required in the region of highest temperature is that of static pressure, a measurement which is relatively easy to obtain. Therefore, if the advantages seem desirable and due regard is taken of its limitations, Equation [2] might be used in some instances as an approximation.

It is desired, however, to develop a method which retains the advantages of the thermodynamic approach through which "point values" of temperature may be obtained. An instrument employing such a method would then be truly a temperature meter. One method for accomplishing this is outlined in the following section.

Proposed Thermodynamic Method of Measuring Temperature

The following analysis is presented to demonstrate the underlying assumptions and procedure for development of an equation expressing the thermodynamic static temperature of a gas stream in terms of other properties (8). Consider a point 1 to be any arbitrarily selected point in a stream of gas flowing subsonically at any velocity or temperature in a duct of any shape and at a pressure which is low relative to the critical pressure. The mass velocity of the gas at point 1, Fig. 3, may be expressed as $G_1 = \rho_1 V_1$. The equation of state for many gases over a range of temperatures and pressure usually encountered in engineering prac-

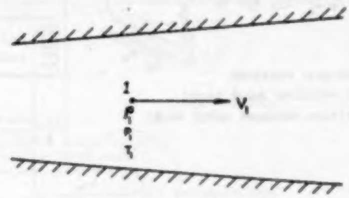

Fig. 3

tice may be represented accurately by $P = \rho RT$. From the steady-flow energy equation for this gas the following relation holds (9)

$$\frac{P_{01}}{P_1} = \left[1 + \frac{k-1}{2}\mathbf{M}_1^2\right]^{\frac{k}{k-1}} \quad \text{[3]}$$

Also, for a gas of this type the speed of sound is $c_1 = \sqrt{kR_1T_1g_0}$.

Now, from the definition of Mach number, $\mathbf{M} = V/c$, and Equation [3] the thermodynamic static temperature at the arbitrarily selected point 1 is found to be

$$T_1 = \frac{2g_0}{R_1}\left(\frac{P_1}{G_1}\right)^2\left(\frac{k}{k-1}\right)\left[\left(\frac{P_{01}}{P_1}\right)^{\frac{k-1}{k}} - 1\right] \quad \text{[4]}$$

This then is an equation relating the gas static temperature to other gas and flow properties, all at point 1. The accuracy of the determination of T_1 depends upon the precision and accuracy of the measurements of other quantities in Equation [4].

Temperature Probe and Instrumentation. Examining Equation [4], it is found that R_1 and k and P_1, G_1, and P_{01} must be determined at the point at which T_1 is to be evaluated. The experimental setup required to do this is shown in Fig. 4.

Here immersed in a stream of flowing gas is a cooled probe mounted so that its axis is parallel to the direction of flow. The other end of the probe is connected to the inlet of a pump whose purpose is to "suck" a certain amount of the mass of the flowing gas through the open end of the probe. This small mass of gas is then carried along the probe ducts where it is cooled in a heat exchanger and then measured by passing it across a calibrated orifice plate. This mass of gas is exactly equal to that which passed from the gas stream through the open end of the probe. Since the probe area is known at this point the parameter G_1, which is W/A, is evaluated.

The mass rate of flow through the probe is assured to be the same mass rate of flow which would pass through an area equal to that of the open end of the probe if the probe were not present by adjusting the flow to equalize the static pressure inside the

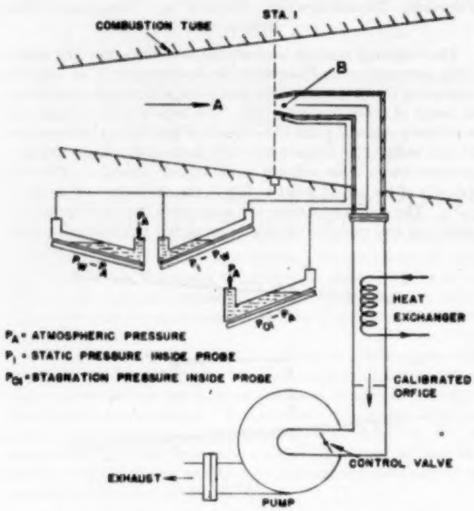

FIG. 4 SCHEMATIC DIAGRAM OF INSTRUMENTATION FOR PROPOSED METHOD

opening of the probe and the static pressure of the gas stream in the same plane. This is very important in order that the calculated T_1 be representative of the true static temperature of the gas stream at the point from which the mass is removed.

The static pressure P_1 can be determined from a static pressure tap in the duct wall in the plane of the probe opening. If such an arrangement is neither convenient nor practical, it would be possible to measure this pressure at static openings in the outside surface of the probe.

The stagnation pressure of the flowing gases is taken from a stagnation tube centered inside the probe and just aft of its opening, Fig. 5. Its proximity to the open end of the probe is such that the pressure it registers will vary by a negligible amount from the stagnation pressure at the plane of the entrance of the probe. It is placed far enough aft, however, so that its effect will be negligible on the flow into the probe.

To insure that this tube does not induce a premature "choking" of the flow inside the probe when the free-stream velocity is close to sonic, the internal flow area is increased gradually for a short distance downstream from the entrance. Such a configuration makes it improbable that the gas would accelerate after it enters the probe.

The temperature probe shown in Figs. 5, 6, and 7, consists of two concentric tubes with axial partitions in the annular space to separate the incoming and outgoing flow of cooling water. The presence of the cooling water enables the instrument to be used at higher temperature than could be measured with an uncooled probe. There are two static-pressure taps at the inner surface of the entrance of the probe which facilitate the alignment of the probe with the gas stream and also the adjustment of the aspirated flow. The stagnation pressure in the probe is measured by a conventional tube at the axis of the probe. Small-diameter tubes are used to convey these pressures to the outside of the probe where manometer connections are made. The probe is constructed entirely of stainless steel.

Effect of Gas Composition. It is noted that Equation [4] involves terms which are dependent upon gas composition, namely, the gas constant R, and the ratio of specific heats, k. Since the equilibrium composition of combustion products is a function of temperature (and partial pressure of each constituent), an explanation of the use of k and R in Equation [4] is required. For many purposes the effect of gas composition upon the value of R can be neglected since even at stoichiometric mixture ratios for most hydrocarbon fuels, the weight of fuel is less than 7 per cent that of the air. However, if this refinement is required, a satisfactory value for R can be determined from a chemical analysis of the gas, by calculation knowing the fuel-air ratio, or from the tables of reference (10). We generally cannot neglect the variations in k with changes in gas composition, however. A change in k from that of atmospheric air ($k = 1.4$) to 1.3, results in a change in the factor $k/k - 1$ of 24 per cent. It would appear, then, that the use of Equation [4] in the calculation of temperature of high-velocity combustion gases would require accurate knowledge of the gas composition. Fortunately, this is not the case. Examining the effect of k on the value of the calculated temperature from this equation, we see the happy coincidence that its effect is practically negligible. Appearing in Equation [4] first as a factor and then as an exponent which is the reciprocal of this factor, the factor $k/k - 1$ has a damping influence upon the exponent $k - 1/k$. This behavior is evident from a series expansion of Equation [4]

$$T_1 = \frac{2g_0}{R_1}\left(\frac{P_1}{G_1}\right)^2 \frac{\Delta P}{P_1}\left[1 + \frac{x-1}{2!}\left(\frac{\Delta P}{P_1}\right) + \frac{(x-1)\,(x-2)}{3!}\left(\frac{\Delta P}{P_1}\right)^2 + \ldots\right] \ldots\ldots [5]$$

where

$$x = \frac{k-1}{k} \quad \text{and} \quad \Delta P = P_{01} - P_1$$

Now, Equation [5] can be used to evaluate with any desired precision the effect of different values of k upon the calculated temperature T_1. To do this it is evident that we have only to evaluate the series

$$S = 1 + \frac{x-1}{2!}\left(\frac{\Delta P}{P_1}\right) + \frac{(x-1)\,(x-2)}{3!}\left(\frac{\Delta P}{P_1}\right)^2 + \ldots\ldots [6]$$

Because the effect of various values of k will depend upon the ratio ($\Delta P/P_1$), two values for this ratio are chosen; $\Delta P = 3$ in. of water for P_1 of 1 atm, and then for a "choked" condition, or local Mach number of unity. This selection represents the opposite extremes of ordinary combustion problems and, therefore, should give a complete picture of the maximum and minimum effects of k. The range of specific-heat ratios selected is 1.400 to 1.000. A k of 1.400 is for pure air at 70 F, and a k of 1.000 represents no known gas but would be an extremely severe mixture of high-density gases, including all that is believed possible in ordinary combustions problems. Therefore this selection should give a comprehensive picture of the effects of all imaginable values of k.

Basing a percentagewise effect of various values of k for each pressure ratio on the value of T_1 for $k = 1.250$, the results are given in Table 2.

It is evident from Table 2 that at low ratios of $\Delta P/P_1$ (low velocities) wide differences in k have essentially a zero effect on the value of the "calculated" temperature T_1. At the choked condition, the maximum possible $\Delta P/P_1$, the effect of k is noticeable but quite small, being of the order of 1 per cent for the values

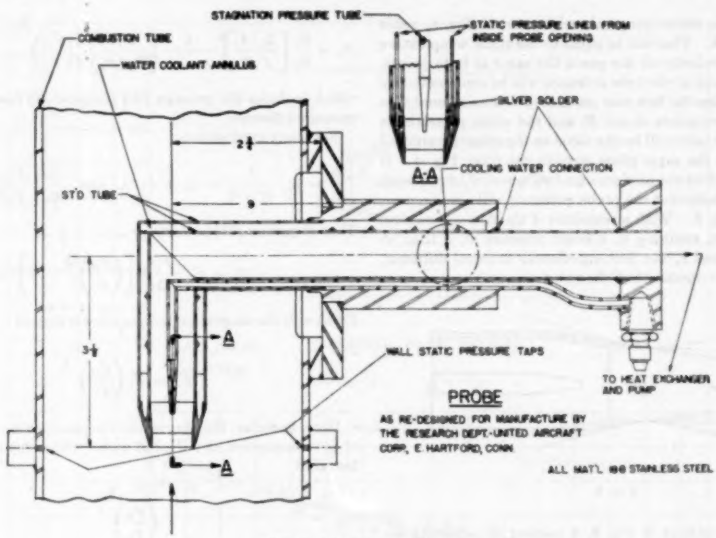

FIG. 5 DETAILS OF PROBE

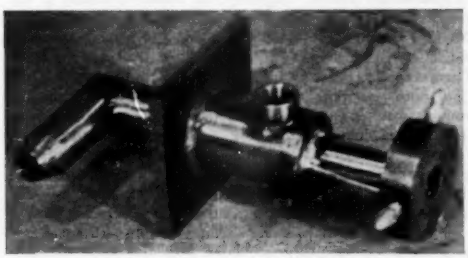

FIG. 6 TEMPERATURE PROBE

TABLE 2 EFFECT OF VARIOUS k-VALUES

		ΔP = 3 in. H_2O		Choked, (M_1 = 1)	
k	$x = \frac{k-1}{k}$	S	ΔT_1*, per cent	S	ΔT_1* per cent
1.400	0.2860	0.997479	0.0418	0.7000	2.87
1.350	0.2595	0.997279	0.0218	0.6940	1.99
1.300	0.2310	0.997174	0.0113	0.6875	1.03
1.250	0.2000	0.997062	0	0.6805	0
1.200	0.1667	0.996941	0.0121	0.6730	1.10
1.150	0.1305	0.996804	0.0260	0.6660	2.13
1.100	0.0909	0.996664	0.0398	0.6585	3.23
1.000	0	0.996328	0.0735	0.6390	6.10

* Negative signs omitted.

of k common to combustion systems. We have then, in Equation [4], an expression relating the static thermodynamic temperature at any point in a stream of high-velocity compressible gases to other properties of the flow which are convenient and practical to measure. Furthermore, this expression with k = 1.250 is so formulated that the calculated temperature is for practical purposes independent of gas composition. Further refinement may be obtained by using in Equation [4] a better value of k for the particular gas.

FIG. 7 PROBE BEING INSERTED INTO COMBUSTION DUCT

Effect of Variations in Aspirated Flow. The temperature determined by use of Equation [4] and the apparatus shown in

Figs. 4 and 5 is the static temperature at point B, Fig. 8, inside the probe entrance. This will be equal to the static temperature at point A if the velocity of the gas is the same at both points. Then the streamlines at the tube entrance will be represented by lines 2 in Fig. 8; also the flow rate per unit of cross-sectional area will be the same at points A and B, and the static pressures at point B within the tube will be the same as the static pressure of the gas stream in the same plane outside the tube, Fig. 4. If the aspirated flow does not produce equal values of W/A at points A and B, the streamlines at the probe entrance will assume positions 1 or 3 in Fig. 8. With streamlines 3 the flow experiences external expansion, resulting in a lower pressure at B than at A; with streamlines 1, the flow experiences external diffusion, resulting in a higher pressure at B than at A.

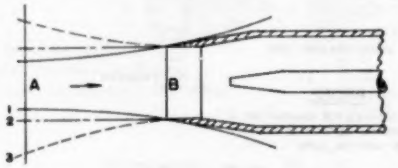

FIG. 8

Streamline flow of type 2, Fig. 8, is assured by adjusting the aspirated flow to equalize the static pressures measured within the probe at point B, Fig. 5, and at the duct wall, point W. Because of inherent combined installation and instrument errors, the actual static pressures at these points may not be exactly equal when the regulating manometer indicates equality, though their differences will be small. The effect of this error appears as a difference between the temperatures at points A and B, Fig. 8, their ratio being given by

$$\frac{T_B}{T_A} = \left(\frac{P_B}{P_A}\right)^{\frac{k-1}{k}} \qquad \text{[7]}$$

Consider the effect of a difference in static pressure of ϵ

$$P_B - P_A = \epsilon \qquad \text{[8]}$$

Then Equation [7] expanded in series form becomes

$$\frac{T_B}{T_A} = 1 + x\left(\frac{\epsilon}{P_A}\right) + \frac{x(x-1)}{2!}\left(\frac{\epsilon}{P_A}\right)^2 + \frac{x(x-1)(x-2)}{3!}\left(\frac{\epsilon}{P_A}\right)^3 + \ldots \qquad \text{[9]}$$

For $P_A = 14.7$ psia and $k = 1.3$, and $\epsilon = 0.2$ in. H_2O

$$\frac{T_B}{T_A} = 1.0001133$$

or an error of 0.01133 per cent, which is indeed small. From Equation [9] it is observed that this error becomes even smaller in atmospheres of higher pressure.

Other Forms of Equation [4]. If the measurement of G_1 of Equation [4] is obtained by an orifice

$$G_1 = C_1 K \frac{A_2}{A_1}\left[2g_0 \frac{P_2}{R_2 T_2} \Delta P_2\right]^{1/2} \qquad \text{[10]}$$

where subscript 2 refers to conditions at the orifice. K is the orifice flow coefficient. Combining this with Equation [4] results in

$$T_1 = \frac{R_2}{R_1}\left[\frac{A_1/A_2}{C_1 K}\right]^2 \frac{k}{k-1}\left[\frac{P_1^2}{P_2 \Delta P_2}\right]\left\{\left(\frac{P_{01}}{P_1}\right)^{\frac{k-1}{k}} - 1\right\} T_2 \qquad \text{[11]}$$

which includes the pressure and temperature readings which are measured directly.

For many applications

$$\frac{R_2}{R_1} = 1; \quad \frac{k}{k-1} = C_3 = C_5^{-1}, \quad \text{and} \quad \frac{R_2}{R_1}\left[\frac{A_1/A_2}{C_1 K}\right]^2 \frac{k}{k-1} = C_4$$

Then Equation [11] becomes

$$T_1 = C_4 \frac{P_1^2}{P_2 \Delta P_2}\left[\left(\frac{P_{01}}{P_1}\right)^{C_5} - 1\right] T_2 \qquad \text{[12]}$$

Further, if the stagnation temperature is desired

$$T_{01} = T_1 \left(\frac{P_{01}}{P_1}\right)^{\frac{k-1}{k}} \qquad \text{[13]}$$

Here, however, the stagnation temperature is not independent of gas composition as is T_1, but varies with composition to the extent that

$$\left(\frac{P_{01}}{P_1}\right)^{\frac{k-1}{k}}$$

varies with k.

Experimental Results. Experimental results available at the present time are for atmospheric air flowing at approximately 50–60 fps and 70 F, and for the products of combustion of Cambridge City gas flowing at approximately 70–165 fps in the range of temperatures 1100 to 1500 F.

For both the "hot" and "cold" runs the air or combustion products was blown vertically upward through the 5-in-diam stainless-steel duct shown in Fig. 7. The temperature probe is shown being inserted and will be at the duct center line facing upstream at a point approximately 11 diam from the duct inlet where suitable flow straighteners are located. For the cold runs the entire system was in an isothermal environment so that it was necessary to make a single temperature measurement as a check on the temperature calculated from the probe measurements. This was accomplished by inserting a triple-shielded calibrated chromel-alumel thermocouple at the duct center line 10 in. downstream from the temperature-probe entrance. For the hot runs, however, an axial temperature gradient existed in the duct so a single thermocouple measurement was unsatisfactory. Instead, two additional triple-shielded chromel-alumel thermocouples were placed upstream from the probe, which were used in conjunction with the downstream thermocouple to determine the axial temperature gradient at various levels of temperature in the duct. All thermocouples contained a heated shield, the input to which was controllable so as to allow for a zero difference in temperature between the measuring thermocouple and the first shield. This design made it unnecessary to compensate for the effects of radiation. During test runs with the probe, the two upstream thermocouples were removed to permit unobstructed flow before the probe, temperature measurements being taken as a check on the downstream thermocouple only. The temperature at the entrance of the probe was obtained by correcting the downstream thermocouple reading with the previously determined gradient. The data obtained for the hot and cold runs are shown in Fig. 9 which in a sense is a calibration curve for the particular probe used in these experiments.

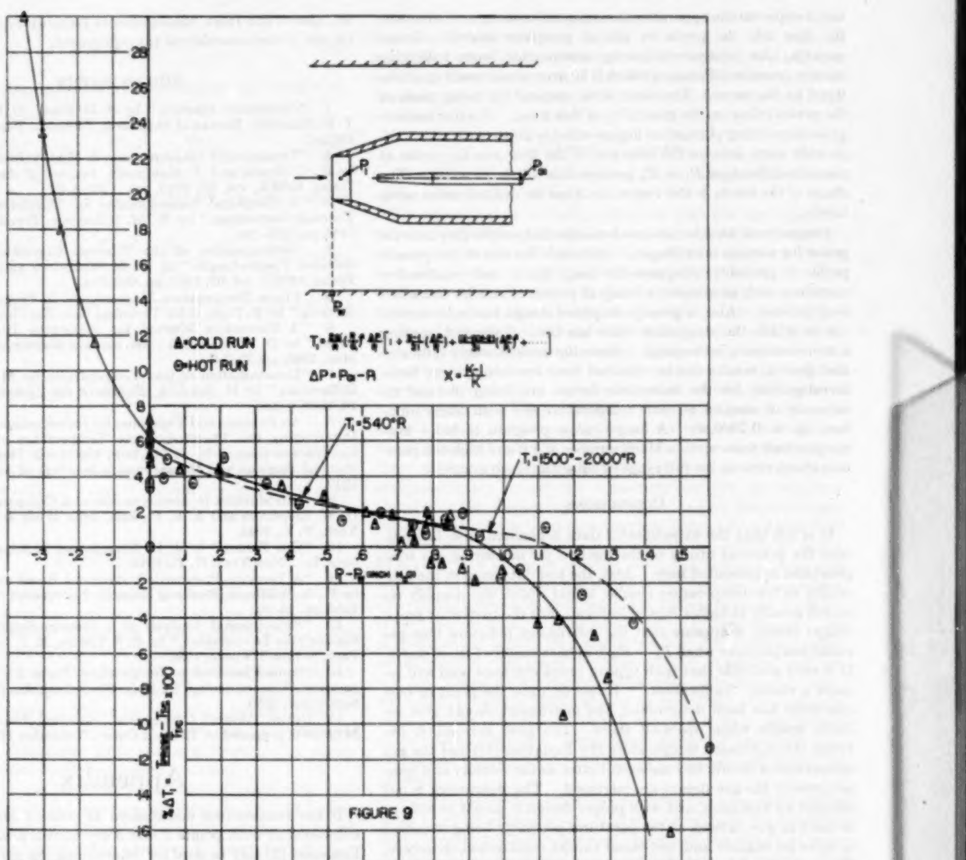

FIG. 9 DATA FOR HOT AND COLD RUNS

In Fig. 9 the percentage error in the calculated static temperature by Equations [4] and [5] is plotted against $P_1 - P_w$, a quantity which best represents the nature of the flow into the probe. Two curves are shown, one for the cold runs at approximately 70 F and one for the hot runs at approximately 1500 F. While several important things are shown by these curves, perhaps the most significant is the fact that they fall almost one over the other. This indicates the independency of the curves upon level of temperature and gas composition as the two curves represent air flowing at 70 F and products of combustion at 1500 F. The importance of this fact is that much detailed study can be made of the flow into the probe inlet using a simple and well-behaved gas like air and obtain results which are applicable to those of combustion products at higher temperatures, without the complications of high-temperature experimentation.

When $P_1 - P_w$ is negative, the streamlines entering the probe are converging. Separation of the flow probably occurs at the relatively sharp-edged entrance, Fig. 5, resulting in a greater ΔP and a smaller W/A or G_1 than is proper, which in turn cause the calculated temperature by Equation [4] or [5] to be too high. The effect of this type of flow into the probe is very severe as can be seen from Fig. 9 where small changes in $P_1 - P_w$ cause large percentage changes in the calculated temperature. Although the effects of P_1 being less than P_w are serious, they can be avoided by simply not operating in that regimé.

As $P_1 - P_w$ becomes greater than zero the percentage change in the calculated temperature approaches zero. This indicates that for the particular probe used the measurements in this region of ΔP and W/A or G_1 are becoming more representative of their true values. Also, the rate of change of the percentage error in the calculated temperature with changes in $P_1 - P_w$ is much less than when $P_1 - P_w$ is negative. It is possible that flow in this region has greater stability because of the smaller possibility of there being separation at the inlet of the probe.

At greater values of $P_1 - P_w$ the percentage error in the calculated temperature is shown to decrease rapidly negatively. This variation was not expected, and its validity is somewhat doubtful. To obtain values of $P_1 - P_w$ in this range it was neces-

sary to operate the apparatus at maximum capacity and to reduce the flow into the probe to almost complete shutoff. Consequently, the pressure-measuring instruments were indicating minute pressure differences which if in error would result in a false trend to the curve. Therefore little emphasis is being made at the present time on the generality of this trend. Further investigations are being planned on higher-velocity air streams which will provide more data on the behavior of the flow into the probe at pressure differences $P_1 - P_w$ greater than 1.0 in. of water. The shape of the curve in this region can then be defined more accurately.

Future work includes an aerodynamic study of the flow into the probe for various inlet shapes. Although the size of the present probe is probably adequate for large ducts and combustion chambers such as ramjets, a study of probes of smaller diameters is of interest. Also, a greatly simplified design has been worked out in which the stagnation tube has been eliminated, making a more compact instrument. Since the present study indicates that general results can be obtained from low-temperature tests, investigations for the immediate future are being planned on subsonic air streams at room temperature and with Mach numbers up to 0.70–0.80. A longer-range program includes low-temperature tests up to a Mach number of 1.0 and high-temperature check runs in the full range of subsonic Mach numbers.

Conclusions

It is felt that the experimental data accumulated so far indicate the practical utility of the method for measuring gas temperatures as presented here. Also, the test data suggest the generality of low-temperature results, a fact which will simplify research greatly at higher flow velocities. For the particular probe design tested, it appears that the instrument indicates true gas static temperature when $P_1 - P_w$ is approximately 1 in. of water. It is very probable that each type of probe entrance used will require a similar "calibration." However, once the point of best operation has been determined, the instrument should give reliable results when operated there. The good correlation between the calculated temperature (by Equation [4]) and the gas temperatures should become even better as the velocity and temperature of the gas stream are increased. The instrument is not affected by radiation, and with proper design it should be able to be used in gas streams at temperatures presently being obtained in turbojet engines and test-stand ramjet combustion chambers. The instrument is rugged, not subject to corrosion, is relatively simple to build, and is easily installed. Maintenance should not be a problem.

Finally, the two important basic qualities should be restated: The instrument indicates a point-value of temperature, hence it is a "temperature meter"; and inherent in the derivation of the method is the property that the equation describing the temperature is practically independent of the composition of the gas being measured, over a wide range of compositions expected in present and future combustion problems.

Acknowledgments

The authors wish to express their appreciation to Mr. R. C. Molloy, Executive Research Engineer, Mr. A. E. Wetherbee, and Mr. J. W. Tumavicus, Chief of Wind Tunnel Design, all of the Research Department, United Aircraft Corporation, East Hartford, Conn., for their interest in this project and for providing the vital pieces of equipment needed for the research. Special thanks are also given to Professors Gordon B. Wilkes and Lucien R. Vianey of the M.I.T. Heat Measurements Laboratory, for their assistance in overcoming the technical problems arising in the design and operation of the test equipment. Mr. Edward Hartel, also of the Heat Measurements Laboratory, rendered valuable aid in the assembly of the equipment.

BIBLIOGRAPHY

1 "Pyrometric Practice," by P. D. Foote, C. O. Fairchild, and T. R. Harrison, Bureau of Standards Technical Paper no. 170, 1921, 326 pp.

2 "Temperature Measurements in High-Velocity Air Streams," by H. C. Hottel and A. Kalitinsky, *Journal of Applied Mechanics*, Trans. ASME, vol. 67, 1945, pp. A-25–A-32.

3 "A Graphical Determination of Unshielded-Thermocouple Thermal Corrections," by W. M. Rohsenow, Trans. ASME, vol. 68, 1946, pp. 195–198.

4 "Determination of the Thermal Correction for a Single-Shielded Thermocouple," by W. M. Rohsenow and J. P. Hunsaker, Trans. ASME, vol. 69, 1947, pp. 699–704.

5 "Flame Temperature Measurement in Propulsive Ducts and Rockets," by B. Pugh, RAE Technical Note No. Gas 19, April, 1946.

6 "A Pneumatic Method for Measuring High Temperature Gases," by D. W. Moore, Jr., *Aeronautical Engineering Review*, vol. 7, May, 1948, pp. 30–34.

7 "Determination of Gas Temperatures by Means of Pressure Differences," by H. Schmick, *Zeitschrift für Technische Physik*, vol. 10, 1929, p. 146.

8 "An Analysis and Experimental Investigation of a Method for Determining the Thermodynamic Temperature of High Velocity Combustion Gases," by J. A. Clark, SM thesis, Department of Mechanical Engineering, Massachusetts Institute of Technology, May, 1949.

9 "Introduction to Aerodynamics of a Compressible Fluid," by H. W. Liepmann and A. E. Puckett, John Wiley & Sons, Inc., New York, N. Y., 1945.

10 "Gas Tables," by J. H. Keenan and J. Kaye, John Wiley & Sons, Inc., New York, N. Y., 1948.

11 "A Versatile Pneumatic Instrument Based on Critical Flow," by W. A. Wildhack, *Review of Scientific Instruments*, vol. 21, January, 1950, pp. 25–30.

12 "Experimental Analysis of a Pressure-Sensitive System for Sensing Gas Temperature," by R. S. Cesaro, R. J. Koenig, and G. J. Pack, NACA TN 2043, 1950.

13 "Sonic-Flow-Orifice Temperature Probe for High-Gas-Temperature Measurements," by P. L. Blackshear, Jr., NACA TN 2167, September, 1950.

14 United Aircraft Corporation, Research Department Report M12133-6, prepared by Richard Curry, November 16, 1949.

Appendix

If the temperature distribution at point 2 and velocity distributions at both points 2 and 3 are known a modified form of Equation [2] may be used for determining the mean temperature at point 3, Fig. 2.

Define flow rate, average density, and average temperature, as follows

$$\left.\begin{aligned} w &\equiv \int_A \rho V dA \\ \bar{\rho} &\equiv P/R\bar{T} \\ \bar{T} &\equiv \frac{1}{w}\int_A T\rho V dA \end{aligned}\right\} \qquad [14]$$

If the mass average velocity is defined as $\bar{V} = w/(\bar{\rho}A)$ then

$$\bar{V} = \frac{1}{A}\int VdA \qquad [15]$$

and

$$\bar{T} = \frac{PA\bar{V}}{Rw} \qquad [16]$$

Define the momentum average velocity as

$$\bar{V}_m \equiv \frac{1}{w}\int_A Vdw = \frac{1}{w}\int_A \rho V^2 dA \qquad [17]$$

Also define

$$J \equiv \bar{V}_m/\bar{V} \qquad [18]$$

Then the momentum equation may be written for a constant-area duct as

$$A(P_2 - P_3) = \frac{w_3}{g_0}\bar{V}_{m3} - \frac{w_2}{g_0}\bar{V}_{m2} \qquad [19]$$

Then a modified Equation [2] is obtained by combining Equations [14] through [19]

$$\bar{T}_3 = \frac{P_3}{P_2}\frac{R_2}{R_3}\frac{\bar{T}_2}{(1+f)^2}\left[\frac{R_2\bar{T}_2 g_0}{\bar{V}_2^2 J_2}\left(1 - \frac{P_3}{P_2}\right) + \frac{J_3}{J_2}\right] \qquad [20]$$

which may be used to determine an average temperature at point 3.

Combining Equation [18] with [15] and [17]

$$J = \frac{A\int_A \rho V^2\,dA}{\left[\int_A V dA\right]\left[\int_A \rho V dA\right]} \qquad [21]$$

The values of J at two points are the same if the ratios of T/T_{CL} and V/V_{CL} are each the same functions of r at the two points. The value of J is unity if V and T are uniform across the duct, e.g., one-dimensional flow.

Discussion

S. W. Greenwood.[4] The authors quote Blackshear who obtained static temperature results with the sodium D line-reversal method higher than the stagnation values obtained with a thermodynamic instrument using two consecutive flow elements. A study of the literature on the line-reversal method indicates that temperature values closely approaching, and in some cases even exceeding, the theoretical values for complete combustion are frequently obtained. The discrepancy between the two sets of results noted by Blackshear may, perhaps, therefore be partly attributed to defects in the line-reversal method.

With regard to the thermodynamic method tentatively proposed by the authors, and centering on Equation [2], the limitations inherent in the assumptions on which the equation is based appear to be quite severe. The value for T_3 determined in practice would be too high, the error depending on the extent to which the basic assumptions were invalid.

It would be interesting to know whether any correlation has been effected between the proposed theory and practical cases of heat addition.

The refinement of Equation [2], given as Equation [20] in the Appendix, requires a knowledge of the velocity distribution at Section 3. It would seem that this requires a knowledge of the density variation across the section, which in turn requires a knowledge of the temperature variation. If this is known, the analysis is not required! Comment on this point would be appreciated.

With respect to Fig. 9, one feels that when $P_1 - P_w$ is zero, then ΔT per cent should also be zero. Could the authors account for the departure from this condition?

It would be interesting to know where the static-pressure taps in the duct wall were placed relative to the probe. Was any investigation made of the effect of varying the position of the taps?

In connection with the proposal of the authors to place free-stream static-pressure taps in the outer wall of the probe, it might be desirable to position such taps in a plane perpendicular to the probe stem, to avoid the influence of the stem and of proximity to the duct walls on the static-pressure readings obtained.

[4] Assistant Research Engineer, Gas Dynamics Laboratory, Department of Mechanical Engineering, McGill University, Montreal, Que., Canada.

Authors' Closure

We wish to thank Mr. Greenwood for his thoughtful and interesting comments on this work.

We agree that it is highly probable that the apparent discrepancy in Blackshear's results may be attributed to irregularities in the sodium D-line method. The conclusions drawn from Mr. Greenwood's literature survey in regard to the sodium D-line method are consistent in character with those of our reference 5, indicating the need for care and caution on the part of the experimenter if this presently widely used technique is to be employed in the measurement of high gas temperatures. Our experience with this method has involved the use of a fairly inexpensive spectrometer in experiments in which our objectives were to attempt to inject liquid sodium at a "point" in a gas stream and to determine the lowest temperature at which reversal could be observed. Attendant to the accomplishment of these objectives we encountered difficulty with obtaining and maintaining the proper slit adjustment on the spectrometer, clogging of the sodium injection system, and an unsatisfactorily sensitive calibration of the comparator lamp, all of which were inherent with our relatively simple setup. In addition we found, in general, not a precise reversal point but rather a band over which it was difficult to assign the exact reversal temperature. Frequently it appeared that one of the D-lines reversed while the other did not, again lending uncertainty and inaccuracies. Our conclusion was that to be more satisfactory the instrumentation would have to be more complicated and expensive and unwieldy. These latter characteristics seem to be found in many successful D-line installations and as such limit their use principally to the laboratory. One of our objectives in this present study was to develop a "temperature meter" of reasonable simplicity and expense at no sacrifice in mechanical reliability nor precision.

We are aware that Equation [2] would not be adequate for many constant area combustion processes owing to the departure from one-dimensional conditions because of the effects of flame holders and asymmetrical fuel injection and combustion. For this reason we re-emphasize the approximate nature which Equation [2] could assume, depending on the conditions of each particular combustion process. To our knowledge no experiments have been conducted on the method of Equation [2]. However, we doubt the value of such experiments, except to the particular individual and apparatus concerned, since the subject method is based on an experimental equation of state and three well-established principles: namely, Newton's Second Law; The Conservation of Mass; and the Second Law of Thermodynamics, each of which has not been contradicted in countless experiments. Thus any experiments using the method of Equation [2] would not check the method but would simply demonstrate the degree of departure of the conditions of the experiment from the assumptions underlying the method. Obviously, the results would have only local significance.

We do not share the enthusiasm of Mr. Greenwood's comment on our Equation [20]. We think a broader viewpoint is possible. It is true that to determine the velocity variation at station 3, Fig. 2, knowledge would be required of the temperature variation. This fact brings out the weakness of all such "bulk" methods and shows the necessity for an instrument which is a "temperature meter," as given by our Equation [4] and discus-

sion. However, once such velocity and temperature profiles have been established, say, as a function of some nondimensional quantity as a Reynolds number, then the J factors can be evaluated. We can visualize the convenience afforded to the experimenter who then uses these J factors in Equation [20] and is able to compute accurately the average downstream static temperature by making one simple measurement in the high-temperature region, namely, the static pressure. It is also conceivable that one might choose to "extrapolate" lower-temperature velocity and temperature profiles in order to improve the approximation of the determination of T_2.

We believe that inherent installation and instrument errors caused the manometer to indicate a zero difference in $P_1 - P_w$ when P_1 was actually less than P_w. This would result in the flow into the probe being similar to case 3, Fig. 8.

The static-pressure taps in the wall were located in the plane of the probe's entrance, as shown in Fig. 5. No investigation was conducted on the effect of changing the location of these pressure taps.

We agree that pressure taps located on the probe itself would probably be best placed in a plane perpendicular to the stem, although recent work at the NACA[8] has shown this not to be particularly critical if reasonable care is observed.

In addition to the comments on Mr. Greenwood's points we wish to make two more. During the initial stages of our experiments we found that excessive cooling of the gas sample was as serious as insufficient cooling. That is, with a high rate of coolant flow, water vapor would condense on the heat-exchanger surfaces resulting in incorrect measurement of mass flow. This was remedied by reducing the cooling flow, thus maintaining the heat-transfer surfaces hotter and dry.

In regard to our comment following Equation [13] it has been pointed out that once the static temperature has been determined, then an accurate value can be calculated for k. This being the case, the stagnation temperature as calculated by our Equation [13] is independent of uncertainties in gas composition.

[8] "Effects of Pressure-Rake Design Parameters on Static-Pressure Measurement for Rakes used in Subsonic Free-Jets", by L. N. Krause, NACA TN 2520 unclassified October 1, 1951.

Some Aspects of Design and Economic Problems Involved in Safe Disposal of Inflammable Vapors From Safety Relief Valves

By S. Chesler[1] and B. W. Jesser,[2] New York, N. Y.

The problem of disposal of inflammable vapors released from safety relief valves in petroleum refineries and similar types of units is treated in this paper. Three approaches are presented which are being employed in the design of pressure-relieving systems with the objective of reducing costs without sacrificing safety: (*a*) Use of diffusion equations to determine maximum concentration of gas at grade when a given quantity is discharged from a safety relief valve into the atmosphere. The solution assists in determining whether an open or closed system should be used. (*b*) Procedure whereby in closed systems, the sizes of discharge piping may be reduced by setting the relief valve below vessel design pressure. (*c*) Application of special type of safety relief valve in closed systems, in order to eliminate or reduce effects of back pressure.

Nomenclature

The following nomenclature is used in the paper:

a = throat area of relief valve, sq in.
C = gas concentration, pcf of air at any point x, y, on ground
C_A = kinetic-energy correction factor for adiabatic flow
C_K = kinetic-energy correction factor for isothermal flow
C_y = horizontal diffusion coefficient
C_z = vertical diffusion coefficient
D = inside diameter of pipe or vessel, in.
d = inside diameter of pipe, ft
E = joint efficiency
f = Fanning friction factor, dimensionless
G = mass velocity of gas, lb per sec per sq ft
g = gravitational constant, 32.17 fps per sec
h = effective stack height, ft
K = coefficient of discharge for relief valves
k = ratio of specific heats, dimensionless
L = equivalent length of pipe, ft
ln = logarithm to natural logarithmic base, e
M = molecular weight of gas, lb per lb mole
n = a number that depends on pressure accumulation within vessel (upstream of relief valve) (for 10 per cent systems n = 0.1, for 25 per cent systems n = 0.25 etc.)
P = absolute pressure of gas, psi
P_A = accumulative pressure within vessel (upstream of relief valve), psig
P_D = design pressure of vessel, psig
P_O = operating pressure in vessel, psig
P_S = set pressure of safety relief valve, psig
p = absolute pressure of gas, psf
r = critical pressure ratio, $(P_2/P_1)_{crit}$; depends on ratio of specific heats, k
S = allowable stress in design of vessels, psi
T = absolute temperature of gas, deg R = (deg F + 460)
t = thickness of vessel, in.
u = mean wind velocity, fph
V = linear velocity of gas, fps
v = specific volume of gas, cu ft per lb = $1/\rho$
W = weight of gas discharged, lb per hr
x = distance from base of stack down wind, ft
y = distance cross-wind from center line of gas stream, ft
ΔP_E = frictional pressure drop in entire length of pipe, based on inlet (upstream) conditions; psi
ΔP = corrected pressure drop, psi = $C_K \Delta P_E$ or $C_A \Delta P_E$
ρ = density of gas, lb per cu ft.

Subscripts:

1 = upstream—at inlet to pipe or at inlet to relief valve (in latter case it refers to accumulative conditions)
2 = downstream—at outlet of pipe or at outlet of relief valve
c = refers to critical flow conditions at end of pipe or in throat of relief valve

Introduction

During the design of nearly all petroleum refineries and similar types of units, the question always arises as to the method of disposal of the inflammable vapors released from safety relief valves. There is the first decision as to whether the discharge shall vent directly to the atmosphere or to a closed system terminating in a refinery flare or a water-quenched stack. If the decision is in favor of the open system, a minimum of additional work is required. However, if a closed system is selected, a considerable number of problems must be solved in order to attain a safe and satisfactory system. In most cases this is a rather expensive system with long large lines meandering all over the refinery. The present paper will not attempt to cover the complete detailed design of such systems since the API is now in the process of preparing an extensive bulletin on the subject of "Pressure Relieving Systems."

This paper will, however, present three approaches presently being employed in the design of pressure-relieving systems in an effort to reduce their costs without sacrificing safety:

1 The first method assists in making the decision of open system versus closed system. It involves the use of diffusion equations

[1] Piping Engineer, The M. W. Kellogg Company.
[2] Head, Piping Analytical Section, The M. W. Kellogg Company. Mem. ASME.

Contributed by the Petroleum Division and presented at the Semi-Annual Meeting, Toronto, Ont., Can., June 11–15, 1951, of The American Society of Mechanical Engineers.

 Manuscript received at ASME Headquarters, May 15, 1951. Paper No. 51—SA-18.

in order to determine the maximum concentration of a gas that might be expected at grade when a given quantity of gas is discharged from a safety relief valve into the atmosphere. The location of this point of maximum concentration also may be determined.

2 The second method presents a procedure whereby, if a closed system is used, the sizes of the discharge piping may be reduced by setting the pop pressure of the conventional safety relief valve below the design pressure of the vessel.

3 The third method also applies to closed systems. It involves the application of a special type of safety relief valve presently being developed in order to eliminate or reduce the effects of back pressure and thus reduce line sizes in the discharge system. Experimental valve-capacity data observed by the authors are included.

In order to give a realistic picture of the cost and economy involved, typical safety relief-valve discharge systems have been set up, sized, and priced for the various alternatives just presented. Also included are cases covering the alternative back pressures permitted by the 1943 API-ASME code (10 per cent) and the 1950 ASME UPV code (25 per cent).

Definition of Terms

"Safety relief valve"—a spring-loaded automatic pressure-actuated relieving device, characterized by pop action and a closed bonnet so that it is suitable for service as either a safety valve or a relief valve. For convenience and in line with usual refinery practice, the term in this paper will be condensed to "relief valve." Furthermore, consideration has been given only to nozzle-type high-lift relief valves.

"Set pressure"—vessel pressure at which relief valve is set to open or pop.

"Opening pressure"—vessel pressure at which there is a measurable opening of disk.

"Relieving pressure"—vessel pressure existing while relief valve is discharging.

"Accumulative pressure"—maximum relieving pressure permitted by code.

"Reseat pressure"—vessel pressure at which valve closes automatically after discharge.

"Blowdown"—difference between opening and reseat pressure.

"Back pressure"—pressure at outlet of relief valve.

"Superimposed back pressure"—back pressure that is exerted at outlet of relief valve by release of vapors from other relief valves tied ir to same closed system.

"Lapse rate"—rate of decrease of atmospheric temperature with altitude.

"Inversion"—meteorological condition wherein atmospheric temperature increases with altitude.

Gas Concentrations Resulting From Discharge Directly to Atmosphere

The decision between an open or a closed relief-valve system is many times an arbitrary one based on local conditions, past practices, and the general feelings of the person or persons making the decision. There is seldom any concrete fact on which to base the decision. Recently, however, this problem has been attacked by making use of the theoretical equations for the dispersion of gases from tall stacks as developed by Bosanquet-Pearson (1)[2] and Sutton (2). These theoretical equations have been applied by Thomas, Hill, and Abersold (3) to a large number of field measurements in which the ground concentrations of SO_2 gas released from tall stacks was determined. Very good agreement with the theory has been indicated.

In essence these diffusion equations define the action of smoke or gases as they leave a stack, turn downwind, and cone out. At some point downwind, the cone reaches the ground, and there the gases are reflected. The point of maximum ground concentration is somewhat downwind of the point where the cone first reaches the ground.

Swift and Murphy (4) used these equations to calculate the maximum ground concentration that would be expected when the relief valves popped on an alkylation unit. Assuming a 1 mile wind, they arrived at a concentration range of 0.44 to 0.55 per cent by volume, which is well below the minimum limit of explosibility (5) of any gas likely to be encountered in that particular case.

The Bosanquet-Pearson formula is given as

$$C = \frac{W}{\sqrt{2\pi C_y C_z}\, ux^2} e^{\left(-\frac{h}{C_z x} - \frac{y^2}{2C_y^2 x^2}\right)} \qquad [1]$$

On differentiation, the location of the maximum ground concentration is shown to be at

$$x = \frac{h}{2C_z} \text{ with } y = 0 \qquad [2]$$

and the maximum ground concentration is given as

$$C_{\max} = \frac{0.216\, W}{uh^2} \left(\frac{C_z}{C_y}\right) \qquad [3]$$

Sutton's formula for maximum ground concentration is exactly the same, except that the numerical constant is 1.09 as great. For the distance between the source and the point of maximum concentration, Sutton's formula yields a figure at least double that of Bosanquet and Pearson.

The diffusion coefficients are functions of both elevation and meteorological conditions. Low values correspond to high elevations and inversion conditions, while high values correspond to low elevations and lapse conditions. Bosanquet-Pearson assumed mean values of $C_y = 0.08$ and $C_z = 0.05$, whereas Sutton showed a range of 0.07 to 0.21 for C_y and 0.035 to 0.21 for C_z. The work of Thomas, Hill, and Abersold showed the best agreement between theoretical equations and field measurements when diffusion coefficients of 0.05 to 0.07 were used. This more or less confirmed the information of Best (6), who found that, above stack heights of 20 to 25 m, vertical and horizontal diffusion coefficients are about equal, yielding a C_z/C_y ratio of 1.

In order to facilitate the use of the Bosanquet-Pearson equation (1), a plot, Fig. 1, has been prepared showing the discharge rate of vapor versus maximum ground concentration for various stack heights. This plot is based on a wind velocity of 1 mph and a C_z/C_y ratio of 1.00. Results from Fig. 1 should be corrected for the appropriate ratio of C_z/C_y.

To date most of the work with the diffusion equations has been applied to stacks handling material closely associated with air and at low stack velocities. In applying these equations to the discharge from relief valves to the atmosphere, consideration must be given to factors not inherent in the equations, namely, stack velocity, density, and the effect of diluents. Then there is also the question of point source versus line source.

Von Hohenleiten and Wolf (7) included stack velocity as one of their variables in a model study of smoke plumes, prior to the building of the Riverside Station of the Baltimore Consolidated Gas & Electric Company. They found that stack velocity has a considerable effect on the elevation of the plume. Fig. 2(a) reproduces one of their plots and indicates the difference in smoke plumes produced by stack velocities of 15 and 50 fps with a

[2] Numbers in parentheses refer to the Bibliography at the end of the paper.

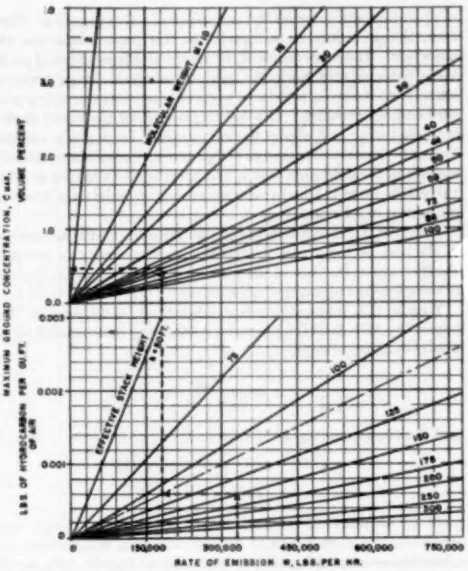

FIG. 1 MAXIMUM GROUND CONCENTRATION VERSUS RATE OF EMISSION FOR VARIOUS STACK HEIGHTS

(Basis: Bosanquet-Pearson equation, $C_{max} = \frac{0.216W}{uh^2}\left[\frac{C_z}{C_y}\right]$; $C_z/C_y = 1$; wind velocity (u) = 1 mph.)

10-mph wind. With a lower wind velocity, the larger stack velocity should be even more effective in placing the plume at a higher elevation. Studies made after the completion of the plant at Baltimore showed that the correlation between model and actual plant was very good. Furthermore, the results with a 50-fps velocity were so encouraging that, when subsequent units were added, they were designed for a 90-fps velocity, and nozzles were incorporated in the stack outlets. Although the velocities involved are much lower than the 500–1000 fps that might be obtained in a relief-valve discharge pipe, the experience at Baltimore does give a qualitative indication of what can be expected.

Taylor, Grimmett, and Comings (8) determined the velocity and momentum profiles of jets of air mixing with air through velocity ranges of 30 to 800 fps. Their study was carried out to a distance 30 diam from the nozzle, at which point the instantaneous velocity at the axis of the jet was still 22 per cent of the initial velocity. Furthermore, these authors showed that the original air from the jet has been diluted with 7.5 volumes of air by entrainment at the 30-diam location. Albertson, et al (9) in a similar study found that the center-line velocity at 100 diam was still 6 per cent of the initial velocity, and the dilution was 18 volumes at 65 diam.

Combining the foregoing observations and applying them to the vertical discharge from a relief valve into an atmosphere moving horizontally at 1 mph, it is reasonable to assume that the flow pattern would be as shown in Fig. 2(b). The gases would first rise in a vertical cone for some distance and then would roll over into the horizontal. It appears that this phenomenon can best be incorporated into the Bosanquet-Pearson equation by using an "effective stack height." This effective stack height would equal the height of the actual outlet plus an allowance for velocity for which 60 to 100 diam of the outlet-pipe size appears to be a reasonable figure.

Since the Bosanquet-Pearson and Sutton equations are based on eddy diffusion, density is not considered as a factor. However, density may enter the over-all phenomenon by exerting its effect before the diffusion process starts. This is forcibly brought out by Thomas, Hill, and Abersold (3) in their discussion of the effect of temperature. They point out that with low wind velocities, smoke at high temperatures will rise to high levels above the stack before coning out according to the diffusion equations, whereas with high wind velocities, the hot gases are blown nearly horizontally from the top of the stack, and thus temperature and density effects are practically negligible. Therefore, with low wind velocity and density less than air, one would expect a gas to rise before coning out, and with density greater than air to fall vertically before coning out. This latter effect has definitely been observed in refineries on many occasions when hydrocarbon vapor has been seen to roll out of the top of a stack and drop toward the earth.

This approach to the effect of density, however, neglects any consideration of velocity of emission. In the discharge from relief valves these velocities are so high that by the time the vertical-velocity component of the issuing stream has been reduced to the magnitude where the difference in density between the stream and the air will have any effect, the stream has "coned" out considerably, and the diffusion process is well under way. Thus the theorized pattern under low wind and high stack velocities as indicated in Fig. 2(b), should not be changed in any appreciable manner by density effects.

FIG. 2(a) EFFECT OF MODERATE STACK VELOCITY ON SMOKE PATTERN, SHOWING UPPER AND LOWER LIMITS OF SMOKE PATH (10-mph wind and 167-ft stack elevation. Courtesy of von Hohenleiten and Wolf, ref. 7.)

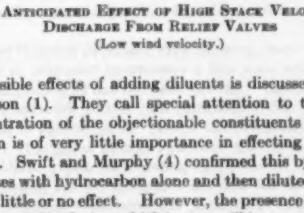

FIG. 2(b) ANTICIPATED EFFECT OF HIGH STACK VELOCITY ON GAS DISCHARGE FROM RELIEF VALVES (Low wind velocity.)

The possible effects of adding diluents is discussed by Bosanquet-Pearson (1). They call special attention to the fact that the concentration of the objectionable constituents at the point of emission is of very little importance in effecting ground concentration. Swift and Murphy (4) confirmed this by calculating several cases with hydrocarbon alone and then diluted with steam and found little or no effect. However, the presence of steam will increase the stack velocity, which in turn will increase the effective stack height. Steam is normally tied into most relief-valve dis-

charge vents anyway and, in some cases, it may be advisable to increase the size of the steam tie-in line and make the admission of steam automatic. Everything possible should be done to increase the velocity of emission even to the point of putting nozzles at the outlets of the discharge pipes.

The Bosanquet-Pearson Equation [1] is based on a point source of emission. The original reference also includes an equation for a line source, such as a battery of chimneys. Neither of these equations fits precisely the refinery situation where relief valves are to be discharged to the atmosphere. For an individual unit, the outlet pipes are close enough together so that the total quantity discharged may be considered as emanating from a single central source at an average height. When there is a group of units involved, it appears best to consider each unit as a point source. The maximum concentration at any given point may then be assumed to be equal to the sum of the individual concentrations resulting from gas release from the various units. The individual concentrations may be determined from Equation [1] or [3].

Effect of Setting Relief Valves Below Vessel Design Pressures on Closed Discharge Systems

The sizing of a closed system collecting vapors released from conventional-type relief valves is governed by the maximum permissible back pressure at the valve outlet. As is well known, this conventional type of valve responds to the full impact of the back pressure and as such operates essentially on the differential that exists between the pressure upstream of the relief valve and that immediately downstream, i.e., the back pressure. In view of this behavior the pressure drop available for vapor flow in the discharge system is equal to the pressure accumulation within the vessel as permitted by the governing code. At present, practically all petroleum vessels are designed in accordance with one of the following Unfired Pressure Vessel Codes: (*a*) 1943 API-ASME, (*b*) 1949 ASME, or (*c*) 1950 ASME. The pressure accumulation permitted by the first two codes is 10 per cent of the design pressure. The same is true of the 1950 ASME code, except that, in the case of fire condition, this code permits 20 per cent accumulation. It is also important to note that the Non-Mandatory Appendix M of this code states that in "manifold discharge systems, ... the header should be so designed as to limit the back pressure to approximately 25 per cent of the set pressure of the lowest set valve." Thus it can be assumed that all refining units designed to the 1950 ASME UPV code will probably have "25 per cent discharge systems," while those designed to 1943 API-ASME and 1949 ASME will have "10 per cent discharge systems." Since the number of states which, at present, have approved the 1950 ASME UPV code is rather limited, most of the systems presently being designed must legally be "10 per cent systems."

For vessels whose design pressures are fairly low and where the quantity to be relieved is quite large, the pipe sizes in the closed systems become very large if the system is to accommodate the discharge from the relief valves within the foregoing back pressure limitations.

If a larger back pressure were available, it would permit a reduction in pipe sizes and a consequent reduction in the cost of the closed system. One way that this can be accomplished, without violating code limitations, is by setting the relief valve below the design pressure of the vessel. Thus, instead of the pressure drop available for the discharge system being only 10 per cent (or 25 per cent) of the design pressure, the drop available would be this figure plus the difference between the set pressure and the design pressure. Of course, the immediate objection to such a procedure is that it would decrease the spread between the operating pressure and the set pressure, and thus limit the flexibility of operation and increase the frequency of valve popping. However, the procedure recommended in this paper eliminates this objection. The set pressure of the relief valve is established on the same basis as that normally used to establish design pressure, namely, to secure a satisfactory spread between operating pressure and set pressure. The design pressure of the vessel is then increased over and above the set pressure by a given amount. Not only does this increase in design pressure result in substantial savings in the discharge piping, but there is also a saving in relief-valve cost since the higher design pressure results in a lower requirement of relieving area.

However, an increase in the design pressure means an increase in the cost of the vessel. Therefore it is necessary to compare the increase in the cost of the vessel with the decrease in the cost of the discharge piping and relief valves.

Within the internal-pressure limitations considered in this paper, the API-ASME formula for calculating the corroded thickness of cylindrical shells

$$t = \frac{P_D D}{2SE - P_D} \qquad [4]$$

and the corresponding ASME formula

$$t = \frac{P_D D}{2SE - 1.2P_D} \qquad [5]$$

yield for all practical purposes the same results for design temperatures not exceeding 650 F. Beyond this temperature the allowable stresses differ slightly and lead to slightly different results. However, since the design conditions considered herein have been selected arbitrarily, there is no loss in generality if an over-all API-ASME basis is used.

Fig. 3 shows a plot of the required corroded thickness of cylindrical shells for various internal pressures. The chart, as indicated, is based on the API-ASME formula and is applicable to vessels designed for a temperature not greater than 650 F, and a joint efficiency of 80 per cent. As explained previously, there is no loss in generality in using this basic joint efficiency.

The line on the chart marked minimum thickness represents the API-ASME code requirement as expressed by the formula

$$t = \frac{D + 100}{1000} \qquad [6]$$

and is independent of the design temperature.

Points, representing diameters and design pressures of vessels, to the left of the line marked minimum thickness, indicate minimum-thickness vessels, whereas, points to the right of this line indicate that the thickness is determined by pressure. Thus, in the case of vessels with design temperature equal to or less than 650 F and lying to the left of the minimum-thickness line in Fig. 3, the design pressure may be increased up to that corresponding to the minimum thickness with no additional cost for the cylindrical shell. The heads may have to be made heavier and reinforcing pads at nozzles added, or increased in thickness. Because of the many variables involved, it is impractical to develop any general economic relation between incremental increase in vessel cost and savings in discharge piping. Nevertheless, experience has indicated that wherever vessels are operating at low pressures and relieving into closed systems, it definitely pays to put a spread between the set pressure and design pressure. It is not always necessary nor even advisable to raise the design pressure to that corresponding to minimum thickness. Five or ten pounds may sometimes be sufficient. Furthermore, the procedure is not necessarily limited to vessels with design temperatures at or below 650 F. That merely limits the use of Fig. 3.

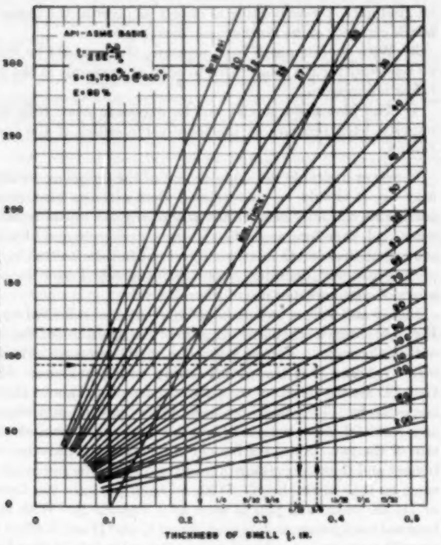

FIG. 3 REQUIRED THICKNESS OF CYLINDRICAL SHELLS FOR INTERNAL PRESSURE

In following the foregoing procedure there is one precaution that must be taken. Due to the fact that the vessels involved have relatively low set pressures, indiscriminate raising of the design pressure and a consequent wide spread between accumulative pressure and set pressure, may result in the back pressure being above the critical pressure. To check this point, the following general formula may be used in order to determine for any given set pressure P_S, what maximum design pressure P_D may be used without exceeding the critical condition

$$P_D = \frac{1}{(1+n)(1-r)} P_S - \frac{\text{atm pressure}}{(1+n)} \ldots\ldots [7]$$

where n is a number that depends on the permissible accumulation; for 10 per cent accumulation $n = 0.1$; for 25 per cent accumulation $n = 0.25$, etc; r is the critical pressure ratio $(P_2/P_1)_{crit}$ that depends on the ratio of specific heats, k.

Assuming a critical ratio of 0.55 and an atmospheric pressure of 14.7 psi, one obtains:

For 10 per cent systems

$$P_D = 2.02\, P_S - 13.4 \ldots\ldots [8]$$

For 25 per cent systems

$$P_D = 1.78\, P_S - 11.8 \ldots\ldots [8a]$$

If it is desired to raise the design pressure higher than the figure resulting from Equation [8] or [8a], then it is necessary that the relief-valve area for the vessel be calculated from the noncritical formula

$$W = 2404Ka \sqrt{\left(\frac{P_1}{v_1}\right)\left(\frac{k}{k-1}\right)\left[\left(\frac{P_2}{P_1}\right)^{2/k} - \left(\frac{P_2}{P_1}\right)^{1+k/k}\right]} \ldots [9]$$

The simple case of a single vessel 10 ft diam operating at 10 psig and releasing 160,000 lb per hr of 300 F and 62-molecular-weight vapor to a flare 2000 ft away will serve to illustrate the savings that may be derived by following the procedure recommended. Table 1 serves to summarize the results of this illustration. If it is assumed that the normal basis for spread between operating pressure P_O, and design pressure P_D, is 10 per cent or 10 lb whichever is greater, the design and set pressures for the conventional procedure will be 20 psig. The set pressure under all columns of the recommended procedure will also be 20 lb. By using Equations [8] and [8a], the maximum design pressure for the critical flow case is 27 psig and 24 psig, respectively. If a higher design pressure is desired, reference to Fig. 3 indicates that it may be increased to 40 psig without increasing shell thickness for the noncritical flow case. Accumulative pressure P_A is obtained by multiplying the design pressure by 1.1 or 1.25, respectively, for the 10 per cent or 25 per cent systems. The back pressure available for the design of the discharge system is the accumulative pressure minus the set pressure. Critical pressure (gage) = 0.55 (P_A + 14.7) − 14.7. The line size and safety relief-valve area are calculated following conventional practices except that Equation [9] is used for the noncritical flow case.

Reference to Table 1 clearly indicates that substantial savings can be achieved by setting relief valves below design pressure when minimum-thickness vessels are involved. For the 10 per cent system, the size of the discharge line was reduced from 26 to 16 in., and the net total cost reduced from $46,900 to $24,800. For the 25 per cent system, the line size was reduced from 22 to 14 in., and the cost from $42,000 to $21,900. Such savings can be made without any sacrifice in safety or operating flexibility and with a probable saving in engineering cost. Experience has indicated that savings of this order are typical but naturally are a function of the extent of the discharge system.

In the case of vessels that lie to the right of the minimum thickness line in Fig. 3, the same procedure with regard to a spread between set and design pressure may be applied, but the savings in general are not as substantial. Normally, the plot of vessel diameter versus design pressure in Fig. 3 will lie between two thicknesses. Since the tower, undoubtedly, will be purchased with the thicker plate, an increase in the design pressure usually may be obtained for the small cost of increasing the size of the

TABLE 1 EFFECT OF SETTING RELIEF VALVE BELOW DESIGN PRESSURE ON MINIMUM-THICKNESS VESSELS

	Conventional procedure		Setting valve below design pressure			
			Critical flow		Noncritical flow	
Designation[a]	10 per cent	25 per cent	10 per cent	25 per cent	10 per cent	25 per cent
Operating pressure	10	10	10	10	10	10
Set pressure	20	20	20	20	20	20
Design pressure	20	20	27	24	40	40
Accumulative pressure	22	25	29.7	30.0	44	50
Back pressure	2	5	9.7	9.9	24	30
Critical pressure	5.5	7.1	9.7	9.9	17.6	20.9
Line size, in.	26	22	18	18	16	14
Relief-valve area, sq in.	50.7	50.7	42.3	45.4	33.4	33.4
Installed piping cost[b]	$46,900	$42,000	$34,500	$34,500	$23,400	$20,500
Incremental vessel cost	0	0	$ 1,100	$ 1,100	$ 1,400	$ 1,400
Total net cost	$46,900	$42,000	$35,600	$35,600	$24,800	$21,900

[a] All pressures are gage.
[b] Includes relief valves.

reinforcing pads and the thickness of the tower heads. For example, an 8-ft tower designed for 80 psig requires, according to Fig. 3, a corroded thickness of slightly over or $^{11}/_{16}$ in. which would require a $^{3}/_{4}$-in. plate, corresponding to a design pressure of 85 psig. Therefore, if the set pressure is maintained at 80 psig and the design pressure raised to 85 psig, then there will be an additional 5 psi available for the discharge system. In some cases where one particular tower is the bottleneck in the design of a discharge system, it may be found economically feasible to jump a plate thickness by $^{1}/_{16}$ in. or more.

Use of Relief Valves That Operate Independently of Back Pressure

Another approach to the problem of reducing discharge-line size involves the use of a special type of relief valve so designed that the effect of back pressure on the operation of the valve is essentially eliminated. For convenience and due to the lack of any better generic name for this special type of relief valve, such valves will be referred to in this paper as "back pressure" relief valves, as contrasted with the "conventional" relief valve.

The potentialities involved in the use of a good back-pressure valve are best illustrated by reference to Fig. 4. The capacity curve for a conventional relief valve holds up fairly well until a back pressure of about 10 per cent is reached. Then it falls off rapidly and is usually closed at 15 to 18 per cent back pressure. By contrast, the theoretical nozzle curve maintains capacity up to the critical point and then tapers off gradually to 0 at 100 per cent back pressure. Even at 90 per cent back pressure, the capacity has dropped only to 65 per cent. To anybody who has been juggling around relief-valve discharge systems with an over-all available back pressure of only 2 or 3 lbs, the thought of designing a system based on this curve would be a welcome relief.

In the development of a good back-pressure relief valve there are four main conditions that must be achieved. They are as follows:

1 With a superimposed back pressure at the valve outlet the valve should pop when the contents of the vessel reach the set pressure.

2 After the valve pops and the vessel reaches the accumulative pressure, the valve should attain its full lift and its rated capacity against back pressure. The rated capacity should be maintained until the back pressure reaches critical and then, with further increase in back pressure, the capacity should fall off gradually, approximating as closely as possible the theoretical nozzle capacity curve for the noncritical region.

3 With superimposed back pressure, there should be little or no tendency for the relief valve to open at pressures in the vessel below set pressure.

4 The blowdown should not be excessive even with superimposed back pressure at the relief-valve outlet at the time of closing.

However desirable the achievement of the foregoing conditions may be, it should be remembered that extreme back-pressure conditions can only occur when practically the entire refinery is upset and, therefore, variations in the set pressure and blowdown somewhat broader than normally permitted are tolerable. Capacity, however, definitely should be established over the entire range of contemplated use of the relief valve.

Figs. 5 and 6 show two makes of conventional relief valves, and Fig. 7(a) shows a schematic diagram of the operation of the forces within the valve. Forces A are due to the pressure within the vessel. Force B is the counteracting spring pressure. Forces C and D are the results of back pressure below and above the disk, respectively. This back pressure either may be superimposed or a result of vapor released from the valve itself, or a combination of the two. Since the bonnet is enclosed, the pressure in the bonnet and thus the pressure above the disk will be essentially the same as that in the bowl. With no back pressure (no forces C or D) the valve will pop as soon as A exceeds B. With superimposed back pressure, however, forces C and D are in effect and, since D operates over a greater area, the valve is held closed until the pressure in the vessel builds up to the set pressure plus the back pressure. A similar situation exists when the valve is open. As soon as the back pressure becomes greater than the difference between the relieving pressure and the set pressure, the valve will close. Reaction effects of the vapor on the under side of the disk and the effects of the secondary orifice will tend to keep the valve open somewhat longer, but only to the extent of about 5 per cent of the set pressure.

First attempts to develop a back-pressure relief valve involved eliminating the vent between the bowl and the bonnet. The bonnet was then vented to atmosphere to release any vapors that leaked past the disk and the guide. With the bonnet under atmospheric pressure, forces D were eliminated [see Fig. 7(b)]. This solved the situation to some degree when the valve was open and creating its own back pressure. However, when the valve was in the closed position with a superimposed back pressure at the valve

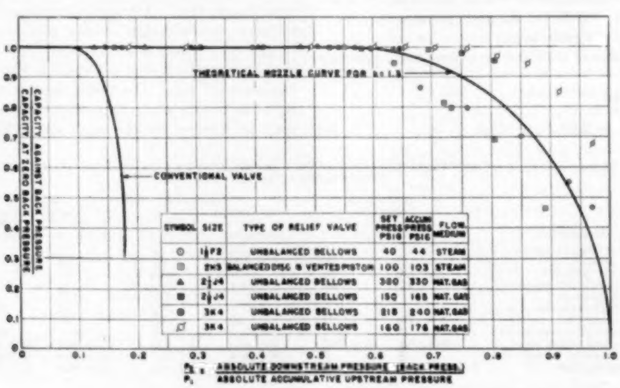

Fig. 4 Effect of Back Pressure on Capacity of Relief Valves

outlet, forces C would act in conjunction with A against B, and the disk would be lifted off the seat at vessel pressures well below set pressure.

Since that time the valve manufacturers in co-operation with some of the oil companies have been working on the development of a satisfactory back-pressure relief valve. Many types and designs have been tried out and tested but failed in one way or another to meet the desired requirements. However, developments have now reached the stage where installations of back-pressure valves are being made in both isolated test installations and complete refinery installations.

Back-pressure relief valves presently under consideration are in two general categories, namely, the balanced-disk and piston valve and the bellows valve. One form of the balanced-disk and piston group is illustrated in Fig. 8, and might be called the sealed-piston type. It is a development from the vented bonnet valve in which a secondary piston has been added (assuming the disk itself is the primary piston). The area of this secondary piston has been balanced against the seat area (i.e., the diameter of the secondary piston equals the diameter of the seat of the nozzle). A hole is located in the guide so as to permit the back pressure to be exerted both above and below the extended portions of the disk (or primary piston). The secondary piston makes

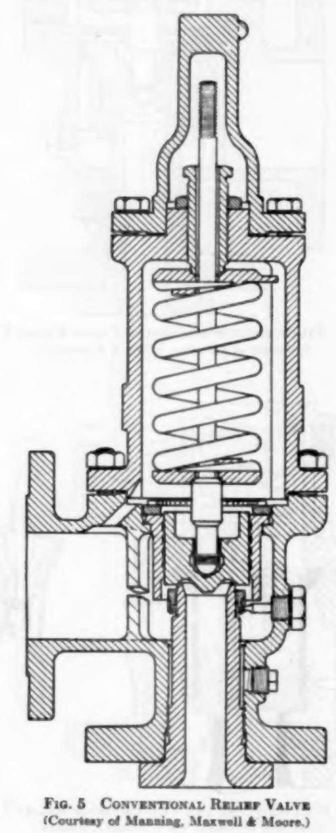

Fig. 5 Conventional Relief Valve
(Courtesy of Manning, Maxwell & Moore.)

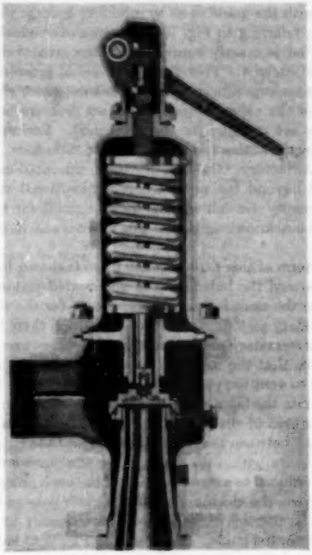

Fig. 6 Conventional Relief Valve
(Courtesy of Farris Engineering Company.)

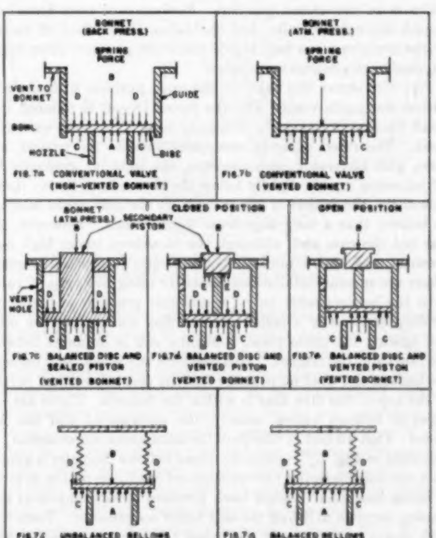

Fig. 7 Schematic Diagrams Showing Operation of Forces on Relief-Valve Disk

a close fit with the guide so as to minimize leakage into the bonnet. Thus, referring to Fig. 7(*e*), the area over which the forces D are exerted is exactly equivalent to the area over which the forces C are exerted. Therefore, with vessel pressure below set pressure and a superimposed back pressure, there should be no tendency for the valve to open before set pressure or to be held closed after set pressure has been reached. Performance tests witnessed by the authors confirmed these conclusions. Blowdown was also satisfactory. On capacity tests, the rated capacity was maintained beyond the point where conventional valves close, but the capacity did fall off rapidly at a point far short of the critical. It is acknowledged that this valve is still in the development stage.

Another form of this type of relief valve is shown in Fig. 9 and might be termed the balanced-disk and vented-piston valve. It is similar to the sealed-piston valve, except for the construction of the secondary piston. In the closed position there is a close fit between the secondary piston and the guide. However, the piston is recessed so that the moment the valve is opened, a large area is available to vent the gases from within the guide. These gases are vented into the bonnet and out the bonnet vent to the atmosphere. The area of the hole in the guide is considerably smaller than the area between the recessed piston and the guide. Therefore the pressure within the guide, when the valve is in the open position, is reduced to a small fraction of the back pressure.

Furthermore, the ejector effect of the gases passing by the hole in the guide as they leave the valve has a tendency to reduce the pressure within the guide. Reference to Fig. 7(*d*) indicates that in the closed position, the vented-piston valve performs essentially in the same manner as the sealed-piston valve, Fig. 7(*c*). Forces D operate over the entire top area of the disk, but forces E in the opposite direction counteract a portion of these forces. Since the areas are so balanced that $D - E = C$, there is no net effect resulting from back-pressure forces acting on the disk when the valve is in the closed position. Performance tests have confirmed this substantially, and the disk neither lifted off its seat prematurely nor was held closed above set pressure when superimposed back pressure was applied.

Fig. 7(*e*) shows the valve in the open position with the area within the guide vented and the forces D and E reduced to a small fraction of forces C. Capacity tests with steam were very good. The rated capacity was maintained to the critical, and then, with increasing back pressure, the capacity gradually fell off following a path slightly below the theoretical curve. As for blowdown, the release of pressure above the seat might lead one to believe that a long blowdown would result. However, this was not the case and, although the blowdown under high back pressure was above normal requirements, it was satisfactory. There are several installations presently using this type of valve.

In the bellows relief valve, a different principle is used. By welding one end of a bellows to the disk and sealing the other end against the guide plate, a definite seal is obtained between the bowl and the bonnet. This prevents any gases from entering the bonnet and thus no pressure force is exerted on that portion of the top of the disk that is within the bellows. There are two types of bellows valves, namely, the unbalanced and the balanced. Figs. 10 and 11 illustrate the unbalanced construction. As indicated in Fig. 7(*f*), where the mean bellows diameter is greater than the seat diameter, this unbalanced condition results in forces D being less than C when back pressure is superimposed, thus causing the disk to lift off the seat below set pressure. Tests with both steam and gas have confirmed this point. Capacity tests on the unbalanced bellows valves have been highly successful. Tests with gas showed that rated capacity was maintained to critical. Beyond that point the data followed a fairly smooth curve somewhat above the theoretical. Tests on two different

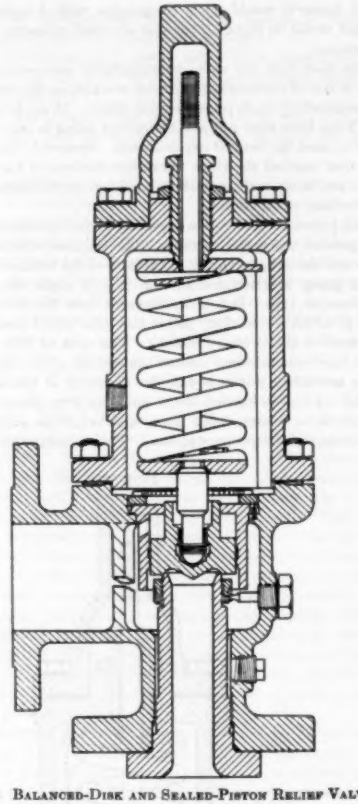

Fig. 8 Balanced-Disk and Sealed-Piston Relief Valve
(Courtesy of Manning, Maxwell & Moore.)

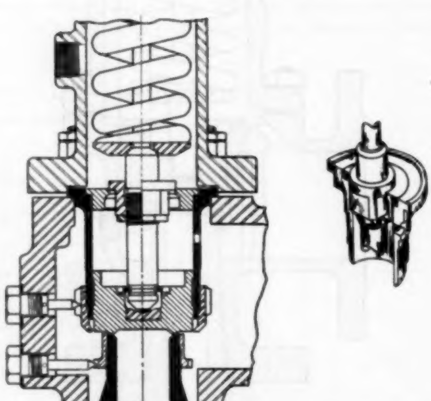

Fig. 9 Balanced-Disk and Vented-Piston Relief Valve
(Courtesy of Crosby Valve & Gage Company.)

valve sizes and at two different pressure ranges were in surprisingly good agreement from a capacity point of view. In a test with steam, good results were obtained, except that beyond the critical the capacity was somewhat below the theoretical.

The unbalanced bellows relief valve has been used in corrosive and asphalt service where variable back pressure is not a factor. It also can be used where there is a single tower discharging to a flare or vent line; or where there is one large vessel discharging into a system which collects only discharges of insignificant quantities from other vessels. In such cases only the large vessel can be equipped with unbalanced bellows relief valves. However, for the usual type of discharge system, handling the gas release from many towers, this valve is not satisfactory and must be considered as a development stage toward the desired end.

The balanced bellows relief valve is illustrated in Fig. 12 and the pressure effects in Fig. 7(g). By reducing the mean diameter of the bellows until it equals the diameter of the seat, the pressure effects of forces D and C are equalized. In this way the disadvantage of the unbalanced bellows valve in opening below set pressure is eliminated. Unfortunately, the authors have not had the opportunity to witness performance tests on the balanced bellows valves. The manufacturer points out that the only difference between the balanced and unbalanced valves is the reduction of the bellows diameter and the mechanical rearrangement of the moving parts so as to fit them within the smaller bellows. The size and relation of all other parts remain the same. Thus it is their thought and contention that the balanced valve should have essentially the same capacity as the unbalanced valve. There is another prevalent opinion that, by the very operation of balancing the valve, a condition has been set up whereby full lift may not be achieved with a resultant loss and inconsistency in capacity. Performance tests should clarify this situation. At present there are several complete installations—both in service and under construction—using balanced bellows valves.

The capacity data observed by the authors during their investigation of the back-pressure problem are covered in Fig. 4. These data are plotted as the ratio of the capacity of the valve at any given back pressure to the capacity at zero back pressure versus the ratio of absolute back pressure to absolute accumulative

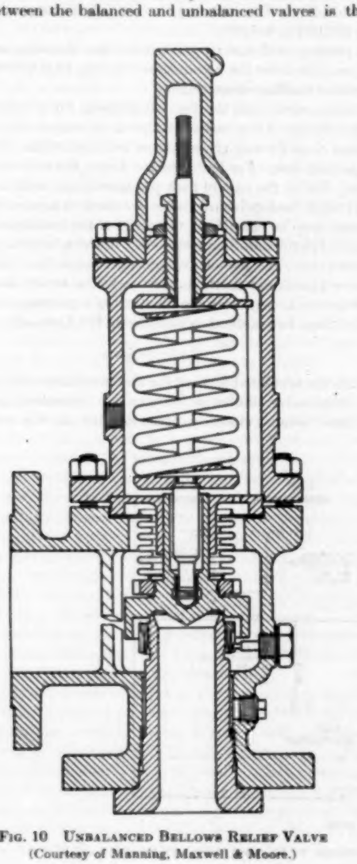

Fig. 10 Unbalanced Bellows Relief Valve
(Courtesy of Manning, Maxwell & Moore.)

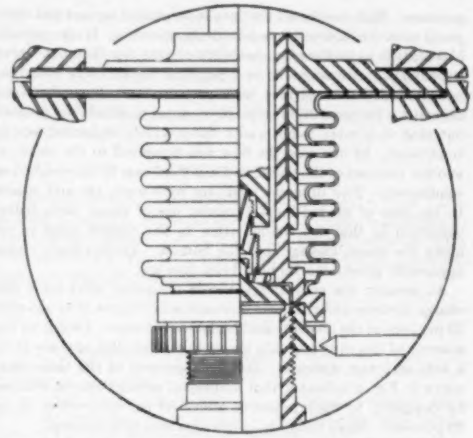

Fig. 11 Unbalanced Bellows Relief Valve
(Courtesy of Farris Engineering Company.)

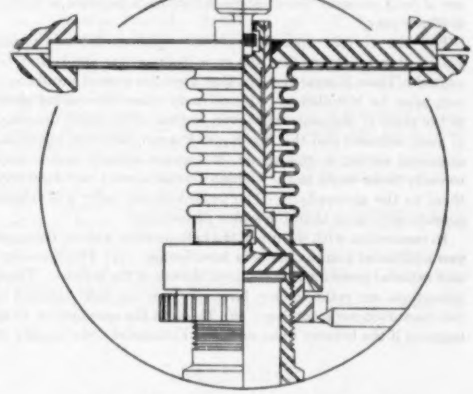

Fig. 12 Balanced Bellows Relief Valve
(Courtesy of Farris Engineering Company.)

pressure. This enables all the data to be plotted against and compared with the theoretical nozzle-discharge curve. It also permits observation as to the reproducibility of data for different valve sizes and pressure ranges in the noncritical region. The tested capacity of all valves at zero back pressure was above the rated capacity. In connection with these data, it should be pointed out that they were taken under three widely separated sets of conditions. In one case the flow was measured to the valve, in another case out of the valve, and in a third case it was weighed as condensate. Two different mediums were used, gas and steam. In the case of vented bonnet valves, use of steam gives better operation in that the condensation in the bonnet helps to remove the steam leakage into the bonnet. Furthermore, steam apparently gives a shorter blowdown than gas.

At present, the general practice in designing relief-valve discharge systems utilizing back-pressure relief valves is to use only 50 per cent of the absolute accumulative pressure. Owing to the scarcity of the capacity data above this point, this appears to be a safe and wise decision. However, perusal of the theoretical curve in Fig. 4 indicates that additional savings can be realized by designing to back pressures above 50 per cent—even up to 90 per cent. More test data in this area should be secured.

It should be pointed out that, for low-pressure vessels, the procedure previously described, of setting the conventional relief valve below the design pressure results in a larger back pressure available for the discharge system than would result from the use of back-pressure relief valves (where back pressure is limited to 50 per cent).

For the correct operation of the balanced-disk and piston valves, it is necessary that the gases leaking into the bonnet be vented. There is some thought that an entire second parallel system must be installed in order to carry away the vented gases to the point of disposal. However, in view of the small quantity of gases released and the Bosanquet-Pearson diffusion equations discussed earlier in this paper, it appears entirely satisfactory to carry these vents to the highest available point and discharge them to the atmosphere. The vented-piston valve will release considerably more than the sealed piston valve.

In connection with the use of the bellows relief valves, there are two additional points that bear mentioning. (*a*) There are certain external pressure limitations on the use of the bellows. These limitations are rather wide; however, they are fully covered in the manufacturer's catalog. (*b*) There is the question of what happens if the bellows leaks or fails. Fortunately, the quality of bellows is continually improving but, nevertheless, the possibility of leakage or failure is always present. If it does fail, the valve will operate in the same manner as the conventional valve and thus, if the valve is called on to operate against a high back pressure, it will be necessary for the vessel pressure to build up to a pressure in excess of the originally contemplated figure in order for the valve to open or remain open.

In order to evaluate the savings that may be achieved by using back-pressure relief valves, a typical refinery-flare system, consisting of several units was laid out, Fig. 13. The line sizes were calculated using 10 per cent and 25 per cent systems with conventional relief valves, and 50 per cent and 80 per cent systems using back-pressure relief valves except on those vessels where excess pressure was available, and thus the premium for the back pressure valve could not be justified. Table 2 summarizes the results of the line calculations and the installed costs for the various systems. From this table the reduction in line sizes and cost that can be achieved by the use of back-pressure relief valves is readily apparent. The main refinery header has been decreased from 28 in. for the 10 per cent case with conventional valves to 16 in. for the 80 per cent case with back-pressure valves. Similar reductions in line sizes were made for the individual leads and other headers. The reduction in cost for the two cases cited was from $89,900 to $58,600.

In passing, it should be pointed out that the comparable cost of an open system for the layout shown in Fig. 13 is $6600, including the cost of snuffing steam piping.

In connection with the line calculations for a relief-valve discharge system, it is a rather prevalent procedure to calculate the pressure drop for any given line on the basis of the average pressure in that line. For low pressure drops, the error is not appreciable. But in the case of high pressure drops, such as those produced when back-pressure valves are used, it is essential that the pressure drop be calculated, using either the isothermal approach of Lobo, Friend, and Skaperdas (10), or the adiabatic approach of Lapple (11). The use of average pressure rather than the adiabatic or isothermal methods may result in errors as high as 25 to 30 per cent. An example illustrating a pressure-drop calculation by these two methods is included in the Appendix.

Conclusions

From the tabulated costs of the systems illustrated, it is evident that relief-valve discharge systems are expensive propositions. Therefore, before a closed system is decided on, due consideration

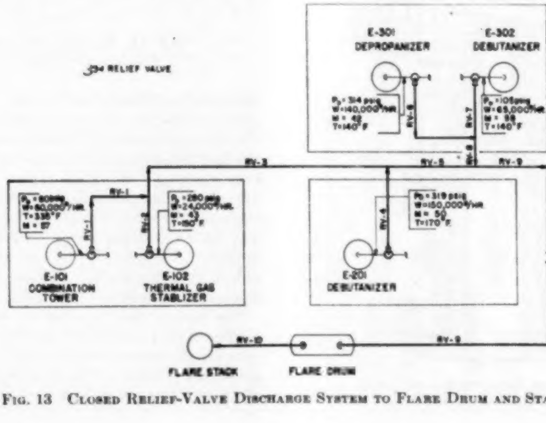

Fig. 13 Closed Relief-Valve Discharge System to Flare Drum and Stack

TABLE 2 EFFECT OF USING BACK-PRESSURE RELIEF VALVES IN A REFINERY FLARE SYSTEM

Back pressure	—Conventional— relief valves 10 per cent	25 per cent	—Back-pressure— relief valves 50 per cent	80 per cent
	—Line sizes, in.—			
Line RV-1[a]	14	12	8	8
Line RV-2[a]	4	3	3	3
Line RV-3[a]	18	16	10	10
Line RV-4[a]	10	6	6	6
Line RV-5[a]	24	18	14	12
Line RV-6[a]	8	6	6	6
Line RV-7[a]	12	8	6	6
Line RV-8[a]	16	12	10	8
Line RV-9[a]	28	22	20	16
Line RV-10[a]	28	22	20	16
Cost of variable items[b]	$67,300	$53,400	$44,300	$36,000
Cost of constant items[c]	$22,600	$22,600	$22,600	$22,600
Total cost	$89,900	$76,000	$66,900	$58,600

[a] See Fig. 13 for identification of line numbers.
[b] Includes installed cost of piping and relief valves, etc.
[c] Includes cost of flare drum, stack, foundations, pump, supports, etc.

should be given to an open system. With the Bosanquet-Pearson equation and proper allowance for the velocity of emission of the vapors, the degree and location of the maximum ground concentration can be ascertained. These data together with the layout of the refinery and surrounding territory should permit an evaluation of the degree of risk involved in an open system.

It should be remembered that in at least one respect an open system is safer than a closed system. In cases where one or more vessels in a refinery are out of service and the relief valve is to be removed, there is no risk at all with an open system. However, with a closed system, there is almost invariably some slight gas pressure in the system, and thus the removal of any relief valve opens up the system until a blind flange can be placed over the opening. Furthermore, there is always the possibility of a pop while the relief valve is being removed.

If an open system is selected, the point of release of the gases to the atmosphere should be at the highest possible point with the largest possible velocity of emission consistent with the pressure available. In this connection, where excess pressure is available, consideration should be given to nozzles at the pipe outlet in order to increase velocity. In addition, where low-pressure towers are involved either back-pressure valves should be used or the relief valve should be set below design pressure so that more static pressure is available for conversion into velocity.

The use of the open system is naturally not applicable to heavier vapors, (approximately 80 molecular weight and higher) because of the tendency to condense. Recommended practice in those cases is a closed system to a water-quenched stack which may also serve to handle the furnace blowdown.

When closed systems are required for one reason or another, the cost of the system can be reduced considerably by the two means presented, namely, setting the relief valve below the design pressure, and the use of back-pressure relief valves. The former is particularly advantageous for minimum-thickness vessels where the increased vessel costs resulting from raising the design pressure are usually very small compared to the savings in piping and relief valves in a closed discharge system. In cases above the minimum-thickness range, the advantages are limited somewhat but, on occasions, the method may have considerable value where one vessel is the "bottleneck" of the system.

The use of back-pressure valves at the present time should be limited to back pressures not exceeding 50 per cent of the accumulative absolute pressure, owing to lack of sufficient capacity tests for the range above critical. Development and testing in the range above critical should be continued so that eventually it will be possible to design with confidence to any back pressure. With the present 50 per cent limitation on back-pressure valves, the application to low-pressure towers is not as effective as the procedure of setting the relief valve below the design pressure.

In the case of balanced-disk valves that depend upon venting the bonnet, it is the opinion of the authors that, in most cases, the vent may be released to the atmosphere rather than be carried in a separate pilot system. If the gases are released at a high point with the largest possible velocity, the diffusion equations would indicate practically no risk at all because of the small quantity involved.

Acknowledgments

The authors wish to express their appreciation to Crosby Valve & Gage Company, Farris Engineering Company, and Manning Maxwell and Moore, for carrying out the performance tests. The assistance of Mr. V. J. Reamy, who carried out all the calculations, is also acknowledged.

BIBLIOGRAPHY

1 "The Spread of Smoke and Gases From Chimneys," by C. H. Bosanquet and J. L. Pearson, Transactions, Faraday Society, vol. 32, 1936, pp. 1249–1264.

2 "The Theoretical Distribution of Airborne Pollution From Factory Chimneys," by O. G. Sutton, Roy. Meteorological Society Quarterly Journal, vol. 73, 1947, pp. 426–435.

3 "Dispersion of Gases From Tall Stacks," by M. D. Thomas, G. R. Hill, and J. N. Abersold, *Industrial and Engineering Chemistry*, vol. 41, 1949, pp. 2409–2417.

4 "Waste Hydrocarbon Gas Disposal From an Alkylation Unit," by J. J. Swift and J. J. Murphy, The M. W. Kellogg Company Development Report, 1950 (unpublished).

5 "Chemical Engineer's Handbook," by J. H. Perry, third edition, McGraw-Hill Book Company, Inc., New York, N. Y., 1950, p. 1585.

6 "Transfer of Heat and Momentum in the Lowest Layers of the Atmosphere," by A. C. Best, Geophysical Memoirs, Great Britain Meteorological Office, London, England, no. 65, 1935.

7 "Wind-Tunnel Tests to Establish Stack Height for Riverside Generating Station," by H. L. von Hohenleiten and E. F. Wolf, Trans. ASME, vol. 64, 1942, pp. 671–683.

8 "Isothermal Free Jets of Air Mixing With Air," by J. F. Taylor, H. L. Grimmett, and E. W. Comings, *Chemical Engineering Progress*, vol. 47, April, 1951, pp. 175–180.

9 "Diffusion of Submerged Jets," by M. L. Albertson, Y. B. Dai, R. A. Jensen, and H. Rouse, Trans. American Society of Civil Engineers, vol. 115, 1950, pp. 639–697.

10 "Pressure Drop in the Flow of Compressible Fluids," by W. E. Lobo, L. Friend, and G. T. Skaperdas, *Industrial and Engineering Chemistry*, vol. 34, 1942, pp. 821–823.

11 "Isothermal and Adiabatic Flow of Compressible Fluids," by C. E. Lapple, Trans. AIChE, vol. 39, 1943, pp. 385–432.

Appendix

Pressure Drop for Flow of Compressible Fluids in Pipes

For small pressure drops the density of a vapor or a gas is very nearly constant and, just as in the case of liquid flow, the Fanning equation can be used for calculating the frictional losses for vapor flow in pipes.

However, for large pressure drops the density varies markedly from point to point along the line, thereby introducing changes in the kinetic energy. Since the Fanning equation makes no allowance for these changes in the kinetic energy, a basic pressure-drop formula for the flow of compressible fluids in straight horizontal pipes of uniform cross section must be used.

Isothermal Flow of Gases. Lobo, Friend, and Skaperdas (10) have developed the following pressure-drop equation applicable to isothermal flow of ideal gases in straight horizontal pipes of uniform cross section

$$1 - \left(\frac{P_2}{P_1}\right)^2 + \frac{G^2}{g p_1 \rho_1} \ln \left(\frac{P_1}{P_2}\right)^2 = \frac{2\Delta P_F}{P_1} \qquad \text{[10]}$$

This can be rearranged in the form

$$\frac{2\Delta P_E}{P_1} = 1 - \left(1 - C_K \frac{\Delta P_E}{P_1}\right)^2 + \frac{G^2}{gp_1\rho_1} \ln \left(1 - C_K \frac{\Delta P_E}{P_1}\right)^2 \quad [11]$$

The curves shown in Fig. 14, entitled "Kinetic Energy Correction for Pressure Drop for Isothermal Flow of Gases," are based on Equation [11]. This chart gives kinetic-energy corrections for various ratios of $\Delta P_E/P_1$ corresponding to various values of

$$\frac{G^2}{gp_1\rho_1} = 5.594 \times 10^{-7} \frac{W^2}{D^4 P_1 \rho_1} \quad [12]$$

It should be remembered that ΔP_E is the friction loss, based on inlet (or upstream) conditions, in the entire length of pipe; so that the corrected (actual) pressure drop ΔP is equal to $C_K \Delta P_E$.

Note that the curves shown in Fig. 14 terminate at a broken line marked critical velocity. Points on this broken line thus represent the maximum pressure drop that can be obtained in a given length of line of a given diameter for a given flow and inlet conditions, for velocities beyond the critical (acoustic), cannot be obtained in pipes of uniform cross section.

The critical velocity for isothermal flow is given by

$$V_c = 68 \sqrt{\frac{P_c}{\rho_c}} \quad [13]$$

If the velocity at the pipe exit is critical, then $P_c = P_2$ and $\rho_c = \rho_2$.

Adiabatic Flow of Gases. Adiabatic flow of ideal gases (with friction) in straight horizontal pipes of uniform cross section has been treated by Lapple (11), and others. However, the charts which Lapple prepared do not lend themselves very readily to the type of problems that involve the determination of pressure at the end of the line when the flow and the pipe-inlet conditions are known. Furthermore, the form of his equations is not applicable directly, without transformations and rearrangements, to the method of pressure-drop calculations used by the authors.

Equations for adiabatic flow comparable in form to those obtained by Lobo, Friend, and Skaperdas for isothermal flow are desirable.

One such equation can be obtained directly by integrating the energy-balance equation

$$v dp + \frac{V dV}{g} + \frac{2f V^2 dL}{gd} = 0 \quad [14]$$

utilizing the equation of continuity

$$G = \frac{V}{v} \quad [15]$$

and the equation of state for adiabatic flow

$$pv + \left(\frac{k-1}{k}\right) \frac{V^2}{2g} = \text{const} \quad [16]$$

The result of the foregoing integration leads to the following expression

$$\left[1 - \left(\frac{\rho_2}{\rho_1}\right)^2\right] \left[1 + \left(\frac{k-1}{2k}\right) \frac{G^2}{gp_1\rho_1}\right] - \left(\frac{k+1}{2k}\right) \frac{G^2}{gp_1\rho_1} \ln \left(\frac{\rho_1}{\rho_2}\right)^2 = \frac{2\Delta P_E}{P_1} \quad [17]$$

The equation of state, Equation [16], can be expressed as follows

$$\frac{\rho_2}{\rho_1} - \left(\frac{k-1}{2k}\right) \frac{G^2}{gp_1\rho_1} \left[\frac{\rho_1}{\rho_2} - \frac{\rho_2}{\rho_1}\right] = \frac{P_2}{P_1} = 1 - C_A \frac{\Delta P_E}{P_1} \quad [18]$$

where C_A is the kinetic-energy correction factor for adiabatic flow.

Equations [17] and [18] are pressure-drop equations for the flow of ideal gases in straight horizontal pipes of uniform cross section for adiabatic process with friction.

Note that for $k = 1$, Equation [18] reduces to $p_1v_1 = p_2v_2$, and Equation [17] reduces to Equation [10], i.e., they reduce to the isothermal case.

The temperature at the end of the pipe, obtained from the ideal gas law and Equation [18], is given by

$$T_2 = T_1 \left(\frac{P_2}{P_1}\right)\left(\frac{\rho_1}{\rho_2}\right) = T_1 \left\{1 - \left(\frac{k-1}{2k}\right) \frac{G^2}{gp_1\rho_1} \left[\left(\frac{\rho_1}{\rho_2}\right)^2 - 1\right]\right\} \quad [19]$$

The critical velocity for adiabatic flow is represented by the expression

$$V_c = 68 \sqrt{\frac{kP_c}{\rho_c}} \quad [20]$$

Numerical Example. The following example is presented in order to illustrate the use of the foregoing equations, as well as to compare the results obtained for the isothermal, the adiabatic, and the average density methods.

A 16-in. sch 30 pipe 1600 ft long, is to handle 440,000 lb per hr of vapor whose $M = 48$. The pipe-inlet conditions are $P_1 = 75$ psia and $T_1 = 625$ deg R; $k = 1.2$; viscosity = 0.01 cps. Estimate the total pressure drop in the line.

Isothermal Solution

$$\rho_1 = \frac{MP_1}{10.73 T_1} = \frac{48 \times 75}{10.73 \times 625} = 0.536 \text{ pcf}$$

Friction loss, based on upstream conditions and the Fanning equation is equal to 28.8 psi = ΔP_E

$$\frac{\Delta P_E}{P_1} = \frac{28.8}{75} = 0.384$$

$$5.594 \times 10^{-7} \frac{W^2}{D^4 P_1 \rho_1} = \frac{5.594 \times 10^{-7} \times (4.4 \times 10^5)^2}{15.25^4 \times 75 \times 0.536} = 0.0498$$

Enter Fig. 14 at $\Delta P_E/P_1 = 0.384$ and go up to the curve that corresponds to 0.0498 and then horizontally to the left or right and read $C_K = 1.670$. Hence the corrected (actual) pressure drop

$$\Delta P = C_K \Delta P_E = 1.670 \times 28.8 = 48.2 \text{ psi}$$

$$\text{Outlet pressure} = 75 - 48.2 = 26.8 \text{ psia}$$

Adiabatic Solution. Since charts are not available at present, a numerical approximation can be obtained directly from Equations [17] and [18].

Note that the right-hand member of Equation [17] is equal to

$$2\left(\frac{\Delta P_E}{P_1}\right) = 2 \times 0.384 = 0.768$$

The coefficients of the left-hand member of Equation [17] are easily calculated since k is known and

$$\frac{G^2}{gp_1\rho_1} = 0.0498$$

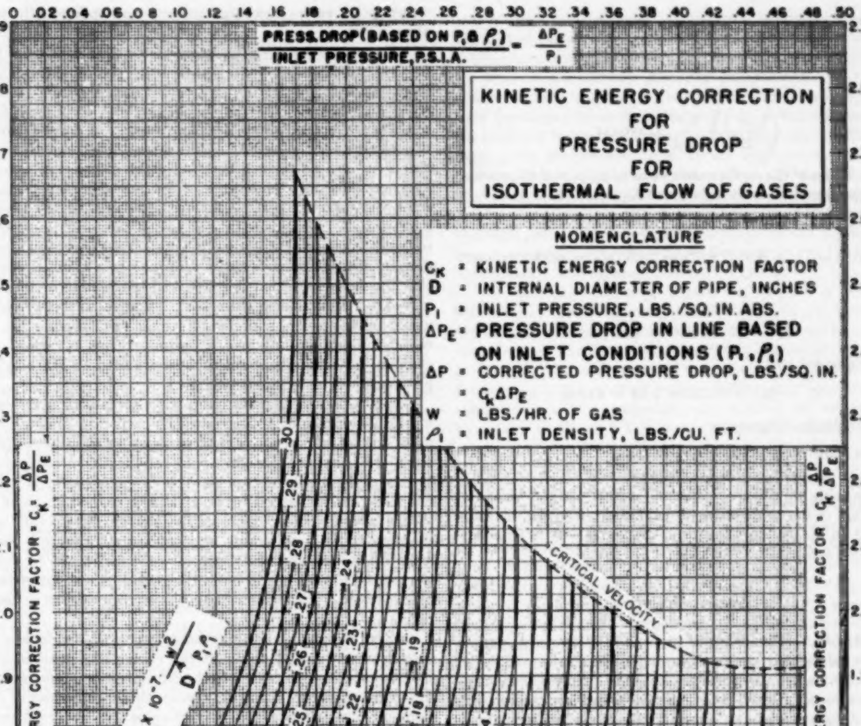

Fig. 14 Kinetic-Energy Correction for Pressure Drop for Isothermal Flow of Gases

Thus

$$\left(\frac{k-1}{2k}\right)\frac{G^2}{gp_1\rho_1} = 0.0041$$

and

$$\left(\frac{k+1}{2k}\right)\frac{G^2}{gp_1\rho_1} = 0.0454$$

For these values of the coefficients a value of $\rho_1/\rho_2 = 2.62$ provides a good approximation to the solution of Equation [17].

Substituting this value in Equation [18] one obtains

$$\frac{P_2}{P_1} = 0.373 \text{ or } P_2 = 0.373 \times 75 = 28.0 \text{ psia} = \text{outlet pressure}$$

Hence

$$\Delta P = 75 - 28.0 = 47.0 \text{ psi}$$

Using Equation [19]

$$T_2 = 625 \times 0.373 \times 2.62 = 610 \text{ R}$$

a drop of 15 deg in temperature.

Solution Based on Average Density in Line:

Leads to a total pressure drop of 38.5 psi.

The foregoing results show that the isothermal and adiabatic solutions are of the same order of magnitude, whereas the solution based on the average density in the line is seen to be about 25 per cent in error.

Discussion

F. L. Maker.[4] The problems in disposal of discharge vapors from relief valves have increased in magnitude greatly within the past 15 or 20 years, in large part because of the development of catalytic-cracking plants, and polymerization and alkylation plants, and the attendant butane and butene separation columns. The cracking plants generate very large quantities of gases at relatively low pressures, and the large process quantities and large reflux ratios of the butane columns mean very large requirements for relief valves. Hence a simple computation shows that the volume of explosive mixture of vapor and air that might conceivably exist if a single cause, such as a cooling-water failure, should cause a large number of relief valves to pop simultaneously, results in a frighteningly large cloud. (A similar computation many years ago, before conservation measures were adopted, indicated the normal discharge of gas being vented into the air from the many natural gasoline plants over Kettleman Hills was sufficient to make a cloud of explosive mixture $^3/_4$ mile thick, and that it would be unsafe for an airplane to fly over the field.)

The authors compare "open" versus "closed" systems, give a suggestion for reducing the sizes of discharge lines if a closed system is used, and discuss test results of special modifications of safety valves to permit operation at higher back pressures, thereby permitting smaller discharge lines.

The authors quite evidently prefer what they call an open system, which involves discharging the vapors from relief valves at the highest practicable point in each plant. There is much to be said in favor of this practice, particularly where the molecular weight of the gases is not large, and the quantities involved are individually not too great. In fact, even where a closed system may be used for some plants, it is not uncommon for them to have many relief valves discharge directly and individually to the atmosphere.

A discharge system leading gases from a number of relief valves to a central discharge point is most often chosen, when it is, because of the magnitude of the possible discharge and the excessively large cloud of explosive vapor that may result, say, from a single cause such as failure of cooling water. A flare to ignite the vapors removes the hazard. This central discharge system and flare may also be favored because of the presence of poisonous hydrogen-sulphide components, which might be dangerous even when the concentration has reduced to less than the lower explosive limit. (Incidentally, the use of the term closed system to indicate a system of leading the discharged vapors to a central flare or disposal point is really a misnomer. There is a system that has been used that is really a closed system in which the gases are led to a closed gasholder. "Central discharge system" would appear to be a preferable term, even though the term closed system has attained a certain degree of usage. The chemical-absorption systems such as are used on HF alkylation plants are also really closed systems.)

It might be well to point out a few alternatives in the case of individual discharge arrangements for separate plants. If the plant has a fired heater (or if there is one on an adjacent plant), one way to dispose of the gases is to lead the discharge pipes up to the top of the stack and turn them so the vapors will mix with the flue gases and be heated by them and be carried up along with the flue gases. If the vapors are hot enough, even if they have a specific gravity considerably greater than air, they will have to mix with enough air before they are sufficiently cool to settle to the ground that they will have necessarily passed out of the explosive range. This system has been used in a number of installations.

Another possibility, if the discharge vapors are available at high enough pressure, is to discharge the vapors into injectors so designed that they will draw into the injectors a large enough quantity of air to insure a mixture below the lower explosive limit. Computations indicate that this method is feasible for a discharge of butane vapor of the order of 100,000 lb per hr without too elaborate an installation, but discharge to the top of a stack is considered effective and cheaper.

Multiple jets spread out over a large area also would serve the purpose.

The reasons favoring a central discharge system are as follows:

1 Very large vapor quantities.
2 Low pressure at which gases are available.
3 Possible poisonous contents, such as H_2S.
4 Possible liquid components in discharge streams.

The last condition is frequently encountered in cracking plants where, in an emergency, dump valves, automatically or manually controlled, dump the hot liquid contents of a vessel into a discharge tank under the surface of water or into a type of jet condenser through which water is flowing. Such liquid streams that will partly flash to vapor upon release of pressure should not, of course, be released at an elevation to be scattered over a large area.

A central discharge system either must have a method of storing the vapors (gasholder), absorbing them chemically (as in the case of HF), condensing them (if condensable), burning them as in a flare, or discharging them at such a temperature that they will rise to a safe height.

The usual method is to have a flare continuously burning to ignite the vapors. In some cases the size of the flame will be enormous as the gas quantities may be at the rate of 5,000,000 cfh. The heat generated may destroy the burner installation, as

[4] Engineering Specialist, California Research and Development Company, San Francisco, Calif. Mem. ASME.

it may be difficult to arrange to get an excess of air sufficient to keep the temperature of combustion within limits.

An alternative method, instead of burning the gas in air, is to arrange to burn a stream of air in the gas. By proper construction it is possible to supply enough air to heat the mass of flue gas and unburned vapor hot enough to rise to a height sufficient to insure safe diffusion before any heavy vapors can return to ground level.

The authors suggest that where a central discharge system is used, it may be economical to design the vessels for a higher pressure than is required for process reasons because of the saving in cost of the discharge piping systems thereby made possible. To do this deliberately is an interesting suggestion, and the authors' figures justify it for the cases discussed. They note that there may be only small extra costs involved in many cases where the thickness of the shell is fixed by the minimum-thickness criterion rather than by the process pressure. In this connection it may be noted that many designers have for years followed the practice of designing vessels with heads and nozzles strong enough to develop the full strength of the shell, whether this is fixed by the minimum-thickness criterion or by extra material added for corrosion. Among other things, this permits making a hydrostatic test that will stress the shell joints adequately. Whether it is desirable to use the excess margin between process pressure and allowable relief-valve setting for obtaining extra back pressure in the discharge lines can be looked at from another point of view. It is usually considered more desirable not to have the relief valves pop at all, and usually there are one or more means provided to prevent this happening, such as automatic shutoffs for heat sources, dumping of liquid, and so forth. If there is a margin of pressure available, it should be considered whether the safety valve should not be set at the highest allowable pressure and permit these other safeguards to function. They do not rate officially as substitutes for relief valves, but actually may prevent the pressure rising to the relief-valve popping point.

In regard to the provisions of the codes, the question of accumulation being limited to 10 per cent (or 20 per cent for fire exposure, in the 1950 ASME Code) has nothing to do with the sizing of the discharging piping, provided the relief valve is so constructed that its capacity is not reduced by the back pressure. Note that the "25 per cent discharge systems" are in the nonmandatory section of the 1950 ASME Code, and the 1943 API Code does not cover the discharge piping. It may be questioned whether there is any legal requirement for a discharge system to have a less back pressure than 10 per cent of the discharge pressure, providing this does not increase the accumulation above 10 per cent.

What this means as to the construction of the relief valve is discussed as follows:

Relief valves used in petroleum plants have been developed largely by modification of steam safety valves. The authors' Figs. 7(*a*) and 7(*b*) show what they term "nonvented bonnet" and "vented bonnet" arrangements. It should be remarked that the manufacturers' standard practice has been to furnish relief valves in which the bonnet is not vented to the atmosphere but is vented to the discharge space, as in Fig. 7(*a*), unless the purchaser specifies differently. As the authors remark, the result of this arrangement is to insure that any back pressure, resulting either from the operation of the valve or of another valve on the same discharge line, causes an extra force acting on top of the disk, which is additive to the spring pressure, and tending to cause it to close, or in the case of back pressure from another valve, tending to prevent it opening at its set pressure.

Venting the bonnet to atmosphere and plugging or omitting the conventional connection from bonnet space to discharge space results, in general, in an uplift force on the disk, since the guide is generally larger in area than the seat circle. This means that back pressure in a discharge pipe due to a second valve operating first makes the second valve open at less than its set pressure. This appears to be safer than having the popping point raised, unless there is considerable disparity of pressures. It has been rumored that in one case a low-pressure vessel connected to the same discharge pipe as the relief valve for a high-pressure vessel was ruptured by the back pressure from the high-pressure valve, causing the low-pressure valve to lift and permit an excessive pressure to back into the weaker vessel. (Note that a check valve in the discharge line would prevent this happening.) In general, it may be economical not to connect discharge valves of markedly different pressures into the same line, as the line would have to be designed for the combined capacities and the minimum back pressure, and separate lines may be cheaper.

It is obviously desirable, if possible, to have a relief valve which would have its operation unaffected by the back pressure in the line. Such a valve should not have its capacity reduced by a back pressure less than the critical flow pressure, or roughly, one half of the absolute pressure on the vessel at the time the valve is discharging. The authors state, "Since that time the valve manufacturers in co-operation with some of the oil companies have been working on the development of a satisfactory back-pressure relief valve." While this statement is true, to set the record straight it should be noted that this activity was initiated by the API Committee on Pressure Relieving Devices. This committee about 4 years ago found that there was uncertainty as to the actual discharge capacities of large valves, since there were no facilities for testing them to capacity, and also that the back-pressure effects noted by the authors existed. They communicated with the various manufacturers and, in a meeting at Tulsa, outlined these problems to the manufacturers' representatives and suggested that they form a manufacturers' subcommittee and see what they could do about it. In regard to the elimination of back-pressure effects, the writer submitted a memorandum discussing the situation and pointing out that a balance piston of the same area as the seat should substantially eliminate these effects. The change in design is simple for most relief valves, and, in fact, existing valves can be altered readily. One manufacturer got on the boat quite early because, fortuitously, in some particular nozzle sizes it happened that the seat area and guide area came close to balancing. In the same memorandum the alternative of a bellows was also discussed. The use of a bellows was not new, there being in the record several expired patents showing them, although the purpose was to seal the valve against leakage. The balance piston arrangement is also probably not patentable either. For ordinary situations, the bellows method would appear to be more expensive and have no particular advantages.

The authors' Fig. 4, showing the effectiveness of means to prevent the back pressure of the discharge getting at the back of the disk and causing it to close, is very interesting. It would be of further interest to have included some test data on balanced disk valves without vented piston, such as is illustrated in Fig. 8 of the paper. It is believed the manufacturers of the particular valve shown have some data.

It should be noted that the use of the bellows in itself should not influence the curve for pressure ratios that are greater than the critical ratio, whether or not the bellows are balanced. It is, as a matter of fact, somewhat difficult to understand how some of the curves in this region indicate capacities greater than the theoretical. Presumably this is due to the method of determining the basis. The authors state that they have plotted the ratio of discharge at any back-pressure ratio against discharge at zero back pressure, and this permits comparison with the theoretical discharge-nozzle curve. They do not state that the theoretical curve was based upon the measured diameter of the nozzle throat. They do state that the tested capacity was in all cases above the

rated capacity. The rated capacity, in turn, is based presumably on the nozzle size. It is not to be expected that the manufacturer would intentionally understate the capacity of his valve, so this may indicate some variation in the test methods in the different tests, which is indeed noted in the paper.

If the theoretical curve were based upon the theoretical nozzle, all of the test points would be expected to be below the unity line as the actual nozzles will necessarily have a discharge rate less than a theoretical nozzle. It is to be noted that both valves in Fig. 4, which come below the theoretical nozzle curve, were tested with steam and, presumably, saturated steam. Under these conditions the deviations from the gas law may be of importance. A check of the discharge ratio for a perfect rounded-entrance nozzle, using the steam tables for determining the theoretical flow rate instead of the thermodynamic formula that assumes a constant value of the ratio of specific heats, might be of interest.

It is possible that some of the difficulties with relief valves may be due to keeping the blowdown small. This is desirable for a boiler, which may be operated so close to its popping pressure that it may pop frequently. (Steam-locomotive safety valves frequently pop whenever the train halts.) For process-plant relief valves, which pop much less frequently, it may be questioned whether a low blowdown is of any value if it affects the capacity of the valve adversely from the standpoint of back pressure.

H. F. Newman.[5] Adaptation of Bosanquet-Pearson diffusion equation to the venting of refinery relief valves gives a designer something on which to "hang his hat," as the authors put it. The old rules of thumb must make way for more exact expressions which correlate the variables. The use of the diffusion equations in the analysis of stack and vent performances is already well established.[6] However, even with the equations of Sutton or Bosanquet, the practical man must still tax his best judgment to assign suitable numerical values to the variables in the equations and reflect on the general merit of the solution and his assumptions.

In determining the height of a vent or stack by means of diffusion equations or Fig. 1 of the paper, the designers should keep in mind that a prevailing horizontal wind is usually assumed. This condition may or may not be realized depending not only upon the weather but also upon possible effects of adjacent structures on patterns of air flow. Where flammable materials are discharged from open relief-valve units, the designer should also be mindful of possible drift of vapors to elevated points which may cause ignition such as furnaces, hot stacks, flares, and so forth.

The use of automatic admission of steam on relief-valve discharge vents would seem to invite considerable maintenance to make it as dependable as the relief valves. It should not be substituted as an equivalent of a necessary increment of stack height. If large volumes of flammable vapors must be discharged and there is doubt about the ultimate safe disposal into the atmosphere by means of a vent, the refiner should consider providing a flare system in order to burn the vapors safely at the disposal point.

The authors suggest that economies can be realized through the smaller sizing of relief-valve discharge piping by increasing vessel design pressure and setting the relief valves to open at pressures below the revised design pressures, in order to size discharge piping with greater pressure drop.

Because of the relatively low pressure drops for which these lines ordinarily must be sized, it is easily seen that increase in permissible pressure drop should realize savings in many cases. However, it is declared in the paper that the proposed procedure can be followed without violating code limitations. Paragraph W-604 of the 1943 API-ASME Code states, "The size of outlet pipe shall be such that the pressure drop shall not be more than 10 per cent of the permitted valve-discharge pressure." Until this paragraph of the API-ASME Code is revised to permit the practice suggested by the authors, refiners may wish to proceed with caution if they are on a basis of conformance to this code for statutory reasons. It is our understanding that paragraph W-604 in the proposed revised API-ASME Code, which is not released as yet, will be completely reworded and will probably limit vessel pressure instead of pressure drop in the discharge piping from relief valves.

We should like to inquire whether the authors have any data based on tests they may have conducted using conventional relief valves set to open below the design pressure and operating with the higher back pressures as proposed. It would be of interest to plot such data on a graph such as Fig. 4 of the paper. We note that, according to Fig. 4, conventional valves are reported to be completely inoperative at $P_2/P_1 = 0.18$. This indicates that conventional valves are quite susceptible to the effects of back pressure and tend to become closed as the back pressure rises with respect to the upstream pressure. As is indicated by the authors, the extent of the effect depends upon the various forces acting upon the disk, such as the spring force, the back pressure acting upon the back of the disk as well as kinetic effects of the flowing vapor upon the front and sides of the disk. Under flowing conditions it is probably impossible to calculate with any assurance the magnitudes of the dynamic effects of the vapors on the disk. Thus, although setting the relief valve below the design pressure in effect decreases the spring force upon the disk, it is not entirely clear that the conventional valve should then perform with capacity as computed for the back-pressure valves (right-hand curve in Fig. 4). Rather, one might also expect (in the absence of data to the contrary) that performance of conventional valves under the proposed conditions might fall anywhere between the two curves now shown in Fig. 4. If this were true, it would of course make the proposal to use conventional valves under higher back-pressure conditions unreliable. It is for this reason we would like to see test data to support this proposal.

Because of the dependency of the performance on the mechanical design of relief valves, it is suggested that designers obtain specific information from the manufacturers regarding the effects of back pressure on the performance of the relief valves before attempting the proposed method.

In further regard to the curve for conventional valves in Fig. 4, we note that the 10 per cent rule on back pressure would not be safe for conventional relief valves used in the conventional manner on vessels having design pressures less than approximately 135 psig. For example, for a vessel with design pressure of 100 psig, the maximum accumulated upstream pressure would be 124.7 psia. The 1943 API-ASME Code would permit a back pressure of 11 psig or 24.7 psia. Hence, P_2/P_1 equals 0.199, and according to Fig. 4, the valve should be inoperative. Since this is inconsistent with current design practices and presumably experience with conventional relief valves, we should like to inquire about the types of valves and test conditions that were used to plot the curve for the conventional valves.

Regarding the use of back-pressure relief valves with discharge piping systems sized for more than 10 per cent back pressure, we would be inclined to agree with the authors that development and testing should be continued so that eventually it will be possible to design with confidence to any back pressure. However, we feel that, in considering the present extent of our experience and

[5] Manufacturing Department, Standard Oil Company (Indiana), Whiting, Ind.

[6] Refer, for example, to the "Symposium on Atmospheric Contamination and Purification," *Industrial and Engineering Chemistry*, vol. 41, December, 1949, and the report entitled, "Pollution Control," in *Chemical Engineering*, May, 1950.

knowledge of relief valves and inability to predict flow conditions accurately for complex and extensive header systems, for general design purposes there is still a need to stay below the critical "50 per cent" back pressure. In general, a figure such as 25 per cent would seem to be a suitable first step from the 10 per cent pressure-drop limitation which the API-ASME Code has at present.

It is suggested that designs for higher back pressures be developed in considerable detail with the relief-valve manufacturers, and that they be applied only when the designers can predict with good assurance all the essential variables of the system. Users of high back-pressure systems should perhaps get confirmation of relief-valve capacity, opening pressure and blowdown from the manufacturers, particularly if existing, older valves have to be substituted during the course of regular maintenance into new services involving higher back pressures.

L. P. Stillman.[7] The writer's company is a manufacturer of safety relief valves. This discussion therefore, is necessarily confined to the ability of a safety relief valve to function under each of the disposal methods outlined.

The valve in question is a spring-loaded valve, operating automatically and actuated by the pressure contained in the vessel upon which it is mounted. The sole purpose of this valve is to protect equipment and personnel from the presence of excessive overpressures. The paper clearly indicates, and it is of course logically understood, that all of the methods described therein must depend upon the ability of the safety relief valve to function as required by the disposal method chosen.

If the first stated method of blowing the safety relief valves to the atmosphere is used, then no problem is presented to the manufacturer. Conventional valves of this type are designed to operate with a predetermined pressure differential across the valve. The constant back pressure supplied by the atmosphere readily satisfies this requirement.

The second proposed design method, setting the safety relief valves on closed systems below the vessel design pressure, also satisfies the requirements of the conventional valve design. Since this valve maintains a predetermined differential pressure across the valve, method 2 will result in a fluctuation of the valve set pressure in direct relationship to the variation in back pressure. The opening point at any specific back pressure will be P_S = differential set pressure plus back pressure at valve outlet. The only undesirable result of this method will be a fluttering action in the valve until equilibrium is established between the flow from the valves and the resulting back pressure in the discharge header. When this equilibrium is established, the valves will deliver their rated capacity. It should be pointed out here that this fluttering action under some conditions may result in valve chatter which will damage the valve seating surfaces seriously.

The use of safety relief valves which operate independently of back pressure, as outlined in the third method discussed, is, of course, an ideal solution to this problem, providing valves are available that will function properly under such a condition.

The requirement that the safety relief valves operate independently of back pressure means that the valve must function as follows:

1 Open at a predetermined set pressure regardless of the back pressure imposed upon it.

2 Maintain full lift of the valve disk at all back-pressure levels, so that the valve capacity will follow the theoretical nozzle curve the authors have shown in Fig. 4.

3 Close at not less than 90 per cent of the set pressure under any back-pressure condition.

[7] Manager, Tulsa Products Division, Manning, Maxwell & Moore, Inc., Tulsa, Okla.

Of the three requirements for proper safety-relief-valve action listed, the authors have shown in Fig. 4 only results which demonstrate the possibilities in flow characteristics. They have not attempted to include performance data on the additional requirements of set pressure and blowdown.

It is quite evident, after a complete analysis of extensive development tests covering a period of several years, that when this variable back-pressure condition is imposed, it is quite improbable that satisfactory or consistent valve action will be obtained with any possible design of a spring-loaded valve. These tests indicate further that the performance of a spring-loaded valve, regardless of its design features, is questionable when used against a variable back pressure higher than 25 per cent of the gage set pressure.

The forces which are available to operate such a valve are conflicting and variable at different points in the back-pressure range, to the extent that proper or consistent operation of the safety relief valve cannot be accomplished without the use of auxiliary forces. An application of such auxiliary-force methods, which is consistent with the fundamental concept of safety that dictates the use of safety relief valves, has not yet been conceived. Thus, it would seem that the application of the third method proposed by the authors, as desirable as it certainly is, should await the development of a valve design that is truly and practically independent of back pressure.

The potential value of using the ideal third method outlined in the authors' paper, when closed systems are chosen, is emphasized by the fact that development work to obtain a safety relief valve that will operate independently of back pressure is being continued. By using a different approach to the problem, it is hoped that the successful development of such a valve will soon become a reality.

Authors' Closure

The authors wish to express their appreciation to Messrs. Maker, Newman, and Stillman for the time and effort spent in reviewing and commenting on this paper. Not only have they contributed worth-while constructive criticism, but they also have offered additional information on the subject. As a matter of fact, their presentation, in the main, can be considered as representing an elaboration on the work and opinions of the authors. However, they have raised some points of difference that warrant consideration, and it is to these points that the authors wish to reply.

Mr. Maker states that the authors evidently prefer an open system to a closed system. The authors did not intend to convey this idea but merely wished to call attention to the economic factors involved. There are certain instances where open systems are desirable and there are others where closed systems are required. From the relative costs of the open and the closed systems, it is evident that in some cases the additional money that might be spent on a closed system could more logically be used to provide various means and devices for reducing the possibility of a relief-valve pop and/or minimizing the quantity discharged. This would result in a safer and more economical over-all system. Mr. Maker points out that it is usually considered more desirable not to have the relief valves pop at all, and thus favors setting the valves to open at the design pressure rather than maintaining a spread between the design pressure and a lower set pressure. However, in such a case the size of the relief-valve discharge system, to be in strict accordance with the Code, would be considerably larger and more expensive than that resulting from setting the valve below the design pressure. It was the intention of the authors to indicate the approximate magnitude of this additional increment in cost. Thus the decision as to whether or not to maintain a spread

between the set pressure and the design pressure is again a problem of economics, i.e., a balance between the savings in discharge piping versus the operating advantage of having a higher set pressure. This operating advantage may not materialize, since in many cases with a major upset condition, it is just as likely that the pressure will rise right up to the design pressure as to a reduced set pressure.

Mr. Maker points out that for process-plant relief valves, blowdown is not as critical a factor as it is in the case of boilers. The authors heartily agree and feel that conventional blowdown requirements should be relaxed in order to increase capacity under back pressure conditions.

Mr. Newman is entirely correct in pointing out that Paragraph W-604 of the 1943 API-ASME Code limits the pressure drop in the relief-valve discharge system to 10 per cent of the valve discharge pressure. However, the purpose of this paragraph is to limit the vessel overpressure to 10 per cent of the design pressure. Therefore by setting the relief valve below the design pressure and taking additional pressure drop in the discharge line, but still limiting the overpressure to 10 per cent of the discharge pressure, the spirit of the Code has not been violated. Furthermore, revised editions of the ASME and API-ASME Codes, which have been in the making for several years, have eliminated the phrase referred to. Mr. Newman, in questioning the curve for the conventional valve in Fig. 4, has uncovered an error on the part of the authors. The data obtained for capacities under variable back-pressure conditions for conventional valves were meager and at relatively high set pressures. Consequently, when the data were plotted on the basis of absolute-pressure ratios, there did not appear to be much difference between the points representing different set pressures. However, if data had been obtained for a wide variation of set pressures, say, from 15 psig up, such data would form a family of curves on Fig. 4. However, if the plot were based on the ratio of gage pressures, it would probably appear as one curve. Mr. Newman questions the capacity of a conventional relief valve when the set pressure is below the design pressure and a back pressure greater than 10 per cent of the design pressure is permitted to build up. Although the authors have no data to substantiate their contention, it appears obvious that since the conventional relief valve recognizes only the differential, the capacity should be unaffected. Mr. Stillman in his discussion verifies this point.

Mr. Stillman points out that the actual data included in the paper covered only capacity characteristics and did not include data on the effect of variable back pressure on blowdown and popping pressure. During the tests carried out some data were obtained on variation of blowdown and set pressure. These data were not included in the paper since the authors did not consider them sufficiently complete. However, qualitative discussion indicating the approximate effects of variable back pressure on these two characteristics were included in the paper. Furthermore, as Mr. Maker has pointed out, a small blowdown is not too critical in process-plant operations and may be sacrificed to increase capacity at high back pressure.

The authors believe that Mr. Stillman's and Mr. Newman's contention that back pressure be limited to 25 per cent of the set pressure does not take reasonable advantage of the new type of valve. In view of the data included in the paper, the authors wish to reaffirm their previous conclusion that with certain back-pressure valves, 50 per cent back pressure is a safe design figure.

As a concluding remark, it can be stated that those who discussed this paper, as well as the authors, point to the necessity for additional testing. This testing under variable back-pressure conditions should involve both, the specially designed back-pressure valves and conventional valves. In order to simulate conditions resulting from setting a relief valve below design pressure, the latter should be tested not only for the usual 10 per cent accumulation, but also with accumulations greater than 10 per cent.

The Mamba Engines in the Apollo Aircraft

By B. H. SLATTER,[1] PARKSIDE, COVENTRY, ENGLAND

The installation and operation of Mamba propeller-turbine engines in a civil aeroplane, such as the "Apollo," involved a number of new problems, some of which were fully brought to light only as a result of experience with the engines in the aircraft. The paper describes these problems and the steps which were taken to overcome them either in the design stage or, subsequently, as a result of flight experience.

Introduction

The design of the Mamba power plant involved a number of problems peculiar to propeller-turbine engines, notably with regard to the control of the engine and propeller. It was necessary to consider not only the normal running of the engine but the engine requirements and effects on the aircraft during handling, stopping, and restarting in flight and following various possible types of power-plant failure.

During the early flight testing of the Apollo, various defects came to light in connection with such matters as nacelle ventilation, engine starting, and performance.

It is the purpose of this paper to describe the various problems connected with the Apollo engines which have been encountered and overcome either in the design stage or following experience in the aircraft.

Brief Description of Mamba Power Plants

The Mamba engine embodies a 10-stage axial compressor, six vaporizing combustion chambers, and a two-stage turbine. The compressor and turbine rotors are directly connected together and revolve at a maximum speed of 15,000 rpm.

The rotor system is coupled to the propeller through a compound epicyclic reduction gear having a ratio of 0.097:1.

The bare engine has a maximum diameter of 28 in. and weighs 750 lb. It was designed originally to provide 1000 shp and 300 lb of jet thrust at take-off.

In building this engine into a power unit for the Apollo, the main aims were to keep the frontal area of the nacelle to a minimum, group all the engine accessories on the engine unit, and at the same time, provide good accessibility for maintenance.

The way in which these features were achieved is shown in Figs. 1, 2, and 3. Fig. 1 shows the engine fully cowled, the maximum diameter of the cowling being 31 in. The nose cowling forms the oil tank with a capacity of $3^3/_4$ gal.

Fig. 2 shows how the power plant is divided into three zones by fireproof bulkheads. The engine fuel and oil systems, and the propeller governor and feathering pump are all located round the compressor casing in zone 1, and ready access to the accessories for servicing is provided by hinged and detachable cowlings fitted with toggle fasteners.

A drive is taken from the engine accessories casing through zones 1 and 2 to a bevel box in the leading edge of the wing. Here, the drive is bifurcated and taken outward to subsidiary gearboxes carrying generators, cabin blowers, and hydraulic pumps.

The power plant is readily detachable from the airframe by disconnection of the auxiliary drive shaft, fuel and electric services, and removal of four mounting bolts at the rear of zone 2.

Ventilation of Nacelle

It will be appreciated that the surface temperature at any part of the main components of a gas turbine must be quite close to the temperature of the air at that point inside the casing due to the large volume of air flowing through the engine and the relatively high velocity over the inside walls. It is futile, therefore, to attempt to cool the casing of the engine since the quantity of cooling air must be kept as small as possible in order to minimise drag. It should also be borne in mind that aero-engine fire-extinguisher systems rely on filling the engine bay with a blanket of inert gas, and this method could not be effective with a large flow of air through the nacelle.

However, it is necessary to insure that parts of the aircraft structure adjacent to the engine and such equipment as electrical components are not overheated, and ventilation is necessary for this purpose and to avoid the possibility of the formation of dangerous concentrations of fuel vapor. The compartment around the compressor containing engine accessories (zone 1) is not subject to very high temperatures and no cooling difficulties arise.

Zone 2 is provided with a flow of air to insulate the surrounding heat shield from the combustion chambers, Fig. 4. This flow of air was originally brought from a forward-facing scoop in the slipstream but trouble was experienced with high temperatures outside the heat shield. This trouble was due to the pressurizing of the space inside the heat shield A, by the Pitot entry, causing leakage of hot air into the outer space B. It was overcome by feeding the air to zone A from zone B, the air being extracted from the combustion-chamber zone by means of a rearward-facing louver. This arrangement insures that any leakage at the heat shield is from the cooler zone into the hotter zone and thus gives no trouble.

Starting

To start the engine it is necessary to motor the rotor (and the propeller, since it is always geared to the rotor) up to a speed from which the engine will pull away under its own power. This speed is about 25 per cent of the maximum rpm, and an electric motor, operating from a 24-volt supply and developing a peak power of 8 hp, is employed, the starting cycle having a duration of 30 sec.

At first, some trouble was encountered with starting the engines in the aircraft, the starter motors sometimes failing to accelerate the engines to their self-sustaining speed. The reason for this was that the power requirement represents just about the limit of what can be obtained economically from 24-volt batteries when allowance has been made for voltage drop in cables and connections. Satisfactory starting was not possible unless the batteries were in really good condition and fully charged, and considerable care was taken to insure low-resistance connections throughout.

Satisfactory results were obtained by using either a rectifier, operating from mains supply, or a battery truck incorporating an 18-kw gasoline-driven generator.

---

[1] Experimental Flight Engineer, Armstrong Siddeley Motors Limited.

Contributed by the Aviation and Gas Turbine Power Divisions, Institute of the Aeronautical Sciences, and the Canadian Section of the Society of Automotive Engineers and presented at the Semi-Annual Meeting, Toronto, Ont., Can., June 11-15, 1951, of The American Society of Mechanical Engineers.

Note: Statements and opinions advanced in papers are to be understood as individual expressions of their authors and not those of the Society. Manuscript received at ASME Headquarters, March 2, 1951. Paper No. 51—SA-14.

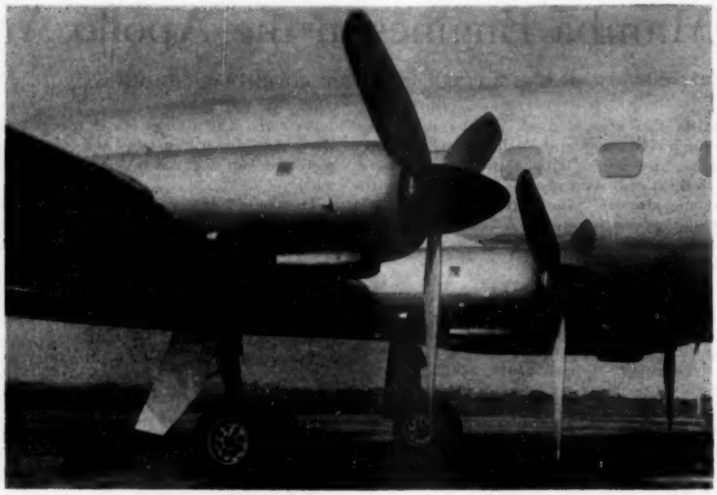

Fig. 1 Mamba Engine Fully Cowled as Installed on the Apollo

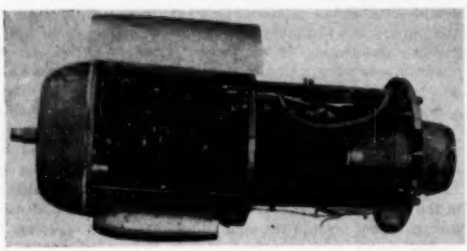

Fig. 2 The Power Plant Is Divided Into Three Zones by Fireproof Bulkheads

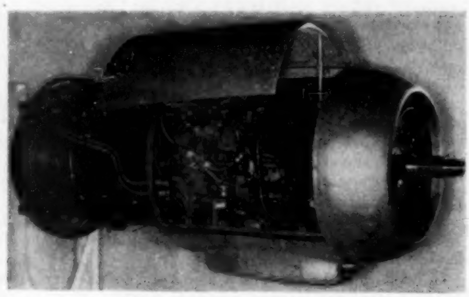

Fig. 3 The Power Plant Showing Engine Accessories

The starting problem emphasizes the fact that turbine engines require higher-capacity ground starting facilities for trouble-free operation than is necessary with piston engines. It probably will prove advantageous to employ higher-voltage starting systems in the future in order to minimize the weight of cables and connections.

Controls

In considering the manner in which an engine of the Mamba type should be controlled, it was necessary to decide first of all what proportion of the total power output should be given to the propeller, the remainder appearing in the exhaust jet.

Calculations, since verified by tests, showed that for air speeds up to 350 mph, the maximum thrust horsepower would be obtained by converting about 85 per cent of the available power into shaft horsepower for the propeller. Theoretically, a small advantage would be obtained by varying this percentage with forward speed by means of a variable propelling nozzle, but, in practice, the additional weight and complication would not be justified.

Unlike a jet engine with fixed propelling nozzle, the rate of fuel feed to a propeller turbine and the speed at which it runs are not fixed automatically by the characteristics of the engine. There are many possible ways in which the engine could be controlled but it was decided to govern speed by means of the propeller, as in piston-engine practice, and the power by scheduling the fuel supply. This arrangement appeared to be as promising as any other possible system and possessed the advantage that the main components required, namely, a propeller speed governor and an automatic fuel-metering control as used on jet engines, were already available so that the amount of development work required could be kept to a minimum.

As the speed and power of the engine are independent, it was next necessary to choose the relationship between these two variables. Fig. 5 indicates diagrammatically the limitations within which this choice may be made. It will be seen that the power/-speed characteristics of a turbine are considerably less flexible than those of a piston engine. In the lower part of the speed range, the power capabilities of the engine are limited either by the maximum temperature which the turbine materials will withstand, or by the possibility of overloading the compressor which results in a breakdown of the aerodynamic flow or "surge." Thus the area A in Fig. 5 cannot be used.

In the remaining area B, a working line was chosen which enabled the engine to develop any given power with the minimum fuel consumption. In practice it was found necessary to shift this ideal working line slightly to the right, as shown by the broken line, to avoid encroaching into the area A when suddenly opening the throttle at low power.

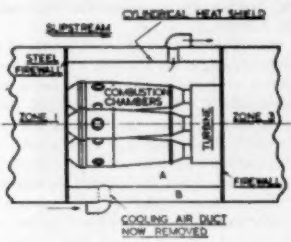

Fig. 4 Cooling Arrangements of Zone 2

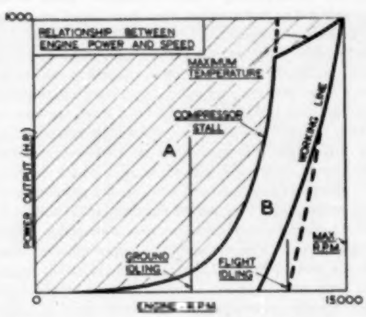

Fig. 5 Relationship Between Engine Power and Speed

Since the speed of the engine is governed by a variable-pitch propeller, it is quite simple to arrange for the engine speed to remain in the range shown by the working line in flight even when the engine power is reduced to zero.

On the ground, however, it is desirable that the engine idling speed should be lower to avoid excessive idling thrust and keep fuel consumption low. The ground idling speed (approximately one half the maximum rpm) is shown in Fig. 5, and this speed corresponds to the fuel flow which provides satisfactory engine starting.

It should be noted that between the ground and flight idling speeds, it is possible to overfuel the engine if the throttle is opened too rapidly, causing the operating point to move into the area A. This caused some trouble during ground handling of the engines in the Apollo, but the introduction of a temperature control, which is dealt with later, provides a satisfactory remedy.

It will be seen that there is no need to provide the pilot with separate control of speed and power and that, in fact, this would be unacceptable since there would be nothing to prevent him from selecting an impossible power at low speed with consequent damage to the engine by overheating.

Thus, to achieve the desired relationship between power and speed, the control lever of the fuel-metering unit and the propeller-governor control lever are both connected to the pilot's throttle. The connection to the propeller governor is made through a servo system which, in effect, enables the governor to anticipate the change in power which is being made when the throttle is moved, thus permitting the rapid and smooth changes in power which an aero engine is required to provide.

The high-pressure cock in the engine fuel system is connected to a separate lever in the cockpit, this lever also being linked to the feathering override on the propeller governor. Thus, if this lever is operated in flight, the fuel supply is cut off, and the propeller control overridden to select coarse pitch simultaneously. The use of mechanical linkages for this control rather than, for example, electrical actuation, is considered desirable because it is most important that the control should function in an emergency such as an engine fire in flight.

Temperature Control

It has been explained in the previous section that the temperature at which the engine operates for a given throttle setting is controlled by a fuel-metering unit. This is a scheduled control; that is, it is designed to pass a quantity of fuel which is estimated to be the engine requirement for a given set of operating conditions.

Bearing in mind that the engine fuel requirement varies with throttle setting, air-intake pressure and temperature, it will be realized that a very sensitive and accurate control would be required to achieve the accuracy of temperature control desired at or near full power when the engine is operating close to the maximum allowable temperature.

Furthermore, the Mamba jet pipe temperature changes about 3 C for every 1 C deviation in ambient-air temperature from standard. Thus, although the standard variation in ambient temperature with altitude can be allowed for in the design of the fuel-metering control, some form of temperature-sensitive control is necessary to allow for the rise in operating temperature which otherwise would occur on a hot day or in the tropics.

To meet these difficulties, the development of a fuel-metering control, sensitive to jet pipe temperature, was undertaken. This unit comprises an electrical amplifier fed with signals from thermocouples in the jet pipe and from a temperature selector linked with the throttle. The output of the amplifier controls a fuel valve.

Although a magnetic amplifier was chosen, rather than the conventional type of amplifier, in the interests of reliability, it is not desirable to rely entirely on a somewhat complicated electric system for the control of the engine. Consequently the temperature-control function is limited to about 30 per cent of the total fuel flow so that it acts as an accurate trimmer of the operating temperature, but any failure of the temperature control could not have a catastrophic effect on the power of the engine.

Apart from providing greater accuracy and consistency of jet pipe temperature than would be possible with any form of scheduled control, the temperature control also performs the very useful function of avoiding overfueling the engine, by opening the throttle rapidly at low rpm on the ground, for example. It does this by reducing the fuel supply to the engine immediately the indicated jet pipe temperature begins to exceed the selected value, and in this way provides a safeguard against maltreatment.

The Propeller

The propellers on the Apollo engines are essentially conventional hydraulically operated variable-pitch propellers, capable of fully feathering and reverse-pitch braking if required.

However, as the ground idling speed of the engine is just over 50 per cent of the maximum speed, and the engine is not capable of producing much power at this speed, it is necessary for the constant speeding range to be extended down to much finer pitch than is normal with piston engines. Apart from considerations of engine power limitations, this is necessary in order to keep the

starting power requirement to a minimum and to avoid excessive thrust for taxiing. Accordingly, the basic pitch stop of the Apollo propellers is set at 6 deg.

The ability of the propeller to operate at very fine pitch produces a difficulty when the possibility of failure of the propeller governor is considered. Following such a failure, the propeller blades would move to fully fine pitch under the influence of the centrifugal twisting moment and cause an intolerable amount of drag. To prevent this possibility a withdrawable pitch stop was developed set at 26 deg. This stop is withdrawn by oil pressure when a solenoid on the governor is energized and automatic operation of the solenoid is provided by a switch fitted to the undercarriage oleo system. This switch is arranged so that the pitch stop is withdrawn only when the aircraft is on the ground and the oleos are compressed due to the weight on the undercarriage.

The withdrawable pitch stop provides safety against any failure of the propeller-pitch-control system at all air speeds up to about 180 mph and enables the engine to continue developing reduced power until this air speed is reached. This covers the range of speed in which control of the aircraft otherwise might prove impossible should the failure occur on an outboard engine. The only remaining danger is the possibility of overspeeding the engine in the event of the propeller moving to fine pitch at high air speeds in excess of 300 mph. The danger of overspeeding is considerably reduced compared with a piston engine owing to the high motoring power which a turbine engine will absorb and the presence of an overspeed governor in the fuel system which cuts off the engine fuel supply when the engine overspeeds by more than 5 per cent.

However, a later development to provide a complete safeguard against propeller control failure at high air speed is a device arranged to lock the pitch of the blades wherever it happens to be at the instant the failure occurs.

Safeguards in Event of Engine-Power Failure

The power required to motor a turbine engine is very much greater than for a piston engine; in the case of the Mamba, the power which it absorbs at full rpm is 75 per cent of the take-off power. Consequently, the drag which the propeller would produce if the engine were allowed to windmill after a power failure would be correspondingly high. For this reason it was particularly desirable to provide some form of automatic feathering, especially during take-off.

The engine embodies a torque meter which operates by measuring the torque reaction on the stationary internal gear in the epicyclic reduction gear between the engine and the propeller. A switch is fitted to this mechanism in such a way that if the propeller attempts to feed more than 50 hp back into the engine, a circuit is closed which overrides the propeller governor to coarsen the propeller pitch.

Thus a complete power failure results in the propeller coarsening pitch automatically and, unless the power is restored immediately, the propeller continues to feather until the drag is negligible.

The "reverse-torque" switch, as it is called, serves another very useful function in connection with restarting an engine in flight, which is dealt with later.

Incidentally, the control arrangements and safety devices which have been described were all tested in flight on a Mamba engine installed in the nose of a Lancaster flying test bed before the Apollo flew. By this means, it was possible not only to carry out general flight development of the Mamba but to prove the efficiency of the various safety devices following simulated engine or propeller control failures, without prejudicing the safety of the aircraft.

Restarting in Flight

In some ways the propeller-turbine engine is easier to start quickly in flight than a pure jet engine because of the fact that the propeller can be used to accelerate the engine rapidly. In effect, it is only necessary to unfeather the propeller with fuel and ignition turned on to achieve effective and rapid starting. There are, however, two features in connection with restarting which are worthy of mention.

Owing to the relatively high effective inertia of a turbine engine, rapid unfeathering could result in a momentary but considerable amount of drag while the propeller feeds power into the engine to accelerate it. Furthermore, should the combustion chambers fail to light, the drag would remain due to the propeller continuing to windmill the engine at high speed. Although the drag involved would not be catastrophic, its effects might be embarrassing, particularly when considering an outboard engine.

However, the "reverse-torque" switch, previously described, deals with restarting admirably without further complication. In effect, it controls the rate of unfeathering of the propeller, preventing more than 50 hp being fed into the engine, and automatically arrests unfeathering while the propeller pitch is still quite coarse, unless the combustion chambers light and the engine begins to develop power.

Some trouble with restarting was experienced during the early flights of the Apollo, the combustion chambers sometimes failing to light. The Mamba embodies vaporizing combustion chambers, and ignition is effected by means of torch igniters and spray jets which direct flame into the vaporizing tubes to heat them quickly during the early part of the starting cycle. To make the ignition circuit switch off automatically, which is desirable to simplify starting procedure and obviate the possibility of the igniters operating for a long period which might result in overheating the vaporizing tubes, arrangements were made originally for the ignition circuit to be cut when the engine reached 5000 rpm.

During a restart in flight, it was found that the engine speed reached 5000 rpm in about 3 sec which was barely sufficient to establish steady combustion. The cure for this trouble was simple and completely effective, a time switch being fitted to control the ignition cycle in place of the engine-speed basis previously employed. By this means, the time the igniters are operating was made independent of the rate of unfeathering of the propeller.

Performance of Engine

The Mamba was originally designed to produce 1000 shp but the predicted power and fuel consumption were not obtained on test. It was found that the efficiencies of the two major components, the compressor and turbine, were lower than had been anticipated, largely because of the relatively small aspect ratio of the blading.

The design top speed for the engine was 14,500 rpm, but rig tests showed that the performance of the compressor based upon a maximum speed of 15,000 rpm would be satisfactory. By making use of this speed increase and other developments, the take-off power of the engine was raised to the design figure on the test bed, although the specific fuel consumption remained higher than predicted, especially at altitude.

These developments had the effect of increasing the gas velocity in the jet pipe, thereby increasing losses and the proportion of the total power left in the jet.

To counter these deficiencies, the aspect ratio of the blading was increased, with resulting increases in air throughput and power output of 25 per cent. A considerable amount of flight development and performance testing of this 1250-hp Mamba was carried out in a Dakota aircraft fitted with these engines, Fig. 6,

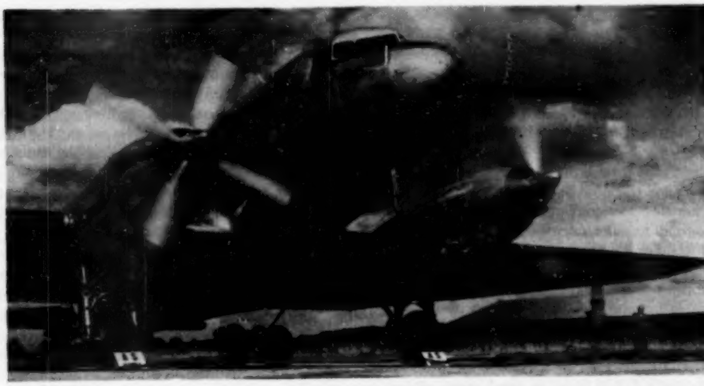

FIG. 6 MAMBA ENGINES OF 1250 HP FITTED IN DAKOTA AIRCRAFT FOR DEVELOPMENT AND TEST PURPOSES

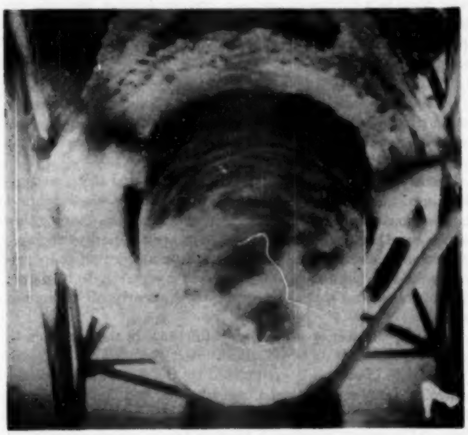

FIG. 7 FLIGHT VIEW OF MAMBA ENGINE RUNNING UNDER ARTIFICIAL ICING CONDITIONS

and a marked improvement in performance, handling characteristics, and serviceability was established.

When these engines are installed in the Apollo, the jet pipe diameters will be increased up to the maximum size permitted by the wing spars in order to revert as far as possible to the intended distribution of power output between the propeller and the jet.

ANTI-ICING

Various methods of insuring reliable engine operation under icing conditions have been considered, and the use of a methanol spray in the engine intake has been chosen for the Apollo.

A single spray jet is fixed to the periphery of the propeller spinner so that the methanol is distributed around the annular intake, the rate of flow required being from 10 to 40 lb per hr depending upon the severity of the icing conditions. Ice formation cannot occur on the leading edge of the engine cowling as the nose cowl forms the oil tank and, therefore, is kept warm.

Testing of the methanol anti-icing system has been carried out on the ground in Canada, and in flight, using artificial icing conditions obtained by means of a water spray mounted in front of the engine. Fig. 7 is a view taken in flight of a Mamba engine running under artificial icing conditions, this particular engine not embodying the oil tank in the nose cowl.

It is interesting to note that, although it was originally feared that the small and relatively fragile blades of the Mamba compressor might be particularly susceptible to damage by ice, the engine has, in fact, suffered no damage under natural or artificial icing conditions in flight even when no anti-icing protection has been provided.

CONCLUSION

Although an engine may reach a satisfactory state of development on the test bed, there remain problems associated with its inclusion in a suitable power plant for application to an aircraft and with its operation in flight.

This paper has described these problems with reference to the Mamba engines in the Apollo and the manner in which they have been overcome, and it is hoped that the experience gained may be of interest.

ACKNOWLEDGMENTS

The author wishes to express his thanks to the Directors of Armstrong Siddeley Motors Limited and to the Ministry of Supply for permission to publish this paper.

Discussion

W. M. HAWKINS, JR.[1] The author's summary of problems encountered with the Mamba engine in a transport airplane has been most thorough. We have not had the problem of actually installing a turbopropeller engine at the writer's company, but we have spent considerable time in the study of turbine-propeller transports and have been aware of many of the problems which were encountered and solved with the Apollo airplane.

The items covered in the paper with which we are in general agreement are as follows:

1 The torquemeters which appear to be desirable and are recommended by the author should be installed in any turbine propeller engine. We feel that the Apollo experience emphasizes this fact, and we urge that the development of other turbine-propeller engines incorporate this device.

[1] Division Engineer, Preliminary Design, Lockheed Aircraft Corporation, Burbank, Calif.

2 The tail-pipe temperature control with an amplifier has always appeared to us to be a relatively dangerous device if it fully controls the engine. Thus the approach which was used with the Mamba, in which the temperature override only controls a small portion of the fuel flow, appears to be a very desirable solution. It is, of course, hoped that someday engines with broader characteristics may be obtained where this kind of control will not be necessary.

3 The installation of the oil tank in the nose appears to be a most ingenious solution for the nose anti-icing. We should be most interested to follow this development and determine whether or not this installation had any detrimental effect, such as overcooling of the oil and whether it actually would suffice as an anti-icing device for the lip.

4 The use of a multiple propeller-blade angle stop appears to us to be an awkward solution and we heartily agree with the suggestion that a propeller control be installed in which the propeller remains at a fixed angle whenever the governor fails. We should like to recommend that in this kind of a system the propeller actually be manually controllable from its fixed angle after a governor failure. Thus the pilot or flight engineer could maintain a semblance of normal operation on an engine without the governor.

5 The recommendation that automatic feathering be installed in the airplane appears to be well founded, and the torquemeter solution for this installation appears to be a very usable and simple system.

Certain items in the paper led to questions on our part, and the writer will list these only to bring them to the attention of those who are developing turbine-propeller engines so that more effort may be spent in their solution.

1 Although this is repetition, we should certainly like to emphasize that a propeller control should be such that it automatically goes into manual control with the propeller at the last blade setting prior to governor failure. In the failure of a governor, the multiple stop system to control overspeeding appears to be awkward and undesirable.

2 The starting of turbine engines should not remain as difficult as at present, requiring extremely high-powered starters. For an engine the size of the Mamba, this was not an insurmountable problem. For larger and larger turbine engines, however, it is a serious consideration for the airline operator, and anything that can be done in the basic concept of the engine to ease this problem should be done.

3 The ability of the turbine propeller to be used as a reverse-thrust device is highly important, and no mention was made of any development program to work out the bugs of this system in the Apollo airplane. We presume, of course, that such is being done and we are interested in following the progress of this work.

4 In some of our studies it appeared desirable to operate a multiple-engine turbine airplane with some of the engines shut down. This would appear to be completely feasible from a starting standpoint and from a drag standpoint. However, the icing problem if such holding has to be done in inclement weather might be extremely severe and, therefore, the alcohol system of anti-icing might have its drawbacks. Furthermore, the use of alcohol always implies a design decision as to how long the anti-icing problem will exist in order that the capacity of the system may be determined. It appears more logical to us that a hot-air system, supplied by all of the engines in combination, would be a more desirable anti-icing system since it could be used for prolonged periods of time, and since it could be used for anti-icing a dead engine. The nose oil tank must be vulnerable to congealing with a dead engine and some sort of heat source should be available to prevent this.

5 The heat shield and vent system described in the Apollo installation gives rise to the question of whether it would not have been more desirable to reduce the ventilation to very nearly zero by the use of a stainless-steel structure in this area. This would have given better fire protection, since the heat-resistant material would have been heavier, and the fire control would have been improved since less air flow would be passing through the area where a fire was being snuffed out. Along the same line, no mention was made of the fire-protection means for the relatively long tail pipe which must be adjacent to important wing structure. It would be interesting to know what measures were taken for heat insulation and fire protection in this area.

In summary, it would appear that the author has been doing very worth while development work in an entirely new field, and he should be commended on his apparent efforts to solve each of the complicated problems in a straightforward and simple fashion. Airline transport today suffers not from the advanced performance and the high speeds which are being achieved, but from the complications which go to added passenger comfort and to the extremely precise controls which are being developed to improve flight safety. The more work that is done to determine the simplest possible solutions to our new problems rather than the installation of more and more gadgets, the better off the airline operator will be from an economy, regularity, and performance standpoint.

C. F. Wood.[3] Although the writer has had no actual experience with the building and operation of the turboprop engine, he has been associated with a study of the controls for a somewhat larger engine than the Mamba.

It is of interest to note that this study indicated the same general approach to the engine-control combination as was developed during the actual testing of the Mamba. A good many other studies have been made where a different type of control arrangement was recommended. However, the simplicity of the Armstrong Siddeley approach to the problem is certainly to be highly recommended and should be applicable to nearly all turboprop engines.

There is, however, a considerable difference in the approach to automatic controls between the United States and England. The English approach is exemplified by the development of the control system for the Mamba engine. The first flight testing on this engine was conducted with a relatively simple control and then, as the testing progressed, refinements of a more complicated nature were added. In the United States the course of development usually follows a somewhat different pattern. A general statement of the entire control problem is made at the beginning of the development. The solution is then obtained by a frontal attack on the entire problem.

In addition, there seems to be some difference between the two countries in the requirements placed on any control system. The difference is concerned chiefly on the responsibility placed on the pilot for the safety of the engine. The attitude taken in the United States is that the pilot should not have to be responsible in any manner for the safety of the engine during any normal flight operation. It is up to the control system to protect the engine almost without regard to the manner in which the power-control levers are operated. This attitude results in a somewhat more complex control system, but on the other hand, leaves the pilot more freedom of operation and allows his attention to be concentrated more directly on the business of flying the airplane.

This writer does not wish to try to evaluate the quality of either of these approaches but merely to point out the difference.

[3] Senior Engineer, Control Development Activity, Aviation Gas Turbine Division, Westinghouse Electric Corporation, Lester, Pa.

It must be said that there are many arguments in favor of both approaches. Actually, it now appears that both countries are moving toward a middle ground in their approach to the problem of controlling aviation gas-turbine engines.

A study of the flight testing of the Allison XT-40 turboprop engines in the U. S. Navy XP5Y-1[4] described a number of operational difficulties. Practically every one of these is discussed in the present paper and its solution given.

One of the more serious problems encountered during the early flight experience with the Allison engine was that of asymmetric thrust. This asymmetry was the result of a mismatch between the control settings on the two outboard engines. It is apparently quite difficult to hold the proper control settings when the engines are operating at low power at low-flight speed. What happened was that the controls were set so that one engine was windmilling, while the other was producing power. Because of the low air speed, the windmilling propeller went to very flat pitch with correspondingly high drag. The difference between the operation of the two engines caused not only a large asymmetric thrust, but also a large rolling moment toward the windmilling engine. This difficulty was avoided on the Mamba by the use of two limiting devices, namely, a low-pitch stop, and a reverse-torque limit. The low-pitch stop is being installed on the XT-40, while the use of a reverse-torque limiting device is being considered.

Attention should be drawn to type of flying test bed used by Armstrong Siddeley for the testing of the Mamba. The use of a well developed airframe such as the Lancaster is eminently suitable. In this manner it is possible to avoid the problems surrounding the early flying of any new airframe. Since the airframe itself is not under test, all attention may be turned to studying the operation of the power plant. Any difficulties with its operation are immediately apparent, whereas with an untried airframe it is sometimes troublesome to distinguish between the operational difficulties due to the power plant and those due to the airframe.

[4] "Flight Experience With Turbine Propeller-Powered Aircraft," by R. C. Loomis and E. D. Shannon, SAE Preprint No. 616.

It should be pointed out that while the Lancaster bomber makes an excellent flying test bed for a turboprop engine such as the Mamba, the Lancaster's effectiveness as a test bed for turbojet engines is limited. A flying test bed for a turbojet engine should be capable of flying to considerably higher altitudes and speeds than are available with the Lancaster. However, the excellence of the Armstrong Siddeley approach to the flight testing of the Mamba engine is adequately demonstrated by the results.

Author's Closure

The suggestion made by Mr. Hawkins that control of the propeller should be possible manually following governor failure is interesting and almost certainly involves the adoption of an electrically operated propeller. The only objection to this arrangement is that the manual override itself would presumably be liable to failure to about the same extent as the governor, in which case there would be no over-all increase in safety.

The author agrees with his remarks concerning starting turbine engines and advocates the use of higher-voltage starters.

The adoption of reversing propellers on the Mamba involves no modifications to the engine itself but makes the propeller controls rather more complicated. Tests have been carried out with satisfactory results.

Various anti-icing systems have been studied and some of them tested. Anti-icing by means of hot air was found to cause an excessive loss of performance. No trouble with congealing of oil in the nose oil tank has been experienced or is anticipated due to the use of a relatively low-viscosity lubricant.

Regarding ventilation of the engine nacelles, in the case of the Apollo, stainless-steel heat shields are employed round the combustion chambers and jet pipe to insure the maximum safety.

In answer to Mr. Wood's discussion, it is true that the initial flight tests of the Mamba were carried out without some of the control-system refinements fitted, but the whole concept of the system had already been worked out and no basic changes have been found necessary in the course of development.

The author would like to correct the impression that he is satisfied to leave the safety of an aero engine in the hands of the pilot. Control systems should be arranged so that no damage can be caused to the engine by any reasonable manipulation of the control levers.

An Instantaneous and Continuous Sodium-Line Reversal Pyrometer

By M. M. EL WAKIL,[1] P. S. MYERS,[2] and O. A. UYEHARA[3]

The theory, development, and calibration of an electro-optical sodium-line reversal pyrometer are given. This pyrometer instantaneously and continuously determines and indicates the black-body temperature of a nonluminous flame made luminous at the sodium wave length by the addition of sodium. Typical data obtained on a spark-ignition engine are presented and compared with data obtained by previous investigators. A correlation of these data with combustion-chamber design indicates the possible existence of a high temperature in the flame front.

THE University of Wisconsin has had a long and continued interest in obtaining a better understanding of the fundamental processes occurring during combustion in an internal-combustion engine. Wilson, Rose, et al, (1, 2, 3)[4] were early pioneers in the field of combustion in a compression-ignition engine. Uyehara, Myers, et al, (4, 5, 6, 7) developed an electro-optical pyrometer capable of following and recording flame temperatures during the combustion process in the compression-ignition engine and used this and other instruments to make additional studies. It is logical that this interest in the mysteries of combustion be extended to cover the field of combustion in a spark-ignition engine. Hence this paper deals with an instrument capable of measuring and recording flame temperatures in a spark-ignition engine. The information on this instrument is presented at this time with the hope that it may be of interest to workers in other fields, and with the expectation that constructive criticism of the ideas presented and the techniques used may prove of benefit when undertaking proposed spark-ignition combustion studies.

As was pointed out previously (4), instantaneous and continuous temperature measurements in an internal-combustion engine are difficult to achieve but are of fundamental importance in any combustion study. The electro-optical pyrometer (4) provides instantaneous and continuous temperature data for a luminous flame but is inoperative on nonluminous gases such as exist during the compression stroke in both the compression- and spark-ignition engine and during normal combustion in the spark-ignition engine.

The sodium-line reversal technique developed by Kurlbaum (8) and Fery (9) has achieved general acceptance as a means of measuring the temperatures of nonluminous gases, although it has not entirely escaped criticism (10). Adaptations of the Kurlbaum-Fery technique by Hershey and Paton (11), Lloyd-Evans and Watts (12), and Rassweiler and Withrow (13) have enabled point-by-point measurements to be made during the combustion processes in the spark-ignition engine. The data obtained in these investigations were the average values over a large number of cycles of questionable reproducibility. This reproducibility was even more questionable in the cases where it was necessary to stop the engine between the recording of the data for individual points. Furthermore, the experimental data represented a time average as well as a cyclic average since the stroboscopic shutter, of necessity, remained open for periods of as much as 18 deg of crank rotation. Nevertheless, the measurements were pioneering in nature and shielded valuable and interesting data on the combustion processes in the spark-ignition engine.

Since the sodium-line reversal method had achieved general acceptance as a means of determining the temperature of nonluminous gases, and since it had been successfully applied to point-by-point temperature measurements, it seemed logical to use the fundamental techniques of this method as the basis for developing an instantaneous and continuous temperature indicator for nonluminous flames. It is believed that the data obtained with this instrument will be valuable in combustion studies of the spark-ignition engine as well as in any other fields where the temperatures of nonluminous gases are rapidly varying and temperature measurements are desired.

The Electro-Optical Reversal Pyrometer

The basic techniques of the method devised by Kurlbaum (8) and Fery (9) are illustrated in Fig. 1. As shown, the radiation

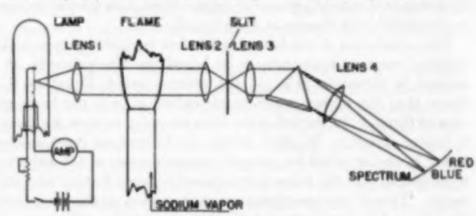

Fig. 1 Apparatus for Standard Sodium-Line Reversal Temperature Determination

from a broad-ribbon tungsten-filament lamp is made parallel by lens 1, passed through the flame which has been made luminous at the sodium wave length by the addition of sodium compound, and focused on the slit of the spectrometer by lens 2. If the flame is luminous only at the sodium wave length, all visible radiation from the lamp, with the exception of the sodium-wave-length radiation, passes unchanged through the flame. The spectral intensity at the sodium wave length is

$$J_{\lambda S} = J_{\lambda L} - A_{\lambda F} J_{\lambda L} + E_{\lambda F} J_{\lambda F} \ldots\ldots\ldots\ldots [1]$$

where

$J_{\lambda S}$ = monochromatic radiation intensity of wave length λ received by the spectrometer

$J_{\lambda L}$ = monochromatic radiation intensity from lamp at wave length λ

[1] Lecturer, College of Engineering, Farouk I University, Alexandria, Egypt.

[2] College of Engineering, University of Wisconsin, Madison, Wis., Mem. ASME.

[3] College of Engineering, University of Wisconsin. Jun. ASME.

[4] Numbers in parentheses refer to Bibliography at end of paper.

Contributed by the Oil and Gas Power Division and presented at the Annual Meeting, New York, N. Y., November 26–December 1, 1950, of The American Society of Mechanical Engineers.

 Manuscript received at ASME Headquarters, October 2, 1950. Paper No. 50—A-94.

$A_{\lambda F}$ = monochromatic absorptivity of flame at wave length λ
$J_{\lambda F}$ = monochromatic radiation intensity from flame at wave length λ

If the sodium-wave-length radiation absorbed by the flame, $A_{\lambda F}J_{\lambda L}$, is greater than the sodium-wave-length radiation emitted by the flame, $J_{\lambda F}$, $J_{\lambda S}$ will be less than $J_{\lambda L}$, and the sodium line will appear dark in comparison with the unabsorbed lamp radiation of other wave lengths. Conversely, if the amount absorbed is less than the amount emitted the sodium line will appear bright. At the reversal point where $J_{\lambda S} = J_{\lambda L}$

$$J_{\lambda L} = \frac{J_{\lambda F}}{A_{\lambda F}} \quad [2]$$

Applying Wien's law which relates the monochromatic radiation intensity of a body to its temperature, and noting that for negligible reflectivity the absorptivity of a body receiving radiation from another body at the same temperature is numerically equal to its emissivity

$$J_{\lambda L} = E_\lambda C_1 \lambda^{-5} e^{\frac{-C_2}{\lambda T_{BBL}}} = C_1 \lambda^{-5} e^{\frac{-C_2}{\lambda T_{AL}}} = C_1 \lambda^{-5} e^{\frac{-C_2}{\lambda T_{BBF}}} \quad [3]$$

where

E_λ = monochromatic emissivity of lamp at wave length λ
C_1, C_2 = known constants
T_{BBL} = black-body temperature of lamp
T_{AL} = apparent temperature of lamp at wave length λ
T_{BBF} = black-body temperature of flame

and thus $T_{BBF} = T_{AL}$.

The standard procedure is then to adjust the temperature of the lamp filament to that temperature at which the sodium line just reverses or blends into the rest of the spectrum. At this temperature the black-body temperature of the flame is equal to the apparent temperature of the lamp which may be measured by a standard optical pyrometer using a correction for the change in emissivity with change in wave length.

The adaptation of the foregoing method for use on flames with rapidly varying temperatures is based on the concepts expressed in Equation [1]. At the reversal point, Equation [1] states that the sodium-wave-length radiation from the lamp as viewed through the flame has the same intensity as when the lamp is viewed directly. In other words, at the reversal point an observer is unable to tell by intensity measurements at the sodium-wave length that the flame is interposed between himself and the lamp. Thus if two spectrometers were sighted on the lamp, one directly and the other through the flame, and if the sodium-wave-length radiation intensities as received through the two spectrometers were always kept equal by varying the lamp temperature, the apparent temperature of the lamp would at all times be equal to the black-body temperature of the flame. Such an arrangement is advantageous over the usual sodium-line reversal arrangement in that the lamp need emit only the sodium-wave length, i.e., it need not emit the other wave lengths of the spectrum which, in the conventional arrangement, are used to detect the point of reversal. Thus a gaseous-discharge lamp, electronic in nature and giving a discontinuous spectrum but capable of following rapid temperature variations, may be substituted for the conventional broad-ribbon tungsten lamp with its high thermal inertia. In addition, phototubes and their associated electronic equipment may be used to detect and maintain equal sodium-wave-length radiation intensity at the two spectrometers. This adaptation enables the electro-optical sodium-line reversal pyrometer to follow and record rapidly varying temperatures such as are found in spark-ignition engines.

Apparatus. A schematic diagram of the electro-optical reversal pyrometer is shown in Fig. 2. Three optical paths are provided for the radiation from the sodium lamp. For the first path the radiation passes through the quartz windows, through the flame in the head of the engine, and into a spectrometer where a photo-

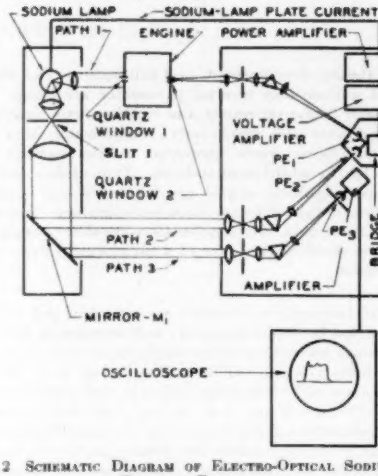

Fig. 2 Schematic Diagram of Electro-Optical Sodium-Line Reversal Pyrometer

tube PE_1, located at the sodium wave length, measures the radiation intensity. The second path by-passes the engine and goes directly to another spectrometer where a second phototube PE_2, also located at the sodium wave length, compares the radiation intensity with that received by PE_1. If the two phototube outputs are not equal, the current through the lamp is adjusted automatically by electronic means until the two phototube outputs are equal. The third radiation path terminates at PE_3. This phototube, when properly calibrated, measures the apparent temperature of the lamp which automatically follows and is equal to the true temperature of the flame as previously explained. As will be discussed later, vapors other than sodium could be used in the lamp. However, it was desired to use a sodium lamp for the present experiments, and thus the smallest commercially available sodium lamp, General Electric Na-1 (14), was used. At its maximum plate current of 3 amp the apparent temperature of this lamp is considerably higher than the temperatures anticipated in the engine.

This lamp was designed for operation on alternating current with a hot filament in each end alternately serving as an electron emitter and as a plate. For the present purpose, both filaments were used only during the warm-up period. While the pyrometer was in actual use one of the filaments was not heated but served only as a plate. A pulsating direct-current voltage related to the flame temperature and supplied by the power amplifier, Fig. 2, was then impressed on this plate.

The intensity of the light emitted by the lamp is a function of the vapor pressure of the sodium in the lamp, of its physical characteristics, and of the current passing through the lamp. Schmellenmeier (15) has found that a 1 per cent rise in vapor pressure inside of the lamp produces a 1 per cent rise in illumination. For this reason the radiation intensity of the lamp was measured directly by PE_3 rather than by measuring the plate current. It was considered expedient, however, to supply external heat to

the lamp, especially during the periods of low-current operation, in order to maintain a relatively constant vapor pressure. For this purpose a heating coil, thermostatically controlled, was wrapped around the neck of the lamp. A standard vacuum flask was placed over the lamp and the heating coil as an aid in minimizing the vapor-pressure fluctuations and reducing the amount of heat required.

As indicated in Fig. 2, a mirror was used to reflect the light rays at a 90-deg angle. The use of this first-surface mirror enabled the three phototubes to be placed close together physically. The slit S_1 was used to compensate for any light absorption or restriction caused by the quartz windows. Further mention of this point will be made in explaining the calibration procedure.

All three phototubes were of the photomultiplier type (931A). The required high voltages were supplied by a voltage-regulated power supply. The output of the two phototubes, PE_1, and PE_2, Fig. 2, were compared by means of a bridge arrangement, and any inequality was amplified by the voltage amplifier. The voltage from the voltage amplifier was fed to a current amplifier capable of supplying the required maximum lamp current of 3 amp. The plate current for the current amplifier and the lamp was supplied by a 220-volt d-c motor generator set. Cathode followers were used wherever low-impedance circuits seemed desirable. It was necessary to consider both the proper sense and phase relationships between the voltage appearing at the bridge and the voltage impressed on the lamp. Thus a phase inverter was inserted between one of the phototubes and the bridge arrangement, to obtain correct sense relationship between the phototubes, and an odd number of stages were used in the amplifier to obtain the proper phase relationships between the bridge and the lamp.

The apparent temperature of the sodium lamp was measured and oscillographically recorded by means of the third phototube PE_3. This function could have been performed by either PE_1 or PE_2, but it was considered better to separate the balancing and measuring circuits.

Quartz windows of the self-cleaning type (7) were used to transmit the radiation through the combustion-chamber walls. It was noticed that a considerable amount of a hard material, probably some lead or sodium compound, was formed around the outside of the quartz rod. This compound did not form on the end of the rod but a small amount of pitting was noted.

Calibration. A source whose temperature is accurately known was desired for calibration of the measuring circuit. The usual techniques of simulating black-body conditions or employing a broad-ribbon tungsten lamp of known emissivity values for calibration purposes were considered inapplicable because of spectrometer imperfections and the monochromacity of the radiation from the sodium lamp. The same considerations, as well as lack of a suitable filter, prevented the use of a standard optical pyrometer to measure the apparent temperature of the sodium-vapor lamp. The calibration technique finally adopted involved calibration of a steady-temperature flame by the standard steady-state sodium-line reversal technique, and the use of this steady-temperature flame to calibrate the electro-optical reversal pyrometer.

As will be explained later, one temperature determination is sufficient to calibrate the measuring circuit. However, for experimental purposes a burner was constructed that would burn city gas, oxygen, and air in any desired proportions. A sodium salt was added to this system which then furnished a steady-temperature flame whose temperature could be varied manually in an attempt to verify the accuracy of the technique and of the equipment, and which could also be used for calibration purposes.

For ease of calibration and in order to utilize existing apparatus, the calibrating equipment was arranged as shown in Fig. 3. The first-surface movable mirror M_2 served the dual purpose of reflecting the radiation from the tungsten lamp through an angle of 90 deg and blocking the radiation from the sodium-vapor lamp. The second first-surface movable mirror M_3, immediately preceding the phototube PE_1, was placed at such an angle that the

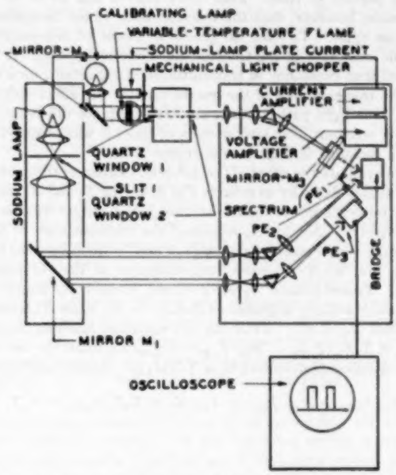

Fig. 3 Schematic Diagram of Electro-Optical Sodium-Line Reversal Pyrometer as Arranged for Calibration Purposes

radiation was reflected upward to a horizontally placed ground glass. When using the broad-ribbon tungsten lamp and the steady-temperature flame the reversal of the sodium-resonance line could thus be visually observed on this ground glass. The chopper was required since the amplifiers were not of the direct-coupled type.

In utilizing the standard steady-state sodium-line reversal technique to determine the temperature of the steady-temperature burner, it was necessary to determine the apparent temperature of the broad-ribbon tungsten lamp. Following the usual practice the apparent temperature of the tungsten lamp at the effective wave length of the standard optical pyrometer (0.665 micron) was determined and this apparent temperature was corrected to the sodium wave length by solving Equation [3] for the two wave lengths involved. The resulting equation is

$$\frac{1}{T_{A\lambda S}} = \frac{1}{T_{A\lambda P}} - \frac{\lambda_S}{C_2} \ln E_{\lambda S} + \frac{\lambda_P}{C_2} \ln E_{\lambda P} \ldots\ldots [4]$$

where

$T_{A\lambda S}$, $T_{A\lambda P}$ = apparent temperature of tungsten lamp at sodium wave length and at wave length of standard optical pyrometer (0.665 micron), respectively

λ_S, λ_P = sodium wave length and standard optical pyrometer wave length, respectively

$E_{\lambda S}$, $E_{\lambda P}$ = monochromatic emissivities of tungsten lamp at sodium and standard optical pyrometer wave lengths, respectively

Consideration must be given to the transmittance of the quartz windows in calibrating the equipment. This transmittance may affect the calibration since the quartz windows are in only one of the three light paths. Their transmittance also will enter into the

calibration since the calibration flame is located in a different position relative to the quartz windows than is the engine flame.

It has been noted already that the quartz windows were of the self-cleaning type. It was anticipated that because of this feature their transmittance would remain constant over relatively long periods of time. Tests have proved this to be so. It is possible, however, that the transmittance varies throughout the engine cycle. To date no practical means of determining the cyclic constancy of the transmittance has been found. It will be noted that constancy of transmittance is important, for a change in the transmittance of the quartz window will affect only one of the three light paths. Since the transmittance did remain relatively constant over long periods of time, it was assumed to remain constant throughout the engine cycle.

To evaluate the effect of the different location of the calibration and engine flame let us refer to Fig. 2, letting X_1 and X_2 represent the transmittance of quartz window 1 and quartz window 2, respectively. Also, let X_3 represent the transmittance of the slit through which passes light paths 2 and 3 which by-pass the engine, and let X_4 represent transmittance of the slit preceding PE_2. Transmittance X_3 is, of course, variable by means of slit S_1, and is initially adjusted so that $X_1 = X_3$, while X_4 is adjusted so that $X_4 = X_2$. Thus the net radiation reaching phototube PE_1 is $X_1X_2(J_{LEF} - A_{EF}J_{LEF}) + J_{EF}X_2$, while the net radiation reaching phototube PE_2 is $X_3X_4J_{LEF}$. At the balance point

$$X_1X_2(J_{LEF} - A_{EF}J_{EF}) + J_{EF}X_2 = X_3X_4J_{LEF} = X_1X_2J_{LEF} \qquad [5]$$

or

$$J_{LEF} = \frac{J_{EF}}{A_{EF}X_1} \qquad [6]$$

where the subscripts EF stand for engine flame. At the same time the measuring phototube, PE_3, will receive radiation of intensity

$$J_{PE(3)EF} = X_1J_{LEF} \qquad [7]$$

With X_3 still fixed at X_1 and X_4 adjusted to compensate for the removal of quartz window 2, let us consider the arrangement shown in Fig. 3 which schematically represents the arrangement of the equipment while using the steady-temperature calibrating flame with the exception that quartz window 2 is in place. Consider the situation when mirrors M_2 and M_3 are inoperative, i.e., the temperature of the calibrating flame has been determined and the flame is now to be used to calibrate the apparatus. Under these conditions, at the balance point

$$X_1(J_{LCF} - A_{CF}J_{LCF} + J_{CF}) = X_1J_{LCF} \qquad [8]$$

or

$$J_{LCF} = J_{CF}/A_{CF} \qquad [9]$$

where the subscripts CF stand for calibrating flame. At the same time the measuring phototube, PE_3, will receive radiation of intensity

$$J_{PE(3)CF} = X_1J_{LCF} \qquad [10]$$

If we have a calibrating flame and an engine flame with the same black-body temperature, then from Equations [6] and [9]

$$J_{CF}/A_{CF} = J_{EF}/A_{EF} = J_{LCF} = J_{LEF}X_1 \qquad [11]$$

Equation [11] shows that the lamp intensity must be greater by the factor X_1 when the engine flame is in position if the engine and calibrating flames are to be at the same temperature. Equations [7] and [10] state that the measuring phototube, PE_3, receives the same fraction of the lamp radiation regardless of which flame is in position. It follows then that even when the calibrating and engine flames are at the same temperature, the oscillographic indication of the phototube, PE_3, will be greater by the amount $1/X_1$ when the engine flame is in position. The value of X_1 must then be determined experimentally and properly accounted for by decreasing the gain of the electronic equipment following phototube PE_3 when it is used on the engine flame, by multiplying the oscillographic deflections by the factor X_1, by changing the front slit of the spectrometer preceding PE_3, or by a properly proportioned combination of the three methods mentioned. In any event the choice between the three methods is made on the basis that approximately full-scale oscillographic deflection from the measuring circuit is desired when the instrument is used on the engine.

The calibration procedure is then as follows: The engine is run for some time under the proposed operating conditions to insure the constancy of X_1 and X_2. The engine is then stopped, quartz window 2 is removed to facilitate visual observations, and a constant, alternating voltage is impressed on the plates of the sodium-vapor lamp. The transmittances of the two light paths to phototubes PE_1 and PE_2 are then made equal by adjusting the slit S_1 so that the output of the balancing circuit is zero. The steady-temperature burner and the required mirrors are then placed in position and after the steady-temperature flame has been adjusted to the desired temperature, the reversal point is achieved by varying the current through the broad-ribbon tungsten flame and is visually noted by means of the mirror M_3. The apparent temperature of the tungsten lamp is then determined by a standard optical pyrometer. This determination, after the proper wave-length correction, yields the true flame temperature. With the temperature of the steady-temperature flame now known, the mirrors are removed from the lines of sight, the light chopper is started, and the steady-temperature flame is used to calibrate the electro-optical reversal pyrometer. Several readings are taken since only one temperature determination is necessary to calibrate the apparatus. The value of X_1 is then determined experimentally by again impressing a constant, alternating voltage on the plate of the sodium lamp, blocking the radiation to the phototube PE_2, and noting the oscillographic deflection with quartz window 1, in place, and when it is removed. Following this determination, both quartz windows are inserted, and the absorption of light paths 1 and 2 are made equal by adjusting the slit of the spectrometer in front of PE_2. This completes the calibration of the electro-optical reversal pyrometer.

If the apparent temperature of the lamp is at all times equal to the true temperature of the steady-temperature calibrating flame, and if the amplification of the measuring circuit is constant and linear with light intensity, then according to Equation [3]

$$J_{LCF} = \frac{J_{CF}}{A_{CF}} = KD = C_1\lambda^{-5}e^{\frac{-C_2}{\lambda T}} \qquad [12]$$

where

J_{LCF}, J_{CF} = radiation intensities of calibrating flame and of sodium lamp, respectively
K = proportionality constant
D = oscillographic deflection of measuring circuit
A_{CF} = monochromatic absorptivity of calibrating flame at a wave length λ

Taking the logarithm of both sides and grouping constant terms

$$\ln D = \ln(\text{const}) - (C_2/\lambda)(1/T) \qquad [13]$$

Equation [13] states that the oscillographic deflection of the measuring circuit, when plotted on semilogarithmic paper against the reciprocal of the absolute temperature, should plot as a straight line of slope $-C_2/\lambda$. In order to check the accuracy of

the equipment, calibration data were taken with the air-oxygen-gas mixture supplied to the burner adjusted to give different flame temperatures. The resulting data are shown in Fig. 4 where the temperature scale is the temperature of the burner flame determined by the steady-state sodium-line reversal technique. As the theory predicts, the data indicate a straight line of slope $-C_2/\lambda$. Thus, when calibrating the equipment, one accurate temperature determination is sufficient to establish the calibration of the equipment, since the slope of the line is known.

Preliminary Results

The engine which was used for the exploratory tests and with which it is planned to conduct future tests, is a Waukesha CFR octane fuel-rating engine having a high-speed crankcase and equipped with a special head and crankshaft. This special head has seven holes as shown in Fig. 4. As will be noted in Fig. 4, two pairs of holes are diametrically opposed and suitable for use with the present equipment. The additional holes provide openings for other instruments as well as a means of initiating combustion at different points in the combustion chamber. Because of the special camshaft the intake valve opens at approximately 25 BTC. The timing of the other valve events is normal.

Instrumentation of the type described in reference (4) enabled temperature-time diagrams with timing marks to be repeatedly shown on an oscillograph. In addition, a pip on the oscillographic trace caused by the occurrence of spark indicated the spark timing. Since it was intended to use the sweep circuit primarily for observation purposes and to use a drum camera for taking future data, no special care was taken to insure a high order of accuracy in this mechanism.

For these exploratory tests the engine speed was held constant at 1200 rpm, the spark at 39 deg BTC, the compression ratio at 6:1, and the inlet cooling-water temperature at 180 F. A leaded laboratory fuel, classified as a "premium-grade" fuel and purchased on the open market, was used. The fuel was injected into the intake duct by an injection pump at a point about 3 in. ahead of the intake valve.

The variable chosen for the exploratory tests was the air-fuel ratio. This particular variable was chosen because comparison data taken with the steady-state point-by-point technique were available in the literature. Since neither the fuel nor the air was metered the "best-power" mixture was determined experimentally. The terms "rich" and "lean" as used in this paper are comparative only.

Both the cyclic reproducibility and irreproducibility were especially apparent in all of the oscillograms taken. For example, the isothermal portion of the oscillogram shown in Fig. 5 does not vary by more than 25 or 50 F between the cycles shown. At the same time the temperature of two of the three cycles shown in Fig. 5 exceeded the lower sensitivity limit of the instrument at approximately top center and decreased to a value below this limit at approximately 80 deg after top center. The third cycle did not exceed the lower sensitivity limit of the instrument until approximately 30 deg after top center and did not drop below this limit until an estimated 130 deg after top center when it had gone off the oscillograph screen. It will be noted that the cyclic reproducibility of the isothermal portion was good for all three air-fuel ratios used (Figs. 5, 6, and 7), while the irreproducibility was more pronounced for the rich and lean mixtures (Figs. 5, 6, and 7).

The occurrence of spark is indicated on the oscillogram and remained relatively constant. It will be noted in Fig. 4 and inferred from the data in Figs. 5, 6, and 7, that the elevation of the spark plug is above the elevation of the line of sight through the quartz window. Apparently the cyclic irreproducibility represents the variation in the time required for the flame to grow and

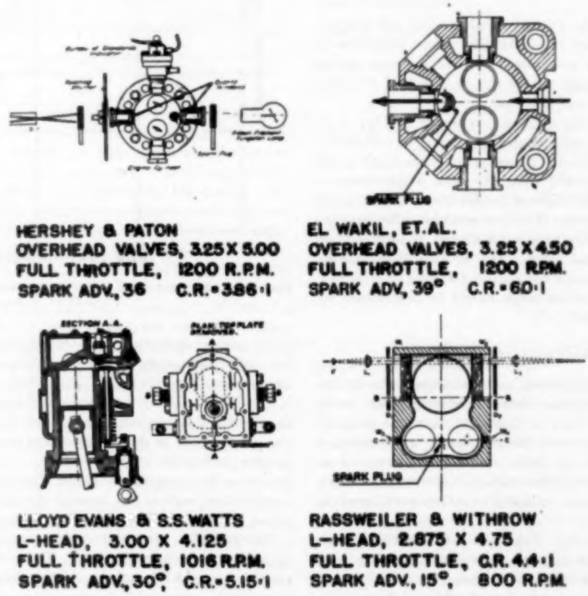

Fig. 4 Combustion-Chamber Arrangement and Operating Data for Different Investigations

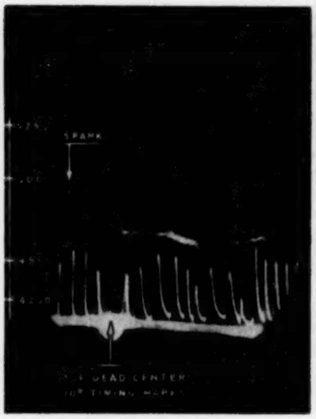

Fig. 5 Temperature-Time Oscillogram Taken With Lean Mixture

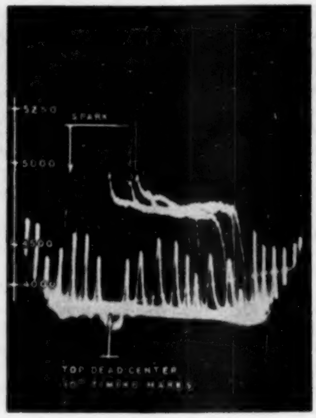

Fig. 6 Temperature-Time Oscillogram Taken With Rich Mixture

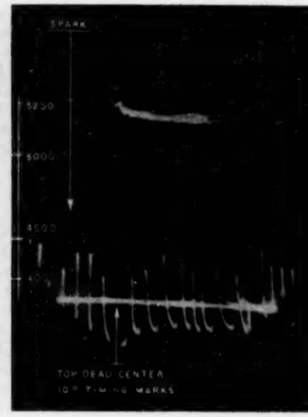

Fig. 7 Temperature-Time Oscillogram Taken With Best-Power Mixture

reach the line of sight of the pyrometer. Some cyclic irreproducibility was to be expected since no particular precautions were taken to insure a homogeneous air-fuel mixture, since previous investigators using the steady-state technique had noted that occasional reversals could be obtained over a fairly large temperature range, and possibly because of the special camshaft used. It will be interesting to determine the extent to which the cycle-to-cycle variation can be minimized or eliminated by supplying a relatively homogeneous air-fuel mixture and by close control of the other engine variables.

The detection of both the cyclic reproducibility and irreproducibility and of their nature illustrates the unique usefulness of the instrument. With this instrument individual cycles can be studied or, if desired, average values can be obtained with the averaging method known and specified.

Deflections scaled from the oscillograms shown in Figs. 5, 6, and 7, were converted to temperature by means of calibration data and are shown as points on a temperature-crank-angle graph in Fig. 8. The trend expected from the data of previous investigators is found, i.e., the highest temperatures are obtained from the best-power mixtures. The temperature difference between the rich and lean mixtures is small and is probably no larger than the experimental error. Any average curve drawn through the points would have a flat portion followed by a portion of decreasing temperature whose slope would be determined by the averaging technique used.

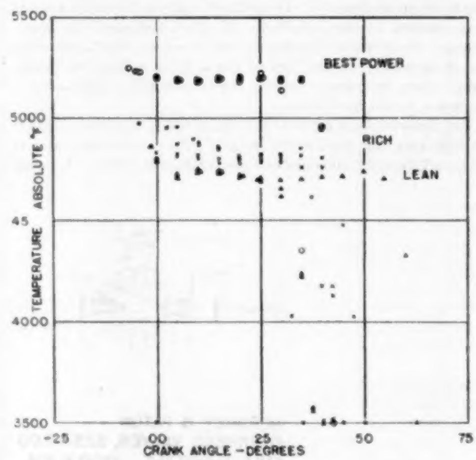

Fig. 8 Variation in Flame-Temperature With Variation in Air-Fuel Ratio

Experimental Accuracy and Techniques

As is true with most instruments and techniques, the instrumentation described has certain characteristics peculiar to it. Since these characteristics must be taken into account properly when interpreting data taken with the instrument, a discussion of these characteristics may be in order. It may also prove of interest to point out technique and instrument improvements which may make the instrument more valuable to others working in the field.

Low-Temperature Sensitivity. Equation [13] states that when the logarithm of the voltage output of the measuring circuit (as measured on the oscillograph) is plotted against the reciprocal of the absolute temperature, a straight line should and does result. It will be noted in Fig. 9 that this results in a rapid decrease in oscillographic deflection with a decrease in temperature, i.e., such low deflections occur at low temperatures that the scaling error becomes inordinately large. This effect will also be noted in Figs. 5, 6, and 7, as an abrupt increase in deflection from an immeasurably small value to a maximum or near-maximum value. Similarly, an abrupt decrease in deflection occurs near the end of the oscillographic indication of temperature. Thus the initial and final points on the temperature graph, Fig. 10, do not represent actual temperature values but merely the initial and final points at which measurable deflections were obtained.

Theoretically, some sodium vapor is always present regardless of the temperature of the gases. However, a practical lower limit exists below which insufficient sodium is present in the vapor state to produce appreciable luminosity at the sodium wave length. The adjustment in the present instrument is such that this lower

limit undoubtedly occurs below the lower temperature limit to which the instrument is sensitive.

The low-temperature sensitivity of the instrument could theoretically be improved by proper choice of the wave lengths used. If Wien's law is differentiated with respect to wave length and

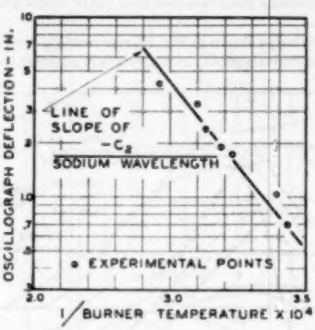

FIG. 9 EXPERIMENTAL FLAME-TEMPERATURE DETERMINATIONS BY ELECTRO-OPTICAL SODIUM-LINE REVERSAL PYROMETER

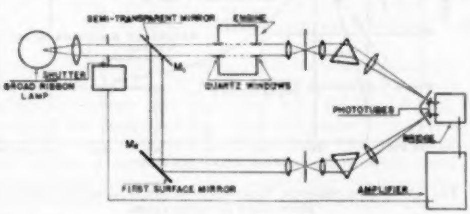

FIG. 10 SCHEMATIC ARRANGEMENT OF ELECTRO-OPTICAL SODIUM LINE REVERSAL PYROMETER USING A VARIABLE TRANSMITTANCE

the differential set equal to zero, it will be found that the product of $T\lambda$ is equal to a constant indicating that the maximum radiation intensity occurs at longer wave lengths as the temperature decreases. Thus a compound with a longer-wave-length resonance line would be more suitable for low-temperature measurements in that higher radiation intensities would result at the same temperature. The use of a compound with a longer wave-length resonance line would also decrease the slope $(-C_2\lambda)$ of the line shown in Fig. 9, and the same oscillographic deflection would represent a greater temperature difference. With these thoughts in mind, other vapors such as potassium (λ = 7664.A) and cassium (λ = 8521.1A) were considered but, for various reasons, such as the unavailability of commercial lamps using these compounds and their possible unknown effects on combustion and the combustion chamber, these and other compounds were rejected in favor of a sodium salt.

Operation of Luminous Flames. The instrumentation described was developed for use on nonluminous flames. However, since there is no definite line of demarcation between a luminous and a nonluminous flame, and vice versa, it might be well to discuss the operation of the instrument when used on a luminous flame.

From a theoretical standpoint, it is immaterial whether the absorption and emission taking place in the flame is caused by the sodium atoms or by small carbon particles—the equations must still be valid under the specified conditions. The equations do assume, however, that one is working with monochromatic radiation, i.e., that one has a perfect spectrometer. On a nonluminous flame a comparatively wide spectrometer entrance slit is permissible and is desirable from sensitivity considerations. However, if a comparatively wide slit is used in conjunction with a luminous flame, the output of PE_1 (Fig. 2), is composed of the output resulting from the side bands present due to spectrometer imperfections as well as that resulting from the radiation at the sodium wave length. At the same time PE_2 (Fig. 2), and the measuring phototube PE_3 (Fig. 2), see only the radiation resulting from the sodium wave length. As previously explained, the bridge circuit automatically maintains equal outputs from the two phototubes PE_1 and PE_2, by adjusting the intensity of the sodium lamp. Thus, even under these conditions, Equation [2] must still be valid and

$$J_{\lambda L} = \frac{J_{(\lambda \pm d\lambda)F}}{A_{\lambda F}}$$

where $J_{(\lambda \pm d\lambda)F}$, however, now includes the intensity of radiation from the side bands $(\lambda + d\lambda)$ and $(\lambda - d\lambda)$ as well as from λ. For a particular flame of fixed temperature and absorptivity $J_{(\lambda + d\lambda)}$ is larger than $J_{\lambda F}$. Since $A_{\lambda F}$ is fixed it follows that $J_{\lambda L}$ is larger when PE_1 receives radiation of intensity $J_{(\lambda \pm d\lambda)F}$, than when PE_1 receives radiation $J_{\lambda F}$. Consequently, the lamp and the measuring circuit could give temperature readings in excess of the black-body temperature of the flame when the instrument is sighted on a luminous flame.

Operation With a Variable Transmittance. As has been previously mentioned, the sodium-vapor lamp requires a maximum current of 3.0 amp for its operation. With the usual type of receiving tube, such currents are achieved only by parallel operation of a large number of tubes, and consequently some other means of modulating the light source might be desirable. If the arrangement shown in Fig. 4 is considered and the analysis previously employed in the development of Equations [1] and [2] is used, it follows that

$$xJ_{\lambda L}R_{\lambda M_1M_2} = xJ_{\lambda L}T_{\lambda M_1} - xJ_{\lambda L}T_{\lambda M_1}A_{\lambda F} + J_{\lambda F} \ldots [14]$$

where

x = transmittance of diaphragm or other means used to modulate the light
$R_{\lambda M_1M_2}$ = combined reflectivity of mirrors M_1 and M_2
$T_{\lambda M_1}$ = transmittance of mirror M_1

In order that equal light intensities will be received by the two phototubes PE_1 and PE_2, Fig. 10, when no flame is present, it will be necessary to adjust the optical paths such that $R_{\lambda M_1M_2} = T_{\lambda M_1}$. With the flame in position and at the balance point where the equation is valid

$$x = \frac{J_{\lambda F}}{A_{\lambda F}\, J_{\lambda L}\, T_{\lambda M_1}} \ldots\ldots\ldots\ldots [15]$$

or if $J_{\lambda L}$ is held constant, x is a function of only the black-body temperature of the flame.

If a suitable variable transmittance could be found the foregoing arrangement would enable a steady-temperature lamp to be used. In addition, the use of a continuous-spectrum light source would help to minimize possible errors encountered in operation on a luminous flame since under these conditions all phototubes (PE_1, PE_2, and PE_3, Fig. 10), would receive side-band radiation as well as the central wave length.

Numerous different methods of modulating the beam of light seem feasible, depending upon the speed of response required. Optical wedges (16) or an ordinary diaphragm would be suitable for very slow operations. For rapid changes, the use of the Kerr cell (17), the Jeffree light valve (18), the P-type crystal (19), or other similar devices would seem feasible. It is hoped that future

development work employing these or other variable transmittances can be carried out.

Nature of Temperature Measured

During the combustion processes in an internal-combustion engine the gases are nonhomogeneous in composition, are in violent physical and chemical agitation, and are neither in chemical nor thermal equilibrium. Thus the thermodynamic terms, "temperature of a flame" or "temperature of the gases in the engine" as used in the preceding discussion are indefinite in meaning until one specifies the measuring and averaging technique used. In other words, one could obtain almost any temperature value desired from such a system by proper choice of the measuring and averaging technique. For example, if one measured the pressure of such a system and calculated the temperature, one value would be obtained, while if some radiation technique, which would weight the high temperatures more heavily, were used, an entirely different answer would be obtained. The following discussion will attempt to point out some of the things that should be considered in evaluating the temperatures measured by the foregoing technique.

It is clear that if the gases are not in thermal equilibrium a spatial average of the temperature must be obtained and that the measured temperature should lie somewhere between the lowest and highest temperatures existing in the gases. Such a problem has been treated by different investigators (16, 20, 21, 22). All of these investigators came to the same conclusions; the measured temperature will lie somewhere between the highest and the lowest temperatures existing in the nonequilibrium system, the measured temperature will be affected by concentration of the radiating substance, and [with the possible exception of the technique used by Bundy and Strong (20)], one cannot determine the temperature and concentration distribution from the measured temperature since the same measured temperature may be given by numerous different temperature and concentration distributions. Experimental confirmation of these conclusions is given by Lewis and von Elbe (23) where temperatures of as much as 100 to 200 F lower were obtained when the flame was totally colored, as compared to point colorations in the high-temperature regions. Confirmation is also given in the work of Bundy and Strong (20) and Buttner, Rosenthal, and Agnew (21), who showed that, even in totally colored flames, the distribution of the radiating particles affected the values of the measured temperatures. Experimental evidence from engine flames will be found in reference (13), where Rassweiler and Withrow found that "self-reversal" could be produced by varying the sodium concentration.

The foregoing reasoning and experimental data emphasize the difficulty in determining the significance of and utilizing combustion-temperature measurements made in internal-combustion engines. These combustion-temperature measurements are further complicated by the possibilities of nonequipartition of energy among the various degrees of freedom of the molecule. This possibility will be mentioned later. At the same time, fairly reproducible combustion-temperature measurements have been made (4, 5, 7, 11, 12, 13).

With the full realization that these data were taken on engines of different design and with different combustion-chamber shapes, under different operating conditions, and in some cases even by entirely different techniques, it was thought that an attempted correlation of combustion-temperature measurements made in spark-ignition engines might be of interest. Accordingly, the available pertinent data from the literature were all plotted to the same scale and are presented in Fig. 11. Fig. 4 presents the shape of the combustion chambers used by the various investigators and as much data on the operating variables as could be obtained from the literature.

Some of the differences between engines can be minimized by plotting the temperature against volume on a log-log scale. Such a plot is shown in Fig. 12 for the data taken by radiation techniques. Since the literature does not give $1/r$ values for the various engines, it was necessary to assume a value of 4.00. Minor variations from this assumed value would affect the scale but little.

Since the curve shown in Fig. 12, representing data taken during the present investigations, includes data in addition to those shown

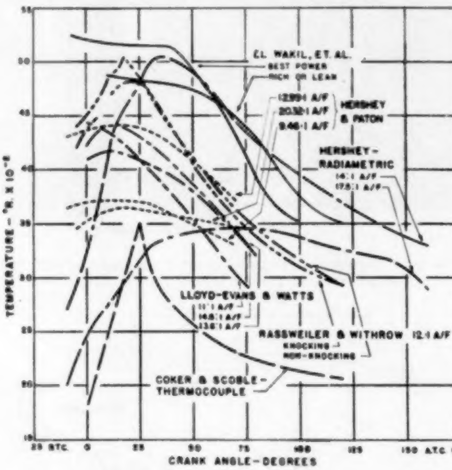

Fig. 11 Graph Showing Temperature Measurements Made by Different Investigators

in Fig. 8, a word of explanation as to the averaging processes used might be in order at this point. The cyclic irreproducibility and the abrupt decrease in deflection at the end of a particular cycle have been noted previously. With the knowledge that the temperature did not go to zero at the end of the abrupt decrease in temperature a value of 3500 R, corresponding to an oscillograph deflection of 0.15 in., was assigned to a curve as soon as the oscillograph deflection became less than 0.15 in. This value and the other measured values were then averaged arithmetically, and a smooth curve drawn through the resulting points. This averaging technique is admittedly imperfect but since the data were used for comparison with point-by-point values and since the type of average obtained by the latter technique is unknown, the method outlined was considered satisfactory.

Inspection of the data shown in Figs. 11 and 12, taken by the sodium-line reversal technique will show lines of two distinctly different slopes, i.e., the data taken by Rassweiler and Withrow (13) and by Lloyd-Evans and Watts (12) show distinctly more of a temperature decrease per crank angle than do the data of Hershey and Paton (11), and that of the present investigation which shows quite "flat" temperature curves. Similar flat temperature curves have been noticed previously in the Diesel engine (7).

Inspection of the information shown in Fig. 4 will suggest at least two possible explanations for the differences in slopes obtained by the different investigators. It will be noticed that the data with the greater negative slope (Rassweiler and Withrow, and Lloyd-Evans and Watts) were taken on head engines, while the flat temperature curves (Hershey and Paton, and El Wakil, et al) were taken on valve-in-head engines. While this is a

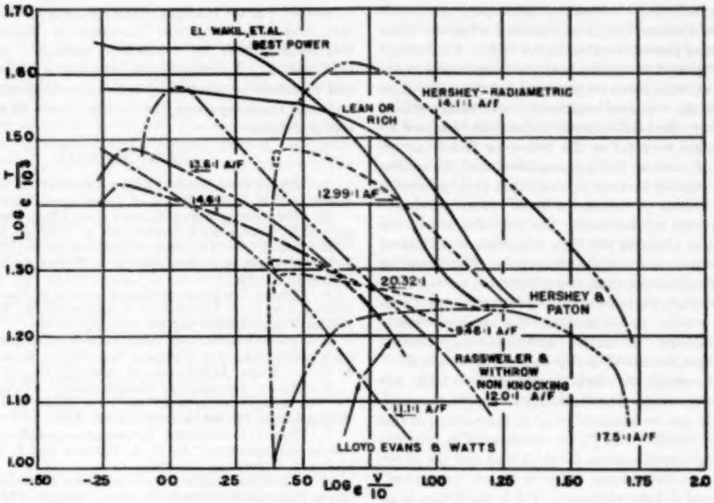

FIG. 12 TEMPERATURE MEASUREMENTS MADE BY DIFFERENT INVESTIGATORS SHOWN ON LOGARITHMIC SCALE

possible explanation, it is not thought to be the most nearly correct and significant explanation. It will also be noticed in Fig. 4 that the flat temperature data were taken with the line of sight, parallel to the flame-front travel (at right angles to the flame front if it were a plane wave), while the other data were taken with the line of sight at right angles to the flame-front travel (parallel to the flame front). It is thought that this second difference in combustion-chamber arrangement is of significance.

The different slopes for the data of the different investigators could be explained by the existence of a high-temperature flame front (possibly even higher than the adiabatic flame temperature). Under this assumption, the data taken with the travel of the flame front at right angles to the line of sight should give an initially high temperature, followed by the expected expansion curve. This is in agreement with the experimental data (Figs. 11 and 12). It is also interesting to note the small initial "pips" visible in Figs. 5, 6, and 7, when the flame front first reaches the line of sight of the electro-optical pyrometer. These experimental pips could be caused by instrument error, and thus at present cannot be accepted as absolute evidence of an initial high temperature, but it is interesting to note their presence. However, these experimental pips were not in evidence when the instrument was sighted on the calibration flame, and the radiation was rapidly and periodically interrupted by the light chopper.

On the other hand, the data taken with the travel of the flame front parallel to the line of sight would be expected to give a flat curve until such time as the high-temperature flame front passed out of the line of sight, while, after the flame front had passed out of the line of sight, the expected expansion curve should be observed. Again, this is in agreement with the experimental facts (Figs. 11 and 12).

Under the foregoing assumption, it would also be expected that the length of this flat portion would vary with the speed of travel of the flame front. Again, the experimental data taken by Hershey and Paton and by the present investigators show this trend. For example, the data of Hershey and Patton show that the lean mixture (20.3:1) gave a very flat curve, the rich mixture (9.46:1) gave a flat portion followed by the predicted expansion curve, and the presumably best-power (12.99:1) mixture gave a very short flat portion, followed by the predicted expansion curve. This trend is in excellent agreement with the speed-of-flame-travel data of Rabezzana and Kalmar (24), who found that a combustion time of approximately 90 deg of crank travel was required for a 20.3:1 mixture, 55 deg for a 9.5:1 mixture, and 45 deg for a 13.6:1 mixture.

If this suggested high flame-front temperature does exist one would also expect that the relative closeness of the flame front to the measuring device would affect the temperature value recorded, (16, 20, 21, 22). The data of the present investigation are inconclusive on this point for, while the flame front is moving away from the measuring device, the pressure and temperature of the unburned gases into which the flame front is advancing are varying and might affect the flame-front temperature in a manner as yet unknown. The data of the present investigation, where the flame front is moving away from the spectrometer, are slightly more flat than the data of Hershey and Paton where the flame front was moving toward the spectroscope.

Additional verification for the suggested high-temperature flame front is found in temperature measurements made on the Diesel engine (4, 5, 6, 7). From the manner in which the fuel is introduced and combustion takes place in the Diesel engine a multiplicity of individual flame fronts would be expected. This multiplicity of flame fronts would be expected to exist for some time after injection has ceased and possibly for a goodly proportion of the expansion stroke because of the imperfect mixing of the fuel and air. Thus if high temperatures did exist in the flame front, a flat temperature curve would be expected. Such flat temperature curves have been found experimentally (4, 5, 7). The "flatness" of these curves caused considerable comment in the accompanying discussions and the foregoing explanation was offered. The data of this investigation would seem to offer conclusive proof that such was the case. Furthermore, the measured Diesel combustion temperatures were not markedly affected by engine operating condition. This is in agreement with the foregoing hypothesis, for the flame-front temperature would probably not be greatly affected by the operating variables.

If the given hypothesis is correct, a previously mentioned abrupt temperature decrease would be expected when the flame front ceased to exist or passed from the line of sight. This abrupt decrease could be expected to terminate at the temperature of the expanding gases and from there on the temperature-crank-angle curve should follow the expected expansion curve rather than a flat curve. However, the oscillographic deflections obtained by either the sodium line reversal or the two-color technique are logarithmic with $1/T$, and, as the temperature drops, the oscillographic deflections rapidly become so small that possible scaling error prevents the taking of conclusive data. More conclusive data could be obtained by increasing the amplification of the measuring circuit and allowing the high-temperature portion of the curve to go off the screen of the oscillograph. This would, of course, preclude simultaneous data being obtained on both the high and low-temperature portions of the curve but it would enable more accurate studies to be made of the low-temperature portion of the expansion. If desired, additional amplification channels and oscillographs would enable both to be obtained.

Unfortunately, the engine on which the studies were made was in the process of being equipped with additional instrumentation, and these data could not be obtained prior to the writing of this paper. The data of Hershey and Paton would seem to bear out this conclusion though, for the curves for the 9.46:1 and the 12.99:1 air-fuel ratio show a flat portion followed by an "expansion" portion. It is planned to take additional data in the future in an attempt to clarify this point.

In view of the experimental confirmation given, it might be well to inquire if any theoretically sound explanation can be found for the suggested high-temperature flame front. Unfortunately, the details of what happens in the flame front are not clear. From the findings of many workers in this and other fields (25) it seems very probable, however, that when the oxidation products are formed from the reactants, a major portion of the energy so released is present in the vibratory degrees of freedom. The sodium atom would be a possible third body to absorb this energy at the time of the reaction or a second body to absorb it after the reaction has taken place. It is also known that the vibratory degrees of freedom of nitrogen, which, after all, forms approximately 80 per cent of the mixture, are excited much more slowly than the translatory degrees of freedom. Thus if a nitrogen molecule absorbed the excess vibratory energy of the reacting molecules its translatory degrees of freedom would quite probably contain an excess of energy over the other degrees of freedom. Thus, in any event, in the flame front the sodium atom would have an excellent opportunity to become excited by molecules having an excess of energy in a particular degree of freedom and to indicate a high temperature. Under the existing high pressures the large number of molecular collisions undoubtedly would cause rapid re-equipartition of energy but, if the flame front had appreciable thickness, the spatial averaging given by the sodium-line reversal technique might well produce the observed experimental results.

One other point might be of interest in comparing the present results with those of the previous investigations. It is noted that the temperatures currently being measured are the highest of all the temperatures shown in Figs. 11 and 12. One possible explanation for this might be the existence of some luminosity in the flame for, as previously mentioned, this luminosity could cause temperature readings in excess of the black-body temperature.

Acknowledgment

Grateful acknowledgment is made to Profs. L. A. Wilson and J. G. Winans for their assistance, and to Gordon Millar who assisted in taking some of the data. This work was supported in part by a grant from the Wisconsin Alumni Research Foundation, and in part by the University of Wisconsin College of Engineering, and by fellowship assistance from the Ethyl Corporation. To these organizations, and to the many students and members of the faculty who have rendered valuable assistance and encouragement, the authors desire to express their sincere gratitude.

BIBLIOGRAPHY

1 "Photo Electric Combustion Analysis," by R. A. Rose, G. C. Wilson, and R. L. Benedict, *SAE Journal*, vol. 39, 1936, pp. 459–468.

2 "Behavior of High and Low Cetane Diesel Fuel," by G. C. Wilson and R. A. Rose, *SAE Journal*, vol. 41, 1937, pp. 343–348.

3 "Duration of Combustion in a Commercial Diesel Engine," by A. F. Robertson, R. A. Rose, and G. C. Wilson, *SAE Journal*, vol. 44, 1939, pp. 117–124.

4 "Flame Temperature Measurements in Internal-Combustion Engines," by O. A. Uyehara, P. S. Myers, K. M. Watson, and L. A. Wilson, Trans. ASME, vol. 68, 1946, pp. 17–30.

5 "Diesel Combustion Temperatures—The Influence of Operating Variables," by O. A. Uyehara, P. S. Myers, K. M. Watson, and L. A. Wilson, Trans. ASME, vol. 69, 1947, pp. 465–477.

6 "Flame Temperature Measurements—Electronic Solution of the Temperature Equations," by P. S. Myers and O. A. Uyehara, Transactions SAE, vol. 1, 1947, pp. 592–601.

7 "Diesel Combustion Temperatures—Influence of Fuels of Selected Composition," by O. A. Uyehara and P. S. Myers, Trans. SAE, vol. 3, 1949, pp. 178–199.

8 "Über das Reflexionvermogen von Flammen," by F. Kurlbaum, *Physikalische Zeitschrift*, vol. 3, 1902, pp. 332–334.

9 "Thermonitrie-Sur La Temperature des Flammes," by M. Ch. Fery, Comptes Rendus, vol. 137, 1903, p. 909.

10 "The Sodium-Line Reversal Method of Determining Flame Temperatures," by W. T. David, *Engineering*, vol. 138, 1934, p. 175. For a reply to his criticisms see "The Sodium-Line Reversal Method of Determining Flame Temperature," by Bernard Lewis and Gunther von Elbe, *Engineering*, vol. 139, 1935, p. 168.

11 "Flame Temperatures in an Internal Combustion Engine Measured by Spectral Line Reversal," by A. E. Hershey and R. F. Paton, University of Illinois Engineering Experiment Station Bulletin 262, Urbana, Ill., October, 1933.

12 "The Measurement of Flame Temperature in a Petrol Engine by the Spectral Line Reversal Method," by S. S. Watts and B. J. Lloyd-Evans, Proceedings of the Physical Society of London, vol. 46, 1934, pp. 444–449.

13 "Flame Temperatures Vary With Knock and Combustion-Chamber Position," by G. G. M. Rassweiler and Lloyd Withrow, Trans. section, *SAE Journal*, vol. 36, 1935, pp. 125–133.

14 "Fundamental Phenomena in Sodium-Vapor Lamps," by C. G. Found, *General Electric Review*, vol. 37, 1934, pp. 269–277. Other discussions are also given in the June through August, 1934, issues of the same magazine.

15 "Sodium Discharge Lamp as Intensity Standard," by H. Schmellenmeier, *Zeitschrift für Physik*, vol. 95, 1933, pp. 705–725.

16 "The Measurement of Flame Temperature," by Ezer Griffiths and J. H. Awberry, Proceedings of the Royal Society of London, vol. 123, 1929, pp. 401–421.

17 Report No. 327, by C. M. Wolfe, Aerojet Engine Company, 1948.

18 British Patent No. 439236; also see *Television and Short Wave World*, vol. 60, No. 99, pp. 260–264 et seq.

19 "Light Modulation by P-Type Crystals," by G. P. Gotschall, *Journal of the Society of Motion Picture Engineers*, vol. 51, July, 1948, pp. 13–20.

20 Report No. 55278, by T. P. Bundy and H. M. Strong, General Electric Company, Schenectady, N. Y., 1948.

21 "A Study of Flame Temperature as Determined by the Sodium Line Reversal Method in Totally and Partially Colored Flames," by H. J. Buttner, I. Rosenthal, and W. J. Agnew, United States Navy, Project Squid, Technical Memorandum No. Pur-13.

22 An unpublished discussion accompanying Reference 7. This may be obtained from SAE Headquarters, 29 West 39th Street, New York, N. Y.

23 "Combustion, Flames and Explosions of Gases," by Bernard Lewis and Gunther von Elbe, Cambridge University Press, 1938.

24 "Factors Controlling Engine Combustion," by H. Rabezzana and S. Kalmar, *Automotive Industry*, vol. 72, 1935, pp. 324, 354, and 394.

25 "Spectroscopy and Combustion Theory," by A. G. Gaydon, Chapman and Hall, Ltd., London, England, 1948.

Discussion

J. H. Hett.[5] The instrumentation and techniques of this paper are so excellent that it may seem captious to raise again the question of the thermal equilibrium of the sodium with the hot gas under all conditions.

The writer and others at the Jet and Flame Laboratory, New York University, have observed for certain types of acetylene-oxygen flames that the spectral brightness at the centers of the sodium line are at least 100 times greater than that of the adjacent continuum. As this continuum has an emissivity of at least 0.4, some preferential excitation of sodium is indicated in this case.

Along analogous lines is a recent communication by Gaydon and Wolfhard.[6] They show that for a low-pressure acetylene-air flame (24 mm of Hg) when a metal vapor such as iron or lead is introduced into the flame, it is found that many of the lines of the spectrum are obtained in emission, even against a background of a full light of a carbon arc (3800 K). They also give a table of line-reversal temperatures which range for the same flame from 2010 K for Na 5890 to 3450 K for Fe 2483.

These observations clearly indicate that the chemical kinetics of sodium needs additional study before full confidence can be given to line-reversal temperatures.

E. W. Landen.[7] The Combustion Laboratory at the University of Wisconsin has had considerable experience in the measurement of instantaneous temperature of the Diesel flame and has now extended these measurements to the Otto-cycle flame. The development of new and better instruments should give us better data so that we can evaluate combustion more satisfactorily, even though the instruments are based on previously known concepts.

There is little we can add to these data on gasoline-engine combustion, and speculation here at this time would contribute very little. It is too bad that a wider span of temperature cannot be utilized in this equipment so that more complete data could be obtained. It is difficult to make a pyrometer of this type or the two-color electronic-optical type to work for all temperatures. The exponential variation of the radiation as a function of the temperature makes the problem difficult. A two-color electronic-optical pyrometer constructed at our laboratory would operate only over a temperature range of 1000 to 1500 F, depending on the limiting peak temperature. There was some choice in the operating range of this instrument.

The authors make some comparison between the peak temperatures in the gasoline and the Diesel combustion. They refer to the "flatness" of the temperature curves from both engines. This may occur in a gasoline engine when the flame front is moving toward or away from the observation point. In the Diesel, however, due to the heterogeneity of burning after ignition, one would expect considerable variation in the observed temperature because the intensity of burning would vary with time, and the density of the flame would not permit always observing the maximum temperatures, although the weighted average would be in that direction. We have obtained temperature-crank angle data from our test engines, and our observations differ depending upon the point of observations. In the precombustion chamber, the temperature remains high for some time, but there is a variation in recorded temperature of as much as 400 F, and exhibiting a high-frequency oscillation. This may be caused by turbulence of the burning mass. The point of observation in the main chamber was selected to view the gases emerging from the precombustion chamber. The temperature-crank angle curve was quite smooth and varied with the load condition on the engine. A plot of the temperature crank angle at the latter observation point is shown in Fig. 13 of this discussion. Two fuels of differing volatility are illustrated here. The heptane - iso-octane blend, being highly volatile, shows a slightly different tempera-

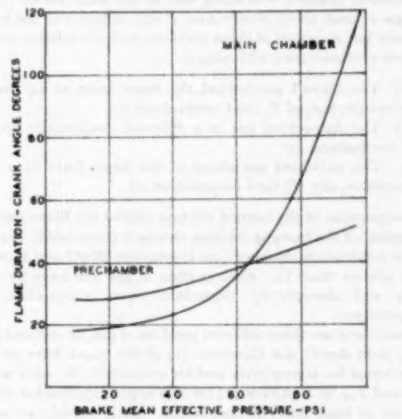

Fig. 14 Flame Duration in Precombustion-Chamber Engine: Speed 1800 Rpm

[5] Jet and Flame Laboratory, New York University, New York N. Y.

[6] "Letter to the Editor," Proceedings of the Physical Society of London, series A, vol. 53, 1950, p. 77.

[7] Caterpillar Tractor Company, Peoria, Ill.

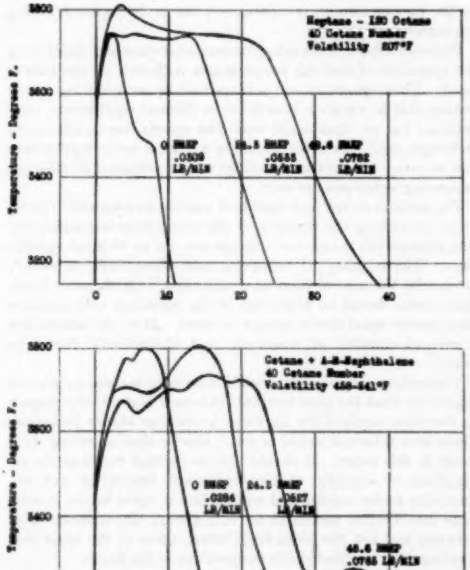

Fig. 13 Crank Angle After Start of Flame

ture-crank angle relationship than does the less volatile fuel even though both have a measured cetane number of 40.

From Fig. 14, herewith, showing the flame duration as a function of bmep, one would expect the flames in the prechamber and main chamber to be of equal duration in this engine at about 60 bmep. The duration from the temperature runs agrees reasonably well with that obtained by other techniques. There is a difference in pressure between the prechamber and the main chamber so that an analysis of the prechamber observations would not exactly fit the main chamber. The temperatures are in the same order of magnitude but differ in duration. This brings up a point in regard to the flatness of the temperature curves shown in reference (4) and (7) of the authors' Bibliography. If the pressures and temperatures were measured in the antichamber, there may be some discrepancy when compared to the events in the main chamber. In our own engines, we know there are differences in pressure between the two combustion chambers. The antichamber of a Diesel engine may give slightly different flame duration and temperature from that of the main chamber.

E. F. Obert.[8] It is noted that the line of sight through the combustion chamber was along that of the flame travel. Then the gas column under observation at any instant was not homogeneous but consisted of three portions (and the relative volume of each portion varied with time):

(*a*) The burned gas behind the flame front at an average temperature, say, of T_1 (and composition x_1).

(*b*) The flame-front gas at a different temperature, say, T_2 (and composition x_2).

(*c*) The unburned gas ahead of the flame front at a third temperature, say, T_3 (and composition x_3).

Compression of the burned mixture behind the flame front by expansion of the burning mixture creates a temperature gradient in the combustion chamber (the Hopkinson effect) and therefore T_1 is greater than T_2. Each portion of gas will have an emissivity and absorptivity dependent upon composition and temperature.

Since there are three different portions of gas, as outlined herewith, then should not Equation [1] of the paper have at least three terms for absorptivity and for intensity? In other words, $A_{\lambda F}$ and $J_{\lambda F}$ in Equation [1] for this engine application should contain at least three distinct terms. As a second part of the same basic question, note that the temperature of each portion of gas has a different value. Then is it permissible to assume that an absorptivity and an emissivity (really, average values) are equal? This was the assumption underlying Equation [3] of the paper. It would appear that no single temperature is being read by the instrument.

That the flat isothermal curves are related more to a "flame-front" temperature and not to an "average" temperature is apparent in Fig. 7, since a 1200 F drop in temperature occurs in about 3 deg of crank movement and certainly an average temperature would not change so rapidly. This drop emphasizes the nonequilibrium of temperature throughout the combustion chamber. In reference (11) of the paper the temperature also approached isothermal when a wide shutter opening (18 deg) was used, and became less so with smaller openings (3 deg). Is there an interrelationship here which is not apparent to the writer?

The flat isothermal portion also may arise from the compression of the already burned gas behind the flame front as combustion takes place. The temperature gradient predicted by theory for a constant-volume combustion tends to maintain the temperature of the first-burned portion as the piston descends. Could this effect be emphasized by the increasing volume of burned products with their high temperature appearing in the line of sight of the instrument at the expense of unburned mixture at a lower temperature? Does the instrument emphasize the highest temperature sighted?

The same explanation might be used for the "pips" shown in the illustrations. If these pips were phenomena of the flame front, maximum values would be expected for overrich mixtures and minimum values for lean mixtures. In the illustrations, however, minimum values occur for the best-power mixture which is a rich mixture. The pips are apparently first sighted either before TDC or before maximum pressure. With the isothermal explanation in mind, would not the pressure probably be rising in the chamber when the pips occur and, therefore, compression of the burned mixture is occurring without a compensating expansion?

A rough calculation indicates that the pips occur in approximately the time that would be required for the flame to travel a distance equal to the diameter of the quartz viewing windows. The authors may care to comment on this coincidence.

[8] Professor of Mechanical Engineering, Northwestern Technological Institute, Evanston, Ill. Mem ASME.

Authors' Closure

The authors appreciate the interest shown by the discussers. They are in agreement with Mr. Hett that in the flame front preferential excitation of sodium does exist and are glad for the confirming experimental evidence set forth by Mr. Hett.

Dr. Landen's data on the Diesel engine are interesting. References (4) and (7) of the main paper do present data taken in the precombustion chamber and his comments are therefore pertinent. It is of interest to note that the temperature-time curves shown by Dr. Landen also are comparatively flat in the region following top center.

Professor Obert raises some fundamental questions concerning the operation of and the temperatures indicated by the instrument. These questions can perhaps best be answered by simply stating that in a system that is not in thermal equilibrium, temperature has no significance until you specify the measurement technique used. In other words, in a system not in equilibrium just as many temperature readings can be obtained as different measuring techniques are used.

The authors do not feel capable of making an unqualified statement concerning the equality of the monochromatic emissivity and absorptivity when the systems are not in thermal equilibrium. The equality of emissivity and absorptivity is always proved for the case of thermal equilibrium. On the other hand, these items should be properties of the substance and therefore once proved equal should always be equal. If so, the assumption of over-all equality of emissivity and absorptivity should be sound.

The authors can conceive possible exceptions to these statements especially when the time interval concerned is short with respect to the time required for an atom to emit or absorb radiation. These time intervals would be much shorter than anything of interest in this paper. It should also be pointed out that the assumption of equality of monochromatic emissivity and absorptivity under nonthermal equilibrium is made in the steady-state line-reversal technique for it is always the apparent temperature and not the black-body temperature of the lamp that is set equal to the black-body temperature of the flame.

No relationship is apparent to the authors between the flat temperature curves obtained by the authors and the flat temperature curves obtained by reference (1) of the main paper with an 18-deg shutter opening.

The flat isothermal curves obtained could be explained by the

increasing volume of the hot burned gases. However, as pointed out in the text, the presence of the "pips," and the abrupt decrease in temperature cause the authors to believe that the correct explanation is the preferential excitation of the sodium in the flame front. This explanation is further confirmed by Professor Obert's observation that the width of the pip is of the same time magnitude as that required for the flame front to pass the quartz window.

AN ASME PAPER

Its Preparation, Submission and Publication, and Presentation

To a large degree the papers prepared and presented under the ASME sponsorship are evidence by which its professional standing and leadership are judged. It follows, therefore, that to qualify for ASME sponsorship, a paper must not only present suitable subject matter, but it must be well written and conform to recognized standards of good English and literary style.

The pamphlet on "AN ASME PAPER" is designed to aid authors in meeting these requirements and to acquaint them with rules of the Society relating to the preparation and submission of manuscripts and accompanying illustrations. It also includes suggestions for the presentation of papers before Society meetings.

CONTENTS